UNIVERSITY OF BIRMINGHAM

INCORPORATION OF URBAN HEAT IN RISK ASSESSMENT: A HEALTH PERSPECTIVE

Charlie John Tomlinson

A thesis submitted to the University of Birmingham for the degree of Doctor of Philosophy.

School of Civil Engineering

College of Engineering and Physical Sciences

University of Birmingham

July 2012

Abstract

This thesis analyses heat health risk spatially in Birmingham (UK) via a combination of remote sensing and GIS techniques, including urban influences which are not generally considered in heat risk assessments or climate change projections. The world's urban population is growing rapidly, and the risk of extreme heat to human health has been highlighted by recent events such as the 2003 heatwave in Europe, where mortality rates significantly increased. This thesis presents a methodology using satellite data to quantify the surface urban heat island of Birmingham at 1 km resolution, with results showing extreme events are much warmer ($\sim$5°C) than average conditions ($\sim$2°C). This urban heat island data is combined with social data in a spatial risk assessment, illustrating that many vulnerable people live in areas of increased heat risk. A custom collection of ground based sensors is utilised to investigate the relationship between surface and air temperatures, finding air temperatures are warmer than LST measurements at night. Then UK Climate Projections 2009 are used to explore the influence of the urban heat island on climate projections in Birmingham, showing that changes could be large (90% increase in minimum temperature under 2080s extreme scenarios).

Acknowledgements

There are a number of thanks due as I finish this thesis. I would like to express my gratitude to my supervisors who have been helpful and supportive throughout this project. Professor Chris Baker, Professor John Thornes and Dr. Lee Chapman were a pleasure to work with. The hands-off nature of their supervision allowed me to develop ideas independently and explore multiple research avenues, but the honest and constructive feedback was appreciated and kept me on track. I have learnt a lot.

Thanks is due to Birmingham City Council for helping focus the research direction towards a "real world" problem and for funding assistance. Particularly to Jonathan Adey, Nick Grayson and Richard Rees. I am grateful to EPSRC for its financial support, and Dr. Mark Sterling from Civil Engineering for his advice and encouragement before embarking upon this PhD.

There are numerous others, too many to list, that I owe thanks to. The editors and anonymous reviewers of the journal papers that accompany this thesis have challenged me and strengthened the work within this thesis. Conversations at conferences, within the department and elsewhere have contributed to my thought process. The fourth floor GEES postgraduate crowd were a useful sounding board and a great social group; I hope we keep in touch.

Finally many thanks to Krystina, family, and friends whose support and continued patience is very much appreciated.

Thanks to you all.

Publications arising from thesis

Tomlinson, C. J., Chapman, L., Thornes, J. E. and Baker, C. J. 'Derivation of Birmingham's summer surface urban heat island from MODIS satellite images.' *International Journal of Climatology*, 32: 214-224. **(2012)** doi: 10.1002/joc.2261

Tomlinson, C. J., Chapman, L., Thornes, J. E. and Baker, C. J. 'Including the urban heat island in spatial heat health risk assessment strategies: a case study for Birmingham, UK.' *International Journal of Health Geographics*, 10(42): 1-14. **(2011)** doi: 10.1186/1476-072X-10-42

Tomlinson, C. J., Chapman, L., Thornes, J. E. and Baker, C. J. 'Remote sensing land surface temperature for meteorology and climatology: a review.' *Meteorological Applications*, 18(3): 296-306. **(2011)** doi: 10.1002/met.287

Tomlinson, C. J., Chapman, L., Thornes, J. E. and Baker, C. J., Prieto-Lopez, T. 'Comparing night time satellite land surface temperature from MODIS and ground measured air temperature across a conurbation.' *Remote Sensing Letters*, 3(8): 657-666. **(2012)** doi: 10.1080/01431161.2012.659354

Tomlinson, C. J., Prieto-Lopez, T., Bassett, R., Chapman, L., Cai, X-M., Thornes, J. E. and Baker, C. J. 'Showcasing urban heat island work in Birmingham - measuring, monitoring, modelling and more.' *Weather*, **(in press)**

Contents

List of Figures

List of Tables

List of Acronymns

ASCCUE : Adaptation Strategies for Climate Change in the Urban Environment

BCC : Birmingham City Council

BEP : Birmingham Environmental Partnership

BKCC: Building Knowledge for a Changing Climate

BUCCANEER : Birmingham Urban Climate Change with Neighbourhood Estimates of Environmental Risk

CCRA : Climate Change Risk Assessment

DEFRA : Department for Environment, Food and Rural Affairs

EMR : ElectroMagnetic Radiation

GCM : Global Circulation Model

GIS : Geographic Information System

GSW : Generalised Split Window (algorithm)

HDI : Hazard Density Index

HH : HouseHold

IB1 : IButton 1

IB2 : IButton 2

IPCC : Intergovernmental Panel on Climate Change

JJA : June, July, August

KTP : Knowledge Transfer Partnership

LCLIP : Local Climate Impacts Profile

LSOA : Lower Super Output Area

MSOA : Medium Super Output Area

LST: Land Surface Temperature

MAUP : Modifiable Areal Unit Problem

MIDAS : Met office Integrated Data Archive System

MODIS : MODerate resolution Imaging Spectroradiometer

NAP : National Adaptation Programme

NDVI : Normalized Difference Vegetation Index

NI : National Indicator

RCM : Regional Climate Model

RTE : Radiative Transfer Equation

SDS : Scientific DataSet

SRES : Special Report Emissions Scenarios

sUHI : Surface Urban Heat Island

TD : Threshold Detector

TIR : Thermal InfraRed

TOA : Top Of Atmosphere

UHI : Urban Heat Island

UKCIP : United Kingdom Climate Impacts Programme

UKCP : United Kingdom Climate Programme

UKCP09 : United Kingdom Climate Projections 2009

USOA : Upper Super Output Area

WG : Weather Generator

WMO : World Meteorological Organisation

Chapter 1

Introduction

The year 2008 marked the first time more than half the world population lived in urban areas, and rapid urban growth is predicted to continue, with urban areas "expected to absorb all the population growth expected over the next four decades", resulting in a predicted urban population of 6.4 billion in 2050 (compared to 3.3 billion in 2007) (United Nations, 2008). This widespread urbanisation has many consequences. At the global scale, this urbanisation and industrialisation is a main cause of climate change, and it is "very likely that anthropogenic greenhouse gas increases caused most of the observed increase in global average temperatures since the mid-20th century" (IPCC, 2007b). At a local scale, the growth of urban areas causes urban heat islands (UHI), where "urban landscapes typically experience higher air temperatures than the surrounding countryside" (Wilby et al., 2011). Global temperatures are expected to rise, the number of people living in urban areas is increasing, and urban areas can be markedly warmer than surrounding countryside. Excessive heat can negatively influence human health and increase mortality rates, having a real impact on society.

This thesis spatially explores heat health risk for the specific conurbation of Birmingham (UK), incorporating high resolution surface UHI (sUHI) measurements from remotely sensed satellite data combined with fine scale social information derived from commercial data. Along-

side this, validation of satellite data against air temperatures has been carried out, and the work has been put in context by considering the sUHI alongside climate change projections.

1.1 Heat risk

There is a growing recognition in the fields of bio-meteorology, epidemiology, climatology and environmental health that heat risk in urban areas is a problem, with scientific literature considering cities in Europe (Kovats and Hajat, 2008), the USA (Basu and Samet, 2002; O'Neill and Ebi, 2009), Australia (Vaneckova et al., 2008) and Asia (Honda, 2007; Tan et al., 2007), among others. Books (Gawith et al., 1999; McMichael et al., 2003) discuss heat risk in the context of climate change, risk and health. Publications such as the "New Civil Engineer" discuss if heatwave risks are being taken seriously in the UK (Stimpson, 2011) and "theWeather", a quarterly magazine of "theWeather Club", discusses UHI's and the potential impact on inhabitants in its Spring 2011 issue. The latest Intergovernmental Panel on Climate Change (IPCC) report; Special Report on Managing the Risks of Extreme Events and Disasters to Advance Climate Change Adaptation (SREX) discusses heat risk and explicitly states that "Urban heat islands pose an additional risk to urban inhabitants" (IPCC, 2012, p. 235) as "Cities can substantially increase local temperatures" (IPCC, 2012, p. 248).

Elevated temperatures cause increased human mortality (Gosling et al., 2009) which is exacerbated in heatwaves resulting in excess deaths. A number of examples are available in the literature such as in the 1995 UK heatwave (Rooney et al., 1998), the 1995 Chicago heatwave (Semenza et al., 1996) or the 2003 European heatwave (Kovats and Kristie, 2006) which affected France (Pirard et al., 2005; Fouillet et al., 2006; Tertre et al., 2006; Filleul et al., 2006), England (Johnson et al., 2005; Kovats et al., 2006), the Netherlands (Garssen et al., 2005), Portugal (Nogueira et al., 2005) and Spain (Simón et al., 2005). There is growing evidence that the intensity, frequency and duration of heatwaves is likely to increase in the future (Meehl and Tebaldi, 2004). This is prompting increased research into heat health risk projections (Knowlton et al., 2007; Luber and McGeehin, 2008), often as part of the broader remit concerning climate change and health (Guest et al., 1999; Kovats et al., 1999; Haines et al., 2006; Costello et al., 2009).

Recent global events have illustrated extreme heat events, for example Australia's summer (2010/2011) has been the hottest and driest summer on record in Perth, having 59 days with

temperatures greater than 30°C and 15 consecutive nights with temperatures not below 20°C (Prichard, 2011). In February 2011 Sydney experienced its hottest heatwave in 150 years of records, peaking at 41.5°C (The Sydney Morning Herald, 2011; 9 News, 2011), and in Adelaide the 1st January 2012 was the hottest start to the year since 1990, with temperatures of 41.6°C (9 News, 2012). In July 2010 Russia had a significant heatwave with the warmest July since at least 1880, where temperatures did not drop below 30°C for over a month, and maximum temperatures touched 37°C (The Economist, 2010; Dole et al., 2011).

It is important to note that this thesis explores air and surface temperatures which are only one aspect of human thermal comfort, which is a large research area (Synnefa et al., 2007; Hacker and Holmes, 2007; Wilson et al., 2008; Indraganti, 2010; Lin et al., 2010). Whilst it is recognised that an enhanced understanding of human thermal comfort would help interpret the heat risk work carried out in this thesis, such an understanding is outside the scope of this thesis.

1.2 Urban heat islands

The urban heat island (UHI) is an extensively studied phenomenon and refers to the difference in temperature between a conurbation and the surrounding rural area (Figure 1.1). There are many factors that contribute to the formation of the UHI. Urban geometry is often cited as the main cause (Oke, 1987), and is frequently parameterised in terms of the sky view factor (Bradley et al., 2002; Svensson, 2004; Unger, 2004) or surface volume compactness (Unger, 2006). Other major influences include the density and population of a conurbation (Oke, 1987) and its associated anthropogenic heat release (Smith et al., 2009), alongside landuse and vegetation cover (Stabler et al., 2005) which affect albedo (Kolokotroni and Giridharan, 2008), emissivity and surface roughness. The cumulative effect of these factors can result in a maximum air UHI of significant magnitude, such as the 7°C measured in London (Watkins et al., 2002) or greater than 8°C in New York City (Gedzelman et al., 2003).

A number of review papers illustrate the significant progress that has been made in the study of the UHI phenomenon, in particular, improving the nature and accuracy of measurements and the development of models (McKendry, 2003; Arnfield, 2005, 2006; Souch and Grimmond, 2006). The quantity of work involved is illustrated in a recent review (Stewart, 2010) that cri-

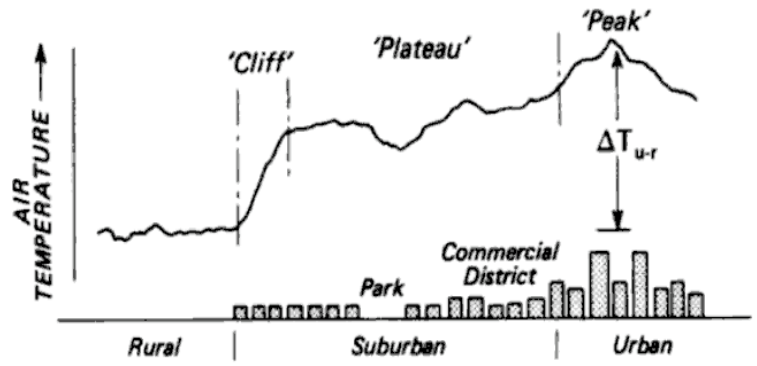

Figure 1.1: Generalised cross-section of a typical UHI (after Oke (1976)).

tiques the literature between 1950 and 2007 and focuses on a sample of 190 studies (from over 500 that were filtered or screened). The results show that "nearly half of all urban heat island magnitudes reported in the sample are judged to be scientifically indefensible". The main areas of weakness identified were controlling for weather, relief or time, and communication of metadata and site characteristics. These areas of weakness will be targeted in order to ensure this thesis is scientifically defensible. Arnfield (2003) offers a review of urban climate research between 1980 and 2001 with a significant focus on the UHI, and one area of weakness identified is the weak validation of models due to the difficulties of measuring the modelled variables. By quantifying the sUHI through measurement techniques (chapter 3) and validating these results (section 5.1) it is hoped this thesis can help model validation in the future.

The difference between air and surface UHI's is mentioned throughout this thesis, with surface UHI's being measured (chapter 3) and the relationship with air temperature explored (section 5.1). Whilst this difference is complicated, Figure 1.2 helps illustrate the the clear spatial and temporal characteristics between both UHI (shown as temperature difference between agricultural and downtown) and measurement techniques (T_{AIR} and Directional Brightness (similar to LST)). This work by Voogt and Oke (2003) shows two temperature transects across Vancouver, Canada; one in the day and one at night. The night transect (a) shows a pronounced temperature increase from the agricultural area through to residential and downtown, clearly illustrating a UHI. This increase is present in both air temperature and directional brightness (LST). Air temperature is consistently higher than directional brightness (apart from some small fluctuations in the mixed rural and water areas) which is similar to work by Jin and Dickinson (2000). In comparison, the day transect (b) shows air temperature lower than direc-

tional brightness, which is similar to work by Gallo et al. (2011) that found that LST was greater than air temperatures in the day. In the day transect a directional brightness UHI is present, but an air temperature UHI is not noticeable.

These two transects help illustrate the difficulties in understanding the UHI and the difference between air and remotely sensed temperatures. This thesis only considers night temperatures; because temperature datasets are not affected by incoming radiation, and the Mosaic data (used in chapter 4) is related to where people live. At night people will be at home sleeping, in the day many people will be at work. Throughout this thesis, UHI will refer to the air urban heat island whilst sUHI will refer to the surface urban heat island (e.g. as quantified in chapter 3).

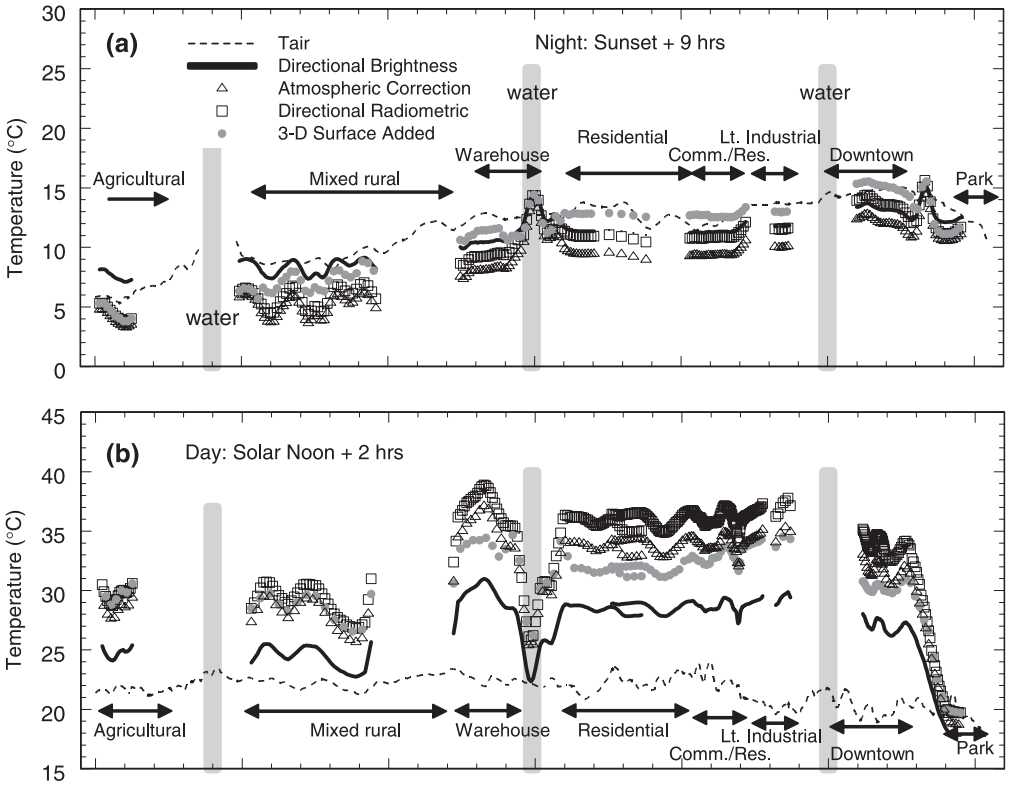

Figure 1.2: Heat island transect across Vancouver, Canada, for (a) nightime and (b) daytime (from Voogt and Oke (2003)).

Interest in the UHI effect is also increasing outside of academia, with reports from London (Greater London Authority, 2006) and the USA (USEPA, 2008) explicitly exploring the UHI. Other studies, for example green infrastructure planning (May, 2010), also require UHI data.

1.3 Climate change

Globally the climate is changing, and there is significant scientific literature available to this effect. In 2007 the IPCC released its Fourth Assessment Report (AR4), which stated "warming of the climate system is unequivocal" (IPCC, 2007a). There is a considerable amount of research done since AR4, which largely reinforces the message that climate change is happening (e.g. rising sea levels, reducing global ice cover, changes in biological systems), and the next IPCC report due in 2014 is expected to build on this evidence base.

1.3.1 Modelling

In the UK, the most comprehensive, scientifically defensible and widely used climate change projections are distributed by the United Kingdom Climate Programme (UKCP), previously known as the United Kingdom Climate Impacts Programme (UKCIP). The most recent projections are those from 2009, known as UKCP09, and these are widely used both within academia (Smith et al., 2011b) and within policy (The Government Office for Science, 2011). Prior to 2009 projections data was released in 1998 and 2002.

> "The UKCP09 Projections provide a basis for studies of impacts and vulnerability and decisions on adaptation to climate change in the UK over the 21st century (Jenkins et al., 2009)."

In UKCP09 there is a significant emphasis on probabilistic based projections, giving a range of potential scenarios; thereby acknowledging the unknown nature of climate change and modelling the future, yet giving a scientific "best guess" that can help inform policy and wider scientific work. However, despite the broad research effort around both the UHI and climate change, an area of research which still requires attention is the inclusion of the UHI phenomenon in climate models. Indeed, a UHI component is notably absent in many models, including the UK Met Office Hadley Centre Regional Climate Model (RCM) which has been used in the UK Climate Programme for both the UKCIP02 (Gawith et al., 2009) and UKCP09 (Jenkins et al., 2009) climate change projections. The UKCP literature makes reference to the UHI as follows:

> "We make no assessment of how the urban heat island may affect change (Jenkins et al., 2009)."
>
> "The UKCP09 probabilistic projections do not include any recognition of urban land-use and there is no account of a potential exacerbation of Urban Heat Island effects under climate change (UK Climate Projections, 2011c)."

Not accounting for the UHI is likely to underestimate future temperatures in urban areas under climate change scenarios. Including the UHI effect in climate models would improve the accessibility of climate data for planners (Gawith et al., 2009), and high resolution measurements of UHI effects would be a useful input for model development and validation. It is only recently that work is being done to try and integrate UHI projections or measurements into UK climate models, and Kershaw et al. (2010) offer a method based on gridded temperature data that can be linked to weather generators and climate models (including UKCP09). In order to integrate UHI data into climate scenarios, accurate and high resolution UHI data is required.

1.3.2 Adaptation

This work fits broadly into the growing field of climate change adaptation, which is accepting that some change is inevitable given historical emissions therefore encouraging adaptation to projected changes. This is different but complimentary when compared to mitigation; the aim of preventing future change, for example by reducing emissions. This work is part of the early foundations for climate change adaptation work in Birmingham.

The field of climate change adaptation is relatively new, and therefore the literature and discourse is correspondingly small. The climate change adaptation strategies of nine global cities, including London, are examined, and Birkmann et al. (2010) calls for a move away the assumption that climate change adaptation has to be purely physical alterations, and towards more emphasis on planning, implementation and evaluation of adaptation. Integrated assessment modelling for climate change adaptation and mitigation is examined by Patt et al. (2010) who finds that there is a bias towards "underestimating the difficulty of adaptation, and hence overestimating the net benefits". It is important to note that the benefits are already being overestimated, which would imply that future assessments should be more conservative. Dis-

cussions in Australia (Palutikof, 2010) consider how to manage extremes and the impact of a reduced water supply.

The climate change adaptation agenda is rapidly gaining traction in the public sector in the UK, for example with reports focussing on "Adapting Institutions to Climate Change" (The Royal Commission on Environmental Pollution, 2010), or "Preparing for Global Climate Change" (Foreign and Commonwealth Office, 2010), and individual cities are preparing adaptation plans. The draft plan for London has been published, with a number of reports available (Greater London Authority, 2012) online ahead of the final report in summer 2012. This project worked closely with Birmingham City Council (BCC) through the Birmingham Environmental Partnership (BEP), with the results feeding into their climate change adaptation work. Between 2008 - 2011 BEP had a number of "National Indicators", of which number 188 (NI 188) was specifically concerned with "Adapting to Climate Change".

> "The indicator measures progress on assessing and managing climate risks and opportunities, and incorporating appropriate action into local authority and partners' strategic planning (Local and Regional Partnership Boards, 2009)."

The indicator had five levels (Table 1.1), and this project was part of a suite of work aiming to help reach the levels by set target dates.

Table 1.1: BEP NI 188 targets.

Level	Result	Target
0	Getting started	Baseline
1	Public commitment and impacts assessment	2008/2009
2	Comprehensive risk assessment	2009/2010
3	Comprehensive action plan	2010/2011
4	Implementation, monitoring and continuous review	n/a

NI188 was part of the National Performance Framework which Local Strategic Partnerships (e.g. BEP) were implementing since their introduction in 2006. The change of government in 2010 brought with it the removal of this framework and the associated indicators, including NI188. BCC chose to keep going until the planned 2011 completion, and despite changes in the political framework, various organisations continue to work in the climate change adaptation area. Recently the UK Climate Change Risk Assessment (CCRA) 2012 (DEFRA, 2012b) was

released, which illustrates the ongoing national work targeting climate change adaptation. Previous reports explored the " International Dimensions of Climate Change" (The Government Office for Science, 2011) for UK policymakers, detailing global level work, whilst Sustainability West Midlands released a local scale report (Sustainability West Midlands, 2012) to coincide with publication of the CCRA. The politics surrounding climate change are often changing, for example the Environment Agency is now tasked with delivering the role of "adapting to climate change", and the Government is developing the National Adaptation Programme (NAP) with Defra (DEFRA, 2012a).

1.4 Thermal remote sensing

Remote sensing is defined as "the science and art of obtaining information about an object, area, or phenomenon through the analysis of data acquired by a device that is not in contact with the object, area or phenomenon under investigation" (Lillesand et al., 2004, p. 763). The general term originated in the 1960's at a similar time to the launch of the first meteorological satellite, the Television InfraRed Observation Satellite (TIROS-1). Usage is growing within the fields of meteorology and climatology, and works in unison with the use of Geographical Information Systems (GIS) (Chapman and Thornes, 2003; Dyras et al., 2005) for spatial analysis. Techniques can provide increased spatial coverage when compared to weather station data (Mendelsohn et al., 2007), and the instantaneous observations, global coverage and improving quality of remotely sensed information is proving increasingly useful (Jin and Shepherd, 2005). Remote sensing offers the ability to work at a number of scales, from local/citywide (Cheval et al., 2009; Cheval and Dumitrescu, 2009), national (Imhoff et al., 2010) and worldwide (Jin, 2004). Regardless of the scale of the study, remote sensing offers an opportunity to provide a consistent and repeatable methodology, suited equally to both quick pilot studies as well as long term monitoring campaigns. Although the initial cost of remote sensing platforms is high, the ease of data availability to end researchers, combined with the often extensive temporal and spatial coverage available, offers a marked improvement to traditional fieldwork campaign studies.

Thermal remote sensing refers to the use of the the thermal infrared spectrum to obtain surface temperature data from remote sensing platforms. This can be useful in studying the sUHI,

and section 2.1 outlines the theory and offers commentary on the various sensors and data available, before chapter 3 uses thermal remote sensing techniques to measure the sUHI of Birmingham.

1.5 Spatial risk assessment

Spatial risk assessment is defined as "the analysis of georeferenced data pertaining to some adverse outcome" (Lawson, 2008). The use of Geographical Information Systems (GIS) for spatial risk assessment work is a growing field, and covers a diverse range of hazards. These include various environmental hazards (Collins et al., 2009; Su et al., 2009), flooding and geological hazards (Fedeski and Gwilliam, 2007), technological hazard (Bolin et al., 2002), hurricanes (Taramelli et al., 2008), fuel poverty (Morrison and Shortt, 2008) and many more. Numerous epidemiological studies combine spatial and statistical analysis to assess risk, for example to explore patterns of cholera (Osei and Duker, 2008), the results of health surveys (Meng et al., 2010), the spatial patterns of cardiac disease (Loughnan et al., 2008), and social disadvantage (Andrey and Jones, 2008), to give a small selection. In comparison, work exploring heat risk spatially has so far been limited, but includes work in Australia (Vaneckova et al., 2010), Canada (Vescovi et al., 2005) and the United States (Reid et al., 2009). Related work in the UK is focussed in the area of climate change adaptation (Gwilliam et al., 2006; Lindley et al., 2006, 2007).

Adding a spatial aspect to risk assessment can be useful but relies upon having data with appropriate spatial information. An overview of spatial risk assessment is given in section 2.2, before the sUHI of Birmingham as measured in chapter 3 is combined with other data in a spatial risk assessment methodology in order to assess heat risk for Birmingham in chapter 4.

1.6 Study area: Birmingham, UK

This project uses Birmingham, the UK's second largest city, as the case study area. Birmingham has an estimated population in 2007 of over 1 million (Office for National Statistics, 2009), and is located in the West Midlands county as shown in Figure 1.3. The city is managed by Birmingham City Council (BCC), the largest local authority in Europe. Other cities, such as

London, are split into much smaller boroughs for local authority management.

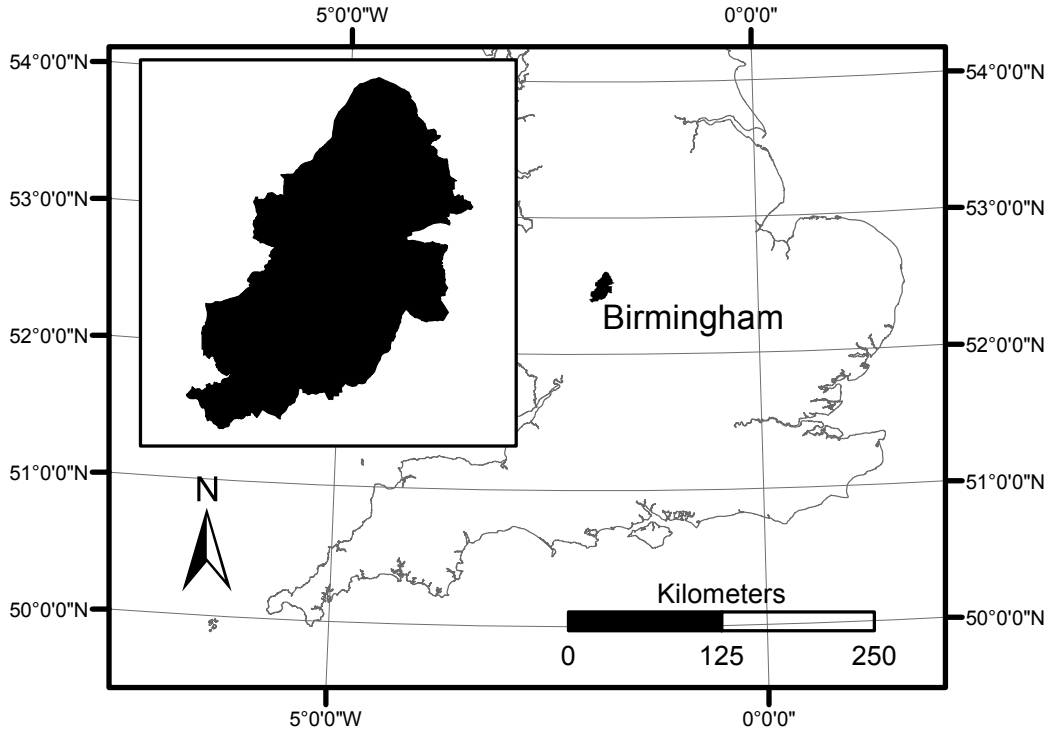

Figure 1.3: Location of Birmingham within the UK. Inset illustrates Birmingham city border.

Birmingham is situated at a reasonably high elevation (∼140 m) on a fairly flat plateau, and extent of the conurbation extends to over approximately 278 km^2. As this project focusses on urban heat it is worth noting that Birmingham did experience high temperatures in the 2003 heatwave, as detailed in the Local Climate Impacts Profile (LCLIP) report (Kotecha et al., 2008), and these temperatures are likely to increase in the future. However, it is recognised that heatwaves outside of the UK can be of a significantly larger magnitude (e.g. Australia and Russia, as in section 1.1) than Birmingham currently experiences. Additional details regarding the study area are detailed in each chapter as appropriate.

1.7 Aims and objectives

The overall aim of this thesis is to assess urban heat health risk spatially in order to create solid foundations for further high resolution urban climatology work focussing on climate change

adaptation. This is based upon incorporating the sUHI effect and high resolution social data for a specific case study area, and developing repeatable methodologies that allow the research to be easily duplicated elsewhere. Current climate change models do not take into account the urban influence on temperatures, and there is limited work exploring heat health risk spatially, especially at high resolutions. This work will develop new baseline datasets for Birmingham, including sUHI and spatial risk, and it is hoped that these can be used for future research, both in Birmingham and elsewhere.

The research is split into a number of specific objectives:

1. Measure the magnitude and spatial extent of the Birmingham sUHI using remotely sensed land surface temperature data to create a repeatable methodology that increases the spatial resolution of previous work.

2. Spatially identify sectors of the population vulnerable to heat health risk for combination with sUHI data to determine if vulnerable people are concentrated in areas with greater sUHI magnitude.

3. Determine how remotely sensed land surface temperature relates to ground measured air temperature in order to validate the use of satellite data for meteorological research including sUHI studies.

4. Consider how future urban temperatures may change when the sUHI is included in climate change projections. Explore the scale of changes and other influences on heat health risk.

1.8 Methodology and structure of thesis

This introductory chapter has outlined some key concepts for the thesis, including heat health risk (section 1.1), the UHI (section 1.2), climate change modelling and adaptation (section 1.3), thermal remote sensing (section 1.4) and spatial risk assessment (section 1.5), as well as detailing the study area (section 1.6) and the research aims and objectives (section 1.7).

The framework for the repeatable methodology described in this thesis is outlined in Figure 1.4. This introduction to the methodological framework is followed by detailed method-

ologies in each chapter. Following literature reviews on remotely sensing land surface temperature (section 2.1) relevant for chapter 3 and spatial risk assessment (section 2.2) relevant for chapter 4, there are three main parts to this thesis.

The first measures the sUHI of Birmingham using remotely sensed satellite data (chapter 3) from the MODIS satellite alongside ground measured meteorological data. This section considers the UHI under different atmospheric conditions at a 1 km resolution.

This sUHI data is then a key input layer into the second section; developing a spatial risk assessment methodology for heat health risk from a social perspective (chapter 4). This makes use of high resolution commercial consumer segmentation data alongside the satellite derived sUHI information.

The third section validates satellite measured temperatures against ground measured air temperature (section 5.1) and offers some climate change related observations (section 5.2). This section makes use of both custom sensors installed across Birmingham, and the UKCP09 climate projections. The thesis finishes (chapter 6) with some overall conclusions alongside ideas for further research.

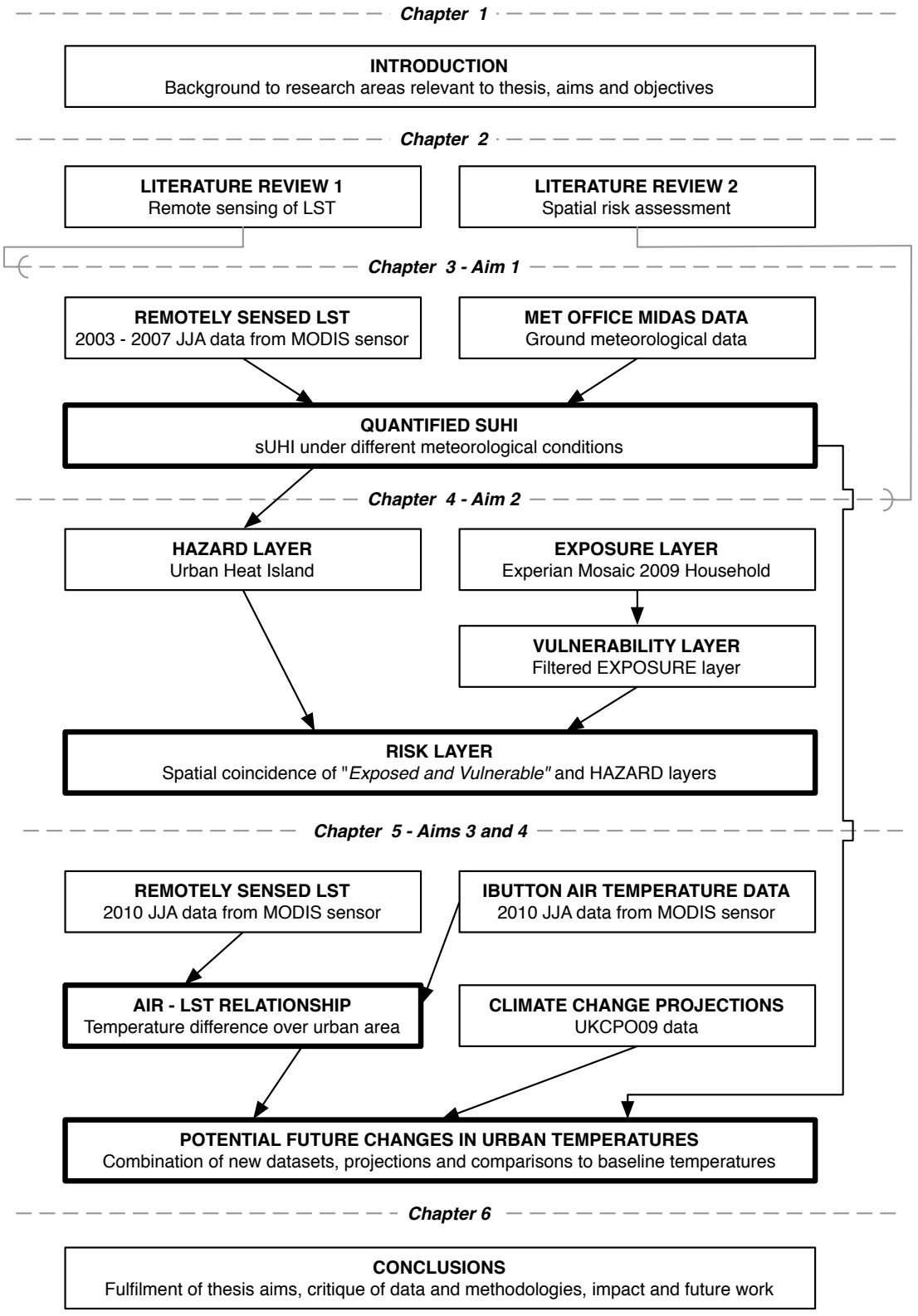

Figure 1.4: Methodological framework for thesis. Bold boxes signify major outputs that fulfill an aim (section 1.7).

Chapter 2

Literature reviews

This chapter offers two distinct literature reviews; the first related to satellite land surface temperature measurements and relevant for chapter 3, and the second detailing spatial risk assessment methods, relevant for chapter 4. The general background literature of interest to the project has been detailed in chapter 1, and individual chapters also offer short reviews of relevant new material.

2.1 Remote sensing of land surface temperature for meteorology

2.1.1 Introduction

A brief overview of remote sensing has been given in section 1.4, and this section reviews remote sensing as a tool for meteorology and climatology, with a particular focus on using remotely sensed data to calculate land surface temperature (LST). In this field, the urban heat island (UHI) is a well-documented phenomenon (see section 1.2 for a more detailed introduction) whereby the climate is unintentionally modified, causing urban areas to be warmer than surrounding rural areas. The UHI was first investigated through satellite techniques in the 1970's (Matson et al., 1978; Price, 1979), but the field is constantly advancing as new developments

in technology (increases in sensor resolution, satellite availability, global coverage, verification methods) and increased understanding of scientific processes come together. Exploration of the UHI effect via satellite techniques is the primary focus of this review and specific studies will be discussed under relevant sensor headings. Other uses, such as calculating cooling degree-days (Stathopoulou et al., 2006) or monitoring heatwaves (Dousset et al., 2010), the impact of urban development on runoff (Herb et al., 2008) and soil surface moisture (Petropoulos et al., 2009) have also been successfully demonstrated. Remotely sensed data can be a useful resource for the modelling community; helping to define input data such as shortwave net radiation for land surface models (Kim and Liang, 2010), or increasing the utility of surface energy balance (Senay et al., 2007) and other climate models (Jin et al., 2007). A number of reviews exist in this general area. For example, see Kidd et al. (2009) for an excellent general overview of satellite meteorology and climatology at the start of the 21st century. With respect to LST, other reviews have covered satellite remote sensing of the UHI (Gallo et al., 1995), the physics, methods and theoretical limitations of LST retrieval (Dash et al., 2001) and Thermal InfraRed (TIR) remote sensing (Prata, 1994; Voogt and Oke, 2003; Weng, 2009). This review differs from other articles as it details multiple sources of data (including timing and availability). It is written with a meteorologist in mind rather than a remote sensing expert and as such it purposefully does not detail software (either commercial or open source) or in depth techniques required to use the datasets described. More details regarding software and techniques used in this thesis are given in chapter 3.

2.1.2 Theory behind LST derivation

This section outlines the theory behind deriving LST from remote sensing techniques, and covers some fundamental details that need to be understood if data are to be used accurately and usefully for sensing the weather. If more detailed information is required, the physics behind deriving LST is explained in more detail in Dash et al. (2002). Several textbooks are also available (e.g. Lillesand et al. (2004)). Alternatively, the specification documents of individual sensors or platforms can be inspected (see links in Table 2.1).

A fundamental requirement for remote sensing is the detection of electromagnetic radiation (EMR) by sensors on a remote sensing platform. This is useful as different objects emit EMR in

Table 2.1: Current LST capable sensors and satellite information.

Sensor	Satellite	Spatial resolution	Orbital frequency	TIR spectral bands (μm)	Image acquisition (local time)	Data available since	Website
Landsat ETM+	Landsat 7	60 m [1]	16 days	(6) 10.4 - 12.5	∼10:00	1999 [2]	http://pubs.usgs.gov/fs/2010/3026/ http://landsat.gsfc.nasa.gov/
MODIS	Aqua	∼1 km	Twice Daily	(31) 10.78 - 11.28 (32) 11.77 - 12.27	∼13:30 ∼01:30	2002	http://modis.gsfc.nasa.gov/ https://lpdaac.usgs.gov/lpdaac
MODIS	Terra	∼1 km	Twice Daily	(31) 10.78 - 11.28 (32) 11.77 - 12.27	∼10:30 ∼22:30	2000	/products/modis_overview
ASTER	Terra	90 m	Twice Daily	(10) 8.125 - 8.475 (11) 8.475 - 8.825 (12) 8.925 - 9.275 (13) 10.25 - 10.95 (14) 10.95 - 11.65	Request only	1999	http://asterweb.jpl.nasa.gov/
AVHRR	Multiple NOAA	∼1.1 km	Twice Daily	(4) 10.3 - 11.3 (5) 11.5 - 12.5 [4]	[3]	1979	http://noaasis.noaa.gov/NOAASIS /ml/avhrr.html
AVHRR	MetOP	∼1.1 km	29 Days	(4) 10.3 - 11.3 (5) 11.5 - 12.5	∼09:30	2006	http://www.esa.int/esaLP /ESA7USVTYWC_LPmetop_0.html
AATSR	Envisat	∼1 km	35 Days	11 12	∼10:00	2004 [5]	http://envisat.esa.int/instruments/aatsr/
SEVIRI	Meteosat-8	∼3 km	Geostationary	10.8 12	Every 15 min	2005	http://landsaf.meteo.pt/
GOES Imager	GOES Network [6]	∼4 km	Geostationary	(4) 10.2 - 11.2 (5) 11.5 - 12.5	Every 3 h (full disc)	1974	http://goespoes.gsfc.nasa.gov/goes/

[1] Collected at 60 m but resampled to 30 m.
[2] Landsat 7 ETM+ data from 1999, TM data from Landsat 4 and 5 available since 1982 at 120 m spatial resolution.
[3] AVHRR is carried on >10 NOAA satellites; see http://ivm.cr.usgs.gov/tables.php for full orbital details of each.
[4] AVHRR/3 Characteristics.
[5] LST product currently available since 2004. Planned application to historical data will result in data from 1991 onwards.
[6] Status of network available: http://www.oso.noaa.gov/goesstatus/

different ways, so the spectral response can be analysed. Within the EMR spectrum (Figure 2.1), the wavelength of most use for LST measurements is the thermal infrared (TIR), between 8 - 15 μm. However, one exception to this is passive microwave which has been used for LST measurement in China (Chen et al., 2010), USA (McFarland et al., 1990), Canadian sub-arctic (Fily, 2003) and indeed globally (Peterson et al., 2000; Williams et al., 2000). Passive microwave measurements tend to be limited in the sense that they typically offer a very coarse resolution (in the tens of km). For this reason, this review will focus on TIR sensors, which are more commonly used and offer higher resolution data.

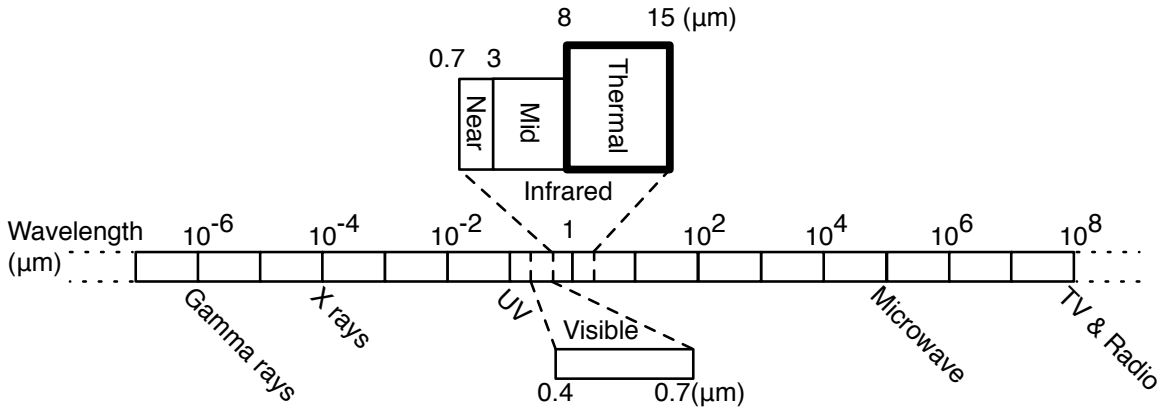

Figure 2.1: The electromagnetic spectrum arranged by wavelength. Thermal infrared highlighted in bold. Adapted from Lillesand et al. (2004).

Satellite TIR sensors receive EMR which can be quantified in the form of measurements of Top Of Atmosphere (TOA) radiances. This includes upwelling radiance emitted from the ground, upwelling radiance from the atmosphere, and the downwelling radiance emitted by the atmosphere and reflected from the ground. During the day there is both emission and reflection of EMR, but during the night sensed EMR is restricted to only emission. The inverse of Planck's law (the energy emitted by a surface is directly related to its temperature) is used to derive blackbody/brightness temperatures from TOA radiances. TOA radiances are then converted to LST by correcting for three main effects; atmospheric attenuation, angular effects and spectral emissivity values at the surface. Atmospheric attenuation (absorption, reflection or refraction and scattering) will alter the EMR as it passes through the atmosphere, resulting in differences between TOA radiances and LST. Within TIR wavelengths, most attenuation is due to water vapour and aerosols. Angular effects are a product of the variety in viewing angles

resulting in wavelength shifting which must be compensated for when estimating radiances (Dash et al., 2002). Spectral emissivity refers to the relative ability of a surface to emit radiation and can be highly variable due to the heterogeneity of land, and is influenced by surface cover, vegetation cover and soil moisture. Quantification of emissivity is achieved by considering the ratio of energy emitted by a surface with respect to the energy emitted by a blackbody at the same temperature. However, calculations are complicated because natural surfaces do not behave like a black body and thus need correction using typical emissivity values (Table 2.2). These corrections are done through complex algorithms, alongside extensive validation and verification, resulting in a final product that can be used by a meteorologist.

Table 2.2: Typical emissivity values of common materials (Lillesand et al., 2004).

Material	Typical average emissivity (over 8-14 μm)
Wet Snow	0.98 - 0.99
Healthy Green Vegetation	0.96 - 0.99
Wet Soil	0.95 - 0.98
Brick	0.93 - 0.94
Wood	0.93 - 0.94
Dry Vegetation	0.88 - 0.94
Dry Snow	0.85 - 0.90
Glass	0.77 - 0.81
Aluminium Foil	0.03 - 0.07

Orbital satellite remote sensing methods are limited by image acquisition time which is set by the orbital characteristics of the relevant satellite and means that readings at specific times cannot be obtained or requested unless they match the orbit. Geostationary satellites, which stay in the same position relative to the earth, offer a greatly increased temporal resolution at the expense of reducing spatial resolution and coverage area. Examples of sensors on geostationary platforms covered in this review include GOES and SEVERI sensors. However, not all images may be accurate, as high zenith angles result in a lengthened atmospheric path that can result in less accurate images (Streutker, 2003). Many images come with additional metadata (such as quality control Scientific Data Sets) that can help recognise this problem. It is also worth noting that not all images are readily available, despite orbital paths. Archives may be corrupt, or the satellite may have been offline or maneuvering in such a way that meant observations were not collected. Hence, if a study has a specific temporal requirement it can therefore be useful to check multiple potential sources. Choice of image timing is also important, for example

Rigo et al. (2006) found that MODIS LST was more accurate at night compared to the daytime, and the AATSR target accuracy is 2.5K for daytime, increasing to 1K at night time (Noyes et al., 2007). Similarly, Hartz et al. (2006) found night time ASTER images could better observe neighbourhood climatic conditions. Limitations of resolution are being investigated, and algorithms have been developed to sharpen thermal images to increase the resolution (Dominguez et al., 2011). A serious limitation of TIR satellite remote sensing techniques is the requirement for clear skies in order to derive accurate readings; hence cloud cover can be a serious problem. Dependent on the research requirements, composite images from multiple passes can often be created in order to construct an image without cloud cover limitations (Neteler, 2010), or algorithms can be used to estimate pixels (Jin and Dickinson, 2000). Alternatively, modelling or passive microwave remote sensing could be used (Wan, 2008) if increased coverage is required. An effect of this is that seasonal differences can influence image availability (increased cloud cover) and accuracy (increased rainfall causing wet surfaces leading to unreliable LST measurements), for example winter study periods can be more difficult (Rajasekar and Weng, 2008).

Two main algorithmic approaches are used for conversions, the radiative transfer equation (RTE) and the generalised split window technique (GSW). These techniques are explained in detail elsewhere (Dash et al., 2001; Weng, 2009) and as such are not covered in detail here. The GSW technique in the 11 and 12 μm channels is used by AATSR, AVHRR, MODIS and SEVIRI products, and in simple terms uses adjacent channels with different properties to calculate atmospheric attenuation. Nine different split window algorithms have been evaluated (Yu et al., 2008), concluding that accuracies are dependent on having reliable *a priori* emissivity data. This is one difficulty with remotely sensed imagery covering large areas; assumptions of average emissivity across a heterogeneous area (discussed in section 5.1). It is important to note that single channel products such as Landsat TM / ETM+ cannot use a GSW technique, and are therefore generally considered less accurate as they will not be correcting for atmospheric attenuation at the time of overpass, although under certain conditions single window methods can provide a reasonable estimate of LST (Platt and Prata, 1993).

The differences between satellite derived LST and ground measured air temperature is one area that is still not fully understood, but a brief discussion is included in section 1.2 and this is the subject of work in section 5.1. Reviews (Arnfield, 2003; Weng, 2009) cite research that de-

tails both similarities between air and LST (Nichol, 1994) and differences (Weller and Thornes, 2001). Related work includes comparing LST and air temperatures over large areas and multiple ecosystems in Africa (Vancutsem et al., 2010), and using MODIS LST data to estimate air temperature in China (Yan et al., 2009).

2.1.3 Satellites and sensors

There are a number of different satellite remote sensing platforms with multiple sensors in the TIR spectrum, giving the modern meteorologist a number of potentially useful datasets to measure LST. Datasets are available for different time periods, at different resolutions, with varying accuracy, therefore this section outlines the various datasets available, ordered by launch date (Figure 2.2). Currently operating satellites are also summarised in Table 2.1. Some comparisons between datasets exist, for example between MODIS and ASTER (Pu et al., 2006) and these are discussed as appropriate. This review will focus on satellite based sensors, as they offer global coverage and good availability. Airborne sensors (e.g. ATLAS (Gluch et al., 2006) or AHS (Sobrino et al., 2006)) can offer greater spatial and thermal resolution, but generally airborne data are only available for small areas and at significant cost to the end user. Similarly this review does not detail private or commercial satellites, as these are generally not as accessible for researchers.

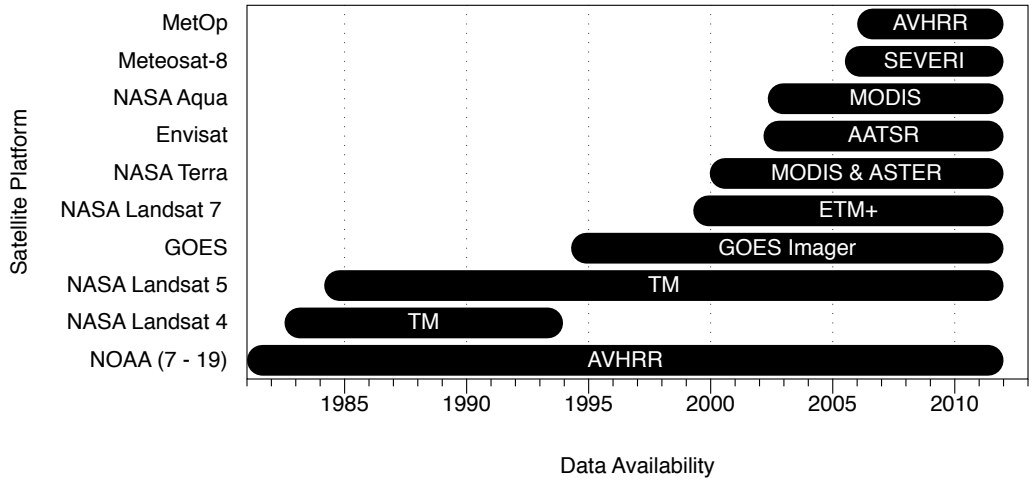

Figure 2.2: Timeline of satellite launches and associated sensor data availability. Data availability to 2012 indicates ongoing availability.

AVHRR

The Advanced Very High Resolution Radiometer (AVHRR) sensor has been on a number of National Oceanic and Atmospheric Administration (NOAA) satellites and is currently operational on NOAA-15,-16,-17,-18,-19, offering at least daily coverage, but restricted to daytime images. The spatial resolution is $\sim$1.1 km and LST is derived from TIR channels 4 (10.3 - 11.3 μm) and 5 (11.5 - 12.5 μm), with a global dataset provided through the sun-synchronous orbit. Data are available from the NOAA Comprehensive Large Array Stewardship System (NOAA, 2012) and the High Resolution Picture Transmission software (Taylor, 2012) can be useful for analysis. MetOP, the EUMETSAT satellite platform, also has an AVHRR sensor with an orbital repeat time of 29 days. Comparative studies of AVHRR algorithms exist which offer more details (Ottle and Vidal-Madjar, 1992; Vázquez et al., 1997).

A strength of the AVHRR sensor is that there is a relatively long historical record of data, and correspondingly a significant body of research that has utilised the sensor for many different uses. A notable use of AVHRR data has been in the creation of an 18 year (1981 - 1998) diurnal LST dataset (Jin, 2004) at 8 km resolution globally for snow free land surfaces. It gives monthly diurnally-averaged, minimum and maximum skin temperatures. This long term record is not possible with most other sensors as the historical data are not available, as the satellites and sensors were not developed or in space yet. Matson et al. (1978) used VHRR (the forerunner to AVHRR) data for sUHI analysis of the US, detecting over 50, and LST investigations in Northern Italy used AVHRR (Ulivieri and Cannizzaro, 1985). Other studies using AVHRR include Gallo et al. (1993) who investigated the surface temperature and vegetation index for 37 cities in the United States, particularly noting the consistent nature of the data when studying the sUHI. Lee (1993) used AVHRR to study the sUHI in South Korea and more recently AVHRR data has been used to study the growth of the sUHI in Houston, Texas, USA between 1985 - 1987 and 1999 - 2001, with the results showing a growth in magnitude of 35%, and a growth in area between 38% and 88% depending on method (Streutker, 2003). Stathopoulou and Cartalis (2009) used AVHRR data from Greece and applied downscaling techniques to increase the output resolution (1 km $>$ 120 m), helping to address the inevitable balancing between spatial and temporal resolution. A significant weakness of AVHRR include the lack of availability of night time images.

Landsat

The Landsat series of satellites are probably the most well known, with the longest record of earth observations from space. The Thematic Mapper (TM) on Landsat 4 and 5 had a visible resolution of 30 m and a TIR resolution of 120 m (band 6, 10.4 - 12.5 μm). Landsat 4 and 5 are no longer continually collecting data, but Landsat 7's Enhanced Thematic Mapper (ETM+) collects thermal data at a 60m resolution (also band 6, 10.4 - 12.5 μm). Landsat 7 has a near polar sun-synchronous orbit with a revisit time of 16 days, meaning that a given point on earth should be imaged at approximately the same local time ($\sim$10:00h) every 16 days. The ETM+ offers some of the highest resolution thermal resolution measurements from space, and data are available freely from the U.S. Geological Survey (USGS) online (USGS, 2012a,b), however data from 2003 onwards is impaired due to failure of the scan line corrector. This results in only $\sim$80% of each scene being captured. The Landsat data archive has only been freely available since 2008, therefore the number of studies has increased in recent years. A disadvantage of data from Landsat is that it is not collected at night, and the thermal calibration is limited. More details on the Landsat project are available (Headley, 2010), and the Landsat Data Continuity Mission (LCDM) aims to continue the long term Landsat record.

In the USA, Aniello et al. (1995) used Landsat TM data to help map micro sUHI's (hot spots within a city) in Dallas, Texas, USA by combining both the thermal band (6) and extracted tree cover data from an unsupervised classification. One satellite image was used and the results showed that micro sUHI's were highest in the centre, and were generally resulting from a lack of tree cover. Weng et al. (2004) use Landsat ETM+ to link LST to Normalized Difference Vegetation Index (NDVI) in Indianapolis, USA which resulted in results linking LST to different land cover types and Xian and Crane (2006) use both Landsat TM and ETM+ to explore the thermal characteristics of urban areas in Tampa Bay and Florida, USA finding that land use and land cover fundamentally affect the thermal results. Weng (2003) used three Landsat TM images (from 1989, 1996 and 1997) to study the sUHI in Guangzhou, China alongside fractal analysis with the result that two significant heat islands existed in the city. Further work has been done in China (Chen et al., 2006; Li et al., 2009), including combining Landsat ETM+ with computational fluid dynamic (CFD) modelling in Wuhan, China (Li and Yu, 2008). The combination of remote sensing and modelling was found to be mutually complementary. In Europe,

Stathopoulou and Cartalis (2007) uses Landsat ETM+ data to explore daytime sUHI across the major cities in Greece using a method that incorporates the CORINE land cover classification to superimpose land cover based emissivity values to create a mean surface temperature by land cover.

Resampling (generally using the nearest neighbour algorithm) the thermal band to lower resolutions (e.g. 30 m to match the visible spectrum) is a common technique (Weng, 2003; Weng et al., 2004; Xian and Crane, 2006; Cao et al., 2010) in order to simplify analysis. Landsat has a great strength in terms of spatial resolution, however its 16 day revisit time and lack of night time image aquisition is limiting at the temporal scale. Stathopoulou and Cartalis (2007) discusses how future studies may focus on a time series of images as the UHI strongly depends on synoptic weather conditions. The spatial resolution of 60m on Landsat ETM+ does allow individual hotspots to be picked out (Aniello et al., 1995; Stathopoulou and Cartalis, 2007) and work is still using the ETM+ sensor (Boudhar et al., 2011).

GOES

The Geostationary Operational Environmental Satellite (GOES) system is a network of geostationary satellites carrying the GOES Imager, a multispectral instrument offering two channels in the TIR (10.2 – 11.2 and 11.5 – 12.5 μm) with an at nadir resolution of $\sim$4 km. GOES related studies discuss algorithm development for dual thermal channel sensors (e.g. on GOES-8 and -10) (Sun, 2003) and single thermal channel sensors (e.g. GOES M-Q) (Sun et al., 2004). An evaluation of GOES LST retrievals over the USA is given by Pinker et al. (2009). An illustration of an advantage of geostationary satellites is shown by Sun et al. (2006), which measures the diurnal temperature range across the USA, possible due to the high temporal availability of data. An interesting study links MODIS data as a calibration source for GOES data, resulting in a 1 km LST dataset at half-hourly temporal resolution and a measured accuracy better than 2°C (Inamdar et al., 2008).

MODIS

The MODerate resolution Imaging Spectroradiometer (MODIS) sensor is carried on both NASA's Aqua and Terra satellites that have near polar orbits resulting in two images per satellite per day. Image acquisition on Aqua is $\sim$13:30h and 01:30h and Terra is $\sim$10:30h and 22:30h local

time. This is a high temporal resolution, and the spatial resolution is $\sim$1 km. Data are available from the USGS Land Processes Distributed Active Archive Center (NASA Land Processes Distributed Active Archive Center, 2011a) and useful LST products include MYD11A1 (Aqua) and MOD11A1 (Terra) which are the daily LST and emissivity at 1 km. Other products include 8 day 1 km data (M*D11A2) and others. These LST products primarily use TIR bands 31 (10.78 - 11.28 μm) and 32 (11.77 - 12.27 μm) combined with split window algorithms (Wan and Dozier, 1996) which multiple studies have tested (Wan, 2002; Wan et al., 2004; Coll et al., 2005; Wan, 2008) with results suggesting accuracies greater than 1 K over homogenous surfaces. A useful tool for processing data in ESRI ArcMap is the Marine Geospace Ecology Tools (MGET) plugin (Roberts et al., 2010), or the standalone MODIS Reprojection Tool (NASA Land Processes Distributed Active Archive Center, 2011b).

There are a number of studies that use MODIS LST data within the urban climatology fields. Within Europe, Pongrácz et al. (2010) explored the sUHI of nine central European cities and find that the most intense sUHI occurs during daytime in the summer period. Work has looked at the ten most populated cities of Hungary (Pongrácz et al., 2006). Studies in Bucharest used MODIS to calculate the sUHI in summer months (Cheval and Dumitrescu, 2009) and under heatwave conditions (Cheval et al., 2009). Globally, Hung et al. (2006) quantified the sUHI in eight Asian mega-cities using MODIS data, Jin et al. (2005) analysed various cities including Beijing and New York and Imhoff et al. (2010) used MODIS data averaged over three years to calculate sUHI's across the United States.

MODIS data has been used extensively outside of the UHI field. Other surface measurements include observing the impacts of agriculture on rural surface temperatures in North America (Ge, 2010) and measuring water temperature and heat flux over a hydroelectric reservoir in Brazil (Alcântara et al., 2010). Atmospheric studies estimate aerosol optical depth (an important influence on the radiation budget) in America, Canada, China and Africa (Liang et al., 2006), and help detect clear sky, low level temperature inversions in the polar regions (Liu and Key, 2003). In cooler areas, MODIS has been used for frost risk assessment in Bolivia (Pouteau et al., 2010) and permafrost monitoring in Siberia (Langer et al., 2010). Outside of the meteorology domain, MODIS data has been used to help epidemiological studies of tick borne diseases (Neteler, 2005) and more. A strength of the MODIS sensor is the compromise between regular image acquisition and reasonable spatial resolution, in comparison to other sensors that

offer higher spatial resolution but lower temporal resolution (e.g. Landsat), or higher temporal resolution but lower spatial resolution (e.g. SEVIRI).

ASTER

The Advanced Spaceborne Thermal Emission and Reflection Radiometer (ASTER) operates at a very high resolution (90 m), and calculates surface temperature (AST08 product) using the Temperature Emissivity Separation (TES) algorithm (Gillespie and Rokugawa, 1998). ASTER has five TIR bands, and full technical details are available in Yamaguchi et al. (1998). ASTER is based on the NASA Terra satellite platform, but is fundamentally different from other sensors discussed in this review in that it is request only, with fees payable for data. Hence, data are only acquired if a specific request has been detailed and paid for, and therefore the historical data are limited and costly. This is a significant restriction, given the difficulties of ensuring suitable atmospheric and weather conditions for a specific future request, and obviously limits historical studies. However the 90 m resolution is high, only comparable with Landsat when considering the spatial scale, and ASTER has the potential for better temporal coverage, given the Terra satellite has a twice daily pass.

ASTER images have been used for a number of studies. They were used to compare LST to urban biophysical descriptors (such as impervious surface, green vegetation and soil) in Indianapolis, USA through linear spectral mixture analysis and multiple regression models, with the results that impervious surfaces and hot objects were positively correlated with LST whereas vegetation and cold objects were negatively correlated (Lu and Weng, 2006). An ASTER image was used alongside a 148 km vehicle traverse of Hong Kong in order to compare air and remotely sensed temperatures (Nichol et al., 2009) and ASTER (for thermal use) and IKONOS data (for high resolution (4 m) visible and near infrared use) were combined to explore the cooling effect of urban parks in Nagoya, Japan (Cao et al., 2010).

There are frequent comparisons between ASTER and MODIS data, for example in verification. This is because ASTER and MODIS are complementary in scale ($\sim$1 km and 90 m) and are based on the same satellite platform, so image acquisition occurs at the same time, height and location which aids comparison. Land surface emissivity and radiometric temperatures have been compared with good agreement over desert in the USA and savannah in Africa (Jacob et al., 2004). Direct comparisons between three correction approaches over the Loess Plateau

in China have reduced the discrepancies between ASTER and MODIS data (Liu et al., 2007). Longterm ground based longwave radiation between 2000 and 2007 have been compared to ASTER and MODIS images for both LST and emissivity (Wang and Liang, 2009).

AATSR

The Advanced Along Track Scanning Radiometer (AATSR) is carried onboard the European Space Agency (ESA) ENVironment SATellite (ENVISAT) which was launched in 2002. This was the third instrument in a series (ATSR-1 and ATSR-2) which started with the Along Track Scanning Radiometer (ATSR-1) in 1991. The primary objective of all missions to date has been for sea surface temperature (SST) collection. ENVISAT is in a sun-synchronous polar orbit with a 35 day repeat cycle, which means data availability is lower than others. The LST product is relatively new, being operational from March 2004 for data from the AATSR, and the TIR bands 11 and 12 μm are used to provide LST at $\sim$1 km resolution. However the algorithms developed will be applied to historical data from the previous sensors (ATSR-1 and ATSR-2) resulting in an LST dataset starting in 1991; however the timeline for completion is unknown. The AATSR literature is primarily concerned with the theoretical science for algorithm development (Prata, 2002), evaluation of algorithms (Sòria and Sobrino, 2007) or validation (Coll et al., 2005; Noyes et al., 2007; Coll et al., 2009). AATSR has been used for monthly LST mapping over Europe (Joan and Cesar, 2009), and more broadly for drought prediction (Djepa, 2011), estimating evapotranspiration (Liu et al., 2010) and detection of snow covered areas (Istomina et al., 2010). In the future more studies utilising AATSR can be anticipated, although the long orbital repeat cycle means other sensors may be better suited.

SEVIRI

The Spinning Enhanced Visible and Infrared Imager (SEVIRI) is an instrument on Meteosat-8 that uses a generalized split window algorithm (detailed in Sobrino (2004)) to calculate LST from two thermal channels (10.8 and 12 μm). The satellite application facility on land surface analysis (LSA SAF) is responsible for generation and archiving of the data. Meteosat Second Generation (MSG) is a geostationary satellite so therefore has different characteristics to other orbital satellites this review has examined. It has a very high temporal resolution of 15 minutes (theoretical maximum of 96 images/day) but the area covered is constant and not global. All

the land pixels within the Meteosat disc that are below a 60 degree viewing angle are processed for LST measurements, to avoid excessive atmospheric attenuation and reduced accuracy at higher angles. This results in a spatial pixel resolution of 3 km at nadir (increasing to $\sim$6 km at $> 60^{\circ}$). Schmetz et al. (2002) offer a useful introduction to the MSG instrument. The high temporal resolution has a number of advantages, namely it has a much greater chance of getting cloud free images of a study area due to the number that are taken, and it enables the potential to study the diurnal LST pattern. Meteosat data have been available since July 2005 for the complete Meteosat disc (February 2005 for Europe).

Trigo et al. (2008) compare Meteosat LST with MODIS LST over three locations and find that Meteosat temperatures are warmer than MODIS, particularly in the daytime. A comparison between MODIS and Meteosat LST has also been carried out focussing on the heatwave in Athens, Greece during July 2007 (Retalis et al., 2010) and the results show significant correlation both between each other and between air temperature measurements, which agrees with other air temperature and Meteosat LST comparisons that also perform well (Nieto et al., 2011).

Due to the high temporal resolution, it is theoretically possible to study the diurnal sUHI. In practice this is limited by cloud cover, however recent work outlines a methodology for reconstructing cloud contaminated pixels (Lu et al., 2011) that allows the diurnal variation to be studied in detail. In other fields this high temporal resolution is useful, for example for hazard modelling such as near real time forest fire monitoring (Umamaheshwaran et al., 2007).

2.1.4 Future developments

The future for remote sensing LST retrievals is focussed on two main areas; that of improved or replacement physical sensors and platforms, and that of improvements in data manipulation of current, historical and future data. In terms of data manipulation there is potential for improved algorithms, for example improved cloud masking or emissivity calculations. These will rely on ongoing validation and testing across a variety of landscapes and sensors, and could improve existing as well as future data.

Regarding the near future of sensors and satellite platforms, a number of relevant projects are in development. The Landsat Data Continuity Mission (LDCM) intends to continue the long Landsat data series (USGS, 2007), and is planned to be launched in December 2012 with 120

m resolution in two thermal channels. The European Space Agency (ESA) Sentinel-3 satellites are planned for launch from 2013, offering a Sea and Land Surface Temperature Radiometer (SLSTR) with a 1 km resolution in the thermal channels and a daily revisit time. The geostationary GOES-R satellite is due in 2015, with a 2 km resolution in the thermal channels from a new Advanced Baseline Imager (ABI) (Yunyue et al., 2009). The National Polar-orbiting Operational Environmental Satellite System (NPOESS) is due to launch in 2016, designed to replace NASA's Aqua, Terra and Aura satellites and offering the Visible and Infrared Imagery Radiometer Suite (VIIRS) sensor for LST. An interesting sensor in development is the Hyperspectral InfraRed Imager (HyspIRI) from NASA that is hopefully planned for launch in 2015, offering a $\sim$60 m resolution in the thermal bands and a repeat cycle of 5 or 16 days. This is still in a planning phase and more details are available (NASA / JPL, 2012) but this offers the next generation of space based thermal sensors. Coupled with these large "traditional" missions, in the future there is likely to be an increase in "small satellites" (Sandau et al., 2010) that enable relatively quick and inexpensive missions, which could for example help to observe dynamic weather systems. Future increases in spatial resolution of sensors combined with the high temporal resolution that geostationary platforms can provide is likely to offer the most useful data, however this offers considerable scientific challenges.

2.1.5 Conclusions

This review has given an overview of remote sensing techniques, sensors and research of interest to the meteorological and climatological community for LST detection and monitoring. It is clear that the focus of research has been surrounding the UHI phenomenon, but a significant research gap still exists which is the quantification of the relationship between measured air temperatures and remotely sensed LST data. Indeed, as Nichol et al. (2009) state this "remains the greatest unknown in remotely sensed studies of heat islands", and this statement is still applicable to any study utilising LST data as a proxy for air temperature. The importance of being able to relate LST to air temperature is especially important when such datasets are being used to inform policy decisions or communicate outside of the scientific community, for example with Birmingham City Council (section 1.3). This relationship is explored in section 5.1.

A significant advantage of remote sensing data and techniques is their truly global coverage

and scope, but despite this there is a low number of studies focussing on many geographical areas, and a limited number that integrate additional ground data. Remote sensing techniques offer access to data that would otherwise be unobtainable, therefore the requirement for defensible verification and accuracy measurements is considerable. Alongside this, the increasing need for data and intensifying analysis will necessitate using remote sensing data alongside other datasets from numerous sources, resulting in an integral role for remote sensing techniques within the meteorological and climatological communities.

2.1.6 Summary

This review clearly illustrates the advantages (e.g. global coverage, regular data acquisition, no need for ground sensors) to using remotely sensed data to measure LST, and the potential such data has for sUHI measurements. A key element of this thesis is measuring the sUHI for Birmingham, which is possible using remotely sensed data due to the global coverage. From the sensors analysed, MODIS offer a good balance of regular timing and reasonable resolution alongside free and readily accessible data, making it ideal for this thesis. Using such data to measure Birmingham's sUHI is undertaken in chapter 3.

2.2 Spatial risk assessment for climate change adaptation

2.2.1 Introduction

This chapter gives a brief overview of the spatial risk assessment field, building on section 1.5 and focussing on techniques and methods that can be utilised later in the thesis to explore heat health risk spatially (chapter 4). After some discussion around risk and associated terminology and a risk matrix example this review focusses on spatial risk assessment. Crichtons's risk triangle is explained, followed by notes on spatial scale and standardisation and weighting procedures. Next a number of studies are briefly discussed. It should be noted that the techniques mentioned in this chapter are not exhaustive; there are numerous other theories and methods that can be relevant to spatial risk assessment. For example Suddle and Ale (2005) develop a methodology that adds a third parameter of height when exploring risk of buildings around roads and railways, but such specific techniques will not be discussed in detail.

Greiving et al. (2006) offers a useful general introduction to some previous spatial risk assessment concepts, and is critical of existing risk assessment methodologies such as the "Natural

Hazard Index for Megacities" (Munich Re, 2003) used by the re-insurance company Munich Re, or the "Total Place Vulnerability Index" (Cutter et al., 1997) developed in the Hazard Research Lab at the University of South Carolina. These two methods help indicate the variety in the risk assessment field, as they focus on economic losses and social vulnerability respectively. An alternative is suggested, named the "Integrated Risk Assessment of Multi-Hazards", designed for international risk assessment at a regional scale, aggregating a number of risks to arrive at a "total risk potential". The lack of data on hazards is mentioned as a problem, perhaps due to the wide ranging methodology encompassing a number of hazards. Concentrating on a single hazard would offer better results.

In relation to quantitative risk assessment, Apostolakis (2004) emphasises the importance of risk informed decision making, as opposed to risk based decision making - highlighting the need for critique and review of the evidence base resulting from risk assessment work.

2.2.2 Quantitative risk assessment theory

The quantification of risk and its definition is large, and Kaplan and Garrick (1981) offers a useful discussion that is still relevant today. The word originates in the mid 17th century, from the French "risque" and Italian "risco" (meaning danger) and the Oxford English Dictionary (Soanes and Stevenson, 2005) today defines risk as:

> noun; a situation involving exposure to danger.
> verb; expose (someone or something valued) to danger, harm, or loss.

There are numerous related terms including damage, probability, uncertainty, hazard, vulnerability, exposure, safeguards and numerous others. Risk encompasses a great variety of fields; safety risk, economic risk, investment risk, political risk, military risk, business risk, health risk and many more. The general nature of risk is illustrated through the International Organisation for Standardization's "Risk management - performance and guidelines" (ISO 31000:2009 (ISO, 2009)) which notes that the guidelines are not specific to any industry or sector.

Despite there being numerous applications of risk assessment, there are relatively few key theories that underpin the concept of risk. The key theories include the probability (or likelihood) that a risk will occur, and the impact (or consequence) if it does. These are commonly

tabulated, probability against impact, resulting in a risk matrix table with details e.g. low to high risk for a given set of scenarios.

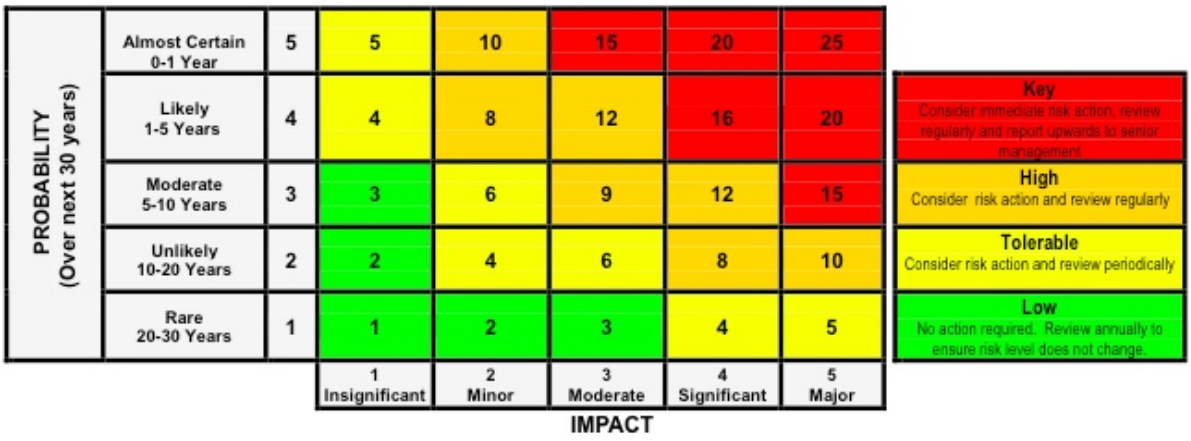

Figure 2.3: Warwickshire LAA risk matrix (Warwickshire LAA, 2008).

An example risk matrix (Figure 2.3) shows the climate change and environmental risk matrix undertaken by the Warwickshire local authority (Warwickshire LAA, 2008), under UKCIP risk assessment guidance (UKCIP, 2009b). The probability of an event is split into five time periods over the next 30 years, and the impact is split into five periods (insignificant to major). The matrix then illustrates, for a given scenario, if the risk is low, tolerable, or high. This matrix is the same for four streams of separate risk areas, but is used here to illustrate theory. A "major environmental threat" (defined as "irreversible environmental degradation with severe legal consequences") would be level 5, but the risk depends on the probability of timing. If this was likely to occur in the next 0 - 10 years (red boxes), then Warwickshire would "Consider immediate risk action, review regularly and report upwards to senior management". In comparison, if this was a rare event, expected to occur within a 20 - 30 year timeframe (yellow box), then it would be a tolerable risk, and Warwickshire would "Consider risk action and review periodically". This helps illustrate how an identical event can be managed differently depending on its probability.

Traditional risk assessment such as this is important, but many hazards are only risks in certain areas. Therefore when doing city–wide assessment a spatial element is vital to understand where risks are and what the impacts would be in specific areas. For example, a flood has different consequences if it occurs in an uninhabited flood plain or a built up urban area. Adding

spatial information to help facilitate understanding of risk is becoming increasingly common, for example Beck and Kropp (2011) explain the idea of "risk cartography" for exploring food risk, helping connect the "unknown unknowns" in relation to production, usage and disposal of food. The perception of risk is also important, and Hess et al. (2011) evaluate how a persons numeracy level relates to their understanding of risk. Unsurprisingly, this study suggests that people with low numeracy skills have more difficulty understanding quantitative risk work, which is important to remember when disseminating research outputs to the wider community.

Crichtons risk triangle

A useful conceptualization that helps to explain risk assessment is that of Crichton's risk triangle, which states that risk is a function of hazard, exposure and vulnerability (Figure 2.4), and all must be coincident for a risk to exist. Crichton's risk triangle and the underlying theory is used for various risk assessments, including natural hazards disaster management and the insurance industry (Crichton, 1999).

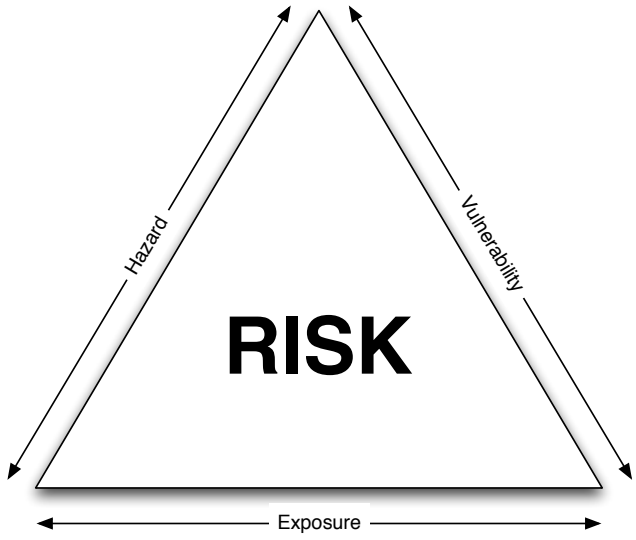

Figure 2.4: Crichton's risk triangle (from Crichton (1999); Gwilliam et al. (2006)).

A hazard is something that may cause risk, for example flooding or sea level rise. Details about each hazard will have various information, for example magnitude and spatial extents (e.g. river flood plain) for certain probability events (e.g. 100 year storm). These can be his-

torical, measured or predicted. Exposure relates what is exposed to the hazard (e.g. what is within the flood plain) of interest (e.g. buildings). Dependent on the industry the exposure information would differ, but for example an insurance company could be interested in how many buildings they insure in the hazard area (the exposed). The third side of the triangle is vulnerability, which is essentially attributes about the exposed items. In the flood plain example this could relate to the flood resistance of individual buildings. A vulnerability table will typically be developed in order to quantify vulnerability. A central theme of the risk triangle is that all three items must be coincident for risk to occur. Although often used in the insurance industry, the risk triangle model is useful for spatial risk assessment as well. The advantages of splitting the definition are that it makes the process clear and transparent and simplifies analysis within a layering system in a GIS, enabling the spatial analysis of risk. A more detailed explanation of Crichton's risk triangle and real world examples of use are available, relating to natural disasters (Crichton, 1999), flooding (Gwilliam et al., 2006; Fedeski and Gwilliam, 2007), and heat risk (Lindley et al., 2006, 2007).

Spatial scale

In spatial risk assessment, the geographical area of study is especially important. The scale is directly relevant to the usability of the results, and is often determined by the scale of available input data. Many studies are at a reasonably large scale, e.g. national (Reid et al., 2009) or state (Vescovi et al., 2005), often due to limitations of data and ease of aggregation at larger scales. When multiple variables are assessed, it is helpful if they share a common spatial hierarchy.

The modifiable areal unit problem (MAUP), initially detailed by Openshaw (1984), discussed recently by Cockings and Martin (2005) and Parenteau and Sawada (2011) is a form of statistical bias that can arise due to summarising point values to areas. The bias is influenced by the choice of areas, and the MAUP should be thought about when designing spatial methodologies. In the UK, this means that Lower Super Output Areas (LSOA) (Office for National Statistics, 2011) may be better aggregation area than wards, census districts or postcodes (Cockings and Martin, 2005). LSOA's are a geographical hierarchy designed for small area statistics, and although they do not have consistent physical size, they are not subject to boundary changes in the future, unlike other areas such as wards or postcodes. This makes them ideal for ongoing studies. A LSOA has a minimum population of 1,000 and an average population of 1,500,

allowing data to be distributed easily without identifying individuals.

Standardisation and weighting

When comparing and combining different variables, it is of benefit if they are standardised to the same scale. Standardisation helps quantify variables and enables statistical analysis and comparisons to be carried out more effectively, and an example standardisation technique is the Hazard Density Index (HDI) (Bolin et al., 2002). This was developed to enable cumulative hazards to be easily compared across census tracts in the U.S., compared to typical methods of just using point source locations for hazards that do not take into account cumulative effects when multiple hazards are in a similar area. The HDI technique offers a "spatially sensitive methodology" (Bolin et al., 2002) that has been successfully used by Grineski and Collins (2008) to assess environmental injustice spatially, and by Collins et al. (2009) to spatially explore vulnerability to environmental hazards.

If numerous standardised variables are being compared, it becomes possible to manually change the weighting of values based on the perceived importance. Weighting variables allows the relative significance to be accounted for, but the process of qualitatively assigning a weighting presents numerous challenges relating to objectives, methods and perspectives (Walker et al., 2011). A typical example where weighting is used is in decision support tools, where the user can vary the weighting and see how the output changes. This interactivity requires a full understanding of the risk process in order to obtain meaningful results. Due to the subjective nature of weighting, equal values are often used in the interests of transparency, for example (Su et al., 2009) used equal weighting when assessing demographic inequality in Los Angeles.

2.2.3 Examples

In the area of spatial risk assessment and climate change adaptation, there are a number of projects that are worth mentioning. Adaptation Strategies for Climate Change in the Urban Environment (ASCCUE) was a project (more details available online (The University of Manchester Centre for Urban Regional Ecology, 2012)) under the Building Knowledge for a Changing Climate (BKCC) initiative. The project used two contrasting case study areas, that of Lewes (a

low lying coastal town in SW England) and Greater Manchester (large conurbation in NW England) in order to look at climate change adaptation when applied to the urban environment, focussing on building integrity, human comfort and urban greenspace. Of note, Crichton's risk triangle was used successfully in a spatial risk assessment methodology for both flooding (Gwilliam et al., 2006; Fedeski and Gwilliam, 2007), and temperature (Lindley et al., 2006, 2007). However, the heat risk work of Lindley et al. (2006, 2007) explicitly does not consider the effect of the UHI.

Green and Blue Space Adaptation for Urban Areas and Eco Towns (GRaBS) was an EU funded project to integrate climate change adaptation into regional planning and development. There were 14 partners (four research institutions and ten European municipalities), including the Town and Country Planning Organisation, the University of Manchester, the London Borough of Sutton, the Northwest Regional Development Agency and Southampton City Council from the UK. One of the four main objectives of the GRaBS project was "to develop an innovative, cost effective and user friendly risk and vulnerability assessment tool, to aid the strategic planning of climate change adaptation responses". More details are available (GRaBS, 2012b) and the GRaBS adaptation action planning toolkit is also available online (GRaBS, 2012a), with interactive mapping both at a European scale and smaller local scales related to partner areas. The tool is used to assess current vulnerability, and not future vulnerability to climate.

Of particular note related to the GRaBS project is the Surface temperature and runoff (STAR) tools, which are "surface temperature and runoff tools for assessing the potential of green infrastructure in adapting urban areas to climate change", and more details are available (The Mersey Forest and The University of Manchester, 2011). This tool builds on the work and models developed in the ASCCUE project (described above), and the surface temperature is an output from a modified urban climate model that uses an energy balance equation to model surface temperature from a number of inputs. This differs to the approach taken in this thesis because it uses modelled data, as opposed to measured data. The complimentary nature of these techniques are discussed later in this thesis.

Other recent work (Oven et al., 2012) as part of the Built Infrastructure for Older People's Care in Conditions of Climate Change (BIOPICCC) project considers climate change and health risks for old people at a regional spatial scale for the UK, and highlights the complexity of undertaking hazard and vulnerability assessments for the future. A future research avenue is

creating fine scale maps at the local scale, as the existing work uses the relatively coarse scale of UKCP09.

The Birmingham Urban Climate Change with Neighbourhood Estimates of Environmental Risk (BUCCANEER) tool is the output of a Knowledge Transfer Partnership between Birmingham City Council and the University of Birmingham. This is a spatial decision support tool for planners to help and inform strategic policies. The tool was developed to integrate various datasets within an easy to use GIS framework in order to enable local authority stakeholders to explore potential changes in the urban climate of Birmingham. The BUCCANEER tool integrates heat risk maps developed in chapter 4.

2.2.4 Conclusion

This short review has given a brief overview of spatial risk assessment techniques, offering an overview of Crichton's risk triangle theory and other areas to be aware of e.g. standardisation, scale, weighting. It is clear that the risk assessment field is extremely broad, encompassing many fields, hence this review focussed on a small number of studies that are of relevance to this thesis. A consistent theme was related to data, and its availability, scale and quality, which directly impacts the final output.

Crichton's risk triangle offers solid foundations for spatial risk assessment that has been successfully used in heat risk related work. The advantage of being able to separate hazard, vulnerability and exposure as clear separate layers in a GIS is a powerful methodology that is used in chapter 4 to assess heat health risk for Birmingham.

2.2.5 Summary

This review has illustrated the risk assessment theory with Crichton's risk triangle, a clearly defined method that can be adapted for spatial risk assessment work. Explanation of spatial scales, standardisation and weighting alongside a brief review of various spatial risk assessment related work has illustrated methods and practice for spatial risk assessment. One area of this thesis is assessing heat risk for Birmingham spatially, which will be possible by utilising information gathered from this review. Crichton's risk triangle offers a good framework to work within, and using this method to explore heat risk spatially for Birmingham is undertaken in chapter 4.

Chapter 3

Measuring summer night surface urban heat island

This chapter aims to produce a simple and transferable technique to quantify the average night surface urban heat island (sUHI) in Birmingham, which can be utilised for spatial risk assessment (chapter 4), and then used in conjunction with climate change scenarios (section 5.2), to inform the evidence base for climate change adaptation, particularly relating to future health risk work.

3.1 Introduction

An introduction to the UHI phenomenon is given in section 1.2, so will not be repeated here. Traditional measurements of the near-surface UHI are often made using pairs of urban/rural weather stations (Kukla et al., 1986; Karl et al., 1988) or air temperature transects (Johnson, 1985; Torok et al., 2001). However, due to a paucity of high resolution air temperature measurements in most cities, including Birmingham, high resolution studies are limited to the measurement of surface temperatures and hence the surface or "skin" (s)UHI as measured by satellites (Streutker, 2003). Surface temperatures are far easier to obtain due to the availability

of products such as the thermal land surface temperature (LST) data from the Moderate Resolution Imaging Spectroradiometer (MODIS) instrument onboard the National Aeronautics and Space Administration's (NASA) Aqua (EOS-PM1) or Terra (EOS-AM1) satellites. A detailed review of land surface temperature measurements from space is given in section 2.1, which influenced the decision to use MODIS data for this work. It is important to note that the relationship between air and surface temperature is not fully understood, and this is the subject of further work in section 5.1. In this chapter the sUHI is investigated and no direct relationship to air temperature is suggested or inferred, but this is explored further in section 5.1.

Studies have explicitly pointed out the negative effects the UHI may have on health (Changnon et al., 1995; Rooney et al., 1998; Basu and Samet, 2002; Conti et al., 2005), particularly when combined with heatwave events. The UHI has also been shown to influence air quality (Huang et al., 2005) and atmospheric pollution (Sarrat et al., 2006) among other things. Heat risk studies (e.g. Lindley et al. (2006)) explicitly mention the lack of a UHI component, despite UHI being described as one of the major problems of the 21st century (Rizwan et al., 2008). For this reason, this study focuses on the summer months of June, July and August (JJA) as these are more likely to cause a heat health risk due to elevated summer temperatures and heatwaves (Rooney et al., 1998; Basu and Samet, 2002). Furthermore, it has been shown that for temperate cities in the northern hemisphere, such as Birmingham, winter UHI's are smaller in both extents and magnitude than summer equivalents (Hung et al., 2006).

3.1.1 Thermal satellite remote sensing techniques

Satellite techniques for remotely sensed thermal measurements are reviewed in section 2.1, illustrating the rapidly advancing field and the variety of sensors and satellite platforms available since the 1970's. The MODIS sensor was deemed to be the most suitable for this work for a number of reasons. Multiple studies have explicitly mentioned the potential and usefulness of the MODIS LST product in UHI research (Rajasekar and Weng, 2008; Cheval et al., 2009), but although MODIS has been operating on the Aqua satellite since 2002, it is only recently that a sufficient archive of data is freely available for analysis. It is for this reason that there are a limited number of studies in the literature that explicitly use MODIS data as a tool for urban climatology. Compared to potential alternatives (discussed in section 2.1) such as the Advanced

Spaceborne Thermal Emission and Reflection Radiometer (ASTER) sensor or Landsat Thermal Mapper (TM) / Enhanced Thermal Mapper Plus (ETM+), the MODIS LST product is considered a coarse resolution ($\sim$1 km) dataset. However, the high temporal resolution (twice daily per satellite) of MODIS makes it ideal for UHI studies. In comparison, the number of images available from ASTER or Landsat is significantly less than MODIS, which combined with the instantaneous observations, global coverage and promising quality of MODIS data (Jin and Shepherd, 2005) makes MODIS an ideal dataset for this work. The increased spatial coverage that satellite remote sensing techniques can provide in comparison to weather station data (Mendelsohn et al., 2007) is the main reason this technique is chosen.

The MODIS LST product has already been used for sUHI investigations in many countries and cities of varying sizes and scales across the globe, with various studies discussed in section 2.1. Notable studies include Hung et al. (2006) who used MODIS to quantify the sUHI in eight Asian mega-cities and Pongrácz et al. (2006) who conducted a similar study on the ten most populated cities of Hungary. However, the most relevant studies for this work is research from Romania where MODIS was used to calculate the average intensity of the sUHI in Bucharest for the month of July between 2000 and 2006 (Cheval and Dumitrescu, 2009) as well as under heatwave conditions in 2007 (Cheval et al., 2009).

3.2 Methodology

3.2.1 Study area

The study area of Birmingham is introduced in section 1.6, but despite its size only has one "urban" weather station (Winterbourne) within the city limits, and one "rural" weather station (Coleshill) approximately 4.5 km from the eastern edge of the city (Figure 3.1). Despite the Winterbourne station previously being classed as "urban" (Johnson, 1985), it is significant distance from the city centre, and located in a green leafy area (Figure 3.2) not representative of an urban area. There is another station in Edgbaston, closer to the CBD, but it is located on a covered reservoir and has limited data availability. The Elmdon weather station, based at Birmingham airport, was not considered due to its location outside the Birmingham study area and the airport setting not being representative for this study. The alternative rural station is Shawbury, but this is located a considerable $\sim$35 km away.

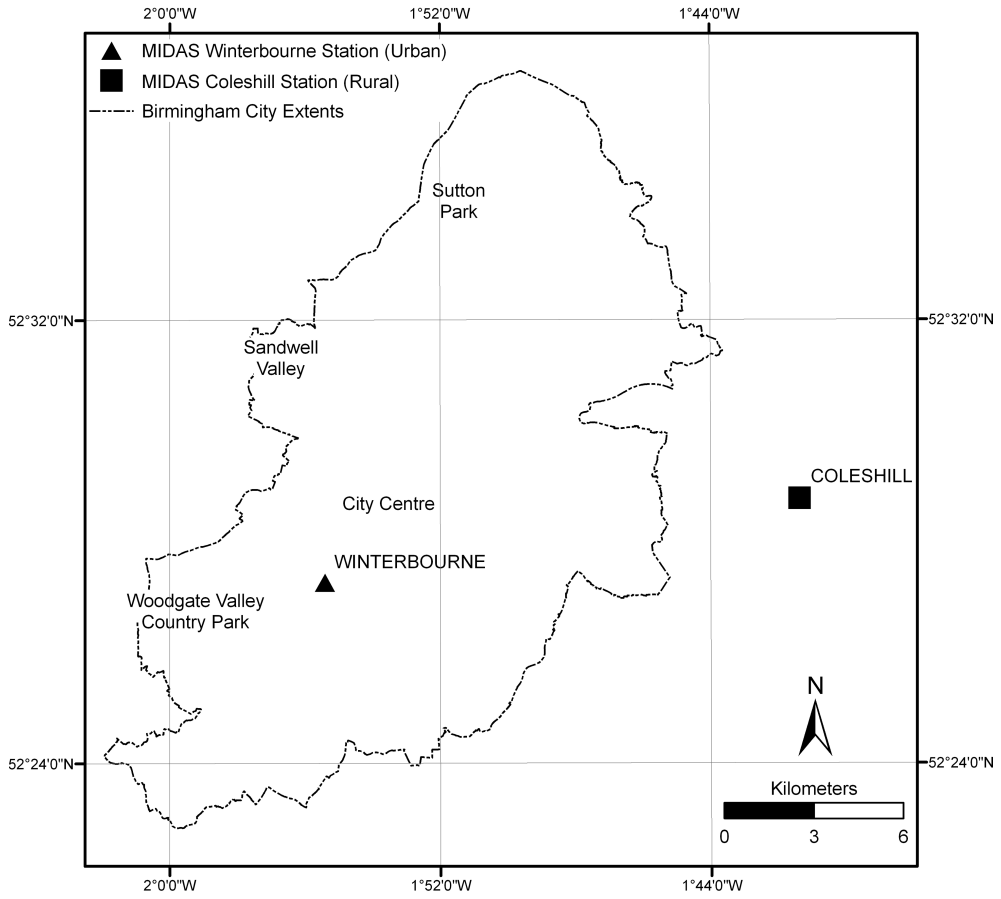

Figure 3.1: Location of Birmingham, local weather stations, and areas of interest.

Previous research into the Birmingham UHI is limited, partly due to the lack of meteorological stations and data. Unwin (1980) compared urban and rural nocturnal minimum weather station measurements and discovered that the near-surface UHI magnitude could reach 5°C in settled anticyclonic conditions. Johnson (1985) used a thermograph transect approach from the city centre out through the SW of Birmingham and recorded a maximum near-surface UHI of approximately 4.5°C during the night. Finally, Bradley et al. (2002) used a 1-Dimensional energy balance model to calculate a calm clear night sUHI intensity of 4.7°C. These few studies contrast with London which has an extensively studied UHI - see Watkins et al. (2002); Wilby (2003); Greater London Authority (2006); Kolokotroni et al. (2007); Kolokotroni and Giridharan (2008); Giridharan and Kolokotroni (2009); Jones and Lister (2009) for recent examples.

Figure 3.2: Winterbourne meteorological station in greenfield setting.

3.2.2 MODIS data

This study uses the MODIS product MYD11A1 (V5) - MODIS/Aqua Land Surface Temperature and Emissivity Daily L3 Global 1 km Grid SIN. Full technical details are available online and so will not be covered here (Wan, 1999; NASA Land Processes Distributed Active Archive Center, 2009). The theory behind LST measurements is outlined in section 1.6, but to reiterate the MODIS LST product uses split window algorithms and techniques (Wan and Dozier, 1996) that correct for atmospheric effects (including absorption and emission) and surface emissivity (inferred from MODIS land-cover calculations) by utilising multiple bands from the 36 available on the MODIS sensor. This addresses many of the "traditional" problems associated with remote sensing measurements of LST, such as emissivity assumptions and unknown or variable atmospheric effects. A number of studies have tested the accuracy of the MODIS LST product with favourable results (Wan, 2002; Wan et al., 2004; Coll et al., 2005; Wan, 2008).

Although the MODIS sensor is carried on both NASA's Aqua and Terra satellites, only images from Aqua (Figure 3.3) are used for this study as the near polar sun-synchronous orbit of Aqua resulted in a night image acquisition time for Birmingham at approximately 01:30h local time (compared to approximately 22:30h using Terra). A night image allows a more precise LST calculation as there is no incoming solar radiation to change the surface radiation balance,

and night time MODIS LST accuracy has found to be better than day time (Rigo et al., 2006). There may be timing differences between air (near-surface) and surface temperature UHI development, but without reliable quantitative evidence the timing of the 01:30h pass seems ideal as (Oke, 1987, p.291) describes maximum air UHI magnitude as three to five hours after sunset, which in the UK summer is around the time of image acquisition.

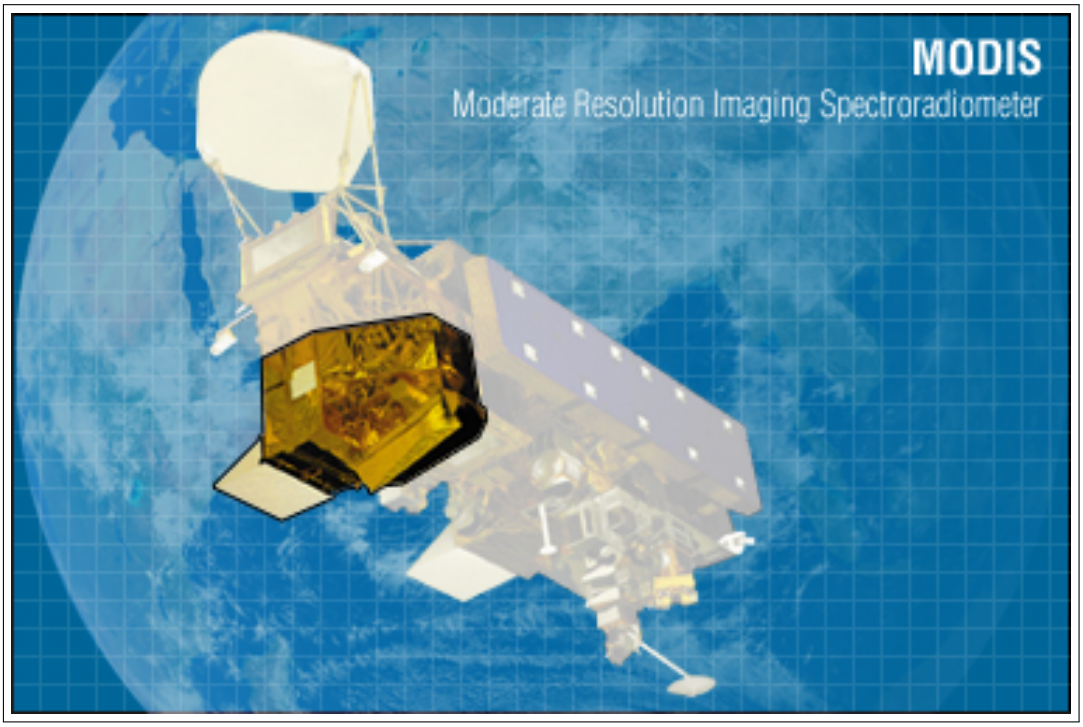

Figure 3.3: MODIS instrument onboard Aqua satellite.

Data were obtained using command line FTP tools (WGET) for the Birmingham study area over the summer months of June, July and August (JJA) for the seven year period between 2003 and 2009 inclusive. Images were batch processed in ESRI ArcMap using the Marine Geospace Ecology Tools (MGET) plugin (Roberts et al., 2010). This processing (Figure 3.4) ultimately resulted in a raster file of each image, geo-referenced and trimmed to the study area, with LST converted to degrees Celsius. Quality control of the images was then achieved by selecting only the raster images that contained 100% LST pixel coverage within the extent of the Birmingham conurbation (Figure 3.1). This last step removed a large amount of the images as MODIS satellite imagery, in common with all thermal infrared sensors, is restricted by cloud cover. The remaining images represented nights with clear skies at the time of the satellite overpass. Indeed, the increased availability of images in the summer months is a major advan-

tage of focussing on the summer sUHI. Difficulties in obtaining sufficient images for analysis in winter (Rajasekar and Weng, 2008), due to increased cloud cover (preventing an image being taken) or increased rainfall (causing wet surfaces leading to unreliable LST measurements), is a barrier for research. Other methods such as modelling or microwave remote sensing must be used if high temporal and high spatial LST data is required without the cloud cover limitations imposed by thermal infrared sensors (Wan, 2008).

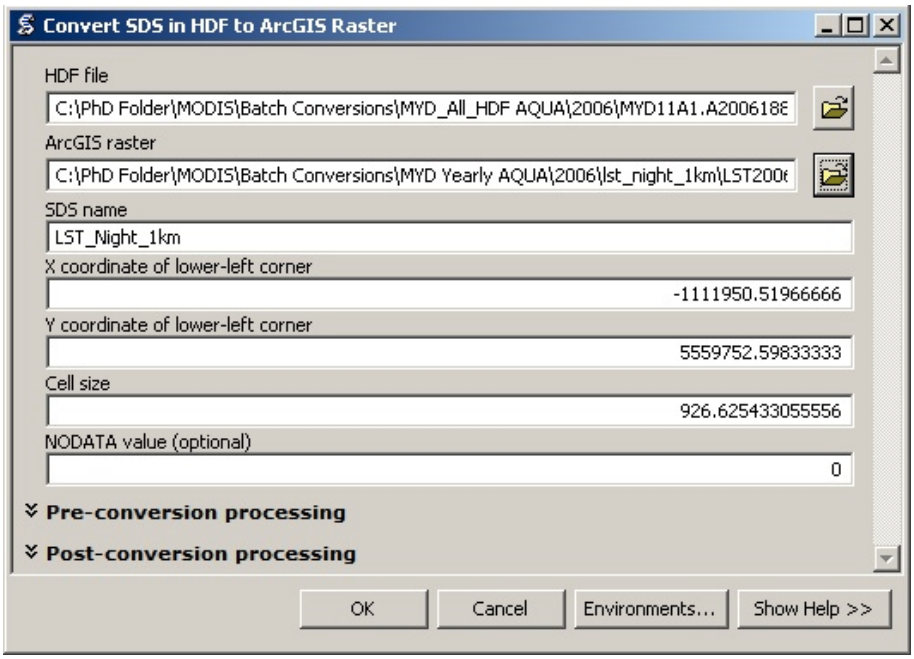

Figure 3.4: Screenshot of MGET plugin for processing MODIS HDF files in ArcGIS.

3.2.3 MIDAS data

The selected images were classified (Table 3.1) into Pasquill-Gifford stability classes (Pasquill and Smith, 1983; Sutherland et al., 1986; Chapman et al., 2001); D (Neutral), E (Slightly Stable), F (Moderately Stable) or G (Extremely Stable) based on the preceding 12 hours weather at Coleshill, a WMO weather station 4.5 km east of Birmingham (Figure 3.1). This weather station was chosen as it is the nearest to the study area which monitors cloud cover. The Met Office MIDAS WH hourly dataset (UK Meteorological Office, 2006) derived from Coleshill was used to average the weather for 12 hours preceding 02:00h (based on the satellite overpass time $\sim$01:30h) for each image in terms of cloud cover, wind speed and present weather code (detailing rain or other atmospheric conditions). Present weather codes detailing mist, smoke,

haze, cloud and fog were allowed (10, 04, 05, 01, 11 respectively) as they can relate directly to local events and have less impact on regional image quality. Automated macro's with validation were developed in Microsoft Excel to automate this repetitive task and avoid user error. This allowed the general atmospheric conditions preceding and including image capture to be summarised and further filtered out images that were unsuitable. Unlike satellite data, MIDAS ground station data can be obtained under all atmospheric situations.

Table 3.1: Classification of Pasquill-Gifford stability classes (adapted from Pasquill and Smith (1983); Chapman et al. (2001).

Surface wind	Pasquill-Gifford Stability Class	
speed (m s^{-1})	Night	
	$\geq$ 4/8 Oktas	$<$ 4/8 Oktas
$<$ 2	G	G
2 - 3	E	F
3 - 5	D	E
5 $>$	D	D

This approach resulted in a total of 63 images for analysis, distributed across the four Pasquill-Gifford stability classes (Table 3.2) and seven years of study (Figure 3.5). An additional classification of MIDAS data was additionally conducted for all summer (JJA) nights over the study period in order to assess the frequency of Pasquill-Gifford classes (Figure 3.6) over the same 12 hour time period.

Table 3.2: Distribution of images and nights across Pasquill-Gifford stability class.

Pasquill-Gifford stability class	Number of nights	Number of images
D	73	6
E	123	20
F	65	22
G	60	15
Total	321	63

Alternative classification options for the Pasquill Gifford stability classes were considered. This included Lamb's weather types (Lamb, 1950, 1972; Hulme and Barrow, 1997) that have been used previously by Unwin (1980). This classification contains both directional components (e.g. North East, East, South East etc) and vorticity components (e.g. anticyclonic, cyclonic), resulting in 28 different categories. Given the relatively small input dataset and the

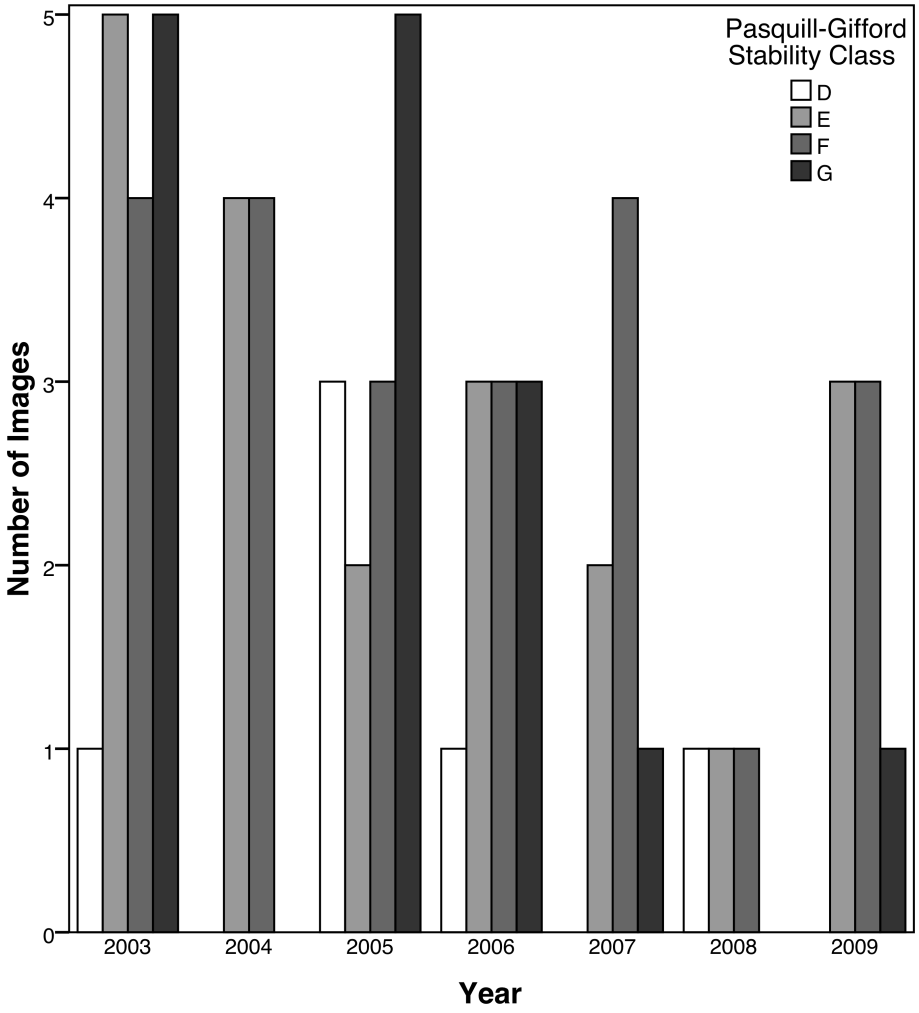

Figure 3.5: Selected images (from JJA) by Pasquill-Gifford class and year.

large number of categories, meaningful analysis would have been difficult, especially as the categories do not include cloudcover, a significant influence on the sUHI (e.g. Morris et al. (2001)). The Monin-Obukhov length (Obukhov, 1971), often used for atmospheric flow modelling in the lower atmospheric boundary layer, was explored, but the simplicity and proven nature (e.g. Chapman et al. (2001)) of Pasquill-Gifford stability classes made them ideal for this study.

3.2.4 Calculation of sUHI magnitude

For each of the four stability classes, spatial averages of LST values were calculated, resulting in a single raster image for each class containing average LST values for each $\sim$1 km cell. The magnitude of the sUHI present in each image was calculated by using a rural reference LST

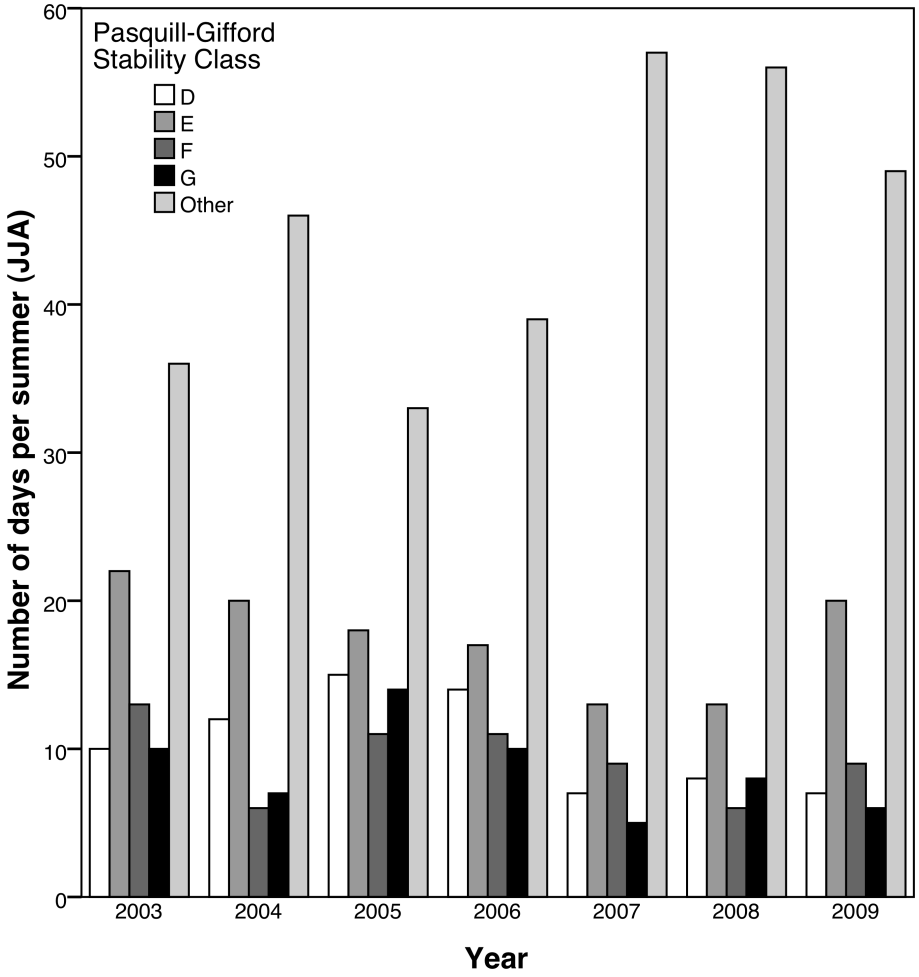

Figure 3.6: Pasquill-Gifford frequency in summer (JJA) 2003-2009. The "Other" class refers to nights that could not be defined into stability classes D, E, F, or G because of the filtering.

value to residualise the temperature value of each pixel across the whole image. Due to its rural location (Figure 3.1), the rural reference LST value was taken as the satellite LST value for the cell containing Coleshill weather station. Although the use of satellite data gave the possibility for choosing any reference area Coleshill was chosen in order to help facilitate potential future research comparing MODIS LST and air temperature (section 5.1). This step left four images, one for each Pasquill–Gifford scenario, with values taken to be sUHI magnitude, measured as LST difference when compared to Coleshill.

3.2.5 Land use data

Finally, in order to investigate the thermal characteristics of differing landuse categories (e.g. Bradley et al. (2002)), every pixel in each of the images was categorised with respect to a com-

mon landuse schema. Owen et al. (2006) derived an eight category urban land use classification from a principal component analysis and cluster analysis based on data from the Ordnance Survey and the UK Centre for Ecology and Hydrology.

1. villages/farms
2. suburban
3. light suburban
4. dense suburban
5. urban/transport
6. urban
7. light urban/open water
8. woodland/open land

The classification scheme was based on 27 different input attributes and the output is a 1 km^2 grid showing similar urban land morphology. Full details are given in Owen et al. (2006). A subset of the whole West Midlands database is used, distributed across Birmingham by frequency (Figure 3.7) and space (Figure 3.8). This classification was chosen for a number of reasons. It splits the urban fabric into multiple urban categories, unlike other classifications (including typical satellite land cover classifications) allowing more in depth comparisons, for example, between different densities of suburbia. Furthermore, it is a similar resolution (1 km^2) to the MODIS data so minimises problems that could arise when generalising between datasets with large differences in scale.

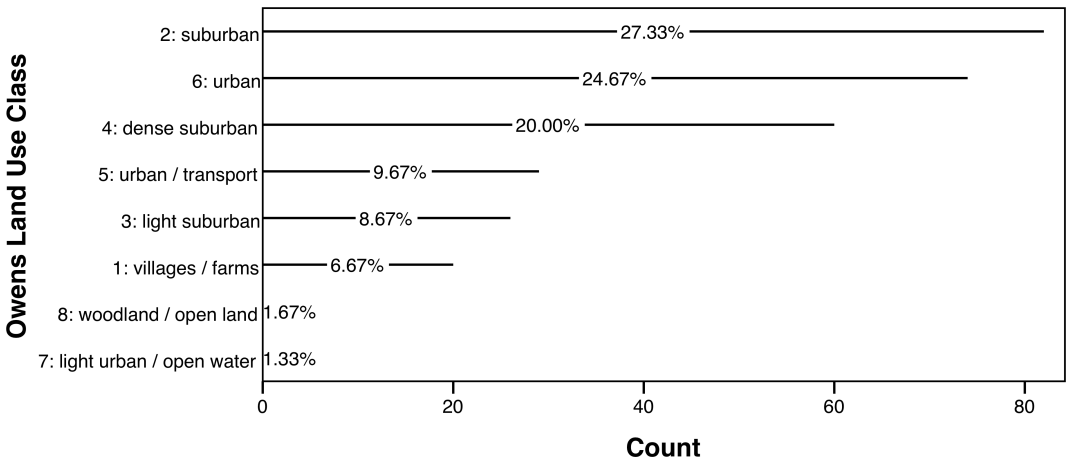

Figure 3.7: Numerical distribution of Owens land classification across Birmingham (after Owen et al. (2006)).

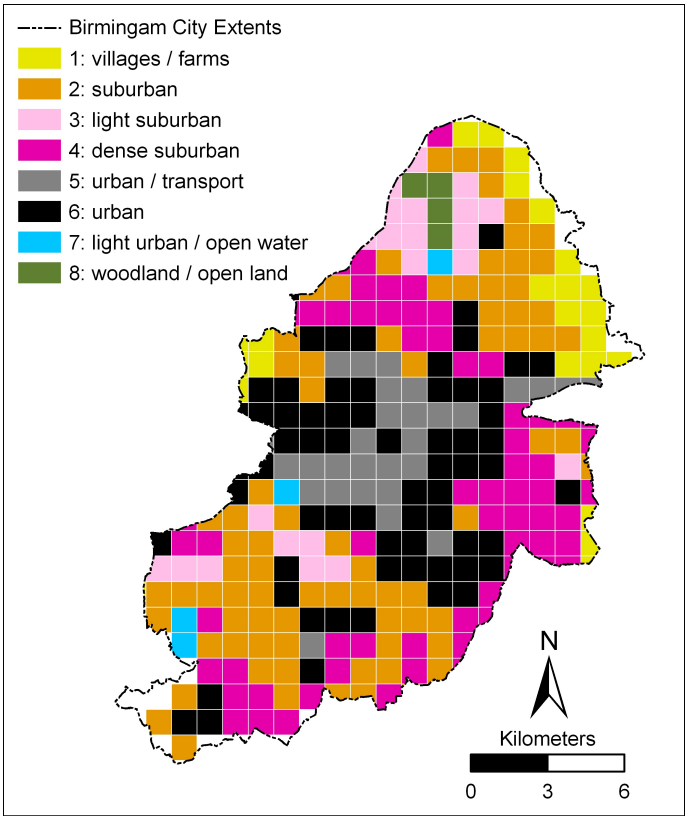

Figure 3.8: Spatial distribution of Owens land classification across Birmingham (after Owen et al. (2006)).

3.3 Results and discussion

3.3.1 Image availability

Both the total number of available images used for each of the Pasquill-Gifford class images as well as the total number of nights categorised in each Pasquill-Gifford class over the study period are detailed in Table 3.2. Here the issue of cloud cover reducing the sample size can clearly be identified as the number of images decreases rapidly between class E and class D due to the increased probability of cloud cover. If cloud cover did not impact image availability, the number of images in class E would be considerably greater as this is the dominant stability class throughout the summer months (Figure 3.6). Furthermore, exploring the distribution of images by year (Figure 3.5) it can be seen that whilst classes E and F are present for every study year, the distribution of classes D and G is less regular. Class D is not present in 2004, 2007 or 2009, whilst class G is not present in 2004 and 2008. The UK Met Office seasonal summaries (Met Office, 2010) can help to explain this, for example 2004 and 2008 summers both had higher

than average (1961-1990) rainfall which helps explain the lack of "Extremely Stable" class G images. Similarly, the year 2003 has the most number of images and was associated with a heatwave (Burt, 2004) which implies increased atmospheric stability.

3.3.2 Atmospheric stability and the Birmingham sUHI

The averaged night sUHI magnitude for the different Pasquill-Gifford stability classes (Figure 3.9) shows a clear increase in sUHI magnitude as atmospheric stability increases. This is expected, and in line with the findings of Morris et al. (2001) who show that increases in cloud cover and wind speed reduce UHI magnitude for Melbourne, Australia. When comparing residualised pixel values (Table 3.3) it can be seen that maximum sUHI magnitude (hottest pixel) decreases through the stability classes. Boxplots of each scenarios sUHI magnitude (Figure 3.10) agree and show an increase in sUHI magnitude as stability increases.

To test for statistical differences between sUHI magnitude under the four Pasquill-Gifford classes, the Friedman Analysis of Variance test (ANOVA) was used with post-hoc Wilcoxon Signed Rank tests. These are non-parametric versions of the repeated measures one way analysis of variance and paired samples students t-test, and were used because the dataset violates assumptions of normality and homogeneity. The results of the Friedman ANOVA confirm that significant differences ($p < 0.01$) in sUHI magnitude exist between at least two scenarios. The Wilcoxon Signed Rank post hoc tests confirm that significant differences ($p < 0.01$) in sUHI magnitude exist between all Pasquill-Gifford changes (D – E, E – F, F – G) when using a Bonferroni corrected significance level of 0.0033. This significance adds confidence to both the methodology used and the underlying MODIS data as the differences agree with expectations.

Clear spatial trends in temperature are evident in all four images and can be clearly delineated by isotherm mapping (Figure 3.9). In general these trends hold for all stability classes, however class D (Neutral) shows weaker trends and lower temperatures. The highest temperatures are consistently seen in the city centre of Birmingham, with a sUHI magnitude >3°C, >2.5°C, >2°C, >1.5°C for Pasquill-Gifford classes G, F, E, D respectively, with isotherm mapping at the 0.5°C interval. Exact LST values are given in Table 3.3. The exact spatial location of the centre of the sUHI moves slightly dependant on stability class, but generally the highest sUHI magnitude is around the central business district which contains Birmingham New

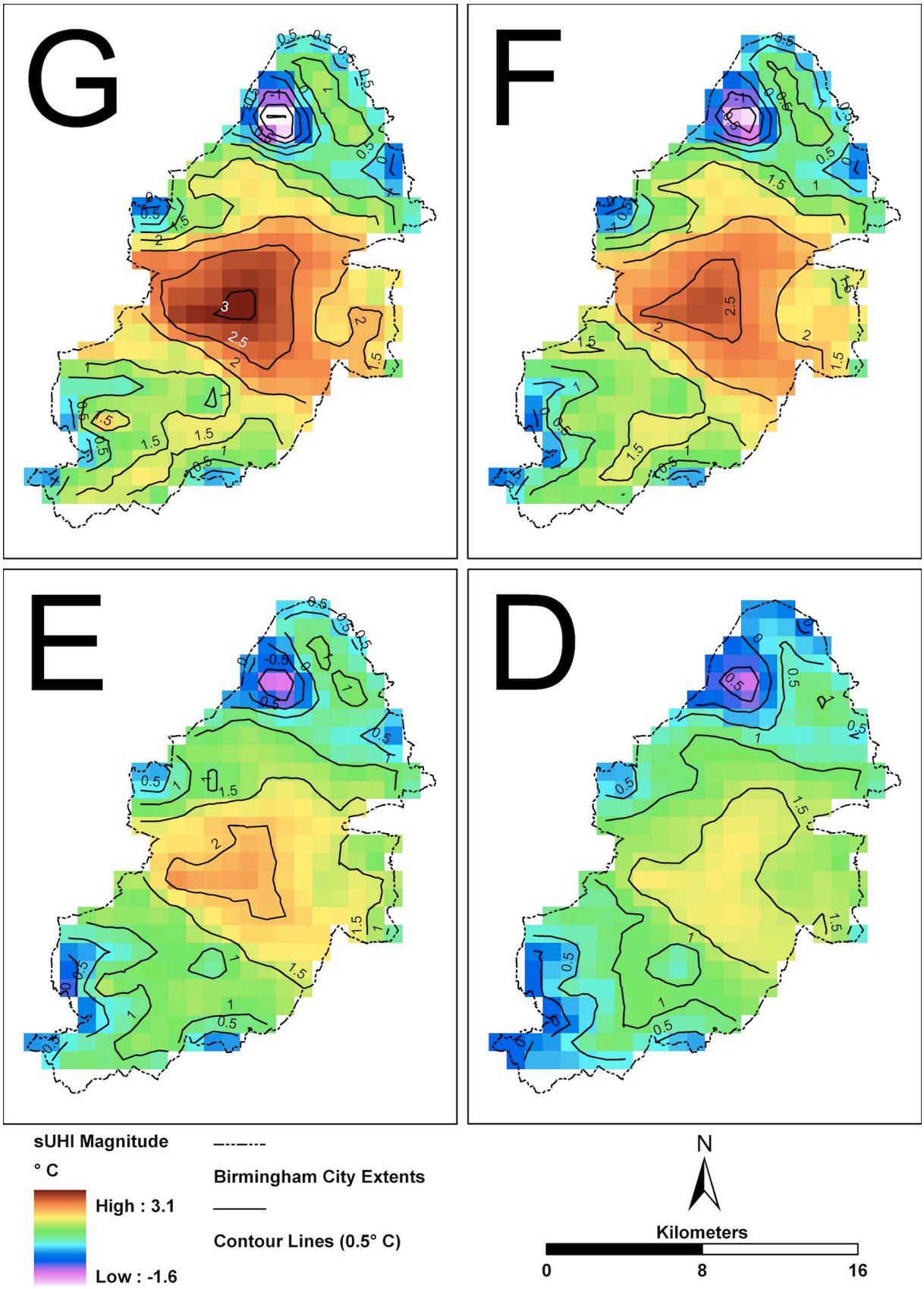

Figure 3.9: sUHI magnitude within Birmingham city extents across Pasquill-Gifford stability classes D, E, F, and G, shown with 0.5°C isotherm lines.

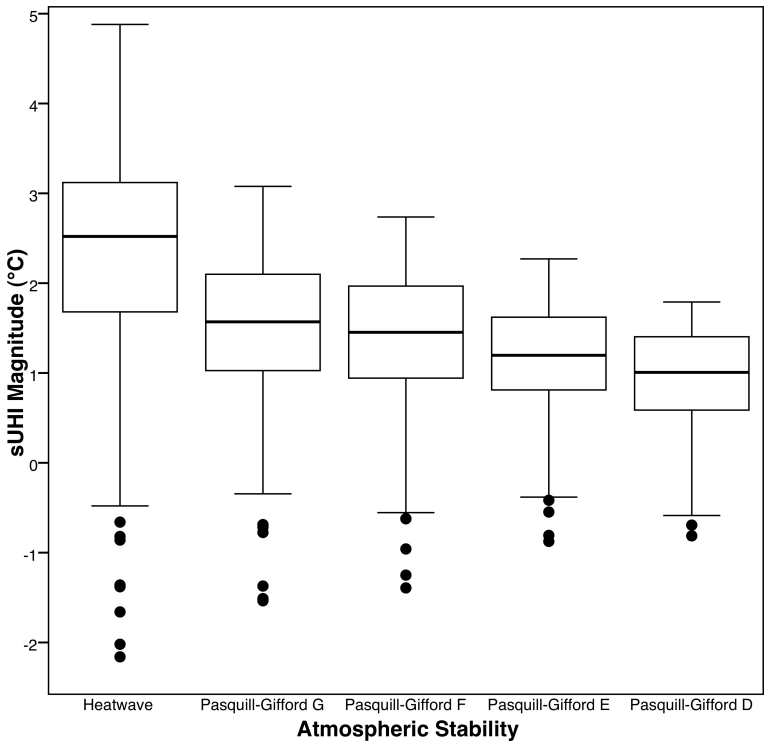

Figure 3.10: Boxplots of sUHI magnitude (°C) for different atmospheric stabilities.

Street Railway station and the main commercial area (Figure 3.1). In the north west corner of Birmingham, all stability classes exhibit a significant cold spot, with maximum magnitudes of <-1.5°C, <-1°C, <-0.5°C, <-0.5°C for Pasquill-Gifford classes G, F, E, D respectively. This area corresponds to Sutton Park Nature Reserve (Figure 3.1) which is the largest area of greenspace in Birmingham (Figure 3.11) covering over 9.5 km^2. This area corresponds to Sutton Park Nature Reserve (shown in Figure 3.11) which is the largest area of greenspace in Birmingham covering over 9.5 km^2 (location shown in Figure 3.1).

Sutton Park is approximately 40m higher than the city centre and accounts for 70% of the outliers shown in (Figure 3.10). Significant temperature gradients are also evident on the western edge of the city extents. These represent the remaining 30% of the outliers in (Figure 3.10) and are caused by a distinct change to an increasingly rural environment containing Sandwell Valley nature reserve as well as numerous golf courses and farms. One particular feature of note is Woodgate Valley Country (shown in Figure 3.12) which is effectively a green corridor running out to rural Worcestershire (location shown in Figure 3.1). Here, the closely spaced isotherm lines delineate a strong temperature gradient between the park and surrounding urban areas. This difference in temperature is particularly noticeable as the southern extents of

the park are bordered by a dense urban (as defined by the (Owen et al., 2006) land use classification) area. Further south there is another strong temperature gradient, explained by more parks, farms and reservoirs.

Figure 3.11: Looking north west across Sutton Park (location 52.5644,-1.8565).

Table 3.3: Residualised pixel comparison for different atmospheric stabilities.

	Temperature (°C)				
	Heatwave	G	F	E	D
Hottest Pixel	4.88	3.08	2.74	2.27	1.79
Coldest Pixel	-2.16	-1.54	-1.39	-0.88	-0.81
Difference	7.04	4.62	4.13	3.15	2.60

3.3.3 Heatwave case study

The Local Climate Impacts Profile (LCLIP) report (Kotecha et al., 2008) for Birmingham is a database of weather events and consequences at a local scale collated from media reports (UKCIP, 2009a). The database identifies various days as "heatwave" events and during the study period, four heatwave events totalling 11 days were identified. Based on this reference, the LCLIP heatwave case study in July 2006 is used as a comparison "extreme event" and the image

Figure 3.12: Looking east across Woodgate Valley country park (location 52.4454, -2.0086).

for the 18th July 2006 was processed using the described techniques (excluding any averaging) to make a fifth scenario for comparison alongside the four Pasquill–Gifford classes.

As illustrated by (Figure 3.13), the averaged images discussed in the previous section can significantly hide the true magnitude of the heat island. Investigating a single image taken 18th July 2006, in the early morning preceding a "heatwave" day, a similar trend is seen. The isotherm mapping (Figure 3.13) shows the same spatial trends already discussed, but with a greater temperature magnitude. The sUHI magnitude peak in the centre is $>$4.5°C, over 1.5°C higher than the "Extremely Stable" Pasquill-Gifford stability class G. A significant cold spot is again seen around Sutton Park, and at the western and south-western city extents. This suggests that an increase in temperatures does not significantly alter the position of the sUHI, but does increase the magnitude of both the sUHI and the Sutton Park cold spot. It is interesting to note that the values (Table 3.3) for a heatwave event are more than double the values for class E, the dominant stability class used in this study.

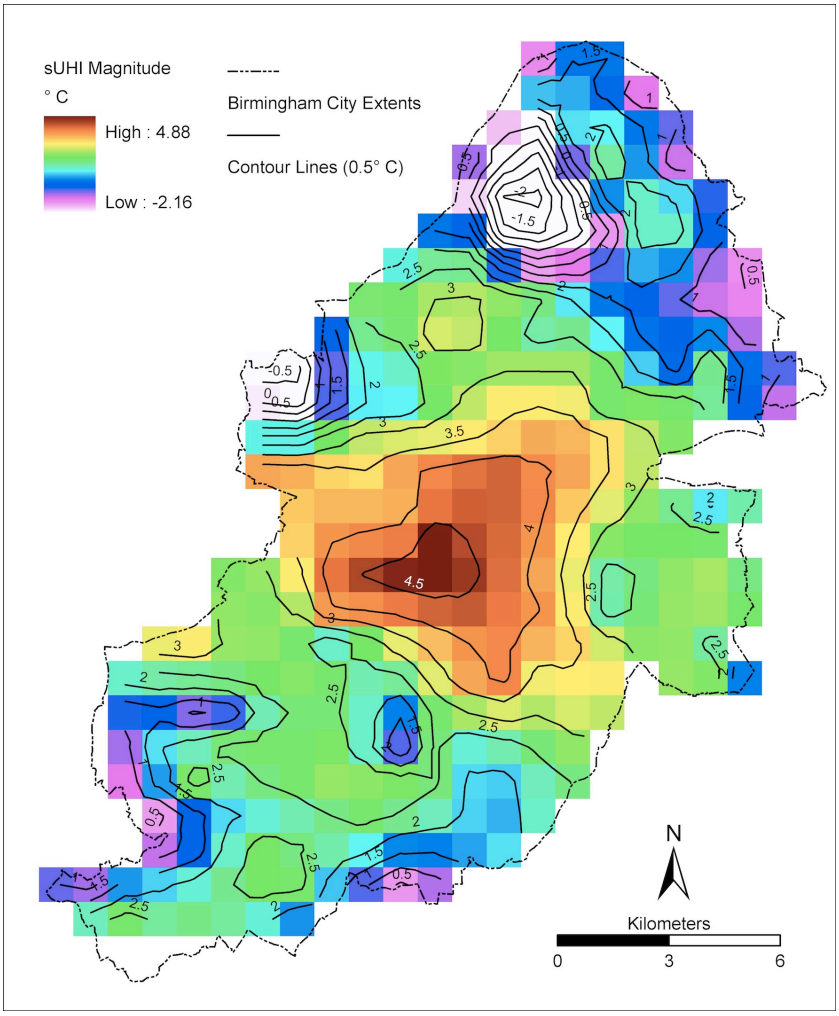

Figure 3.13: sUHI magnitude within Birmingham city extents for heatwave event (18 July 2006), shown with 0.5°C isotherm lines.

3.3.4 Thermal heterogeneity and landuse

Comparing sUHI magnitude across different Pasquill-Gifford stability class by land use (Figure 3.14) shows that in all cases except one, identical trends exist. Mean sUHI magnitude increases across land use classes in the order 8 (woodland/open land), 3 (light suburban), 1 (villages/farms), 7 (light urban/open water), 2 (suburban), 4 (dense suburban), 6 (urban) and finally 5 (urban/transport). The only minor exception is for class D, where the mean values for 1 (villages/farms) and 7 (light urban/open water) switch places and is a likely consequence of the small number of pixels (Figure 3.7) categorised as class 7 (light urban/open water).

Indeed, when applying the Owens Landuse class across Birmingham (Figure 3.7), over 80% of the landuse is explained by just four categories (2 (suburban), 6 (urban), 4 (dense suburban)

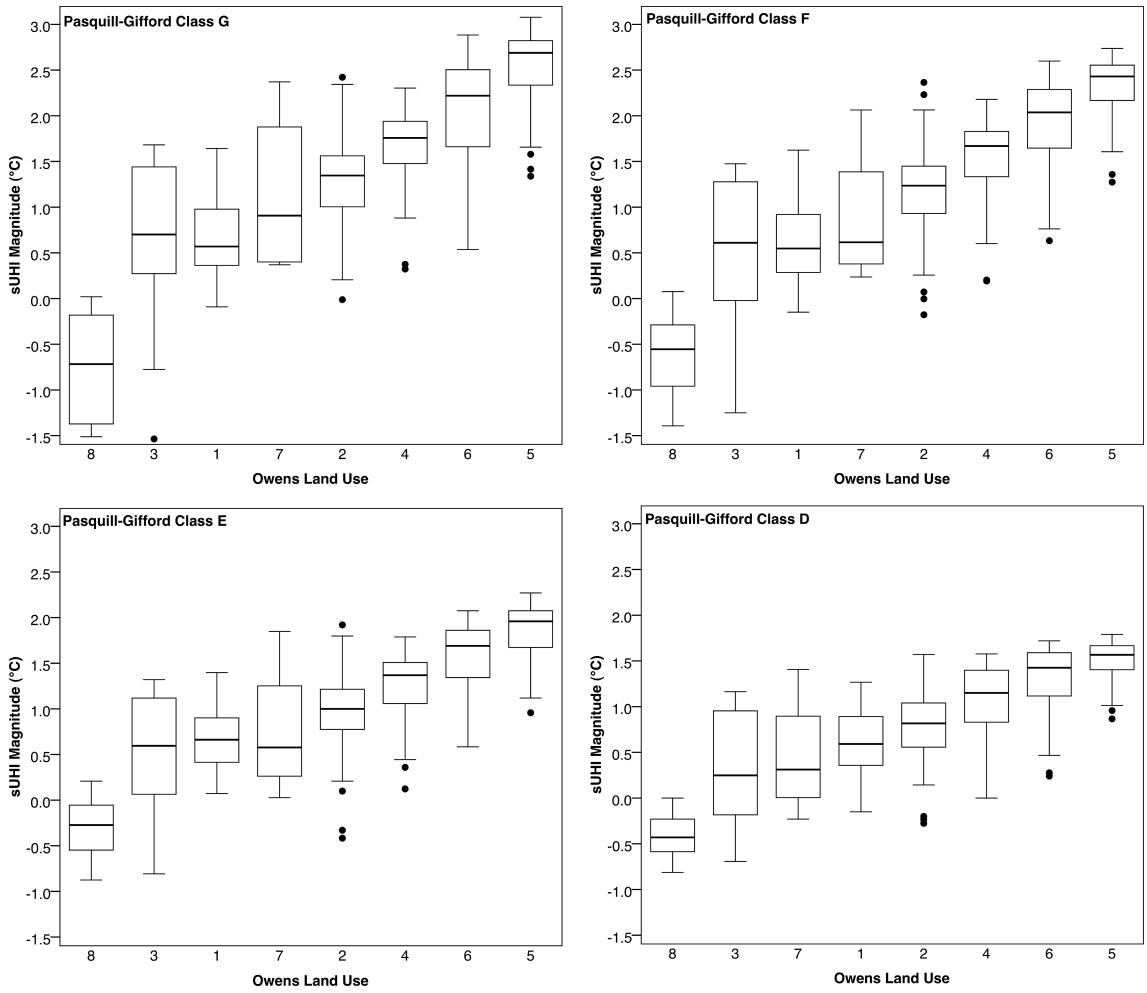

Figure 3.14: sUHI Magnitude for each Pasquill-Gifford class, distributed by Owens land and plotted in order of ascending mean sUHI magnitude. 1 (villages/farms), 2 (sub-urban), 3 (light suburban), 4 (dense suburban), 5 (urban/transport), 6 (urban), 7 (light urban/open water), 8 (woodland/open land).

and 5 (urban / transport)). This is not surprising considering that the classification is an urban classification and the study area is a major urban area. However, it is hard to draw any solid conclusions when considering groups 7 (light urban / open water) and 8 (woodland / open land) as they each make up $< 2\%$ of Owens classification in Birmingham.

To test for statistical differences between sUHI magnitudes and different land use classes, Kruskal Wallis rank order tests were used with post-hoc Wilcoxon rank-sum tests. The results of the Kruskal Wallis rank order tests confirm that significant differences ($p < 0.05$) in sUHI magnitude exist between at least two of the landuse classes in every scenario. The post-hoc Wilcoxon rank-sum tests show that significant differences ($p < 0.05$) exist between a number of land uses for each scenario, when using an appropriate Boneferroni correction factor. When

using a correction factor care must be taken in the interpretation as it becomes easy to reject results, potentially incorrectly. A summary of post-hoc test results (Table 3.4) is split between the full landuse database and a partial landuse database, removing classes 7 (light urban/open water) and 8 (woodland / open land) due to the low sample count (Figure 3.7). The results change considerably as class 7 was showing most of the non-statistically significant change. In all scenarios, there is no statistical difference between landuse 1 (villages/farms) and 3 (light suburban), but this is understandable given the clear similarities between classes detailed in Owen et al. (2006).

Table 3.4: Summary of *post-hoc* Wilcoxon rank-sum tests between landuse comparisons.

	Percentage of statistically significant results ($p < 0.05$) between landuse comparisons	
	Complete landuse (classes 1-8)	Partial landuse (classes 1-6)
	Bonferroni correction factor = 0.0018	Bonferroni correction factor = 0.0033
D (%)	60.71	80.00
E (%)	67.86	93.33
F (%)	67.86	93.33
G (%)	67.86	86.67
Heatwave (%)	64.29	86.67

3.4 Conclusions

The night sUHI of Birmingham has been shown to have considerable variation both spatially and across different levels of atmospheric stability. It has further been shown that landuse has a significant link to sUHI magnitude. The averaged images clearly show a difference in sUHI magnitude under different weather conditions, but the importance of investigating specific case studies such as the heatwave event of July 2006 is illustrated. Such extreme events could have significant consequences, for example in the healthcare sector. They are also likely to increase with climate change. However, when dealing with health impacts, it is ambient temperatures that are more important than surface temperatures. Indeed, a significant research gap that still exists is the relationship between measured surface LST such as used in this study, and air temperature. This is usually calculated by means of an empirical relationship, but in order for this to happen in the Birmingham study area data is required from a larger number of air temperature sensors than is presently available. Work using a pilot study sensor collection is

detailed in section 5.1, and the future plans for a much larger network are discussed in chapter 6. Other future work could compare this dataset with Landsat ETM+ data, of higher spatial resolution (lower temporal) resolution, to try and resolve temperature changes at a finer scale.

Overall, with the increasing interest in climate change adaptation within academia and at a policy level, the growing use of climate change models, and a rapidly rising urban population, there is a growing requirement for accurate high spatial and temporal resolution data relating to the UHI. This study has shown the utility of MODIS in providing a basic appraisal of the sUHI magnitude which is suitable for these growing requirements; including UHI model verification and spatial risk assessment work (chapter 4). The study is significant for several reasons. Many previous UHI studies have focussed on "ideal conditions" in megacities such as London or New York. This study differs from these in terms of the variety of meteorological conditions assessed as well as the size of the city under study (Birmingham can be seen as representative of many mid-latitude cities worldwide). Ultimately, this chapter has presented a repeatable methodology for studying the sUHI of individual conurbations that can be used worldwide with minimal adaptation, regardless of existing surface datasets.

3.5 Summary

This chapter has outlined a repeatable methodology for measuring a conurbation's night sUHI using readily available remotely sensed satellite data, and illustrated the method using Birmingham as a case study. The results clearly show that Birmingham has a significant sUHI, and the quantification of magnitudes under different atmospheric conditions gives a much better understanding of how the sUHI changes. The nature of satellite data allowing measurements at a greatly increased spatial scale has allowed the spatial patterns to be identified in much more detail when compared to the few previous studies in Birmingham, or the alternative measurement techniques such as ground based weather stations.

By accounting for meteorological conditions (via Pasquill-Gifford classes), relief (using a reasonably flat study area) and time (only considering night time measurements) and sharing metadata this chapter targets areas that have made previous UHI studies "scientifically indefensible" (section 1.2).

The GIS data outputs from this chapter, namely quantification of Birmingham's sUHI magnitudes under different atmospheric conditions at a fine spatial scale, allow the UHI to be considered in spatial risk assessment studies. This is a current research gap which chapter 4 analyses.

Chapter 4

Spatial heat health risk assessment

The aim of this chapter is to integrate remotely sensed night surface urban heat island (sUHI) data alongside commercial social segmentation data through a spatial risk assessment methodology in order to highlight potential heat health risk areas. Using Birmingham as a case study area, this chapter will create a heat health risk dataset that can be used as part of wider climate change risk assessment work (see discussions in section 5.2).

4.1 Introduction

The UHI is a well documented phenomenon that has been discussed in section 1.2 and measured for Birmingham using remote sensing techniques in chapter 3. Increased city populations promotes warming from anthropogenic heat release (Smith et al., 2009), hence those that live in inner city areas are subsequently exposed to the UHI effect and can therefore be under increased heat health risk (Rooney et al., 1998; Basu and Samet, 2002; Department of Health, 2009). However, previous spatial risk assessment studies generally don't include the UHI (Lindley et al., 2006). With rates of urbanisation continuing to increase (the United Nations (2008) predicting that population growth to 2050 will be absorbed exclusively in urban areas), the need for detailed heat risk assessments is paramount. Although this is an emerging

research area (McCarthy et al., 2010; Grimmond et al., 2010), existing climate change work does not include a UHI component (Gawith et al., 2009; Jenkins et al., 2009), despite it having a considerable influence on the mesoscale climate. Some work has been done to integrate the UHI within the United Kingdom Climate Projections 2009 (UKCP09) (Kershaw et al., 2010), but this is at a much larger scale than this work considers. The result is a present need to integrate climate change projections with UHI data via a piecemeal methodology. Utilising remote sensing techniques (chapter 3) has facilitated high resolution measurements of the spatial extents of the sUHI, which this chapter uses to develop a spatial heat health risk assessment method.

4.1.1 Vulnerable sections of the population

There is evidence to suggest there are upper limits to human adaptation to temperature (Sherwood and Huber, 2010), which makes the consequences of increased temperatures important to understand. Although defining human thresholds for heat risk has many problems (Meze-Hausken, 2008), it is possible to identify vulnerable groups (Table 4.1). High population density has been shown to correlate with areas of higher temperatures (Coutts et al., 2007), and is to be expected given that high population density is often within inner city areas that are also impacted by the UHI. With specific reference to heat health risk, multiple studies have shown that increased population density results in increased risk (Dolney and Sheridan, 2006; Harlan et al., 2006; Hajat and Kosatky, 2010). Therefore it is reasonable to include people living in areas of high population density as vulnerable to heat risk.

Table 4.1: Groups vulnerable to heat risk.

Vulnerable Group	References
Elderly People	(Huynen et al., 2001; Díaz et al., 2002; Conti et al., 2005; Flynn et al., 2005) (Grize et al., 2005; Hajat et al., 2007; Bell et al., 2008) (Department of Health, 2009) (Stafoggia et al., 2006; Vandentorren et al., 2006; Tan, 2008)
Ill Health	(Semenza et al., 1996; Fouillet et al., 2006; Stafoggia et al., 2006) (Kaiser et al., 2001; Naughton et al., 2002)
High Population Density	(Dolney and Sheridan, 2006; Harlan et al., 2006; Hajat and Kosatky, 2010)
High Rise Living	(Semenza et al., 1996; Naughton et al., 2002; Department of Health, 2009)

The elderly population has a relatively high percentage of illness and disability which increases their vulnerability (Tan, 2008). Older, frail individuals are thought to have a lower tolerance to extremes of heat (Flynn et al., 2005), and compounding factors, such as lack of mo-

bility, further increase vulnerability (Vandentorren et al., 2006). This has been illustrated in the literature by studies in Switzerland (Grize et al., 2005), Italy (Conti et al., 2005; Stafoggia et al., 2006), the Netherlands (Huynen et al., 2001), Spain (Díaz et al., 2002), and Latin America (Bell et al., 2008). Within the UK, academic research (Hajat et al., 2007) and the national Department of Health (Department of Health, 2009) recognise that the elderly are vulnerable to heat. Recent work by Oven et al. (2012) as part of the "Built Infrastructure for Older People's Care in Conditions of Climate Change" (BIOPICCC) project also identifies older people as particularly vulnerable to climate related hazards.

Another vulnerable group can be defined as those in "ill health". This includes those with pre-existing illness or impaired health, which could be physical or mental (Kaiser et al., 2001; Naughton et al., 2002). Those with known medical problems and those unable to care for themselves or with limited mobility are at increased risk (Semenza et al., 1996; Stafoggia et al., 2006; O'Neill and Ebi, 2009), and diseases mentioned specifically include respiratory, cardiovascular and the nervous system (Fouillet et al., 2006).

People living on the top floor of flats or high rise buildings have also been found to have increased heat risk, with studies in Chicago in both 1995 (Semenza et al., 1996) and 1999 (Naughton et al., 2002) having similar results, finding that those living on higher floors were subject to increased risk. Within the UK, those in south facing top floor flats are classed as "high risk" by the Department of Health (Department of Health, 2009). The reasons for this increased risk include the build up of temperatures in larger and taller buildings, and the increased exposure to incoming solar radiation resulting in higher temperatures.

Finally, young children are another group that could be at risk, with studies in Australia (Yaron and Niermeyer, 2004), America (McGeehin and Mirabelli, 2001) and the UK (Kovats et al., 2004) outlining the vulnerability of the very young. However, in this chapter children have not been included because of the difficulties in locating detailed data (a consequence of the requirement to target parents or guardians in order to communicate). An effective way to reduce this research gap could be to target schools and embed heat risk education where appropriate.

4.1.2 Spatial risk assessment methodologies

Spatial risk assessment work is an increasing area, with various methodologies utilising Geographical Information Systems (GIS) software to analyse risk spatially. A critique of risk assessment methods in relation to climate change (Pidgeon and Butler, 2009) details how problematic the process can be. However, given the increasing demand for "evidence based decisions" within governance, a form of risk assessment framework is required. Useful background to this area is given in section 1.5 and section 2.2, however the work that is most closely related to this chapter is that of the field of climate change adaptation in the UK (Lindley et al., 2006; Gwilliam et al., 2006; Lindley et al., 2007) arising from the "Adaptation Strategies for Climate Change in the Urban Environment" (ASCCUE) project. The ASCCUE project (also see subsection 2.2.3) developed a risk assessment methodology based on "Crichton's Risk Triangle" (Crichton, 1999). This has been utilised in the UK as part of a broader methodology to assess flood hazard at both a neighbourhood and conurbation scale (Gwilliam et al., 2006; Fedeski and Gwilliam, 2007) and to assess heat risk in relation to climate change (Lindley et al., 2006, 2007). This chapter builds on the methodologies developed in these papers and adds some important developments. In particular, this work focuses on the impact of the sUHI as well as developing objective methods that can easily be replicated nationally.

4.2 Methodology

4.2.1 Study area

Background to Birmingham is given in section 1.6. This study utilises the "Lower layer Super Output Area" (LSOA) (Office for National Statistics, 2011) as a spatial scale. This is because they are a suitable aggregation area to minimise the modifiable areal unit problem (section 2.2.2), should not change in the future, and can be easily distributed as they do not identify individuals. As the LSOA is part of a hierarchy it is easy to change the scale, for example combining a number of LSOA into a Medium layer Super Output Area (MSOA) which adds flexibility to the methodology as it allows comparison with datasets that may only be available at MSOA. There are 641 LSOA within the Birmingham (Figure 4.1) area, numbered from 8881 to 9521 inclusive, with size (km^2) ranging between 0.062 – 8.739, mean 0.418, standard deviation 0.541.

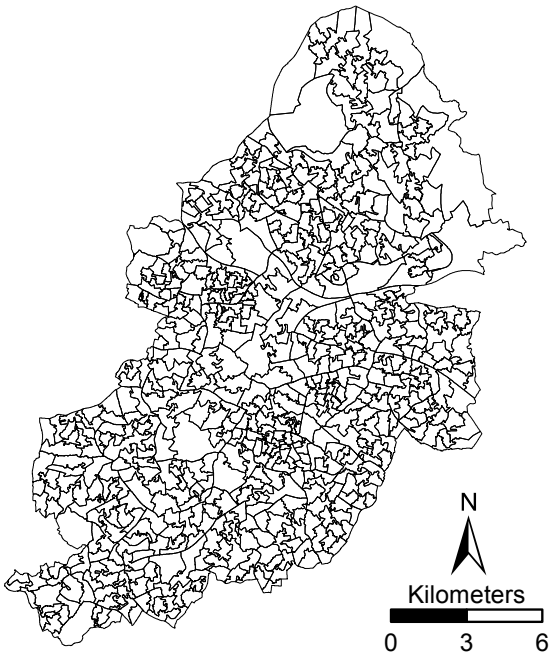

Figure 4.1: Spatial distribution of LSOA's across Birmingham.

Health research with specific reference to the Birmingham area has taken place both within academia; exploring the relationship between mortality and temperature (Fisher, 2009), looking at the 1976 heatwave (Ellis et al., 1980) and through the public sector; looking at climate change and health (May et al., 2010). This previous work has not included a spatial aspect, which is an important research gap given the size and diversity within Birmingham, and particularly when including a UHI component. This work builds upon chapter 3, incorporating the remotely sensed sUHI data in a spatial risk assessment.

4.2.2 Spatial risk assessment

The methodology utilised in this chapter has deliberately been kept simple and transparent in order to remove excessive complicated jargon and help explanation to stakeholders such as Birmingham City Council. However, at this stage it is important to clarify the terminology used in this chapter, as throughout the risk assessment literature there are various terms that have multiple definitions, as outlined in section 2.2. The main risk assessment theory for this chapter uses "Crichton's Risk Triangle" (Figure 2.4) that is explained in section 2.2.2 and details related to its use in this work are outlined below.

A hazard is something that may cause a risk, and in this method the spatial and temporal aspects of the hazard are required, alongside the magnitude. In this case the increase in temperature from the sUHI is being considered, measured from remotely sensed satellite data (chapter 3). The exposure represents what is exposed to the hazard and at a basic level is simply a spatial coincidence between the hazard and the exposure of interest. Various items could be exposed and relevant data about each is required spatially for this method to be useful. Examples could be buildings (with corresponding attributes such as types or value) or people (with attributes such as age or health problems) and this work uses high resolution commercial social segmentation data. Vulnerability refers to which aspects of the exposed elements could be damaged or have adverse outcomes to a given hazard, and this is generally defined by referencing a vulnerability table.

The term vulnerability is also defined by the IPCC (IPCC, 2007b, p. 883) as "the degree to which a system is susceptible to, and unable to cope with, adverse effects of climate change, including climate variability and extremes. Vulnerability is a function of the character, magnitude, and rate of climate change and variation to which a system is exposed, its sensitivity and its adaptive capacity". Comparing the terminology used in the IPCC and this study, the IPCC definition of "vulnerability" is analogous with "risk" and the IPCC term "sensitivity" refers to this studies definition of "vulnerability". The related IPCC term "adaptive capacity" refers to "the ability of a system to adjust to climate change…". Whilst this work does not explicitly discuss adaptive capacity, the methodology allows exploration of adaptive capacity by altering the exposure or vulnerability aspects.

Certain groups are more vulnerable to heat risk, for example the elderly (see subsection 4.1.1). The final risk layer is generated from the spatial coincidence of the hazard layer and the exposed and vulnerable layer. This is a simplification of the ASCCUE work and a flowchart visually illustrates the workflow (Figure 4.2). These methodological changes, which remove the "hazard-exposure" layer and place more emphasis on the "exposed and vulnerable", were chosen due to simplification of data manipulation and ease of explaining to stakeholders. In order to spatially represent each of the hazard, exposure, vulnerability and risk layers a coherent spatial scale is required across all layers. All items of interest are merged at the LSOA scale (Figure 4.1).

A standardisation technique has been employed, in order to illustrate each variable on the

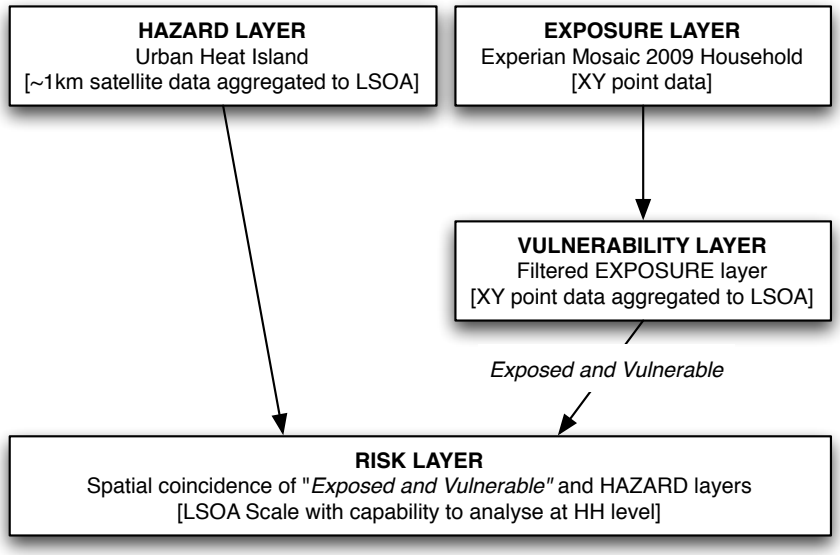

Figure 4.2: Simplified flowchart of GIS spatial risk assessment methodology (adapted and developed from Gwilliam et al. (2006)).

same scale and ensure ease of combining layers of a different nature. This is based on the Hazard Density Index (HDI) (Bolin et al., 2002) that a number of studies have used successfully (Grineski and Collins, 2008; Collins et al., 2009) and further details are given in section 2.2.2. Individual variables are standardised (Equation 4.1) by dividing each variable value by the maximum value of that variable across the complete study area, resulting in a standardised variable between zero (low) and one (high).

$$\frac{\text{LSOA score}}{\text{max LSOA score across Birmingham}} = \text{standardised score for each LSOA} \tag{4.1}$$

When combining layers it is possible to vary the weighting of values based on relative importance, as described in section 2.2.2. However, in this study all weightings have been kept equal in the interests of transparency. Other studies have used equal weighting methods with success (Collins et al., 2009; Su et al., 2009). If weighting of values is varied the process becomes subjective and the resultant maps open to manipulation, therefore appropriate use of weightings requires considerable knowledge concerning all the variables and techniques. It is anticipated that the results of this work will be incorporated into a spatial decision support tool where the weightings can be altered according to specific user requirements. An example of such a tool is the Birmingham Urban Climate Change with Neighbourhood Estimates of Envi-

ronmental Risk (BUCCANEER) tool, the output of a Knowledge Transfer Partnership between Birmingham City Council and the University of Birmingham. This is a spatial decision support tool to be used by planners to help and inform strategic policies.

4.2.3 Hazard layer: sUHI

High resolution sUHI mapping can be obtained through remote sensing methods, as outlined in section 2.1 and carried out in chapter 3. This $\sim$1 km resolution data measuring the magnitude of the night sUHI has been used as the hazard layer. The MODIS remotely sensed image of the night of the 18th July 2006, used as a "heatwave" example (subsection 3.3.3) was resampled and then zonal statistics were carried out in order to facilitate generalisation at the LSOA scale. The mean sUHI magnitude (°C) for each LSOA was taken to standardise the LSOA output on a scale between zero and one, as for other layers. The resultant layer illustrates the spatial pattern of the sUHI across the conurbation on a specific heatwave day, representative of a day with ideal conditions for sUHI generation (low windspeed and low cloud cover). However section 3.3 showed the spatial pattern of the sUHI has been shown to be similar across a number of different meteorological conditions.

The relationship between LST (and therefore sUHI) and measured air temperature is complicated, with techniques such as statistical regression (Yan et al., 2009), solar zenith angle models (Cresswell et al., 1999) or thermodynamics (Sun et al., 2005) often used to explore the relationship. LST and air temperature are not directly comparable, however in the case of the UHI, it is reasonable to believe that spatial trends will be similar when comparing LST and air temperature, and therefore remotely sensed data is a useful dataset as absolute values are not vital in this methodology. This relationship is explored in more detail in section 5.1.

The main alternatives to satellite data for calculating the UHI include ground sensor measurements or model output. There is a paucity of ground sensors in Birmingham, and other approaches (for example transect based (Smith et al., 2011a)) require extensive fieldwork. UHI model's (Martilli, 2007; Grimmond et al., 2010) have been developed, but require considerable work to collate accurate input variables and validate the results. Satellite data is readily available globally, increasing the utility of the methodology.

Overall, the inclusion of the sUHI as the hazard layer explicitly fills a specific research gap

from other heat risk studies. The work could be expanded on, for example to include the possible effects of both climate change and the UHI, and this area is explored in section 5.2.

4.2.4 Exposure layer: Experian Mosaic 2009 data

The exposure layer is made up of detailed commercial social segmentation data from Experian on every household in Birmingham. Experian are a global company focussed on providing information to help business and in the UK they are commonly known for being one of the three credit reference agencies the financial industry uses. Within this chapter, the Experian Mosaic UK 2009 product is used which is a consumer classification for the United Kingdom, providing "an accurate understanding of the demographics, lifestyles and behaviour of all individuals and households in the UK" (Experian, 2009), classifying each household into one of 15 groups, and below that one of 67 types. This exact method is suitable for the UK, but Experian have a number of consumer segmentation products for 29 countries that classify over a billion consumers, so it could be easily adapted to other parts of the developed world. The Mosaic classification is built using 440 data elements, and is updated and verified bi-annually (Experian, 2009).

The Mosaic 2009 dataset was supplied for all of Birmingham at household (HH) level, with each HH including attributes of X and Y location, Mosaic Type and Mosaic Group. For the purposes of this work, HH data is generally aggregated up to LSOA levels as this can be distributed without personal identities being disclosed, whilst still giving a relatively high resolution. However, having access to the HH data gives additional flexibility both for the methodology and analysis. Supplied alongside the raw data was the key to Mosaic types, a document that gave in depth qualitative information for each Mosaic type, including a general overview followed by specific demographic information related to where the type lives, how they live, world views, financial situation and online behaviour. Using a single dataset to underpin the methodology and analysis was a deliberate choice, designed to remove problems of availability and contextual differences that have been illustrated in previous studies (Collins et al., 2009). The data used in this project is at HH level, and details the 427,914 HH contained within Birmingham city extents. Experian offer a risk dataset (Perils), encompassing flood, subsidence, windstorm and freeze risk (Experian, 2012) however heat risk is notably absent, and there-

fore this work also acts as a proof of concept for expanding Experian's risk dataset product portfolio. The exposure layer is point shapefile with one point for each household containing attribute data including Mosaic type; data is summarised into LSOA at a later stage using GIS techniques. Titles of the Mosaic types used in this study are detailed in Table 4.2, and more details are available in the Mosaic 2009 brochure (available online (Experian, 2009)).

Table 4.2: Titles of relevant Mosaic type identified for specific vulnerabilities.

Mosaic Number	Mosaic Titles	Vulnerability
20	Golden Retirement	Elderly
21	Bungalow Quietude	Elderly
22	Beachcombers	Elderly
23	Balcony Downsizers	Elderly
38	Settled Ex-Tenants	Ill
39	Choice Right to Buy	Ill
42	Worn-Out Workers	Ill
43	Streetwise Kids	Ill
44	New Parents in Need	Ill
45	Small Block Singles	Ill
47	Deprived View	Ill
50	Pensioners in Blocks	Elderly
51	Sheltered Seniors	Elderly
52	Meals on Wheels	Elderly
53	Low Spending Elders	Elderly
65	Anti-Materialists	Ill

An alternative data source is the British Census (a decadal survey of every person and household in the UK), and this has been used in other studies (Lindley et al., 2006; Hajat et al., 2007). However, it will take time for data from the recent 2011 Census to become available after being verified and quality assured, and available data from the 2001 Census is now outdated. This work does not use Census data, given the time delay and the future uncertainty over the survey given the recent severe governmental spending cuts. Mosaic uses current year estimates of Census data for 38% of the information used to create the classification, alongside additional datasets and verification. This makes the data more useful as it is upto date. For more information on the classification system, see the brochure online (Experian, 2009).

4.2.5 Vulnerability layer(s): specific vulnerable types

The vulnerability layer is made up of vulnerable types extracted from the exposure layer, made up of Experian Mosaic HH types. Vulnerable types have been defined through a literature

review and justifications for each layer are given in Table 4.1. The following details how each specific vulnerable type was identified and extracted from the data available in the Mosaic dataset.

Elderly people were identified as Mosaic group E, "Active Retirement" (type 20,21,22,23) and L, "Elderly Needs" (type 50,51,52,53). Within these groups, there is a wide range of socioeconomic factors, however all are elderly. The literature identified elderly as a vulnerable type, and whilst affluence can reduce vulnerability, for example by financing air conditioning units, it cannot totally mitigate the vulnerability. The number of HH classed as "elderly" per LSOA was counted and then standardised as discussed.

Other heat risk studies (Lindley et al., 2006) discuss how analysing flats or high rise buildings could be a possible addition to their study. This work uses a combination of datasets to calculate people living in high rise buildings. The Mosaic data gave household locations (including multiple households at the same XY coordinates). Ordnance Survey Mastermap, the highest resolution vector mapping solution available in the UK, details individual buildings at polygon level. Individual building polygons across Birmingham were extracted from Mastermap, and then the number of HH points falling within each polygon was counted. This was then filtered to show only polygons with greater than ten HH within. The rationale behind this number is that buildings with less than ten households are not likely to be sufficiently high rise. This number would be easily altered for use in different cities. Light Detection and Ranging (LIDAR) height data could be combined in order to obtain true height of buildings but this approach was not used because this methodology focuses on using Experian data for ease of repeatability.

Density of households per LSOA was calculated (Equation 4.2) for each LSOA. The result is household density per km^2 that was standardised as per the technique already detailed.

$$\frac{\text{number of HH in LSOA}}{\text{area of LSOA (km}^2\text{)}} = \text{HH density per LSOA} \tag{4.2}$$

The vulnerable group "ill health" was created by a literature and keyword search of the Mosaic 2009 key document for keywords "health" or "illness" followed by qualitative interpretation of the results by a single interpreter to avoid bias. This identified Mosaic types 38, 39, 42, 43, 44, 45, 47, and 65 as including people with ill health. Not all HH will be of ill health, but ex-

amples of the way these groups are described includes “they have health problems “ or “higher levels of illness“ or “many have health issues, including mental health issues“. The number of HH classed as “ill health” per LSOA was counted, and then standardised as described.

4.2.6 Risk layer

To create the final risk layer, the four vulnerability layers were combined into a single “exposed and vulnerable” layer (each weighted at 25%) which was then spatially combined with the hazard layer (each weighted at 50%), a technique that has been used successfully for previous spatial risk assessment (Collins et al., 2009). This process is illustrated in Figure 4.3.

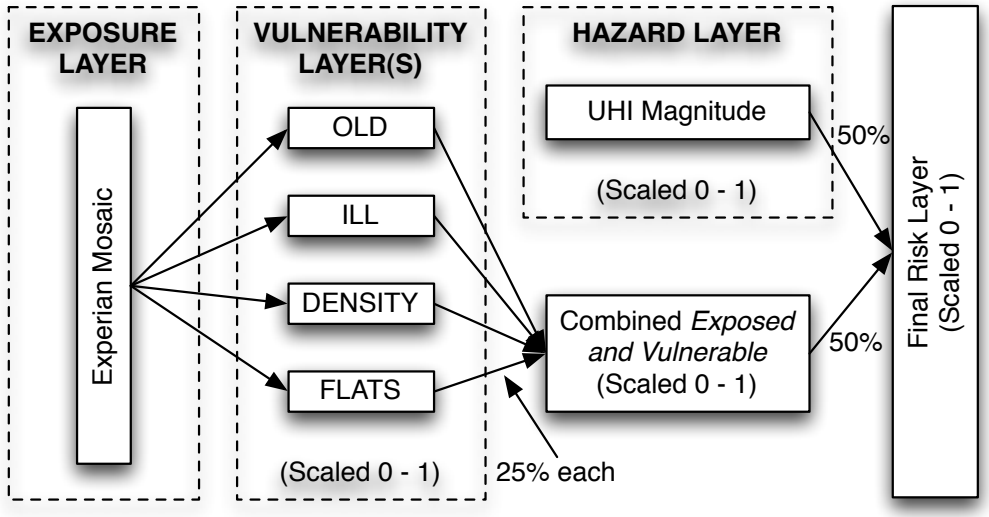

Figure 4.3: Detailed flowchart of spatial risk assessment methodology.

4.3 Results and discussion

When interpreting the results it is important to note that when generalising at the LSOA scale, some data will be masked in a small number of cases. For example, the Sutton Park area in the north of the city that contains the actual park has to be extended to include an area with approximately 1,500 people in order to match the LSOA geography. As this LSOA is physically one of the biggest by area within Birmingham, maps can look skewed.

4.3.1 Spatial trend between the sUHI and exposed and vulnerable

The night sUHI under heatwave conditions at LSOA level (Figure 4.4) reflects the results from chapter 3 and gives confidence that the generalisation to LSOA has not compromised the dataset. A full discussion of the spatial trends is available in chapter 3 but in summary, the highest temperatures are found in the city centre whereas the Sutton Park area in the north of the city is the coolest area. As expected, there is a general trend towards lower temperatures in the suburban areas.

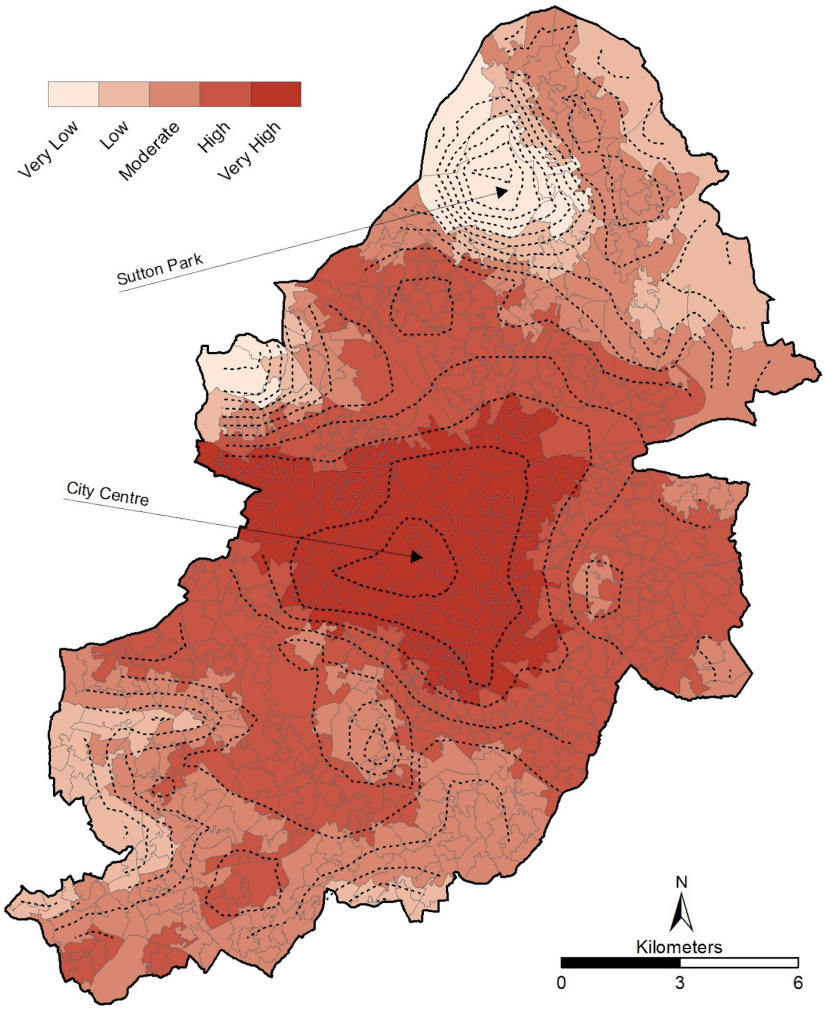

Figure 4.4: Birmingham sUHI under heatwave conditions at LSOA level.

The four main "exposed and vulnerable" layers were displayed in a GIS with natural breaks (Jenks) symbology (Figure 4.5) in order to view groupings inherent in the data. Concentrations

of old people are scattered throughout the city, with distinct clusters in the north. This is not surprising as the northern Sutton Coldfield area is generally regarded as having a slower pace of life, with close proximity to countryside being appealing to the older generation. This also helps explain the lack of elderly people in the city centre, where they are conspicuously absent. There are additional concentrations of older people in the east and towards the south.

Conversely when looking at flats, there is a significant concentration in the city centre, a result of high land costs forcing the development of high rise flats. This property type is unappealing for the majority of elderly people, given the difficulties of access (e.g. steps / lifts) and greater noise levels. Away from the centre, there are other LSOA's with high levels of flats, including small numbers in the north, and even less in the south. For example, clusters can be found in student areas, such as the high rise student housing located on Birmingham City University campus (Area Z, Figure 4.5).

There is less of a visible range when looking at density (detailed in HH per km^2). Again, the highest density LSOA's are located in the city centre, extending north westwards into areas renowned for having a high immigrant population. Conversely, density reduces heading south from the city. For example, Edgbaston (Area Y, Figure 4.5) is an affluent area that also includes the University of Birmingham, Edgbaston golf course and other land uses not associated with households. The north east quarter of the city centre (Area N, Figure 4.5) is also low density, and is an area traditionally associated with industry. However, the overall density levels across the city are generally similar, with local variations between LSOA's dependent on the presence of greenspace (which increase the size of the LSOA area but not numbers of HH).

Finally, significant concentrations in the spatial pattern of people with ill health exist. This is particularly evident across the city centre and in a belt north east of the city centre and towards the cities eastern edge. Pockets are also visible in the south, after noticeable lows in the affluent area of Edgbaston and the transient student population of Selly Oak (Area S, Figure 4.5), who are unlikely to stay in the same place long enough for reliable health statistics to be compiled.

A Spearman's rank order correlation was carried out to determine the statistical relationships between each "exposed and vulnerable" group and the sUHI at the LSOA level (*n=641*). Table 4.3 shows that the results generally agree with the visual interpretation and all relationships are statistically significant ($p < 0.01$) except density vs flats. This lack of correlation may be due to the high number of flats in the city centre, where density is low because significant

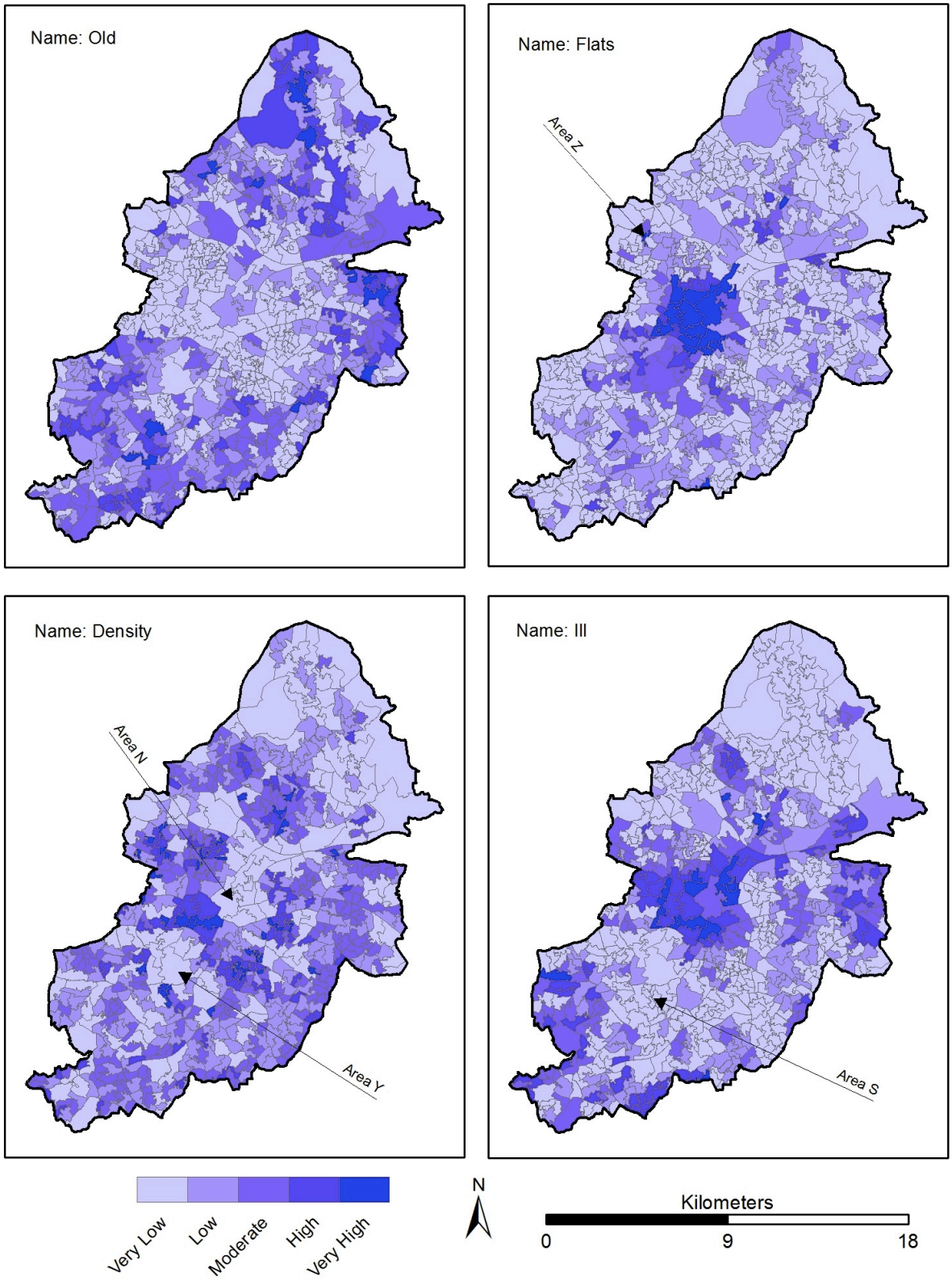

Figure 4.5: Four exposed and vulnerable layers at LSOA level.

LSOA surface coverage is commercial, not residential HH. There is a weak positive correlation between density, flats and illness with the sUHI, showing that as the sUHI increases, the number of "exposed and vulnerable" groups also increases. There is a stronger negative correlation between old people and the sUHI that agrees with the visual interpretation already discussed.

Table 4.3: Spearmans rank correlation coefficient matrix.

	Density	Flats	Ill	Old
Density	-	-	-	-
Flats	0.058*	-	-	-
Ill	0.161**	0.254**	-	-
Old	-0.256**	0.241**	0.158**	-
sUHI (mean)	0.329**	0.125**	0.224**	-0.396**

* Correlation is not significant at the 0.01 level.
** Correlation is significant at the 0.01 level.

When the above four vulnerable groups are combined and equally weighted (Figure 4.6) it is clear to see that the very high risk areas are concentrated around the city centre. This is to be expected due to the individual distributions already discussed, and agrees with previous work in the USA which has found that vulnerability increased in warmer neighbourhoods (Harlan et al., 2006) and that these neighbourhoods had a tendency to be located within the inner city (Reid et al., 2009). Although equal weightings for all layers have been used in this study, it is recognised that features of urban form (e.g. density) can also act as predictors for the UHI. As a result, this can impact the output risk, and is an area that could be explored more in the future when considering different weightings for layers.

4.3.2 The final risk layer

Figure 4.7 shows that the majority of the "very high" risk LSOA's are grouped together in the city centre. It is here where the highest temperatures are experienced as well as the highest number of ill people, number of flats and density. However, additional pockets of "very high" risk also exist and these require additional explanation. As already discussed, a high concentration of flats increases the density of a LSOA. Outside of the city centre, these flats are frequently high rise social housing that is often associated with increased illness in the poorer sections of communities. A typical "high risk" pocket has significant high rise social housing which increases the density, scores highly for flat and often for illness as well.

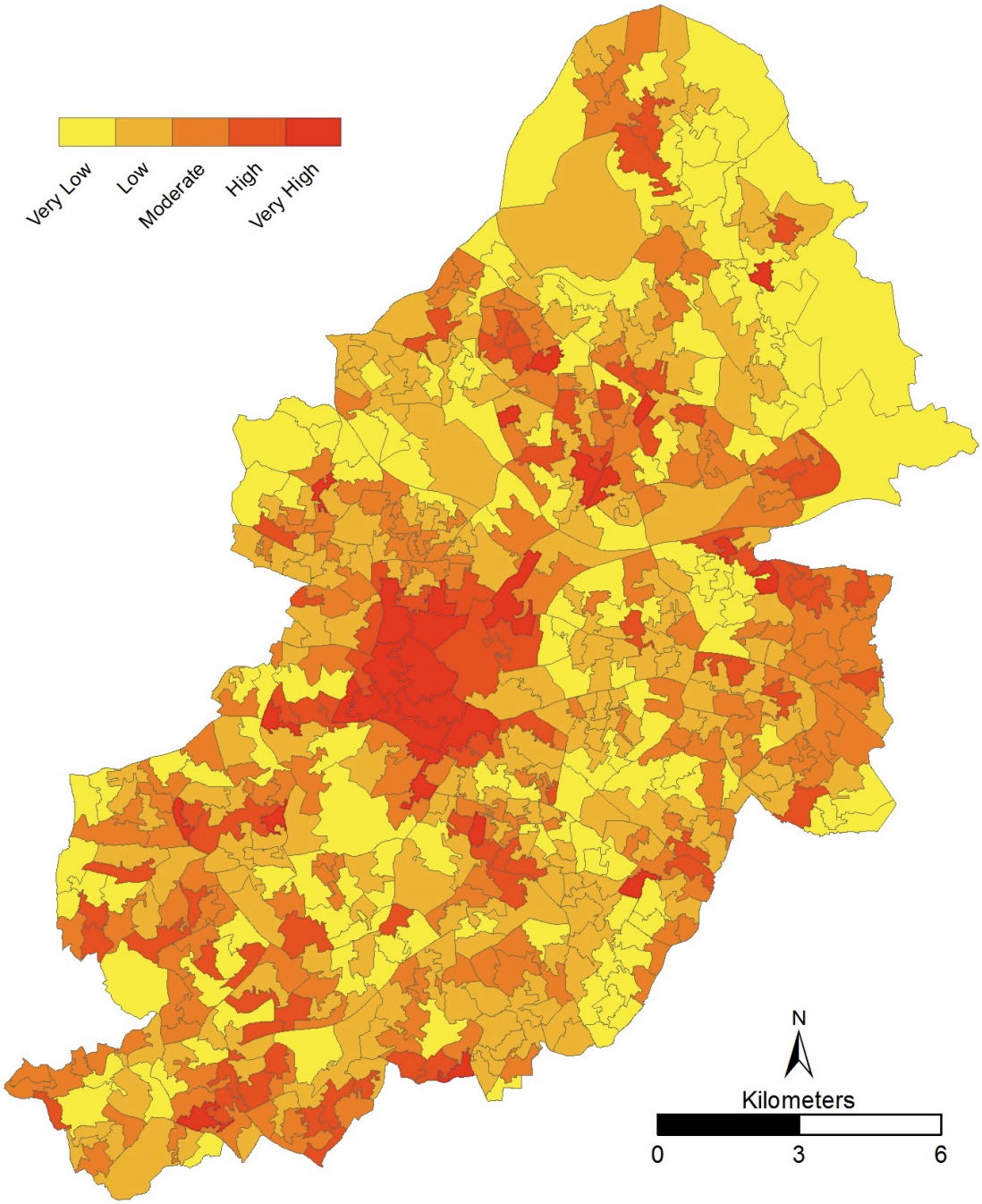

Figure 4.6: Combined (equal weighting) exposed and vulnerable layer at LSOA level.

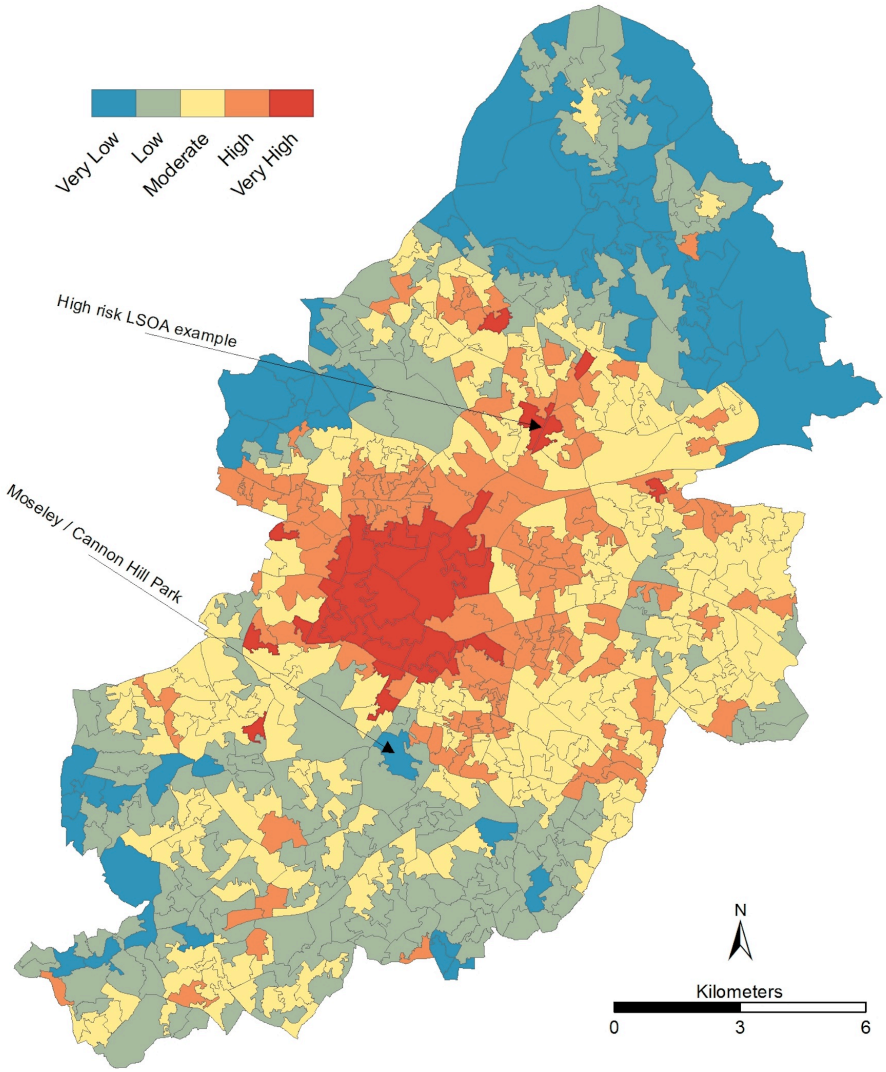

Figure 4.7: Final risk layer at LSOA level.

The lowest risk areas are found in the north west (Sutton Park area) and north east of the city. This is explained by the low and very low sUHI risk coupled with very low "exposed and vulnerable" populations. An anomaly of this area is that it actually has the highest concentration of elderly people, but they are less vulnerable to heat due to their distance from the city centre. Other very low risk areas are evident west of the city centre and scattered south of the city centre. In general these are heavily linked to greenspace; which has the dual effect of ameliorating the UHI and reducing the number of people living in an area. Indeed, a more explicit look at the distribution of greenspace within the conurbation could be useful (e.g. using surface cover analysis (Gill et al., 2008) or energy exchange models (Gill et al., 2007)), given the

benefits of reducing the UHI (Bowler et al., 2010) and improving health inequalities (Mitchell and Popham, 2008).

4.3.3 Household level

A strength of the methodology detailed in this chapter is that once the risk areas have been identified, a subsequent detailed analysis down to HH level can be conducted. Such high resolution work within urban areas is a logical development of previous broader scale work, such as the province wide analysis carried out in Quebec, Canada (Vescovi et al., 2005). A GIS was used to identify 37,477 HH's (or ∼8.76% of 427,914) that fall within the "very high" risk LSOA's (33 out of 641). These HH's can then be profiled using Mosaic type (Figure 4.8), which illustrates the vast majority are either 47 (Deprived view) or 64 (Bright young things), accounting for ∼7,000 HH each. This illustrates a clear divide within the "very high" risk area which is only able to be explored by having access to high resolution underlying datasets such as Mosaic.

> **Type 47:** "poor people who live in high rise blocks of socially owned housing... many have disabilities... characterised by extreme poverty".
>
> **Type 64:** "well educated young high flyers... live in smart inner city areas... mostly modern, purpose built or converted apartments".

Despite living in broadly the same area, the populations are generally separated (Figure 4.9) and are at polarised levels of heat risk. Type 64 typically live in new apartments located within the inner city. These dwellings may have good insulation, air conditioning or even passive cooling. This is a contrast to type 47, who live in older, social apartments located in less desirable areas surrounding the urban core. Unlike type 64, this group is unlikely to have the finances available to make themselves comfortable or safe.

4.4 Conclusions

This study has illustrated a simple methodology for quantifying risk, through a process where each stage can clearly be explained and understood. It offers suggestions for the output to be customised, for example with different weightings or replacement with different hazards

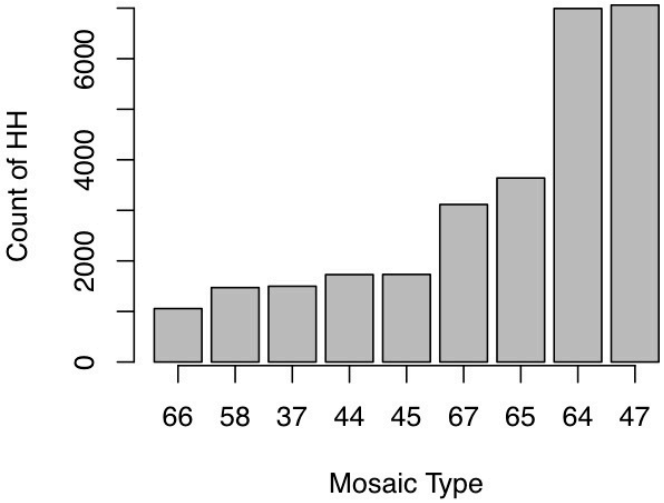

Figure 4.8: Mosaic type within "very high" risk LSOA.

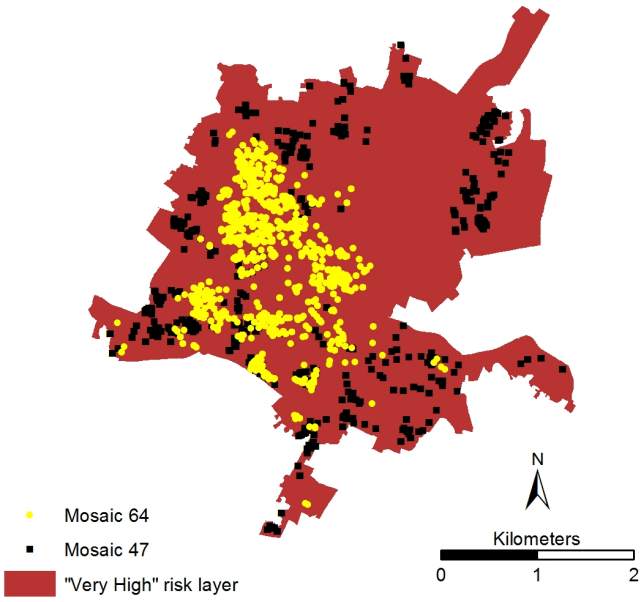

Figure 4.9: Mosaic type 64 and 47 spatial distribution within "very high" risk city centre area.

or risk groups as appropriate. This work offers the foundations for a spatial decision support tool that could be linked to climate change and projection models in order to consider climate change adaptation with a focus on heat health risks. Indeed, such data is potentially of great use to local authorities and health agencies when deciding on targeted campaigns, and the BUCCANEER tool (see subsection 2.2.3) makes use of data from this chapter.

The highest vulnerability is shown to exist in the inner city areas. This result agrees with similar work done in the USA (Harlan et al., 2006; Reid et al., 2009) and is a direct consequence of the increased temperatures associated with the UHI in this area. Furthermore, many of the root causes of the UHI (for example lack of greenspace, high anthropogenic heat output, significant built form) can be linked to vulnerable groups and therefore a feedback loop is created.

The simplicity of the methodology could be significantly refined through further research. For example, throughout this chapter no explicit temperature values have been mentioned. This is deliberate as the focus has been the spatial identification of risk groups. This work assumes that a single day "snapshot" of sUHI data is representative of varying conditions, but an alternative heat hazard layer could be developed using outputs from UHI models, which would allow for flexibility when considering varying conditions. Further work in section 5.2 quantifies potential temperature changes.

A significant research gap is the verification of the results, for example against health and mortality records in association with previous heat events (e.g. heatwave events in 2003 or 2006). This is the focus of ongoing work, but the data is presently not available at both a high temporal and spatial scale, which would be required in order to test for links at LSOA level. The data that is available is of limited utility as it is hard to quantify heat related health issues or mortality with any degree of certainty, and records have unreliable spatial attributes; in that they may relate to a patients home or to the hospital, and significant distances may be present between these. Hospital discharge data could potentially help quantify heat-related health admissions, although again the utility may be restricted due to small datasets and restricted availability.

In summary, the methods shown offer a repeatable methodology that can be utilised in many countries. This is made possible by the flexibility of a GIS based approach, the worldwide availability of the MODIS satellite data and the significant coverage of Experian's segmentation

data throughout the developed world.

4.5 Summary

This chapter has added a social dimension to the quantitative science detailing the areas of Birmingham that are warmer due to the urban heat island effect (chapter 3). High resolution data from Experian was valuable in identifying where people vulnerable to heat risk live in Birmingham. The spatial risk assessment methodology adopted helped clearly and transparently identify that in general, people vulnerable to heat risk live in areas of higher night sUHI magnitude. This is valuable information for local authorities, urban planners and the health sector. The methodology could be used to explore different hazards or risk groups, and further work could use different weightings to explore the relationship between hazard - vulnerability - exposure layers in more detail.

To increase the reliability of these results, the relationship between air temperature (directly associated with human heat risk) and land surface temperature (remotely sensed by satellites and used in this study) should be quantified. This area is the subject of section 5.1. Whilst this chapter offers a snapshot of heat risk, in order to help plan and adapt for future climate change, it is important to consider how temperatures may change. Future scenarios for urban climates are considered in section 5.2.

Chapter 5

Temperature comparisons and climate change

This chapter aims to explore two significant directions for further research, namely the relationship between land surface temperature and air temperature, and links with climate change projections. Both sections are closely related to the previous work and help put this thesis in wider context.

5.1 Comparing satellite land surface temperature and ground measured air temperature

This section aims to explore the relationship between remotely sensed land surface temperature and ground measured air temperature, to help understand how air temperature (the "standard" temperature measurement for stakeholders and meteorology / climatology) may differ to previous work based on land surface temperature.

5.1.1 Introduction

As discussed in subsection 2.1.5, the relationship between air temperature and remotely sensed land surface temperature (LST) is considered "the greatest unknown in remotely sensed studies of heat islands" (Nichol et al., 2009). Additional commentary is given in section 1.2. This thesis includes a remotely sensed study of the surface urban heat island (sUHI) (subsection 2.1.5), and this section aims to explore the "greatest unknown". LST is also an important variable for a number of other uses. These include calculating cooling degree-days (Stathopoulou et al., 2006), for input into models (Jin et al., 2007; Senay et al., 2007; Kim and Liang, 2010), exploring the impact of urban development on runoff (Herb et al., 2008) and soil surface moisture (Petropoulos et al., 2009) and more.

Whilst various studies have explored the absolute accuracy of LST from the MODerate resolution Imaging Spectroradiometer (MODIS) sensor (Snyder et al., 1997; Wan, 2002; Wan et al., 2004; Coll et al., 2005; Wan, 2008), work comparing LST to air temperature is limited. The relationship is clearly complicated, and studies have used techniques such as statistical regression (Jin and Dickinson, 2000; Yan et al., 2009), solar zenith angle models (Cresswell et al., 1999), GIS modelling (Cristóbal et al., 2008) and thermodynamics (Sun et al., 2005) to explore the relationship. Studies have explored daily maximum and minimum temperatures (Mostovoy et al., 2006), linked temperatures to Normalized Difference Vegetation Index (NDVI) (Nieto et al., 2011) and used a variety of ground based sensors including handheld thermography (Hartz et al., 2006) and mobile survey data (Yan et al., 2009; Fung et al., 2009).

There exists a need to understand this relationship between remotely sensed LST (T_{LST}) and ground air temperature (T_{AIR}), for example to validate remotely sensed sUHI studies (chapter 3) help heat health studies (chapter 4) or climate change adaptation planning, where stakeholders are used to dealing with and planning with air temperature data. Previous work has investigated the relationship over vegetated sites (Wang, 2008), accross multiple ecosystems in Africa (Vancutsem et al., 2010) and in mountainous areas (Boudhar et al., 2011), but a research gap exists over urban areas, where the greatest concentrations of people live. General validation of satellite data requires sites larger than a satellite pixel, with homogenous surface cover and flat topography, however these sites are rare and not representative of the urban environment. The relationship becomes increasingly difficult due to the heterogeneous urban

landscape, the variety at sub pixel spatial scales and general paucity of air temperature measuring stations.

This section illustrates the results from a project over the summer (June, July, August) 2010 exploring T_{LST} and T_{AIR} across Birmingham using a custom collection of air temperature loggers and MODIS LST data.

5.1.2 Methodology

Study area

As seen, the background to Birmingham has been given in section 1.6, but for this section it is important to note the city was instrumented with air temperature sensors as outlined below.

This instrumentation was done as part of a Knowledge Transfer Partnership (KTP) between the University of Birmingham and Central Networks, with the aim to look at temperatures in urban electricity substations / transformers and explore how these may alter with climate change. Temperature is a key determinate of both lifespan and efficiency for electricity transformers and substations, so an increased understanding is valuable for the owners of the electricity distribution network.

As such, this thesis had very little control over the experimental methodology, which was designed primarily for the KTP project aims and subject to budget and resource constraints. However, the resulting dataset was unique in its coverage of urban areas and of use as a pilot study. The sensor sampling frequency was set at 30 minute intervals, which was a balance between useful data and logistics of data collection. As the sensors are not enabled for wireless data transmission, a computer had to be physically attached to each sensor in order to download data. As this involved entering an electricity substation, risk assessments and approval from Central Networks was required and Personal Protective Equipment (PPE) needed to be worn. Collecting data from all the sites took $\sim$2 days.

T_{AIR} dataset

This work uses air temperature data obtained via a pilot study consisting of a collection of 28 stations, each containing two iButton air temperature loggers recording at 30 minute intervals across the complete summer period (June, July, August) 2010. The temperature loggers

are small (<20 mm diameter, <10 mm height) and economical (<£30 each), model DS1922L (full details are available online (Maxim, 2011)). The datasheet accuracy is +/-0.5°C between -10°C to +65°C. The temperatures experienced in Birmingham during the study period are well within this range. The distribution of sensors was such that there was a station in every Upper Super Output Area (USOA) (Figure 5.1), and more information is available (Prieto-Lopez et al., 2011).

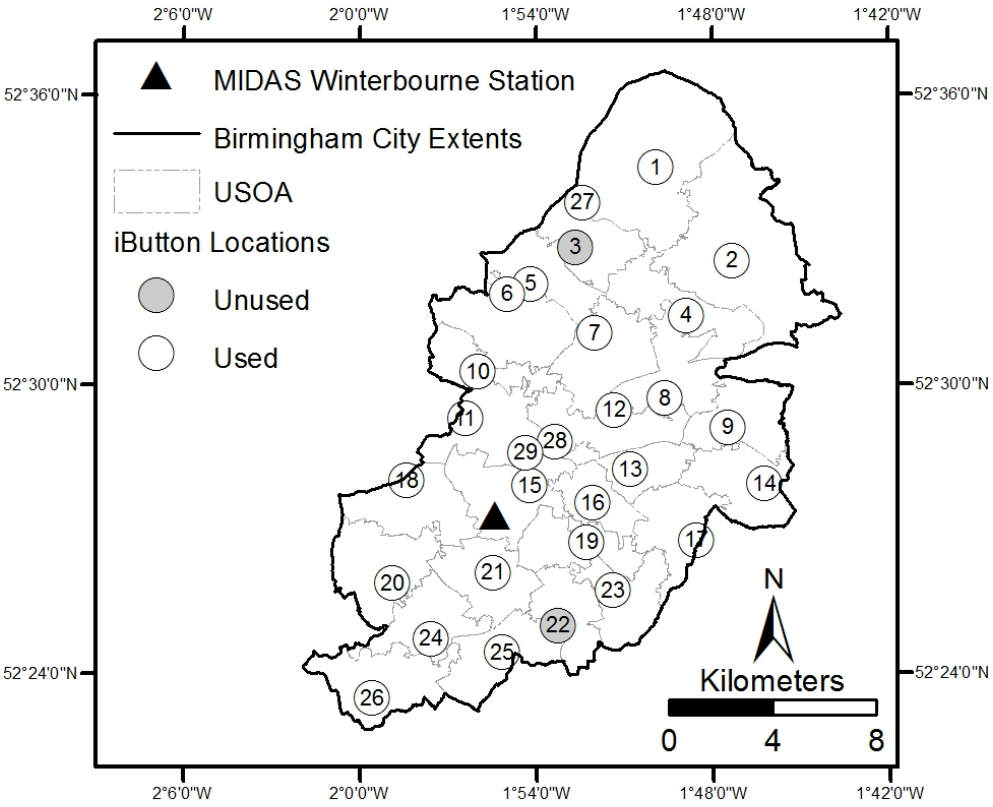

Figure 5.1: Location of Birmingham, iButton Sensors and Met office weather station.

Sensors were installed in pairs next to each other (Figure 5.2) with identical settings in order to check for anomalous data and to ensure that recording still continued if devices failed. Each pair of sensors was installed on the North corner internal wall of an electricity substation (Figure 5.3), because the KTP project required this data. These sites are also secure, to protect devices from vandalism (a problem in urban areas (Oke, 2006)). Prior to installation, all sensors underwent side-by-side comparison which did not show any anomalous data.

However, the effect of local micro-climates caused by being in a small fenced area, and the

Figure 5.2: Pair of iButton temperature loggers installed.

possible effects of variable substation transformer loading influencing temperatures is important to note as a compromise in this methodology. The smallest power (and therefore heat generation) substations were chosen to minimise this. Other data sources were considered, but as seen (subsection 3.2.1) Birmingham has a limited number of UK Met Office weather stations.

Figure 5.3: Example electricity substation.

T_{LST} dataset

Satellite LST data at ∼1 km resolution was obtained from the MODIS sensor on NASA's Aqua satellite. The same MYD11A1 (V5) product was used, as with chapter 3, and technical details are available (Wan, 1999). The Aqua satellite was used to ensure a night (∼01:30h) image that would not have the added complication of incoming solar radiation (important due to the lack of radiation shields on the sensors) and to enable comparison with earlier work in chapter 3 and chapter 4.

Images were selected for further analysis only when they contained 100% pixel coverage within the Birmingham area, as identified via visual inspection. This reduces the amount of images available because cloud cover is a limiting factor when dealing with thermal infrared sensors (see section 2.1). Both "LST_Night_1km" and "Night_view_time" scientific data sets (SDS) were processed in order to obtain LST and ascertain the time of the image acquisition to accurately match with T_{AIR} data.

MODIS data was used following a review of alternatives for satellite LST data (section 2.1) and successful use of MODIS data earlier in this project (chapter 3). Ideal data for this application would be higher resolution (90m) images from ASTER, but data was not available for the study area. It was hoped that airborne thermal flyover data could be used as a verification method for satellite LST data, and therefore as a proxy for T_{AIR}, however data was not available over the study period.

MODIS land cover data

The MYD11A1 (1 km based) product used for T_{LST} is derived from the MYD11_L2 (swath based) product that in turn uses the MOD12Q1 (Land Cover Type) product (details in Wan (2008, 2009)) to estimate emissivity values at each pixel. This was processed for the study area (Figure 5.4) in order to calculate if the underlying emissivity values used in the T_{LST} algorithm had a noticeable effect on the accuracy of T_{LST}. Mostovoy et al. (2006) discusses the importance of *a priori* emissivity data for accurate retrieval of T_{LST}. Further work on emissivity lookup from space (Snyder et al., 1998) has been developed into the V5 product, and details including emissivity values are available (Wan, 2008). Stations were grouped by landcover class and temperatures compared (section 5.1.3).

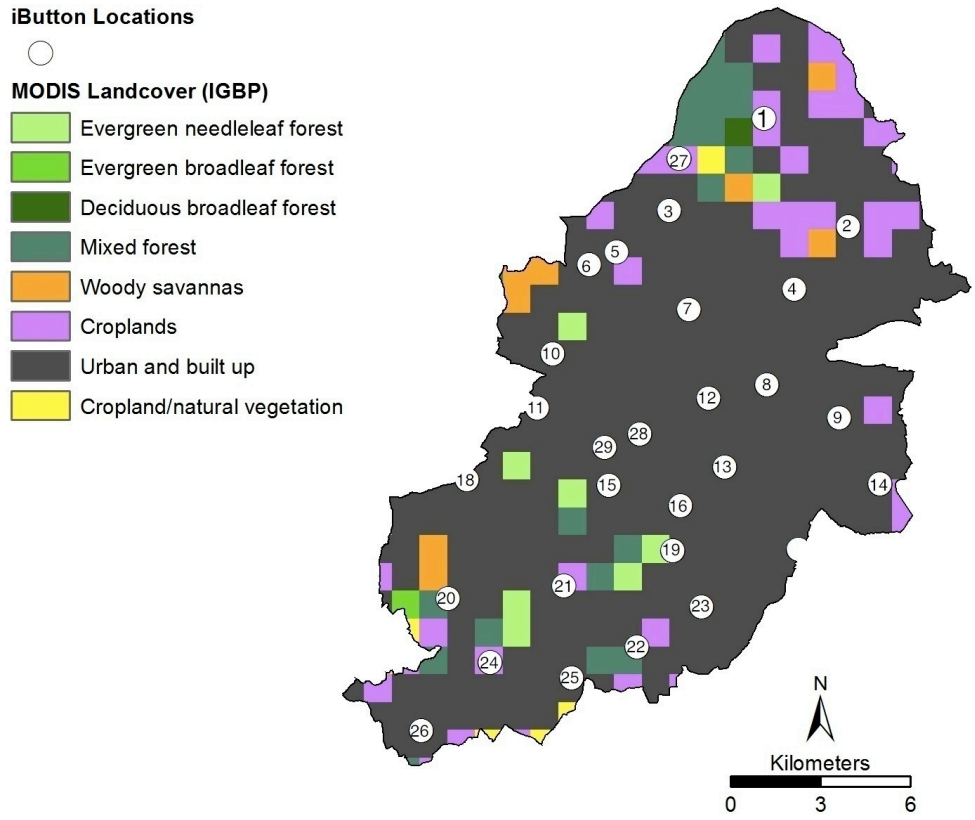

Figure 5.4: MODIS landcover across study area.

Data processing

A geographical information system (GIS) was used to extract LST data at each of the 28 point location where sensors were installed for each of the 13 study nights. No spatial averaging of adjacent pixels surrounding a point location was carried out as this would have increased the already sizeable spatial differences between point locations and ∼1 km pixels. For each image the exact timing of the MODIS image acquisition and hence T_{LST} reading was extracted from the "Night_view_time" SDS and converted to British Summer Time (BST) in order to match sensor data (Table 5.1).

For each station the two sensor readings were checked and averaged as a quality control stage (section 5.1.2). Then temperature data for each station was extracted at the nearest time to each image acquisition (Table 5.1). T_{AIR} and T_{LST} datasets were then combined in order to create a table suitable for analysis including T_{AIR} and T_{LST} data for 28 stations and 13 nights.

Table 5.1: Available MODIS images (*n=13*), timing details and Pasquill-Gifford classification.

Date	Julian Day	Time				Pasquill-Gifford Class
		MODIS (GMT)	MODIS (BST)	Nearest iButton (BST)	Difference (minutes)	
05/06/2010	156	02:42	03:42	03:30	-12	F
17/06/2010	168	01:24	02:24	02:30	+6	F
25/06/2010	176	02:18	03:18	03:30	+12	F
26/06/2010	177	01:18	02:18	02:30	+12	G
27/06/2010	178	02:00	03:00	03:00	0	F
28/06/2010	179	02:48	03:48	04:00	+12	F
03/07/2010	184	01:24	02:24	02:30	+6	F
05/07/2010	186	01:18	02:18	02:30	+12	E
06/07/2010	187	01:54	02:54	03:00	+6	D
11/07/2010	192	02:18	03:18	03:30	+12	D
28/07/2010	209	01:24	02:24	02:30	+6	E
11/08/2010	223	01:30	02:30	03:30	0	E
16/08/2010	228	01:48	02:48	03:00	+12	E

T_{AIR} and T_{LST} availability and accuracy

Across the study period the availability of T_{AIR} data was comprehensive, but comparisons are limited by the availability of T_{LST} data. The remotely sensed T_{LST} data is restricted by cloud cover, resulting in 13 images with 100% coverage across the Birmingham area (Table 5.1). This was reasonable and subsection 3.3.1 found between three and 15 clear sky images per year in the summer periods 2003 - 2009.

Each day (*n=13*) was assigned a Pasquill-Gifford stability class based on preceding 12 hours weather (14:00 - 02:00h) at Coleshill weather station (Table 5.1 and Table 3.1), the nearest station to have both cloud and wind measurement. It was hoped that more data would be available, with a more even distribution of stability classes, allowing an important detailed analysis of differences in the T_{AIR} - T_{LST} relationship under different atmospheric stabilities to be undertaken. Considerable change could be expected, as previous results (chapter 3) showed large changes between stability classes. However, given the low number of images this analysis has not been done in this study.

For data quality control the difference in the two sensors (IB1 and IB2) at the same location was calculated, for each study day and each station location. The majority of differences (*n=325* (13 nights x 25 locations (four stations removed)) in temperature between IB1 and IB2 were small ($>$ 85% are $<$ 0.2°C). The results show $>$ 95% of differences are $<$0.5°C (datasheet

accuracy of the iButton), giving confidence in the sensors. The remaining 5% are from location 22, where all differences are > 1°C, and three readings at other locations between 0.5 and 0.6°C. Location 22 was removed from analysis as the large differences were unexplained, and location three was missing data. Stations 25 and 29 only had one sensor so are not included in the averaging, but for the remaining 25 stations both IB1 and IB2 were averaged together for the same time period.

The maximum difference in timing between T_{LST} image acquisition and T_{AIR} temperature logging was 12 minutes (Table 5.1). This is not believed to be an issue because there is no incoming solar radiation.

5.1.3 Results and discussion

Comparison between T_{AIR} and T_{LST}

Plots (Figure 5.5 and Figure 5.6) comparing T_{LST} and T_{AIR} for all stations on specific nights (Table 5.1) show considerable variation between stations, but T_{AIR} is consistently higher. Across all cases (*n=348* (13 nights * 27 stations (minus 3 missing T_{LST} values))) T_{AIR} is higher than T_{LST}. Maximum temperature differences ($T_{AIR} - T_{LST}$) across all stations and all study nights was 8.55°C, minimum 0.23°C. The average temperature difference at individual stations varied between 1.67°C and 6.39°C which indicates significant station specific variability (Figure 5.7). Considering potential errors in the data of +/- 1°C for T_{LST} (Wan, 2002) and +/- 0.5°C for T_{AIR} (datasheet), in > 85% of cases the measured difference between T_{LST} and T_{AIR} is greater than the combined 1.5°C error.

The results show that it is very likely that actual observed air temperatures will be higher than T_{LST} at night, which agrees with other work (Jin and Dickinson, 2000) that found that T_{AIR} was higher than surface temperature for clear sky nights. However, the studies are not directly comparable given this study is over an urban area, whereas Jin and Dickinson (2000) was over grass and forest.

A brief comparison was undertaken between air temperature at the WMO weather station in the city extents (Winterbourne, see subsection 3.2.1) and the T_{LST} data. Comparison data was available for 11 out of the 13 study days, and the results are shown in Figure 5.5 as station 30, highlighted between vertical bars. Across all 11 days, the difference between T_{AIR} and

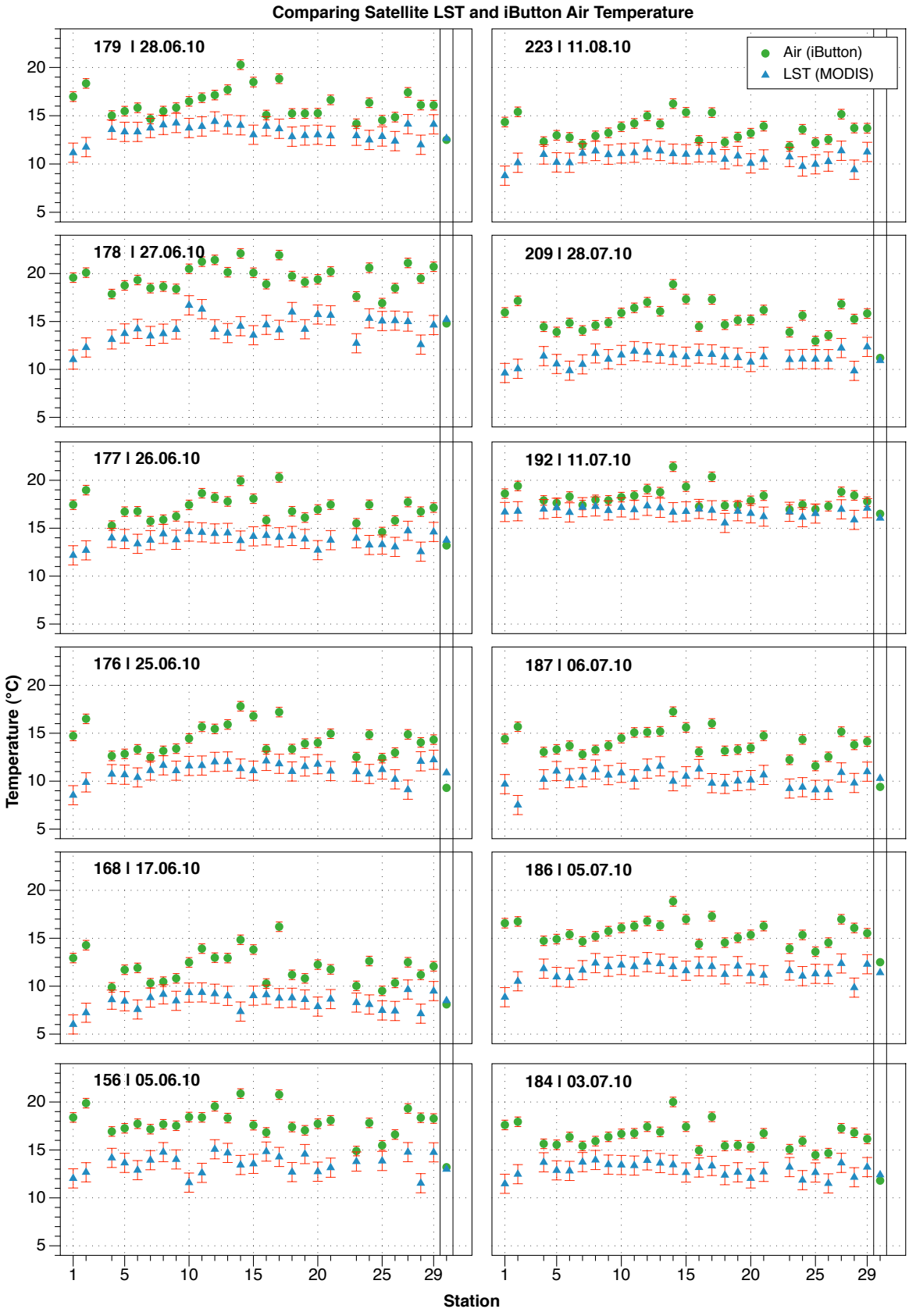

Figure 5.5: Plots of satellite LST vs iButton temperature for nights 1 - 12. Station 30 (between vertical lines) air temperature is Winterbourne (not available for 223).

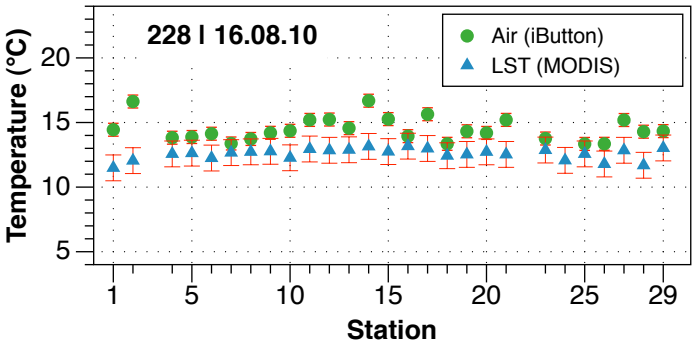

Figure 5.6: Plots of satellite LST vs iButton temperature for night 13. No data from Winterbourne available.

T_{LST} is small; generally < 1 °C. Results show examples of both higher T_{LST} temperatures (day 176 and 187) and higher T_{AIR} (day 186). Although the Winterbourne station results do not agree with the iButton results above, this is expected. The Winterbourne station is a Met Office station, subject to siting regulations which mean it is not representative of an urban area, as explained in subsection 3.2.1 and shown in Figure 3.2. The iButtons may be influenced by local microclimates in electricity substations, but further work is required to test this, which is the subject of the HiTemp project, and recommendations for changes in future work are given in section 6.4.

Regression analysis

Scatterplots of T_{LST} (range 6.01 - 17.33 °C) against T_{AIR} (range 9.52 - 22.11 °C) were plotted for each station, and all resulted in reasonably strong (range 0.72 – 0.98, standard deviation 0.056) positive correlation (Table 5.2). Linear regression was carried out using T_{LST} as the predictor variable and T_{AIR} as the outcome variable for each individual station (Table 5.2).

The slope, intercept and R^2 values from each of the 27 linear regression equations were examined spatially (Figure 5.7), with values displayed scaled over five equal intervals. The range of slope values is less variable (0.57 – 1.02) than either intercept or R^2 values and illustrates the unit change in T_{AIR} if T_{LST} increases by 1°C (all the slope values are statistically significant ($p < 0.05$)). These results are encouraging as the majority (90% $>$ 0.7°C) are close to 1°C which would mean an exact relationship. The spatial trend shows that the lowest values with the greatest inaccuracies (stations 1 and 2) are in the north, and this spatial trend continues across

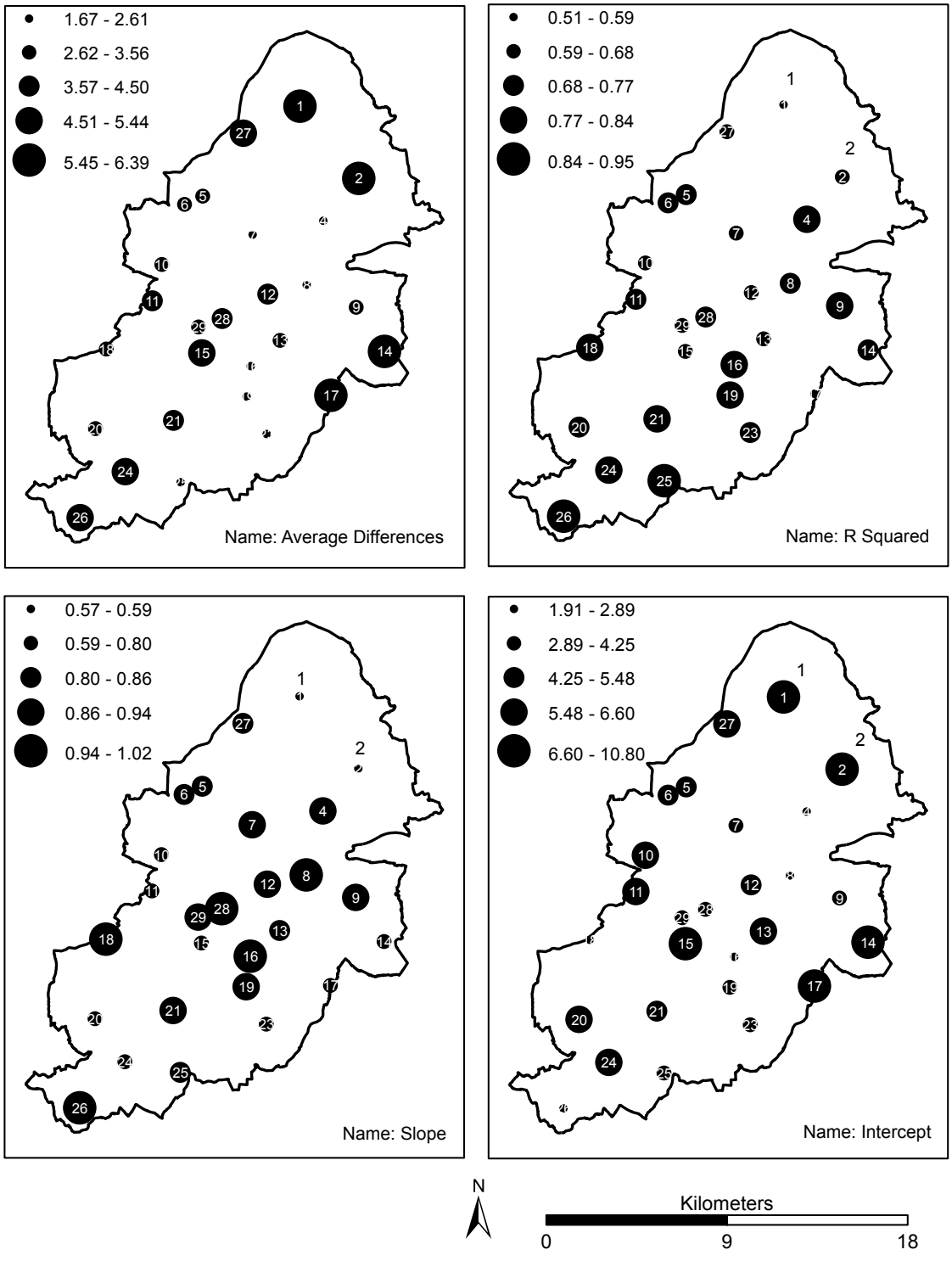

Figure 5.7: Spatial plots of average difference, slope, intercept and R^2.

Table 5.2: Linear regression equation details for each station.

Station	Intercept	Slope	R^2	Correlation (R)
1	10.28*	0.57**	0.51	0.72
2	10.80*	0.59**	0.65	0.80
3	n/a	n/a	n/a	n/a
4	2.89*	0.94**	0.78	0.88
5	4.94*	0.82**	0.74	0.86
6	5.48*	0.84**	0.76	0.87
7	3.35*	0.90**	0.68	0.82
8	2.23*	0.99**	0.77	0.88
9	3.99*	0.90**	0.81	0.90
10	6.03*	0.79**	0.67	0.82
11	6.60*	0.79**	0.71	0.84
12	5.37*	0.88**	0.65	0.80
13	5.71*	0.83**	0.68	0.83
14	8.88*	0.80**	0.73	0.85
15	8.32*	0.70**	0.63	0.79
16	1.90*	0.99**	0.80	0.90
17	8.21*	0.79**	0.59	0.77
18	2.48*	1.02**	0.83	0.91
19	3.99*	0.89**	0.77	0.88
20	5.96*	0.78**	0.74	0.86
21	4.61*	0.94**	0.84	0.92
22	n/a	n/a	n/a	n/a
23	4.25*	0.80**	0.72	0.85
24	6.36*	0.80**	0.80	0.89
25	3.60**	0.84**	0.95	0.98
26	2.78*	1.00**	0.93	0.96
27	6.18*	0.86**	0.66	0.81
28	4.06*	0.97**	0.74	0.86
29	3.58*	0.94**	0.67	0.82

* Not significant at the 0.05 level.
** Significant at the 0.05 level.

the intercept and R^2 values.

The intercept shows considerable variability with a range between 1.9 – 10.8°C (over 80% values <7°C), but all the intercept values are not statistically significant ($p > 0.05$). The intercept shows the estimated T_{AIR} if the measured T_{LST} was 0°C. There are potential inaccuracies in the intercept due to the small range of observed data, however larger figures represent greater inaccuracies. The largest values are again stations 1 and 2, and this may be partially due to the differences in measurement scales. Although measurement scales are the same across the study, in the case of stations 1 and 2, T_{LST} is measured over a ∼1 km^2 area that includes a large urban park (Sutton Park near station 1 - see Figure 3.1). T_{AIR} is a point location within the same ∼1 km^2 area, but with no electricity substations in the park it is placed in a nearby urban area

where temperatures are likely to be higher. Other stations are situated in more homogenous 1 km pixels. Although the lower values appear to be in the centre, station 15 is an obvious anomaly and makes it hard to draw conclusions.

The R^2 value indicates the amount of explained variability in T_{AIR} that T_{LST} can account for and ranges between 0.514 and 0.953 (51.4% - 95.3%). Given that T_{LST} does not take into account other variables such as wind, and is over a significantly larger area than T_{AIR}, R^2 would not be expected to be 100%. Figure 5.7 shows that the lowest values are again in the north (1 & 2), and the highest values (25 and 26) in the south interspersed with a similar spread of values throughout the rest of the conurbation. The low values in the north are likely low due to reasons already mentioned.

Link to emissivity via MODIS landcover

The MODIS landcover map (Figure 5.4) relates to pixel emissivity values used for LST calculation via the split window algorithm. Looking directly at pixels used for analysis (corresponding to sensor locations), most are "Urban and Built Up" (n=*23*), with the remainder (stations 1, 21, 24 and 27) classed as "Cropland" (n=*4*). Comparing average station temperatures split by landuse results in cropland stations (range = 3.88 – 5.73, average = 4.56, n=*4*) having a higher average temperature than urban stations (range = 1.67 – 6.39, average = 3.29, n=*23*), which is unexpected. T-tests between cropland and urban stations indicates the difference in mean temperature is statistically significant ($p < 0.01$). However, this should be repeated with a larger dataset before conclusions are drawn. A weakness of the MODIS data is that urban areas are generalised into a single landuse / emissivity class which cannot adequately represent the complex urban landscape.

5.1.4 Conclusion

This section develops understanding of the relationship between remotely sensed LST and air temperature across a city but it is clear that this area needs considerable continued research. There are numerous questions and problems; for example issue of scale, and the problems and inaccuracies of generalizing a $\sim$1 km^2 pixel (T_{LST}) to a small point location (T_{AIR}).

Whilst no clear relationship was found between T_{AIR} and T_{LST} at the city scale, site-specific

relationships were found to be good when examined in isolation. To develop relationships further other variables would need to be taken into account, including land use and meteorological conditions at the time of measurements. A detailed look into the underlying MODIS algorithms would also be required, and using raw emissivity data from MODIS or an alternative source may yield better results. Increasing the spatial resolution and quality of datasets related to urban areas (e.g. emissivity) would help a number of research areas. An ideal T_{AIR} dataset for this work would be accurate and / or have a high number of stations across the study area. A high number of stations, combined with a calibration network (e.g.full weather stations) would give greater strength to the data and hence results. Further enhancements to this methodology are given in section 6.4.

The result of consistently higher T_{AIR} than T_{LST} across an urban area at night acts as a validation for other work that has utilized MODIS data as a proxy for air temperature (such as chapter 3) and has important implications for heat health studies (such as chapter 4).

The necessity for security of air temperature sensors limits the locations they can be installed, but the location has a significant impact, for example city parks are under represented as no electricity substations are located within them. Using electricity substations also brings with it the risk that changes in transformer loading will alter the local micro climate, however transformer load data was not available to test this.

This work has acted as a pilot study for a much larger project (HiTemp) underway at the Birmingham Urban Climate Lab (BUCL). The HiTemp project is a larger sensor network that will measure T_{AIR} across Birmingham using 25 weather stations combined with over 250 air temperature sensors. This higher density T_{AIR} dataset would allow errors and anomalies to be identified more easily, allow comparisons against a greater number of T_{LST} pixels (and meteorological conditions / atmospheric stability), and increase the accuracy and utility of spatial interpolation techniques, therefore addressing a number of research gaps already identified. A PhD project is planned to explore this field in more detail.

Whilst the global coverage of remotely sensed LST data is becoming increasingly useful, research into the relationship discussed should continue as a better understanding widens the application of LST data to different audiences. Currently using LST data as a proxy measure for night time air temperature measurements can be justified if the limitations discussed are accepted, and it is acknowledged that further work is required.

5.1.5 Summary

This section has compared data from a custom air temperature collection with simultaneous measurements of LST from the MODIS instrument that was used earlier in the thesis to quantify Birmingham's sUHI (chapter 3). The results clearly confirm that this relationship is complicated, especially across a heterogeneous urban area with significantly different measurement scales. The result of note is that at night T_{AIR} is consistently higher than T_{LST} in this study. This has important implications when using LST data, or information derived from LST measurements, for example the sUHI of Birmingham (chapter 3) if the end users are not aware that T_{LST} differs from T_{AIR}.

The limited previous research in this area typically uses small existing datasets, or data from field campaigns over uniform areas. This is unrepresentative of urban areas where the growing majority of people live, therefore utilising a custom collection of air temperature sensors over an urban area has been a valuable exercise - despite the many questions left unanswered.

In the scope of this thesis, the results from this section will be used in section 5.2 to help put work from this thesis in context, and in the wider research community this study has been a useful precursor to larger projects such as HiTemp. It is hoped future work can address can continue research in this area.

5.2 Linking the sUHI to climate change scenarios

5.2.1 Introduction

The night surface urban heat island (sUHI) of Birmingham has already been shown to be considerable (chapter 3) and a number of vulnerable people are situated within the area of higher risk (chapter 4). A logical progression of this work is to link climate change to these results and predict what could happen in the future. Important information is introduced in subsection 1.3.1, namely that the UHI is not currently taken into account in current climate change models. The current approach, assuming that everywhere is a uniform surface with no urban component (e.g. "greenfields"), is likely to underestimate projected temperatures in urban areas, where the majority of people live. It has been described that if the variables influencing the generation of the UHI "do not change significantly in the future, then it is reasonable to add (UKCP09) projections of climate change to a baseline observed urban climate to get a future urban climate" (Jenkins et al., 2009, p.45). This section aims to explore this addition, and

discuss other changes that will influence future urban climate. For example it is also clear that society will change in the future and many cities will increase in size (see chapter 1), and work has suggested that areas of high UHI potential are also those with high population growth potential (McCarthy et al., 2010).

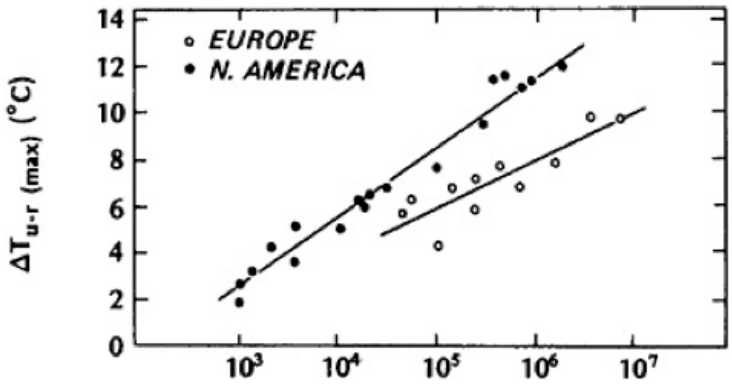

Figure 5.8: Relationship between maximum observed heat island intensity and population for North American and European settlements (Oke, 1987, p. 291).

Although Oke (Oke, 1987, p. 291) has shown that UHI increases with city size (Figure 5.8), it is also important to note that not all cities will increase in size. Although the global population is increasing, there are a number of "shrinking cities", and Emmanuel and Krüger (2012) study Glasgow, UK, as an example. The UHI is found not to decrease, despite city populations decreasing, as the urban fabric is still largely in place. Summer overheating is mentioned as a future possibility, but the main point is the potential opportunity for shrinking cities to reinvent themselves as energy and carbon efficient, utilising "spare" heat from the UHI e.g. for ground source heating. Zhu et al. (2010) have explored this further, finding the "extractable geothermal energy beneath Cologne [Germany] is 2.5 times the residential heating demand of the whole city".

The heat risk from heatwaves, such as the 2003 European heatwave has already been discussed (see section 1.1), and previous chapters have quantified the sUHI chapter 3 and explored where people vulnerable to heat risk live (chapter 4). It has been shown that it is "very likely that human influence has at least doubled the risk of a heatwave" of similar magnitude to 2003 since instrumental records began in 1851 (Stott et al., 2004). There are wider meteorological changes that may impact heat risk, for example increasing humidity may exacerbate the impact of extreme summer heat (Haines et al., 2006). It is important to note that increased

temperatures due to climate change may reduce winter deaths as extremes of cold are reduced (Langford and Bentham, 1995), but the literature is increasingly recognising that heat stress in the future will be aggravated by the UHI effect (Kleerekoper et al., 2011). A major research question is the rate that humans will adapt to a warmer climate (Haines et al., 2006). Human adaptation could mean that temperature thresholds are increased, however, there are also suggestions of limits to human adaptation (Sherwood and Huber, 2010). It is only recently that work is starting to look into linking problems of ageing populations and climate change, for example recent work in Australia (Harvison et al., 2011) discusses the failure of current policies to consider climate change alongside the ageing population, despite both being well known. Luber and McGeehin (2008) discusses the UHI and demographic changes (e.g. ageing population) alongside climate change in terms of driving heat-related mortality, concluding that "heatwaves are a significant public health threat in the U.S".

Research is starting to incorporate urban features and climate models at a number of scales, from global (McCarthy et al., 2010) through national (Kershaw et al., 2010) to city scale (Wilby, 2008; Hoffmann et al., 2011). McCarthy et al. (2010) has integrated an urban land surface model in the Hadley Centre Global Climate Model (HadAM3) in order to explore urban effects alongside climate change at a global scale. Kershaw et al. (2010) offers an approach that calculates UHI from gridded temperature data, which could be combined with climate projections and weather generator data from UKCP09, working at a national scale.Wilby (2008) uses a general circulation model with statistical downscaling to project, at a city scale, London's future UHI and ozone concentrations. Hoffmann et al. (2011) used a statistical UHI model and regional climate model (RCM) data with statistical downscaling methods to explore the future UHI for Hamburg, Germany. Other methods are also being explored, for example outside of the UK work by Jin et al. (2007) is incorporating MODIS satellite data in the US National Center for Atmospheric Research (NCAR) Community Land Model Version 2 (CLM2) and other models.

Statistical downscaling techniques, using modelled UHI data alongside modelled climate change data via statistical methods, offer one way to link urban influences with climate change scenarios. However there is potential for problems when combining modelled data with other modelled data, of different spatial and temporal scales, with no reliable way to verify either dataset. UHI modelling (excluding climate information) is a significant undertaking, as illustrated by ongoing work such as Grimmond et al. (2010) which offers a comparison of 33 urban

energy balance models, finding that "in general, the simpler models perform as well as the more complex models based on all statistical measures" illustrating the complexities involved.

Downscaling techniques, to obtain or combine higher resolution information (e.g. urban climate information) from relatively coarse input data (e.g. climate change information from Global Climate Models or Regional Climate Models), will become more important in the future. This section aims to explore potential future changes using simple calculations based on data from UKCP09 and this thesis, namely Birmingham's sUHI and calculations between land surface temperature (LST) and air temperature. This will help place the previous work in context and acknowledge the limitations and scope for further research.

5.2.2 Methodology

Study Area

The general background to Birmingham has been given in section 1.6, but of particular note for this section Birmingham falls within the UKCP09 administrative region of the West Midlands (Figure 5.9), and the majority of Birmingham falls within UKCP09 25 km grid cell with ID 1429.

Met Office heat health risk

This thesis is largely considering the effect of increased heat, with a particular focus on health. The UK Met Office has a "Heat Health Watch" scheme (Met Office, 2012) that operates between 1st June and 15th September each year, with four levels of response based on threshold temperatures (Table 5.3). The thresholds "could have significant effect on health if reached on at least two consecutive days and the intervening night" (Met Office, 2012). When thresholds are passed, warnings are issued which are detailed online and sent to health professionals and social care workers.

- **Green - Summer preparedness and long-term planning**. This is the minimum state of vigilance during the summer. During this time social and healthcare services will ensure that all awareness and background preparedness work is ongoing.
- **Yellow - Alert and readiness**. Triggered as soon as the risk is 60% or above for threshold temperatures being reached in one or more regions on at least two consecutive days and

Figure 5.9: UKCP09 regions showing location of West Midlands.

the intervening night. This is an important stage for social and healthcare services who will be working to ensure readiness and swift action to reduce harm from a potential heatwave.

- **Amber - Heatwave action**. Triggered when the Met Office confirms threshold temperatures for one or more regions have been reached for one day and the following night, and the forecast for the next day is greater than 90% confidence that the day threshold will be met. This stage requires social and healthcare services to target specific actions at high-risk groups.

- **Red - Emergency**. Reached when a heatwave is so severe and/or prolonged that its effects extend outside the health and social care system. At this level, illness and death may occur among the fit and healthy, and not just in high-risk groups.

These thresholds are a useful baseline to compare with current and future scenarios. Birmingham sits in the West Midlands area, where two days with maximum temperatures greater

than 30°C with a night between where the temperature minimum is greater than 15°C would define a heatwave. Globally, the definition of heatwave is variable, for example with the World Meteorological Organisation (WMO) defines a heatwave when the daily maximum temperature exceeds the average maximum temperature by greater than 5°C for five consecutive days. The Met Office heat health watch values will be used as context for this work.

Table 5.3: Met Office Heat Health Watch threshold temperatures (Met Office, 2012).

Region	Day max (°C)	Night min (°C)
North East England	28	15
North West England	30	15
Yorkshire and the Humber	29	15
East Midlands	30	15
West Midlands	**30**	**15**
East of England	30	15
South East England	31	16
London	32	18
South West England	30	15
Wales	30	15

UKCP09 datasets

An introduction to UKCP09 has been given in subsection 1.3.1. The UKCP09 product contain a vast amount of climate change data, giving probabilistic projections for three different scenarios (low, medium and high) which correspond to the Intergovernmental Panel on Climate Change (IPCC) Special Report Emissions Scenarios (SRES), at a 25 km resolution (output of the HadRM3 Regional Climate Model), for a number of overlapping future 30 year time periods (2020s (2010-2039), 2050s (2040-2069), 2080s (2070-2099). They are measured against a baseline of 1961 - 1990, and whilst at the time of release offer the best information available, it is acknowledged that the projections are likely to change over time. They are designed to help long term planning, for example in the climate change adaptation sector, and have been used in research (Jaroszweski et al., 2010; Smith et al., 2011b; Andersson and Chapman, 2011), the public sector (various county councils including Devon, Hampshire, Kent, Oxford) and industry (e.g. Atkins using the weather generator for sewerage monitoring, Severn Trent doing climate change risk assessment) (UK Climate Projections, 2011b). UKCP09 offers reports of "standard" data and a user interface where variables can be changed, resulting in over a billion possible output data combinations.

There is a Weather Generator (WG), outputting a synthetic time series at a daily scale (not a future weather forecast) on a downscaled 5 km grid. This does not integrate any extra climate information, but can be used alongside the Threshold Detector (TD) to explore potential future events. The WG and TD have not been used in this work, but are discussed as a potential area for future work.

There are three main uncertainties in climate projections (Jenkins et al., 2009) despite the Bayesian probability methods allowing both model uncertainty and multiple emissions scenarios.

1. Natural climate variability e.g. changes in volcanic or solar activity that cannot be predicted.

2. Modelling uncertainty e.g. a less than perfect understanding of the processes being modelled, and an inability to verify outputs.

3. Future emissions uncertainty e.g. unknown future emissions and pollutants due to human choices.

It is explicitly stated that "the UKCP09 probabilistic projections do not include any recognition of urban land-use and there is no account of a potential exacerbation of Urban Heat Island effects under climate change" (UK Climate Projections, 2011c), however it is important to note that this may change in future generations of UKCP product as "the new generation HadRM3 model does include a representation of the Urban Heat Island by including in each grid square a score of urban-ness" (UK Climate Projections, 2011c). This new generation of model is again at 25 km resolution, so downscaling techniques combined with other datasets will be required in order to investigate at higher resolutions. This study uses 1 km^2 data alongside UKCP09 outputs in order to explore at a sub-city scale.

There are obvious general trends shown in UKCP09 that are of note for heat health related studies, such as "increases in the number of days with high temperatures are found everywhere....Increases in the number of 10-day dry spells across the UK are found" (Jenkins et al., 2009) however this work aims to look in more detail. Of particular interest to this study are the land based variables relating to "Mean daily minimum temperature increase" and "Change

in temperature of the warmest night (99th percentile of daily maximum temperature in a season)". These variables relate to minimum temperatures, typically measured at night, which aligns with the other research completed in this thesis. A limitation is that minimum temperatures do not match exactly with the ∼01:30h data used elsewhere in this thesis. However, UKCP09 data does not have specific times, and satellite data is limited by overpass time, so this limitation is not easily overcome. Future data from high resolution ground based sensor networks would improve this.

UKCP09 key findings for the West Midlands mean daily minimum temperature increase were tabulated (Table 5.4) from UKCP09 data available online (UK Climate Projections, 2011d). This data illustrates the mean night temperature increase for the summer (JJA) period, across the complete West Midlands region. This can be associated with typical sUHI conditions.

Table 5.4: Summer mean daily minimum temperature (°C) increase in West Midlands under different UKCP09 scenarios.

	Low			Medium			High		
	10%	50%	90%	10%	50%	90%	10%	50%	90%
2020s	0.6	1.6	2.8	0.5	1.5	2.8	0.5	1.5	2.7
2050s	1.0	2.4	4.3	1.1	2.7	4.8	1.4	3.1	5.3
2080s	1.1	3.0	5.3	1.8	3.9	6.8	2.5	5.0	8.4

The UK Climate Predictions User Interface was used to explore potential future scenarios. The variable "change in temperature of the warmest night" was used to explore potential extreme events in the future for the 2080s scenario. This variable is based on the 99th percentile daily minimum temperature for a season, and this approximates to one night per summer (JJA) season (UK Climate Projections, 2011a). This can be associated with maximum sUHI conditions, as the meteorological conditions for the warmest night are likely to correspond to periods of high atmospheric stability that have been shown to produce the highest sUHI magnitude.

sUHI data

Data for Birmingham's night sUHI was taken from section 3.3, shown in Table 3.3. Given the limitations of thermal satellite remote sensing in terms of continual data collection, it is difficult to quantify a "mean summer sUHI' as data is only available for some nights. The dominant

stability class was shown to be class E (subsection 3.3.1) "Slightly Stable" which can be used as a reasonable proxy for mean sUHI given the available data (2.27°C). The results from the "heatwave" example will be used as a proxy for future extremes (4.88°C).

It is important to note again the difference between sUHI and UHI, as explored in section 5.1. This found that air temperature was consistently higher than surface temperature, but with significant site specific variability. The mean value for T_{AIR} - T_{LST} was calculated to be ∼3.5°C, implying that air temperatures on average are 3.5°C warmer than measured LST, as used to derive sUHI. As already discussed (subsection 5.1.4) considerable further research would be required to accurately quantify the AIR - LST differences. The value of 3.5°C will be used in this work, with the understanding that there are considerable limitations and the figure is illustrative rather than absolute. Future work outlined in the conclusions section 6.4 offers ideas for continuing this research.

Modelling of the UHI is a considerable research area; see reviews (Masson, 2005; Martilli, 2007) and model comparisons (Grimmond et al., 2010). Continued modelling of potential future UHI scenarios will offer additional datasets to pursue this important area of interest. It is useful to note that UKCP09 is of limited use when trying to predict future UHI generation as it does not include key variables, for example it does not include a wind component which influences the UHI.

Current temperatures

To put this work in context it is useful to understand typical summer mean daily minimum temperatures for the West Midlands. The UKCP09 baseline (1961-1990) for summer mean daily minimum temperature for the West Midlands is 10.22°C (Met Office, 2011).

An extreme, for example, 26/27th June 2011 had extremely warm temperatures, and the minimum temperature for the morning of the 27th was 15.9°C as measured at Coleshill (UK Meteorological Office, 2006), the weather station used as a rural reference station (subsection 3.2.1). This night was noted as "uncomfortably warm, no lower than 19.9°C at Benson (Oxon)" (Eden, 2011), an interesting point to note as Benson is only ∼80miles from the Coleshill weather station yet was 4°C warmer. This disparity helps illustrate the limitations of studying one area and making wider generalisations.

5.2.3 Results and discussion

These results and discussions should be viewed with caution. An relevant concept is that of Wilby's "envelope of uncertainty" in relation to climate change adaptation (Wilby and Dessai, 2010). As Figure 5.10 illustrates, there is a "cascade of uncertainty" when different levels (or input data) are considered, leading to an increase in permutations (of results). When looking at the following results, the significant amount of uncertainty should be remembered, however the results should help put this thesis in context and provoke questions for future research.

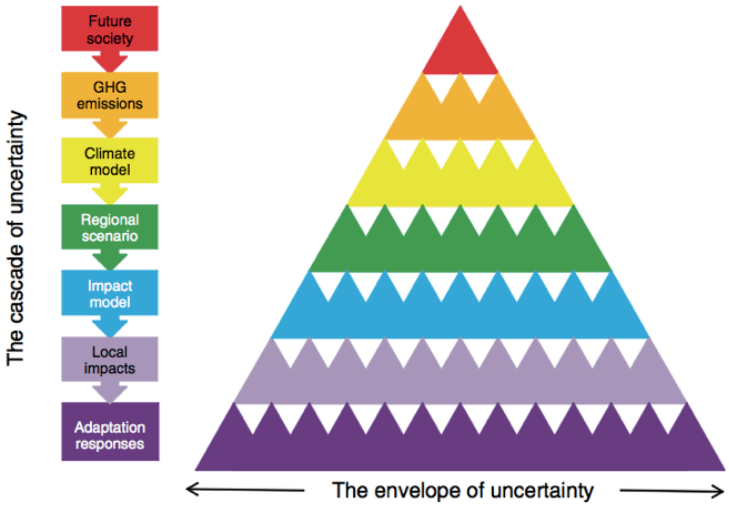

Figure 5.10: A cascade of uncertainty (Wilby and Dessai, 2010). Increasing number of triangles at each level illustrate the growing number of permutations and hence an increasing envelope of uncertainty.

UKCP09 data combined with sUHI data

The range of summer mean daily minimum temperature increase is shown in Table 5.4, with the central estimates varying between 1.6°C – 5.0°C (low emissions scenario in 2020s through to high emissions in the 2050s). This is a considerable range, but not unexpected given the large time periods and differing scenarios. Table 5.4 details the probabilistic data as 10% (very unlikely to be less than) through 50% (central estimate) to 90% (very unlikely to be more than) in standard UKCP09 terminology. The mean minimum temperature can be associated with a typical night. By the 2080s the increase under the central estimate of the high emissions scenario is 5.0°C, and it is very unlikely to be less than 2.5°C and is very unlikely to be more than 8.4°C.

It is clear to see this is a significant range, highlighting the uncertainty in climate predictions, although as expected the range for nearer timescales and lower emissions is smaller, for example 0.6°C - 2.8°C with central estimate of 1.6°C for 2020s low scenario. All the temperatures increase over time, emissions scenarios, and probability as expected, except the 2020s. Temperatures decrease (by 0.1°C) or stay the same through each scenario for the 2020s. These minor variations with no clear progression are to be expected in the near future, but given the small scale (0.1°C) and the "cascade of uncertainty" throughout this chapter it is not anticipated to cause an issue.

These temperatures are only associated with climate change; adding typical sUHI values increases these results.

Table 5.5: Summer mean minimum temperature (°C) increase with addition of sUHI class E.

	Low			Medium			High		
	10%	50%	90%	10%	50%	90%	10%	50%	90%
2020s	2.8	3.8	5.0	2.7	3.7	5.0	2.7	3.7	4.9
2050s	3.2	4.6	6.5	3.3	4.9	7.0	3.6	5.3	7.5
2080s	3.3	5.2	7.5	4.0	6.1	9.0	4.7	7.2	10.6

The calculated results if future mean daily minimum temperature increase based on UKCP09 outputs are added to sUHI measurements from dominant summer stability class E (detailed above) are illustrated in Table 5.5. This can be considered an estimate of future summer mean temperature increase in areas of high sUHI, for example the city centre. It is interesting to note that even the low scenarios in the 2020s has a 10% estimate (very unlikely to be less than) of nearly 3°C, and the 90% (very unlikely to be more than) estimate for high emissions scenario in the 2080s is over 10°C. These are significant temperatures when considering the baseline summer night minimum temperature is currently ∼10°C and the Met Office heat health night threshold is 15°C, and these are average results. Extremes are investigated below.

UKCP09 data combined with sUHI data and air temperature increases

The below (Table 5.6) illustrates the results from adding the average increase of air temperature over remotely sensed LST onto the UKPC09 mean summer minimum temperature with remotely sensed sUHI (Table 5.5). Whilst this calculation should be viewed with caution, it is important to include because it helps illustrate the significant uncertainty surrounding fu-

ture projections. It is logical to include the average difference between air temperature and remotely sensed temperature in order to compare similar values (e.g. air temperature). However, the addition of the air temperature correction factor is larger than the sUHI figures. As discussed earlier in the thesis, significant further work would be required to understand this with more confidence. Looking at Table 5.6 the scale of values is significant when compared to baseline minimum temperatures of 10.22°C and the Met Office heat health night threshold of 15°C. For example, the central estimate of the temperature increase is 10.7°C in the 2080s high scenario, which is higher than the current baseline temperature of 10.22°C. This implies that temperatures could more than double.

Table 5.6: Summer mean minimum temperature (°C) increase with addition of sUHI class E and air temperature correction.

	Low			Medium			High		
	10%	50%	90%	10%	50%	90%	10%	50%	90%
2020s	6.3	7.3	8.5	6.2	7.2	8.5	6.2	7.2	8.4
2050s	6.7	8.1	10.0	6.8	8.4	10.5	7.1	8.8	11.0
2080s	6.8	8.7	11.0	7.5	9.6	12.5	8.2	10.7	14.1

Considering extremes

A single "extreme" heatwave case was examined, using high emissions scenarios for the "change in temperature of the warmest night" and heatwave sUHI data, and the air temperature correction. The high emissions scenario was used to illustrate the likely maximum "extreme" cases. Table 5.7 show the results which as expected are considerably higher than previous results, as both the UKCP09 and sUHI data is higher. Considering that a warm night in 2011 had minimum temperatures of 15.9°C, the results estimate that in the 2080s under high emissions scenario, the temperature could be close to 30°C (15.9°C + 13.6°C). This nearly 90% increase is significant, and brings the night time temperature close to the current Met Office heat health watch limits for daytime temperatures. These results show that for both average and extreme scenarios, temperatures may increase by approximately 100%.

Work has shown that on a global scale change in excess mortality due to heat stress may increase by 100% - 1000% dependent on country, assuming no adaptation or acclimatisation takes place (Takahashi et al., 2012). This agrees with work by Wilby (2008) which also shows

Table 5.7: UKCP09 high emissions change in temperature of warmest night with addition of sUHI and air temperature correction (°C).

	High scenario 50% estimate		
		+ sUHI	
			+ air difference
2020s	1.5	6.4	9.9
2050s	3.4	8.3	11.8
2080s	5.2	10.1	13.6

increasing risks to human health in urban areas, and helps put questions of human adaptation in context – by the 2080s are humans capable of adapting to such temperature increases? What can be done to help adapt to the situation? Future extreme temperatures may put considerable pressure on human populations, and our response is hard to envisage.

Scale

The temperature scale of these potential changes is important to note, especially as there is limited work available to quantify thresholds. However recent work looking at Paris in the heatwave of 2003 suggests that mortality risk for old people doubles with a $\sim$0.5°C LST increase (Dousset, 2011). Issues of spatial scale are relevant, and the impact of urban scales compared to modelling scales is important. This is a subject mentioned above, and downscaling methods and incorporation of datasets of significantly different spatial scale is an ongoing research area. However, Jin et al. (2007) points out that the collective impact of all the global urban regions is unknown, so although the impact of a single urban area on global climate may be small, this work should also be considered at the global scale.

5.2.4 Conclusion

There are a considerable unknowns relating to the future UHI which the above calculations cannot take into account. Simple addition is basic but gives an idea of scale if things were to continue "business as usual". Physically the size of a city is likely to change over time, alongside considerable change in the built form, which will have a significant impact on the UHI. The increasing recognition of urban greenspace and green roofs (Lazzarin et al., 2005; Feng et al., 2010; Williams et al., 2010) may have a positive effect in terms of reducing the UHI

if they are implemented widely. Alongside these physical changes, the social fabric of a city will also change in ways that are hard to predict.

Individual cities are unique, and some will grow outwards, whereas others will be constrained by physical features (e.g. mountains) or legislation (e.g. development limits) which will put increasing pressure due to a rising population in the same area. These changes will influence where vulnerable people live, for example over time the poor inner city areas may be redeveloped into more affluent areas, displacing the more vulnerable to areas outside of the maximum UHI. These kind of changes will be difficult to predict and plan for, despite the efforts of urban planners.

The anthropogenic heat output of a future city is another variable that is hard to predict, yet influences the UHI. Anthropogenic heat release is linked to energy supply and use, particularly from buildings and transport. New, greener, renewable, more efficient power sources and decreased reliance on the combustion engine may decrease anthropogenic heat output, or conversely, increased fossil fuel use and needless consumption may increase anthropogenic heat output. Regardless, anthropogenic heat output and its associated influence on the UHI and urban temperatures is likely to change in the future.

Feedback loops that can be predicted e.g. increasing temperatures fuelling the increased use of air conditioning units and corresponding power increase will mix with feedback loops that are not yet known or understood. This work has been considering outdoor temperatures, but of significant importance is indoor thermal comfort, which is a separate research area in itself.

Future work should look in more detail at the above figures and could use the UKCP09 weather generator and threshold detector in order to help quantify the future recurrence of extremes such as heatwaves. Research is underway at Birmingham University looking at the "Impacts on Health of Heat Waves in UK Cities Enhanced by Climate Change and the Urban Heat Island Effect", which should seek to address a number of the issues raised in this section. However, the complexity in undertaking future hazard and vulnerability assessments which has been identified in this section and other research (Oven et al., 2012) is a problem without an easy answer.

5.2.5 Summary

This section has used simple addition of UKCP09 climate change scenarios, measured night sUHI data, and example air - LST relationships to consider the scale of potential future changes in urban temperatures. The work highlights the considerable uncertainty when trying to incorporate datasets of varying accuracy, scale, timing and origin in order to consider future changes in urban temperatures that may increase heat risk. In placing the work contained in this thesis in wider context, bigger questions are asked. For example, will humans adapt to future night temperatures which are as warm as current daytime heatwave alert threshold temperatures?

The limitations presented, such as the use of surface temperatures which are not incorporated in climate projections, via a basic relationship with air temperatures which are included in climate projections, offers considerable scope for improvement through further research. Surface temperatures are an easily accessible global dataset, therefore an improved way to link them with climate projections would be valuable.

The results should be taken as illustrative, but in spite of the large "envelope of uncertainty", it is clear that urban temperatures are likely to increase significantly in the future, and there is very little understanding of both the physical and human adaptation processes that will happen alongside these changes.

Chapter 6

Conclusions

The focus of this thesis has been to investigate urban heat health risk spatially for the city of Birmingham in the UK. This work has been carried out using various datasets, including remotely sensed land surface temperature, commercial social segmentation data, ground measured air temperature from a custom sensor collection and climate projections from UKCP09 that has no urban component. Research and analysis using each dataset individually offers interesting results, but it is the combination of multiple datasets from a variety of disciplines in this thesis that has enabled the spatial risk of urban heat health to be investigated.

6.1 Fulfilment of aims of the thesis

This thesis had four main objectives, introduced in section 1.7. Each objective is detailed below, with a short discussion summarising the outcomes in relation to this thesis.

1. Measure the magnitude and spatial extent of the Birmingham surface urban heat island using remotely sensed land surface temperature data to create a simple and repeatable methodology that increases the spatial resolution of previous work.

This thesis measured the magnitude and spatial extents of the Birmingham surface urban heat island (sUHI) in chapter 3. This work resulted in a quantified night sUHI for Birmingham, derived from MODIS remotely sensed land surface temperature data. At a 1 km resolution, this work significantly increased the spatial resolution when compared to previous work which was typically limited to measurements from a pair of weather stations, or limited fieldwork.

This data was cross referenced with a ground reference station in order to consider the influence of different meteorological conditions; a particularly novel aspect of this thesis. Under "neutral" conditions, the sUHI magnitude in the city centre was $\sim$1.5°C but under heatwave conditions, this increased to $\sim$4.5°C. The use of a categorisation scheme (stability classes) is a strength of this thesis that future work should seek to include.

This methodology used easy accessible remotely sensed data with global coverage means it could be repeated elsewhere. The dataset from this chapter, namely a quantified night sUHI of Birmingham, was subsequently used as an input to the following objective, and is being used for ongoing research at Birmingham University relating to UHI modelling verification. The results of chapter 3 have been published in the "International Journal of Climatology" (Tomlinson et al., 2012a) which already has four citations.

2. Spatially identify sectors of the population vulnerable to heat health risk for combination with surface urban heat island data to determine if vulnerable people are concentrated in areas with greater urban heat island magnitude.

The exploration of vulnerable people was detailed in chapter 4. This work considered social data at an extremely high household level resolution in order to spatially identify vulnerable sectors of the population. This was combined through a spatial risk assessment methodology with night sUHI temperature data obtained from chapter 3.

This work determined that in Birmingham, generally vulnerable people are concentrated in the area with greatest sUHI magnitude, although the exact vulnerability of the population was mixed throughout the warmest areas. The warmest areas contain both high risk and low risk populations which is only quantifiable due to the use of new datasets in this area. This work also identified high risk pockets elsewhere, as well as sections of the city that were low risk. A strength of this chapter is the high resolution scale of the data, allowing work to identify

vulnerable houses at risk if required, but the flexibility to aggregate to lower resolution data for dissemination without breaching privacy or data protection legislation.

The dataset from this chapter, namely a heat health risk map for Birmingham alongside a transparent and modifiable method for creating the final risk map, has been used by other work at Birmingham University considering climate change adaptation. This work resulted in a publication in the "International Journal of Health Geographics" (Tomlinson et al., 2011) which already has four citations.

3. Determine how remotely sensed land surface temperature relates to ground measured air temperature in order to validate the use of satellite data for meteorological research including surface urban heat island studies.

Heatwave definitions and heat health risk work require information on air temperature, but land surface temperature data can be easier to obtain at greater spatial scales, as shown by objective one. Therefore it was necessary to compare land surface temperature and ground measured air temperature, which was the subject of section 5.1.

This used a pilot collection of air temperature sensors (iButtons) across Birmingham combined with remotely sensed land surface temperature from MODIS to tentatively conclude that LST measurements are consistently lower than air temperature measurements at night over the urban area of Birmingham in the summer. There was considerable site specific variability within the comparisons, with the range of temperature differences 0.23 °C - 8.55 °C. However when examined in isolation, site specific relationships were found to be good.

This work helped validate the use of satellite data for meteorological research, but highlighted problems and weaknesses which require more work to be understood. A strength of this work is that it clearly highlights the difficulties in measurements over urban areas, but underlines the importance of pursuing this research avenue. Further research at the University of Birmingham is helping to address this; the HiTemp project will develop an enhanced air temperature dataset which could be used to explore LST relationships in more detail. This work was presented at the "International Symposium on Remote Sensing of the Environment 2011" and subsequently expanded and published in "Remote Sensing Letters" (Tomlinson et al., 2012b).

4. Consider how future urban temperatures may change when the surface urban heat island is included in climate change projections. Explore the scale of changes and other influences on heat health risk.

Urban areas are not currently included in UKCP09 climate change projections, requiring additional data and methods in order to integrate urban effects. This final objective was addressed in section 5.2, and used UKCP09 climate change projection data alongside sUHI data from previous chapters to add context to the thesis.

Results showed that whilst there are considerable questions around future temperatures and adaptation, the scale of change could be significant. For example, in extreme events in the 2080s, the night summer minimum temperature could be nearly as warm as the current Met Office heat health watch threshold daytime temperature (30 °C). This is a nearly 90% increase on current conditions, which is a considerable increase and their may be numerous impacts. Considering normal UHI conditions under the medium scenario in the 2050's the summer mean minimum temperature increase is over 8°C.

Despite raising numerous questions that cannot be answered easily, this section illustrated the importance of including the sUHI in climate change projections as it can make a significant difference to urban temperatures, where the majority of people live. This work was presented at the "Royal Meteorological Society Student Conference 2011", and subsequently invited for submission to the publication "Weather". This has been accepted and is currently in press.

6.2 Critique of thesis

There are a number of uncertainties in the methodologies used in this thesis. These can be broadly split into accuracy of data and validity of methodologies, and for both there are a number of issues and questions that arise. These have been discussed throughout this thesis, but this section briefly outlines the main areas of interest. The multiple peer-reviewed publications arising from this thesis have been discussed in section 6.1, which has ensured rigorous and defensible scientific work, despite the critique outlined below. Plans for future work are discussed in section 6.4 which address many of these shortcomings.

6.2.1 Data

This thesis has relied upon numerous datasets, and therefore the validity of the research is directly related to the quality and accuracy of these input datasets. Remotely sensed MODIS data has been used as a core dataset, upon which further work has built upon. The MODIS data used measures land surface temperature at a relatively coarse resolution ($\sim$1 km), and is affected by atmospheric conditions. However, following a comprehensive review, MODIS was deemed the most suitable dataset. Stringent checks were put in place to ensure the most accurate data was used, but this restricted the size of the dataset available (e.g. cloud cover restricting the number of available images). The default MODIS algorithm was used for deriving LST, and algorithm work (e.g. altering emissivity values) was not considered due to the difficulties in obtaining and verifying alternative data. The accuracy of MODIS data has not been extensively tested over urban areas, and the 1 km scale and the variety of groundcover in a heterogeneous urban area is a limitation of the current approach.

Commercial social segmentation data has been used from Experian to add a spatial aspect to human vulnerability. This data is comprehensively checked and rigorously developed by Experian, however the underlying datasets and methodologies are not available to inspect. The most recently available annual data was used at the time of research, but the dataset is updated regularly and it would be possible to easily integrate the most recent data when available. Despite the detailed nature of this data it would be useful to have additional information, for example on young children, in order to spatially assess their vulnerability.

Air temperature has been used from both Met Office stations and a custom collection of air temperature sensors. Coleshill, the Met Office station used as 'rural' reference station, was assumed to have generally the same conditions (e.g. windspeed, cloud) as the rest of the city for Pasquill-Gifford stability classification. This is reasonable and the only option available to obtain required cloud cover and windspeed data. The collection of iButton air temperature sensors installed within electricity substations is contentious because of the potential for the results to be influenced by local microclimates within the substation, for example increased temperatures when the transformer is under high load. This was the only feasible location for installation given the security risks in urban areas. The data was checked across two devices, and quality control checks did remove some erroneous data. The field of urban climatology

is gaining traction in Birmingham, with recently funded projects such as HiTemp (see subsection 5.1.4) installing extensive networks to increase the resolution of much required datasets, and developments including a new city centre weather station illustrating the cities commitment. Such advances are increasing the amount and quality of data available for such research in Birmingham, which has the capability to positively impact future work.

The UKCP09 climate change projections data used to illustrate potential future change are the most upto date and scientifically defensible climate change data for the UK, but do not take into account urban areas. However as discussed in section 5.2, climate change research is ongoing and the probabilistic data illustrates the considerable uncertainty in this field, and there are no other realistic or sensible options in terms of UK climate change projection data. This thesis was sure to explicitly discuss the uncertainty to ensure readers are aware of the situation.

6.2.2 Methodologies

There are a number of methodologies used in this thesis, both quantitative and qualitative. This thesis only used Birmingham as a case study area. Whilst some of the findings could be generalised to cities elsewhere, much of the work is only of relevance to Birmingham. However, the methodologies introduced were designed to be replicable elsewhere, for example globally for the remotely sensed sUHI work, and in any developed nation with available customer segmentation data for the risk assessment work. The main limitations to replicability are linked to the scales of available data, for example small settlements may not have enough satellite coverage for meaningful results.

The UHI has been a major area of focus throughout this work, and the measured surface UHI has been used to estimate the air UHI. However, the work exploring the relationship between LST and air temperatures has many concerns and difficulties, in particular due to the heterogeneous urban landscape and the differences in scale. This limitation has been discussed and emphasised throughout the thesis, and it is felt that sufficient explanation and reasoning around the limitations has justified including this important work, highlighting the lack of understanding between surface and air temperatures in complex urban areas. Future increases in data availability will help develop methodologies to address this. Recommendations for

changes in the experimental design are given in section 6.4.

Throughout the thesis only night temperatures are considered, leaving daytime temperatures as a significant gap. Data was not available for a daytime study, and incoming solar radiation would have caused complications, therefore it was decided to exclusively study night temperatures. Similarly, this thesis has only considered outside temperatures, when the implications for human comfort will also be felt inside, forming part of a complex bio-meteorological relationship. Emphasis has been placed on the importance of investigating specific case studies, for example heatwave events, as the results can be significantly different to typical or averaged measurements. However, a limited number of specific events have been investigated due to limitations in study period timings and data availability. These gaps are highlighted as areas for future work (section 6.4).

The qualitative method of identifying vulnerable people via literature review then associating vulnerabilities with specific consumer groups raises concerns because it is subjective and the vulnerabilities and groupings are not perfectly matched. However, this is the highest resolution and most current dataset available containing social information, and analysis was undertaken by one researcher to avoid bias. It was not possible to obtain actual records e.g. hospital admissions/deaths for the study area, which would have helped validate the use of consumer segmentation data. The spatial risk assessment work used equal weightings of different input layers to reach its conclusions. As certain variables are related, e.g. poorer people often live in high rise buildings, this may create a feedback loop that influences the results. Equal weightings were chosen as an unbiased starting point, with the expectation that further work could change weightings with the understanding that such changes could manipulate the results.

The work on climate change uses a simple addition method to represent a complex problem. Whilst the method is simplistic, it is justified as the uncertainty associated with underlying datasets (e.g. UKCP09, LST - air relationship) is significant, questioning the value of complicated analysis. The simplistic method is transparent and clearly highlights areas of weakness.

6.3 Impact

As explained in subsection 1.3.2, this thesis was aiming to help the Birmingham Environmental Partnership (BEP) and Birmingham City Council (BCC) reach defined targets against National Indicator 188 "Adapting to Climate Change". BEP successfully reached their targets as shown in Table 6.1 and BEP's Annual reports (2008-2009 level 1 (Birmingham Environmental Partnership, 2009), 2009-2010 level 2 (Birmingham Environmental Partnership, 2010)) and via the Birmingham Climate Change Action Plan (Birmingham City Council and Birmingham Environmental Partnership, 2011). The action plan outlines a framework for implementing adaptation in the city based on an evidence base that this thesis contributed to. Work contained in this thesis was the winner of the Local Authority Research + Intelligence Association (LARIA) "Excellence in Research" award 2009.

Table 6.1: BEP NI 188 targets and outcome.

Level	Result	Target	Outcome
0	Getting started	Baseline	n/a
1	Public commitment and impacts assessment	2008/2009	Reached
2	Comprehensive risk assessment	2009/2010	Reached
3	Comprehensive action plan	2010/2011	Reached
4	Implementation, monitoring and continuous review	n/a	n/a

Research contained in this thesis has also influenced other sectors outside of academia. The Wildlife Trust for Birmingham and the Black Country investigated the economic value of urban green infrastructure (Holzinger, 2011) and required urban heat island information. Other work on the evidence base for Birmingham's green infrastructure by Birmingham City Council made use of UHI data (May, 2010), and work funded by DEFRA looking at health effects of climate change in the West Midlands (May et al., 2010) also integrated UHI research arising from this thesis.

6.4 Future work

Following the results presented in this thesis, there is considerable scope for further work in this sizeable and growing research area. There are a number of ways future work could continue, and these have been discussed in conclusions within individual chapters (see section 3.5,

section 4.4, subsection 5.1.4, subsection 5.2.4).

There are a number of avenues for future work technically. It would be useful to incorporate additional thermal datasets alongside the MODIS data used in chapter 3, for example high resolution satellite data from Landsat or future instruments. This could be further enhanced by using aerial flyover thermal data from commissioned flights of extremely high resolution. Additional thermal datasets would not only help in verification, but could help downscale satellite images and provide increased opportunities for data e.g. on cloudy nights. This work would have to be carefully undertaken to ensure that different scenarios are accounted for. Further climate change work could integrate the weather generator and threshold detector from UKCP09, which could help predict the frequency of future extreme events.

Limitations surrounding the current understanding of the relationship between air and land surface temperatures presents a significant area of future research. This thesis has presented work using a pilot air temperature sensor collection, but as discussed in section 5.1 and repeated in section 6.2 there is considerable scope for further work given the significant limitations encountered. The uncertainty in the results is a weakness in this approach, but there is no clear alternative for integrating remotely sensed data with air temperatures and climate change scenarios. Further verification from enhanced ground based sensor networks such as HiTemp, an ongoing research project at the University of Birmingham (discussed in subsection 5.1.4) will help further research. However the difficulties in comparing LST to air temperatures is not likely to be solved easily, but remotely sensed LST is likely to increase in use given its global coverage and ease of access. This has a linked effect on the incorporation of urban influences in climate change models, and it will be interesting to see how further research progresses in this area. Urban climatology is a growing field, driven in part by the increasing concern relating to climate change and the very real pressure placed on urban areas due to their explosive growth.

Other research angles offer opportunity for future work. This thesis focussed on the health impacts of heat risk, but there are other areas where excess heat can cause significant problems. Various infrastructure has heat thresholds, from electricity substations (increased heat reduces efficiency) to railways (increased heat reduces speed limits in order to help lower track buckles). Tarmac has heat tolerances, which may cause issues on roads. Both infrastructure and health impacts have an economic impact, which could be widespread. Tourism is influenced by temperatures, and businesses are reliant on reliable infrastructure and healthy populations.

If high temperatures are causing transport issues (e.g. rails buckling and tarmac melting) this impacts both supply of goods and customers. If high temperatures are putting pressure on electricity providers, prices may increase or supplies become unreliable. If vulnerable people are being impacted by heat, hospitals may be under increasing pressure. These examples, and many more possibilities, give some idea as to the potential negative impact of high heat risk. Further work could take a holistic approach, combining many different studies to analyse the complete picture.

There are a number of recommendations for repeating aspects of this thesis in other urban areas in the UK or elsewhere. These recommendations take into account the critique of this thesis (section 6.2), the findings of this thesis and the limitations already discussed.

The study area should be chosen carefully to ensure that the results are useful and the area chosen does not exclude significant local factors. In the case of Birmingham the city boundaries are a sensible area, but in other urban areas the surrounding area may need to be included e.g. if the main urban core is on the boundary, or if significant altitude differences exist. It is important to choose the temporal scale carefully, especially when using multiple datasets, to ensure they are compatible. For example, the social data (used in chapter 4) relates to peoples homes, so may not be as accurate when analysing alongside daytime UHI data, as many people will work or be away from home.

When exploring the UHI the use of stability classes should be considered essential, in order to begin to understand the changing temperature magnitudes under different atmospheric stabilities. It would be prudent to include multiple extreme examples, to assess the full range of temperatures. This is especially important when considering consequences that are exacerbated by extremes e.g. health.

It would be possible to refine the social segmentation classification scheme used in chapter 4 and update it to the most recent version. The Mosaic dataset is updated regularly and therefore in the future comparisons could be made over (relatively short) timescales. Although the Mosaic dataset is extremely powerful, it would be interesting to view the underlying data which may enable the classification to become more quantitative. The weighting of the risk assessment methodology (chapter 4) is an area where future work would be of value; experimenting with weighting and doing sensitivity tests would illustrate the range of results possible. The work would be particularly important if it was being incorporated into a tool that allowed

users to change weightings without fully understanding the consequences.

If repeating section 5.1, or comparing satellite LST to ground measured air temperatures, changes to the experimental design would be advised. In particular, it would be appropriate to install sensors at a standard height with radiation shields and in environments away from potential microclimates. Although this is difficult in urban areas, future work may be able to make use of the forthcoming Met Office guidelines for urban weather stations, which are currently in development. It would be helpful to have a number of sensors within a 1 km pixel, in order to analyse multiple air temperature measurements against specific pixels. This could be combined with higher resolution remotely sensed data which would likely improve the results. It would be ideal if measurements could be taken remotely and automatically; not having to manually download results in the field would save time and resources whilst enabling data to be analysed more quickly e.g. live temperature maps. Further work could be done to explore land use / type characteristics surrounding sensors and within pixels to see how this alters the results. An additional comparison should be made between installed sensors (low cost and large numbers) and weather stations (high cost low numbers) to help calibrate the installed sensors. Many of these changes in experimental design are being tested in the HiTemp project (see subsection 5.1.4).

In an increasingly urbanised world, the urban influence on temperatures and the associated effect on health is gaining attention, highlighted by recent heatwave events that have caused increased mortality. The corresponding lack of urban influence in climate change predictions is a research gap that is only recently being addressed. This thesis has shown that urban influences can be significant, particularly in extreme conditions, and many vulnerable people live in areas of increased risk. To be able to accurately and reliably quantify current conditions is an extremely important first stage, but continued research will be required to assess future changes and help adapt and prepare for a warmer future world.

List of References

9 News. 'Sydney heatwave breaks 150-year-old record.' URL `http://news.ninemsn.com.au/national/8206775/sydney-heatwave-sizzles-into-its-sixth-day`, **2011**. Accessed Nov 2011.

9 News. 'Australia endures record heatwave.' URL `http://news.ninemsn.com.au/national/8397898/australia-endures-record-heatwave`, **2012**. Accessed Jan 2012.

Alcântara, E. H., Stech, J. L., Lorenzzetti, J. A., Bonnet, M. P., Casamitjana, X., Assireu, A. T., and Novo, E. M. L. d. M. 'Remote sensing of water surface temperature and heat flux over a tropical hydroelectric reservoir.' *Remote Sensing of Environment*, 114(11):2651–2665, **2010**. doi:10.1016/j.rse.2010.06.002.

Andersson, A. K. and Chapman, L. 'The impact of climate change on winter road maintenance and traffic accidents in West Midlands, UK.' *Accident Analysis & Prevention*, 43(1):284–289, **2011**. doi:10.1016/j.aap.2010.08.025.

Andrey, J. and Jones, B. 'The dynamic nature of social disadvantage: implications for hazard exposure and vulnerability in Greater Vancouver.' *Canadian Geographer / Le Géographe canadien*, 52(2):146–168, **2008**.

Aniello, C., Morgan, K., Busbey, A., and Newland, L. 'Mapping micro-urban heat islands using Landsat TM and a GIS.' *Computers & Geosciences*, 21(8):965–967, **1995**. doi:10.1016/0098-3004(95)00033-5.

Apostolakis, G. 'How useful is quantitative risk assessment?' *Risk Analysis*, 24(3):515–520, **2004**.

Arnfield, A. J. 'Two decades of urban climate research: a review of turbulence, exchanges of energy and water, and the urban heat island.' *International Journal of Climatology*, 23(1):1–26, **2003**.

Arnfield, A. J. 'Micro- and mesoclimatology.' *Progress in Physical Geography*, 29(3):426–437, **2005**. doi:10.1191/0309133305pp458pr.

Arnfield, A. J. 'Micro-and mesoclimatology.' *Progress in Physical Geography*, 30:677–689, **2006**. doi:10.1177/0309133306071150.

Basu, R. and Samet, J. M. 'Relation between elevated ambient temperature and mortality: a review of the epidemiologic evidence.' *Epidemiologic reviews*, 24(2):190–202, **2002**. doi:10.1093/epirev/mxf007.

Beck, G. and Kropp, C. 'Infrastructures of risk: a mapping approach towards controversies on risks.' *Journal of Risk Research*, 14(1):1–16, **2011**. doi:10.1080/13669877.2010.505348.

Bell, M. L., O'Neill, M. S., Ranjit, N., Borja-Aburto, V. H., Cifuentes, L. A., and Gouveia, N. C. 'Vulnerability to heat-related mortality in Latin America: A case-crossover study in Sao Paulo, Brazil, Santiago, Chile and Mexico City, Mexico.' *International Journal of Epidemiology*, 37(4):796–804, **2008**. doi:10.1093/ije/dyn094.

Birkmann, J., Garschagen, M., Kraas, F., and Quang, N. 'Adaptive urban governance: new challenges for the second generation of urban adaptation strategies to climate change.' *Sustainability Science*, 5(2):185–206, **2010**. doi:10.1007/s11625-010-0111-3.

Birmingham City Council and Birmingham Environmental Partnership. 'Birmingham Climate Change Adaptation Action Plan 2012+ : Preparing Birmingham for Climate Change Impacts.' URL `http://www.bebirmingham.org.uk/uploads/BCCAAP_final.pdf`, **2011**. Accessed Aug 2012.

Birmingham Environmental Partnership. '08/09 Annual Report.' URL http://www.bebirmingham.org.uk/uploads/BEP%20Annual%20Report%2008-09.pdf, **2009**. Accessed Aug 2012.

Birmingham Environmental Partnership. '09/10 Annual Report.' URL http://www.bebirmingham.org.uk/documents/BEP_Annual_Report_09-10.pdf, **2010**. Accessed Aug 2012.

Bolin, B., Nelson, A., Hackett, E., and Pijawka, K. 'The ecology of technological risk in a Sunbelt city.' *Environment and Planning A*, 34(2):317–339, **2002**.

Boudhar, A., Duchemin, B., Hanich, L., Boulet, G., and Chehbouni, A. 'Spatial distribution of the air temperature in mountainous areas using satellite thermal infra-red data.' *Comptes Rendus Geoscience*, 343(1):32–42, **2011**. doi:10.1016/j.crte.2010.11.004.

Bowler, D. E., Buyung-Ali, L., Knight, T. M., and Pullin, A. S. 'Urban greening to cool towns and cities: A systematic review of the empirical evidence.' *Landscape And Urban Planning*, 97(3):147–155, **2010**. doi:10.1016/j.landurbplan.2010.05.006.

Bradley, A., Thornes, J. E., Chapman, L., Unwin, D., and Roy, M. 'Modelling spatial and temporal road thermal climatology in rural and urban areas using a GIS.' *Climate Research*, 22(1):41–55, **2002**. doi:10.3354/cr022041.

Burt, S. 'The August 2003 heatwave in the United Kingdom: Part 1-Maximum temperatures and historical precedents.' *Weather*, 59(8):199–208, **2004**. doi:10.1256/wea.10.04A.

Cao, X., Onishi, A., Chen, J., and Imura, H. 'Quantifying the cool island intensity of urban parks using ASTER and IKONOS data.' *Landscape And Urban Planning*, 96(4):224–231, **2010**. doi:10.1016/j.landurbplan.2010.03.008.

Changnon, S., Kunkel, K., and Reinke, B. 'Impacts and responses to the 1995 heat wave: A call to action.' *Bulletin of the American Meteorological Society*, 77(7):1497–1505, **1995**. doi:10.1175/1520-0477(1996)077<1497:IARTTH>2.0.CO;2.

Chapman, L. and Thornes, J. E. 'The use of geographical information systems in climatology and meteorology.' *Progress in Physical Geography*, 27(3):313–330, **2003**. doi:10.1191/0309133303pp384ra.

Chapman, L., Thornes, J. E., and Bradley, A. 'Modelling of road surface temperature from a geographical parameter database. Part 1: Statistical.' *Meteorological Applications*, 8(4):409–419, **2001**. doi:10.1017/S1350482701004030.

Chen, S.-s., Chen, X.-z., Chen, W.-q., Su, Y.-x., and Li, D. 'A simple retrieval method of land surface temperature from AMSR-E passive microwave data - A case study over Southern China during the strong snow disaster of 2008.' *International Journal of Applied Earth Observations and Geoinformation*, pages 1–12, **2010**. doi:10.1016/j.jag.2010.09.007.

Chen, X., Zhao, H., Li, P., and Yin, Z. 'Remote sensing image-based analysis of the relationship between urban heat island and land use/cover changes.' *Remote Sensing of Environment*, 104(2):133–146, **2006**. doi:10.1016/j.rse.2005.11.016.

Cheval, S. and Dumitrescu, A. 'The July urban heat island of Bucharest as derived from modis images.' *Theoretical And Applied Climatology*, 96(1-2):145–153, **2009**. doi:10.1007/s00704-008-0019-3.

Cheval, S., Dumitrescu, A., and Bell, A. 'The urban heat island of Bucharest during the extreme high temperatures of July 2007.' *Theoretical And Applied Climatology*, 97(3-4):391–401, **2009**. doi:10.1007/s00704-008-0088-3.

Cockings, S. and Martin, D. 'Zone design for environment and health studies using pre-aggregated data.' *Social Science & Medicine*, 60(12):2729–2742, **2005**.

Coll, C., Caselles, V., Galve, J., Valor, E., Niclos, R., Sanchez, J., and Rivas, R. 'Ground measurements for the validation of land surface temperatures derived from AATSR and MODIS data.' *Remote Sensing of Environment*, 97(3):288–300, **2005**. doi:10.1016/j.rse.2005.05.007.

Coll, C., Hook, S. J., and Galve, J. M. 'Land Surface Temperature From the Advanced Along-Track Scanning Radiometer: Validation Over Inland Waters and Vegetated Surfaces.' *IEEE Transactions on Geoscience and Remote Sensing*, 47(1):350–360, **2009**. doi:10.1109/TGRS.2008.2002912.

Collins, T., Grineski, S., and de Lourdes Romo Aguilar, M. 'Vulnerability to environmental hazards in the Ciudad Juárez (Mexico)-El Paso (USA) metropolis: A model for spatial risk assessment in transnational context.' *Applied Geography*, 29(3):448–461, **2009**. doi:10.1016/j.apgeog.2008.10.005.

Conti, S., Meli, P., Minelli, G., Solimini, R., Toccaceli, V., Vichi, M., Beltrano, C., and Perini, L. 'Epidemiologic study of mortality during the Summer 2003 heat wave in Italy.' *Environmental research*, 98(3):390–399, **2005**. doi:10.1016/j.envres.2004.10.009.

Costello, A., Abbas, M., Allen, A., Ball, S., and Bell, S. 'Managing the health effects of climate change.' *Lancet*, 373:1693–1733, **2009**.

Coutts, A. M., Beringer, J., and Tapper, N. J. 'Impact of increasing urban density on local climate: Spatial and temporal variations in the surface energy balance in Melbourne, Australia.' *Journal of Applied Meteorology and Climatology*, 46(4):477–493, **2007**. doi:10.1175/JAM2462.1.

Cresswell, M. P., Morse, A. P., Thomson, M. C., and Connor, S. J. 'Estimating surface air temperatures, from Meteosat land surface temperatures, using an empirical solar zenith angle model.' *International Journal Of Remote Sensing*, 20(6):1125–1132, **1999**. doi:10.1080/014311699212885.

Crichton, D. 'The Risk Triangle.' In 'Natural disaster management: a presentation to commemorate the International Decade for Natural Disaster Reduction (IDNDR), 1990-2000,' Tudor Rose, **1999**.

Cristóbal, J., Ninyerola, M., and Pons, X. 'Modeling air temperature through a combination of remote sensing and GIS data.' *Journal of Geophysical Research*, 113, **2008**. doi:10.1029/2007JD009318.

Cutter, S. L., Mitchell, J. T., and Scott, M. S. *Handbook for conducting a GIS-based hazards assessment at the county level*. Hazards Research Lab, Department of Geography, University of South Carolina, **1997**.

Dash, P., Gottsche, F., Olesen, F., and Fischer, H. 'Retrieval of land surface temperature and emissivity from satellite data: Physics, theoretical limitations and current methods.' *Journal of the Indian Society of Remote Sensing*, 29(1):23–30, **2001**.

Dash, P., Gottsche, F. M., Olesen, F. S., and Fischer, H. 'Land surface temperature and emissivity estimation from passive sensor data: Theory and practice-current trends.' *International Journal Of Remote Sensing*, 23(13):2563–2594, **2002**. doi:10.1080/01431160110115041.

DEFRA. 'National Adaptation Programme.' URL `http://www.defra.gov.uk/environment/climate/government/nap/`, **2012**a. Accessed Aug 2012.

DEFRA. 'UK Climate Change Risk Assessment 2012.' Technical report, Defra, **2012**b.

Department of Health. 'NHS Heatwave Plan for England - Protecting Health and Reducing Harm from Extreme Heat and Heatwaves, 2009 Edition.' Technical report, Department of Health, **2009**.

Díaz, J., Jordán, A., García, R., López, C., Alberdi, J., Hernández, E., and Otero, A. 'Heat waves in Madrid 1986-1997: effects on the health of the elderly.' *International Archives of Occupational and Environmental Health*, 75(3):163–170, **2002**. doi:10.1007/s00420-001-0290-4.

Djepa, V. 'Drought prediction using the Along Track Scanning Radiometer (ATSR2) on board ERS2 satellite.' *Advances in Space Research*, 48(1):56–60, **2011**. doi:10.1016/j.asr.2011.01.026.

Dole, R., Hoerling, M., Perlwitz, J., Eischeid, J., Pegion, P., Zhang, T., Quan, X.-W., Xu, T., and Murray, D. 'Was there a basis for anticipating the 2010 Russian heat wave?' *Geophysical Research Letters*, 38(6), **2011**. doi:10.1029/2010GL046582.

Dolney, T. and Sheridan, S. 'The relationship between extreme heat and ambulance response calls for the city of Toronto, Ontario, Canada.' *Environmental research*, 101:94–103, **2006**. doi:10.1016/j.envres.2005.08.008.

Dominguez, A., Kleissl, J., Luvall, J. C., and Rickman, D. L. 'High-resolution urban thermal sharpener (HUTS).' *Remote Sensing of Environment*, 115(7):1772–1780, **2011**. doi:10.1016/j.rse.2011.03.008.

Dousset, B. 'Surface temperature variability and mortality impact in the Paris region during the August 2003 heat wave.' *International Association for Urban Climate*, 42, **2011**.

Dousset, B., Gourmelon, F., Laaidi, K., Zeghnoun, A., Giraudet, E., Bretin, P., Mauri, E., and Vandentorren, S. 'Satellite monitoring of summer heat waves in the Paris metropolitan area.' *International Journal of Climatology*, 31(2):313–323, **2010**. doi:10.1002/joc.2222.

Dyras, I., Dobesch, H., Grueter, E., Perdigao, A., Tveito, O., Thornes, J. E., van der Wel, F., and Bottai, L. 'The use of geographic information systems in climatology and meteorology: COST 719.' *Meteorological Applications*, 12(1):1–5, **2005**. doi:10.1017/S1350482705001544.

Eden, P. 'June 2011 Mostly rather cool and changeable, but brief warm spells early and late.' *Weather*, **2011**.

Ellis, F. P., Princé, H. P., Lovatt, G., and Whittington, R. M. 'Mortality and morbidity in Birmingham during the 1976 heatwave.' *The Quarterly journal of medicine*, 49(193):1–8, **1980**.

Emmanuel, R. and Krüger, E. 'Urban heat island and its impact on climate change resilience in a shrinking city: The case of Glasgow, UK.' *Building and Environment*, 53(C):137–149, **2012**. doi:10.1016/j.buildenv.2012.01.020.

Experian. 'Mosaic UK - the consumer classification of the United Kingdom.' URL `http://www.experian.co.uk/assets/business-strategies/brochures/mosaic-uk-2009-brochure-jun10.pdf`, **2009**. Accessed Jul 2010.

Experian. 'Perils.' URL `http://www.experian.co.uk/consumer-information/perils.html`, **2012**. Accessed Aug 2012.

Fedeski, M. and Gwilliam, J. 'Urban sustainability in the presence of flood and geological hazards: The development of a GIS-based vulnerability and risk assessment methodology.' *Landscape And Urban Planning*, **2007**.

Feng, C., Meng, Q., and Zhang, Y. 'Theoretical and experimental analysis of the energy balance of extensive green roofs.' *Energy And Buildings*, **2010**.

Filleul, L., Filleul, L., Cassadou, S., Cassadou, S., Médina, S., Médina, S., Fabres, P., Fabres, P., Lefranc, A., Lefranc, A., Eilstein, D., Eilstein, D., Tertre, A. L., Tertre, A. L., Pascal, L., Pascal, L., Chardon, B., Chardon, B., Blanchard, M., Blanchard, M., Declercq, C., Declercq, C., Jusot, J.-F., Jusot, J.-F., Prouvost, H., Prouvost, H., Ledrans, M., and Ledrans, M. 'The Relation Between Temperature, Ozone, and Mortality in Nine French Cities During the Heat Wave of 2003.' *Environmental Health Perspectives*, 114(9):1344, **2006**. doi:10.1289/ehp.8328.

Fily, M. 'A simple retrieval method for land surface temperature and fraction of water surface determination from satellite microwave brightness temperatures in sub-arctic areas.' *Remote Sensing of Environment*, 85(3):328–338, **2003**. doi:10.1016/S0034-4257(03)00011-7.

Fisher, P. A. 'An Examination of the Association between Temperature and Mortality in the West Midland from 1981 to 2007 (Masters Thesis).' Technical report, University of Birmingham, **2009**.

Flynn, A., Mcgreevy, C., and Mulkerrin, E. 'Why do older patients die in a heatwave?' *QJM*, 98(3):227, **2005**. doi:10.1093/qjmed/hci025.

Foreign and Commonwealth Office. *Preparing For Global Climate Change - An Adaptation Plan for the FCO*. Foreign and Commonwealth Office, **2010**.

Fouillet, A., Rey, G., Laurent, F., Pavillon, G., Bellec, S., Guihenneuc-Jouyaux, C., Clavel, J., Jougla, E., and Hémon, D. 'Excess mortality related to the August 2003 heat wave in France.' *International Archives of Occupational and Environmental Health*, 80(1):16–24, **2006**. doi:10.1007/s00420-006-0089-4.

Fung, W. Y., Lam, K. S., Nichol, J., and Wong, M. S. 'Derivation of Nighttime Urban Air Temperatures Using a Satellite Thermal Image.' *Journal of Applied Meteorology and Climatology*, 48(4):863–872, **2009**. doi:10.1175/2008JAMC2001.1.

Gallo, K., Hale, R., Tarpley, D., and Yu, Y. 'Evaluation of the Relationship between Air and Land Surface Temperature under Clear- and Cloudy-Sky Conditions.' *Journal of Applied Meteorology and Climatology*, 50(3):767–775, **2011**. doi:10.1175/2010JAMC2460.1.

Gallo, K., McNab, A., Karl, T., Brown, J., Hood, J., and Tarpley, J. 'The Use of NOAA AVHRR Data for Assessment of the Urban Heat-Island Effect.' *Journal of applied meteorology*, 32(5):899–908, **1993**.

Gallo, K., Tarpley, J., McNab, A., and Karl, T. 'Assessment of urban heat islands: a satellite perspective.' *Atmospheric Research*, 37:37–43, **1995**. doi:10.1016/0169-8095(94)00066-M.

Garssen, J., Harmsen, C., and de Beer, J. 'The effect of the summer 2003 heat wave on mortality in the Netherlands.' *Euro surveillance : bulletin européen sur les maladies transmissibles = European communicable disease bulletin*, 10(7):165–168, **2005**.

Gawith, M., Downing, T., and Karacostas, T. 'Heatwaves in a changing climate.' In T. Downing and A. Olsthoorn, editors, 'Climate, Change and Risk,' Routledge, **1999**.

Gawith, M., Street, R., Westaway, R., and Steynor, A. 'Application of the UKCIP02 climate change scenarios: Reflections and lessons learnt.' *Global Environmental Change*, 19:113–121, **2009**. doi:10.1016/j.gloenvcha.2008.09.005.

Ge, J. 'MODIS observed impacts of intensive agriculture on surface temperature in the southern Great Plains.' *International Journal of Climatology*, 30(13):1994–2003, **2010**. doi:10.1002/joc.2093.

Gedzelman, S., Austin, S., Cermak, R., and Stefano, N. 'Mesoscale aspects of the urban heat island around New York City.' *Theoretical And Applied Climatology*, 75:29–42, **2003**. doi:10.1007/s00704-002-0724-2.

Gill, S. E., Handley, J., Ennos, A., and Pauleit, S. 'Adapting Cities for Climate Change: The Role of the Green Infrastructure.' *Built Environment*, 33(1):115–133, **2007**.

Gill, S. E., Handley, J. F., Ennos, A. R., Pauleit, S., Theuray, N., and Lindley, S. J. 'Characterising the urban environment of UK cities and towns: A template for landscape planning.' *Landscape And Urban Planning*, 87(3):210–222, **2008**. doi:10.1016/j.landurbplan.2008.06.008.

Gillespie, A. and Rokugawa, S. 'A temperature and emissivity separation algorithm for Advanced Spaceborne Thermal Emission and Reflection Radiometer (ASTER) images.' *IEEE Transactions on Geoscience and Remote Sensing*, 36(4):1113–1126, **1998**. doi:10.1109/36.700995.

Giridharan, R. and Kolokotroni, M. 'Urban heat island characteristics in London during winter.' *Solar Energy*, 83(9):1668–1682, **2009**. doi:10.1016/j.solener.2009.06.007.

Gluch, R., Quattrochi, D., and Luvall, J. 'A multi-scale approach to urban thermal analysis.' *Remote Sensing of Environment*, 104(2):123–132, **2006**. doi:10.1016/j.rse.2006.01.025.

Gosling, S. N., Lowe, J. A., McGregor, G. R., Pelling, M., and Malamud, B. D. 'Associations between elevated atmospheric temperature and human mortality: a critical review of the literature.' *Climatic Change*, 92(3-4):299–341, **2009**. doi:10.1007/s10584-008-9441-x.

GRaBS. 'GRaBS Adaptation Action Planning Toolkit.' URL `http://www.ppgis.manchester.ac.uk/grabs/`, **2012**a. Accessed Aug 2012.

GRaBS. 'GRaBS Project website.' URL `http://www.grabs-eu.org`, **2012**b. Accessed Aug 2012.

Greater London Authority. 'London's Urban Heat Island: A Summary for Decision Makers.' Technical report, Greater London Authority, **2006**.

Greater London Authority. 'Managing risks and increasing resilience: the Mayor's climate change adaptation strategy.' URL `http://www.london.gov.uk/who-runs-london/mayor/publications/environment/london-climate-change-adaptation-strategy`, **2012**. Accessed Aug 2012.

Greiving, S., Fleischhauer, M., and Lückenkötter, J. 'A Methodology for an integrated risk assessment of spatially relevant hazards.' *Journal of Environmental Planning and Management*, 49(1):1–19, **2006**.

Grimmond, C., Blackett, M., Best, M., Barlow, J., Baik, J.-J., Belcher, S., Bohnenstengel, S., Calmet, I., Chen, F., Dandou, A., Fortuniak, K., Gouvea, M., Hamdi, R., Hendry, M., Kawai, T., Kawamoto, Y., Kondo, H., Krayenhoff, E., Lee, S.-H., Loridan, T., Martilli, A., Masson, V., Miao, S., Oleson, K., Pigeon, G., Porson, A., Ryu, Y.-H., Salamanca, F., Shashua-Bar, L., Steeneveld, G.-J., Tombrou, M., Voogt, J., Young, D., and Zhang, N. 'The International Urban Energy Balance Models Comparison Project: First results from Phase 1.' *Journal of Applied Meteorology and Climatology*, 49(6):1268–1292, **2010**. doi:10.1175/2010JAMC2354.1.

Grineski, S. E. and Collins, T. W. 'Exploring patterns of environmental injustice in the Global South: Maquiladoras in Ciudad Juárez, Mexico.' *Population and Environment*, 29(6):247–270, **2008**. doi:10.1007/s11111-008-0071-z.

Grize, L., Huss, A., Thommen, O., Schindler, C., and Braun-Fahrländer, C. 'Heat wave 2003 and mortality in Switzerland.' *Swiss medical weekly : official journal of the Swiss Society of Infectious Diseases, the Swiss Society of Internal Medicine, the Swiss Society of Pneumology*, 135(13-14):200–205, **2005**. doi:2005/13/smw-11009.

Guest, C., Willson, K., Woodward, A., Hennessy, K., Kalkstein, L., Skinner, C., and Mcmichael, A. 'Climate and mortality in Australia: retrospective study, 1979-1990, and predicted impacts in five major cities in 2030.' *Climate Research*, 13:1–15, **1999**. doi:10.3354/cr013001.

Gwilliam, J., Fedeski, M., Lindley, S. J., Theuray, N., and Handley, J. 'Methods for assessing risk from climate hazards in urban areas.' *Proceedings Of The Institution Of Civil Engineers-Municipal Engineer*, 159(4):245–255, **2006**.

Hacker, J. and Holmes, M. 'Thermal Comfort: Climate Change and the Environmental Design of Buildings in the United Kingdom.' *Built Environment*, 33(1):97–114, **2007**.

Haines, A., Kovats, R. S., Campbell-Lendrum, D., and Corvalan, C. 'Climate change and human health: Impacts, vulnerability and public health.' *Public Health*, 120(7):585–596, **2006**. doi:10.1016/j.puhe.2006.01.002.

Hajat, S. and Kosatky, T. 'Heat-related mortality: a review and exploration of heterogeneity.' *Journal Of Epidemiology And Community Health*, 64(9):753–760, **2010**. doi:10.1136/jech.2009.087999.

Hajat, S., Kovats, R. S., and Lachowycz, K. 'Heat-related and cold-related deaths in England and Wales: who is at risk?' *Occupational and environmental medicine*, 64(2):93–100, **2007**. doi:10.1136/oem.2006.029017.

Harlan, S., Brazel, A., Prashad, L., Stefanov, W., and Larsen, L. 'Neighborhood microclimates and vulnerability to heat stress.' *Social Science & Medicine*, 63(11):2847–2863, **2006**.

Hartz, D., Prashad, L., Hedquist, B., Golden, J., and Brazel, A. 'Linking satellite images and hand-held infrared thermography to observed neighborhood climate conditions.' *Remote Sensing of Environment*, 104(2):190–200, **2006**. doi:10.1016/j.rse.2005.12.019.

Harvison, T., Newman, R., and Judd, B. 'Ageing, the Built Environment and Adaptation to Climate Change.' Technical report, National Climate Change Adaptation Research Facility, **2011**.

Headley, R. 'Landsat: A Global Land-Imaging Project (U.S. Geological Survey Fact Sheet).' URL `http://pubs.usgs.gov/fs/2010/3026`, **2010**. Accessed Aug 2012.

Herb, W., Janke, B., and Mohseni, O. 'Ground surface temperature simulation for different land covers.' *Journal Of Hydrology*, 356:327–343, **2008**.

Hess, R., Visschers, V. H., Siegrist, M., and Keller, C. 'How do people perceive graphical risk communication? The role of subjective numeracy.' *Journal of Risk Research*, 14(1):47–61, **2011**. doi:10.1080/13669877.2010.488745.

Hoffmann, P., Krueger, O., and Heinke, S. K. 'A statistical model for the urban heat island and its application to a climate change scenario.' *International Journal of Climatology*, pages n/a–n/a, **2011**. doi:10.1002/joc.2348.

Holzinger, O. 'The Value of Green Infrastructure in Birmingham and the Black Country - The Total Economic Value of Ecosystem Services provided by the Urban Green Infrastructure.' Technical report, The Wildlife Trust for Birmingham and The Black Country, **2011**.

Honda, Y. 'Impact of climate change on human health in Asia and Japan.' *Global Environmental Research*, 11:33–28, **2007**.

Huang, H., Ooka, R., and Kato, S. 'Urban thermal environment measurements and numerical simulation for an actual complex urban area covering a large district heating and cooling system in summer.' *Atmospheric Environment*, 39:6362–6375, **2005**. doi:10.1016/j.atmosenv.2005.07.018.

Hulme, M. and Barrow, E., editors. *Climate of the British Isles: present, past and future*. Routledge, London, **1997**.

Hung, T., Uchihama, D., Ochi, S., and Yasuoka, Y. 'Assessment with satellite data of the urban heat island effects in Asian mega cities.' *International Journal Of Applied Earth Observation And Geoinformation*, 8(1):34–48, **2006**. doi:10.1016/j.jag.2005.05.003.

Huynen, M. M., Martens, P., Schram, D., Weijenberg, M. P., and Kunst, A. E. 'The impact of heat waves and cold spells on mortality rates in the Dutch population.' *Environmental Health Perspectives*, 109(5):463–470, **2001**.

Imhoff, M., Zhang, P., Wolfe, R., and Bounoua, L. 'Remote sensing of the urban heat island effect across biomes in the continental USA.' *Remote Sensing of Environment*, 114(3):504–513, **2010**.

Inamdar, A. K., French, A., Hook, S., Vaughan, G., and Luckett, W. 'Land surface temperature retrieval at high spatial and temporal resolutions over the southwestern United States.' *Journal of Geophysical Research*, 113(D7):1–18, **2008**. doi:10.1029/2007JD009048.

Indraganti, M. 'Behavioural adaptation and the use of environmental controls in summer for thermal comfort in apartments in India.' *Energy And Buildings*, 42(7):1019–1025, **2010**. doi:10.1016/j.enbuild.2010.01.014.

IPCC. *IPCC Fourth Assessment Report: Climate Change 2007: Synthesis Report"*. Cambridge University Press, **2007**a.

IPCC. *IPCC Fourth Assessment Report: Working Group II Report "Impacts, Adaptation and Vulnerability"*. Cambridge University Press, **2007**b.

IPCC. *Managing the Risks of Extreme Events and Disasters to Advance Climate Change Adaptation. A Special Report of Working Groups I and II of the Intergovernmental Panel on Climate Change*. Cambridge University Press, Cambridge, UK, and New York, NY, USA, **2012**.

ISO. 'ISO 31000:2009 Risk management – Principles and guidelines.' URL `http://www.iso.org/iso/catalogue_detail?csnumber=43170`, **2009**. Accessed Aug 2012.

Istomina, L. G., von Hoyningen-Huene, W., Kokhanovsky, A. A., and Burrows, J. P. 'The detection of cloud-free snow-covered areas using AATSR measurements.' *Atmospheric Measurement Techniques*, 3(4):1005–1017, **2010**. doi:10.5194/amt-3-1005-2010.

Jacob, F., Petitcolin, F., Schmugge, T., Vermote, É., French, A., and Ogawa, K. 'Comparison of land surface emissivity and radiometric temperature derived from MODIS and ASTER sensors.' *Remote Sensing of Environment*, 90(2):137–152, **2004**.

Jaroszweski, D., Chapman, L., and Petts, J. 'Assessing the potential impact of climate change on transportation: the need for an interdisciplinary approach.' *Journal of Transport Geography*, 18(2):331–335, **2010**. doi:10.1016/j.jtrangeo.2009.07.005.

Jenkins, G. J., Murphy, J. M., Sexton, D. S., Lowe, J. A., Jones, P., and Kilsby, C. G. 'UK Climate Projections: Briefing report.' Technical report, Met Office Hadley Centre, Exter, UK, **2009**.

Jin, M. 'Analysis of Land Skin Temperature Using AVHRR Observations.' *Bulletin of the American Meteorological Society*, 85(4):587–600, **2004**. doi:10.1175/BAMS-85-4-587.

Jin, M. and Dickinson, R. 'A generalized algorithm for retrieving cloudy sky skin temperature from satellite thermal infrared radiances.' *Journal of Geophysical Research*, 105(D22):27,037–27,047, **2000**. doi:10.1029/2000JD900318.

Jin, M., Dickinson, R., and Zhang, D. 'The footprint of urban areas on global climate as characterized by MODIS.' *Journal of Climate*, 18(10):1551–1565, **2005**. doi:10.1175/JCLI3334.1.

Jin, M. and Shepherd, J. M. 'Inclusion of Urban Landscape in a Climate Model: How Can Satellite Data Help?' *Bulletin of the American Meteorological Society*, 86(5):681–689, **2005**. doi:10.1175/BAMS-86-5-681.

Jin, M., Shepherd, J. M., and Peters-Lidard, C. 'Development of a parameterization for simulating the urban temperature hazard using satellite observations in climate model.' *Natural Hazards*, 43(2):257–271, **2007**. doi:10.1007/s11069-007-9117-2.

Joan, M. and Cesar, C. 'Monthly Land Surface Temperature maps over European Zone using Advanced Along Track Scanning Radiometer data for 2007.' *Geoscience and Remote Sensing Symposium,2009 IEEE International,IGARSS 2009*, 4:292–295, **2009**. doi:10.1109/IGARSS.2009.5417316.

Johnson, D. 'Urban modification of diurnal temperature cycles in Birmingham, U.K.' *International Journal of Climatology*, 5:221–225, **1985**. doi:10.1002/joc.3370050208.

Johnson, H., Kovats, R. S., McGregor, G., Stedman, J., Gibbs, M., and Walton, H. 'The impact of the 2003 heat wave on daily mortality in England and Wales and the use of rapid weekly mortality estimates.' *Euro surveillance : bulletin européen sur les maladies transmissibles = European communicable disease bulletin*, 10(7):168–171, **2005**.

Jones, P. D. and Lister, D. H. 'The urban heat island in Central London and urban-related warming trends in Central London since 1900.' *Weather*, 64(12):323–327, **2009**. doi:10.1002/wea.432.

Kaiser, R., Rubin, C. H., Henderson, A. K., Wolfe, M. I., Kieszak, S., Parrott, C. L., and Adcock, M. 'Heat-Related Death and Mental Illness During the 1999 Cincinnati Heat Wave.' *The American Journal of Forensic Medicine and Pathology*, 22(3):303–307, **2001**.

Kaplan, S. and Garrick, B. 'On the quantitative definition of risk.' *Risk Analysis*, 1(1):11–27, **1981**.

Karl, T., Diaz, H., and Kukla, G. 'Urbanization: Its detection and effect in the United States climate record.' *Journal of Climate*, 1:1099–1123, **1988**. doi:10.1175/1520-0442(1988)001<1099:UIDAEI>2.0.CO;2.

Kershaw, T., Sanderson, M., Coley, D., and Eames, M. 'Estimation of the urban heat island for UK climate change projections.' *Building Services Engineering Research and Technology*, 31(3):1–13, **2010**. doi:10.1177/0143624410365033.

Kidd, C., Levizzani, V., and Bauer, P. 'A review of satellite meteorology and climatology at the start of the twenty-first century.' *Progress in Physical Geography*, 33(4):474–489, **2009**. doi:10.1177/0309133309346647.

Kim, H.-Y. and Liang, S. 'Development of a hybrid method for estimating land surface shortwave net radiation from MODIS data.' *Remote Sensing of Environment*, 114(11):2393–2402, **2010**. doi:10.1016/j.rse.2010.05.012.

Kleerekoper, L., van Esch, M., and Salcedo, T. B. 'How to make a city climate-proof, addressing the urban heat island effect.' *"Resources, Conservation & Recycling"*, pages 1–9, **2011**. doi:10.1016/j.resconrec.2011.06.004.

Knowlton, K., Lynn, B., Goldberg, R. A., Rosenzweig, C., Hogrefe, C., Rosenthal, J. K., and Kinney, P. L. 'Projecting Heat-Related Mortality Impacts Under a Changing Climate in the New York City Region.' *American Journal Of Public Health*, 97(11):2028–2034, **2007**. doi:10.2105/AJPH.2006.102947.

Kolokotroni, M. and Giridharan, R. 'Urban heat island intensity in London: An investigation of the impact of physical characteristics on changes in outdoor air temperature during summer.' *Solar Energy*, 82(11):986–998, **2008**. doi:10.1016/j.solener.2008.05.004.

Kolokotroni, M., Zhang, Y., and Watkins, R. 'The London Heat Island and building cooling design.' *Solar Energy*, 81(1):102–110, **2007**. doi:10.1016/j.solener.2006.06.005.

Kotecha, R., Thornes, J. E., and Chapman, L. 'Birmingham's Local Climate Impacts Profile (LCLIP).' Technical report, University of Birmingham, **2008**.

Kovats, R. S., Haines, A., Stanwell-Smith, R., Martens, P., Menne, B., and Bertollini, R. 'Climate change and human health in Europe.' *British Medical Journal*, 318(7199):1682–1685, **1999**.

Kovats, R. S. and Hajat, S. 'Heat Stress and Public Health: A Critical Review.' *Annual Review of Public Health*, 29(1):41–55, **2008**. doi:10.1146/annurev.publhealth.29.020907.090843.

Kovats, R. S., Hajat, S., and Wilkinson, P. 'Contrasting patterns of mortality and hospital admissions during hot weather and heat waves in Greater London, UK.' *Occupational and environmental medicine*, 61(11):893–898, **2004**. doi:10.1136/oem.2003.012047.

Kovats, R. S., Johnson, H., and Griffith, C. 'Mortality in southern England during the 2003 heat wave by place of death.' *Health Stat Q*, 29:6–8, **2006**.

Kovats, R. S. and Kristie, L. 'Heatwaves and public health in Europe.' *The European Journal of Public Health*, 16(6):592, **2006**. doi:10.1093/eurpub/ckl049.

Kukla, G., Gavin, J., and Karl, T. 'Urban warming.' *Journal of applied meteorology*, 25:1265–1270, **1986**. doi:10.1175/1520-0450(1986)025<1265:UW>2.0.CO;2.

Lamb, H. H. 'Types and spells of weather around the year in the British Isles : Annual trends, seasonal structure of the year, singularities.' *Quarterly Journal of the Royal Meteorological Society*, 76(330):393–429, **1950**. ISSN 1477-870X. doi:10.1002/qj.49707633005.

Lamb, H. H. 'British Isles Weather types and a register of daily sequence of circulation patterns, 1861-1971.' *Geophysical Memoir*, 116, **1972**.

Langer, M., Westermann, S., and Boike, J. 'Spatial and temporal variations of summer surface temperatures of wet polygonal tundra in Siberia - implications for MODIS LST based permafrost monitoring.' *Remote Sensing of Environment*, 114(9):2059–2069, **2010**. doi:10.1016/j.rse.2010.04.012.

Langford, I. H. and Bentham, G. 'The potential effects of climate change on winter mortality in England and Wales.' *International journal of biometeorology*, 38:141–147, **1995**. doi:10.1007/BF01208491.

Lawson, A. B. *Spatial Risk Assessment*. John Wiley and Sons Ltd, **2008**. ISBN 9780470061596. doi:10.1002/9780470061596.risk0323.

Lazzarin, R., Castellotti, F., and Busato, F. 'Experimental measurements and numerical modelling of a green roof.' *Energy And Buildings*, 37(12):1260–1267, **2005**. doi:10.1016/j.enbuild.2005.02.001.

Lee, H. 'An application of NOAA AVHRR thermal data to the study of urban heat islands.' *Atmospheric Environment. Part B. Urban Atmosphere*, 27(1):1–13, **1993**. doi:10.1016/0957-1272(93)90041-4.

Li, J.-j., Wang, X.-r., Wang, X.-j., Ma, W.-c., and Zhang, H. 'Remote sensing evaluation of urban heat island and its spatial pattern of the Shanghai metropolitan area, China.' *Ecological Complexity*, 6(4):413–420, **2009**. doi:10.1016/j.ecocom.2009.02.002.

Li, K. and Yu, Z. 'Comparative and Combinative Study of Urban Heat island in Wuhan City with Remote Sensing and CFD Simulation.' *Sensors*, 8(10):6692–6703, **2008**. doi:10.3390/s8106692.

Liang, S., Zhong, B., and Fang, H. 'Improved estimation of aerosol optical depth from MODIS imagery over land surfaces.' *Remote Sensing of Environment*, 104(4):416–425, **2006**. doi:10.1016/j.rse.2006.05.016.

Lillesand, T., Kiefer, R., and Chipman, J. *Remote Sensing and Image Interpretation*. Wiley, Chichester, fifth edition, **2004**.

Lin, T.-P., de Dear, R., and Hwang, R.-L. 'Effect of thermal adaptation on seasonal outdoor thermal comfort.' *International Journal of Climatology*, pages n/a–n/a, **2010**. doi:10.1002/joc.2120.

Lindley, S. J., Handley, J., McEvoy, D., and Peet, E. 'The Role of Spatial Risk Assessment in the Context of Planning for Adaptation in UK Urban Areas.' *Built Environment*, 33(1):46–69, **2007**.

Lindley, S. J., Handley, J. F., Theuray, N., Peet, E., and McEvoy, D. 'Adaptation Strategies for Climate Change in the Urban Environment: Assessing Climate Change Related Risk in UK Urban Areas.' *Journal of Risk Research*, 9(5):543–568, **2006**. doi:10.1080/13669870600798020.

Liu, R., Wen, J., Wang, X., Wang, L., Tian, H., Zhang, T., Shi, X., Zhang, J., and LV, S. 'Actual daily evapotranspiration estimated from MERIS and AATSR data over the Chinese Loess Plateau.' *Hydrology and Earth System Sciences*, 14:47–58, **2010**.

Liu, Y. and Key, J. 'Detection and analysis of clear-sky, low-level atmospheric temperature inversions with MODIS.' *Journal Of Atmospheric And Oceanic Technology*, 20(12):1727–1737, **2003**.

Liu, Y., Yamaguchi, Y., and Ke, C. 'Reducing the Discrepancy Between ASTER and MODIS Land Surface Temperature Products.' *Sensors*, 7:3043–3057, **2007**. doi:10.3390/s7123043.

Local and Regional Partnership Boards. 'Adapting to Climate Change: Guidance notes for NI 188, version 1.7.' **2009**.

Loughnan, M., Nicholls, N., and Tapper, N. 'Demographic, seasonal, and spatial differences in acute myocardial infarction admissions to hospital in Melbourne Australia.' *International Journal of Health Geographics*, 7(1):42, **2008**.

Lu, D. and Weng, Q. 'Spectral mixture analysis of ASTER images for examining the relationship between urban thermal features and biophysical descriptors in Indianapolis, Indiana, USA.' *Remote Sensing of Environment*, 104(2):157–167, **2006**. doi:10.1016/j.rse.2005.11.015.

Lu, L., Venus, V., Skidmore, A., Wang, T., and Luo, G. 'Estimating land-surface temperature under clouds using MSG/SEVIRI observations.' *International Journal of Applied Earth Observations and Geoinformation*, 13(2):265–276, **2011**. doi:10.1016/j.jag.2010.12.007.

Luber, G. and McGeehin, M. 'Climate Change and Extreme Heat Events.' *American Journal Of Preventive Medicine*, 35(5):429–435, **2008**. doi:10.1016/j.amepre.2008.08.021.

Martilli, A. 'Current research and future challenges in urban mesoscale modelling.' *International Journal of Climatology*, 27(14):1909–1918, **2007**. doi:10.1002/joc.1620.

Masson, V. 'Urban surface modeling and the meso-scale impact of cities.' *Multiple values selected*, 84(1-3):35–45, **2005**. doi:10.1007/s00704-005-0142-3.

Matson, M., Mcclain, E., McGinnis Jr, D., and Pritchard, J. 'Satellite detection of urban heat islands.' *Monthly Weather Review*, 106(12):1725–1734, **1978**. doi:10.1175/1520-0493(1978)106<1725:SDOUHI>2.0.CO;2.

Maxim. 'DS1922L, DS1922T Temperature Logger iButton with 8KB Datalog Memory.' URL `http://www.maxim-ic.com/datasheet/index.mvp/id/4088`, **2011**. Accessed Aug 2012.

May, E. 'Green Infrastructure: An Evidence Base for Birmingham.' Technical report, Birmingham City Council, **2010**.

May, E., Baiardi, L., Kara, E., Raicchand, S., and Eshareturi, C. 'Health Effects of Climate Change in the West Midlands: Technical Report.' Technical report, DEFRA, **2010**.

McCarthy, M. P., Best, M. J., and Betts, R. A. 'Climate change in cities due to global warming and urban effects.' *Geophysical Research Letters*, 37(9):L09,705, **2010**. doi:10.1029/2010GL042845.

McFarland, M. J., Miller, R. L., and M, U. N. C. 'Land Surface Temperature Derived From the SSM/I Passive Microwave Brightness Temperatures.' *IEEE Transactions on Geoscience and Remote Sensing*, 28(5):839–845, **1990**. doi:10.1109/36.58971.

McGeehin, M. and Mirabelli, M. 'The Potential Impacts of Climate Variability and Change on Temperature-Related Morbidity and Mortality in the United States.' *Environmental Health Perspectives*, 109(2):185–189, **2001**.

McKendry, I. G. 'Applied climatology.' *Progress in Physical Geography*, 27(4):597–606, **2003**. doi:10.1191/0309133303pp397pr.

McMichael, A., Cambell-Lendrum, D., Corvalan, C., Ebi, K., Githeko, A., Scheraga, J., and Woodward, A. *Climate Change and Human Health Risk and Responses*. World Health Organisation, **2003**.

Meehl, G. and Tebaldi, C. 'More intense, more frequent, and longer lasting heat waves in the 21st century.' *Science*, 305(5686):994–997, **2004**. doi:10.1126/science.1098704.

Mendelsohn, R., Kurukulasuriya, P., Basist, A., Kogan, F., and Williams, C. 'Climate analysis with satellite versus weather station data.' *Climatic Change*, 81(1):71–83, **2007**. doi:10.1007/s10584-006-9139-x.

Meng, G., Law, J., and Thompson, M. 'Small-scale health-related indicator acquisition using secondary data spatial interpolation.' *International Journal of Health Geographics*, **2010**.

Met Office. 'UK Climate Summaries.' URL `http://www.metoffice.gov.uk/climate/uk/`, **2010**. Accessed Feb 2010.

Met Office. 'UKCP09: Regional values of 1961-1990 baseline averages.' URL `http://www.metoffice.gov.uk/climatechange/science/monitoring/ukcp09/download/longterm/regional_values.html`, **2011**. Accessed Mar 2012.

Met Office. 'Heat-Health Watch.' URL `http://www.metoffice.gov.uk/weather/uk/heathealth/`, **2012**. Accessed Feb 2012.

Meze-Hausken, E. 'On the (im-)possibilities of defining human climate thresholds.' *Climatic Change*, 89(3-4):299–324, **2008**. doi:10.1007/s10584-007-9392-7.

Mitchell, R. and Popham, F. 'Effect of exposure to natural environment on health inequalities: an observational population study.' *Lancet*, 372(9650):1655–1660, **2008**.

Morris, C., Simmonds, I., and Plummer, N. 'Quantification of the influences of wind and cloud on the nocturnal urban heat island of a large city.' *Journal of applied meteorology*, 40(2):169–182, **2001**. doi:10.1175/1520-0450(2001)040<0169:QOTIOW>2.0.CO;2.

Morrison, C. and Shortt, N. 'Fuel poverty in Scotland: Refining spatial resolution in the Scottish Fuel Poverty Indicator using a GIS-based multiple risk index.' *Health & Place*, 14(4):702–717, **2008**. doi:10.1016/j.healthplace.2007.11.003.

Mostovoy, G., King, R., Reddy, K., Kakani, V., and Filippova, M. 'Statistical estimation of daily maximum and minimum air temperatures from MODIS LST data over the state of Mississippi.' *GIScience & Remote Sensing*, 43(1):78–110, **2006**.

Munich Re. 'Topics—Annual Review: Natural Catastrophes 2002.' **2003**.

NASA / JPL. 'HyspIRI Mission Study.' URL http://hyspiri.jpl.nasa.gov/, **2012**. Accessed Aug 2012.

NASA Land Processes Distributed Active Archive Center. 'MODIS/Aqua Land Surface Temperature and Emissivity Daily L3 Global 1 km Grid SIN.' URL https://lpdaac.usgs.gov/lpdaac/products/modisproductstable/landsurfacetemperatureemissivity/dailyl3global1km/myd11a1, **2009**. Accessed Feb 2009.

NASA Land Processes Distributed Active Archive Center. 'Homepage.' URL https://lpdaac.usgs.gov/, **2011**a. Accessed Aug 2012.

NASA Land Processes Distributed Active Archive Center. 'MODIS Reprojection Tool.' URL https://lpdaac.usgs.gov/tools/modis_reprojection_tool/, **2011**b. Accessed Aug 2012.

Naughton, M., Henderson, A., and Mirabelli, M. 'Heat-related mortality during a 1999 heat wave in Chicago.' *American Journal Of Preventive Medicine*, 22(4):221–227, **2002**. doi:10.1016/S0749-3797(02)00421-X.

Neteler, M. 'Time series processing of MODIS satellite data for landscape epidemiological applications.' *International Journal of Geoinformatics*, 1(1):133–138, **2005**.

Neteler, M. 'Estimating Daily Land Surface Temperatures in Mountainous Environments by Reconstructed MODIS LST Data.' *Remote Sensing*, 2:333–351, **2010**.

Nichol, J. E. 'A GIS-Based Approach to Microclimate Monitoring in Singapore's High-Rise Housing Estates.' *Photogrammetric Engineering and Remote Sensing*, 60(10):1225–1232, **1994**.

Nichol, J. E., Fung, W. Y., Lam, K.-s., and Wong, M. S. 'Urban heat island diagnosis using ASTER satellite images and 'in situ' air temperature.' *Atmospheric Research*, 94(2):276–284, **2009**. doi:10.1016/j.atmosres.2009.06.011.

Nieto, H., Sandholt, I., Aguado, I., Chuvieco, E., and Stisen, S. 'Air temperature estimation with MSG-SEVIRI data: Calibration and validation of the TVX algorithm for the Iberian Peninsula.' *Remote Sensing of Environment*, 115(1):107–116, **2011**. doi:10.1016/j.rse.2010.08.010.

NOAA. 'Comprehensive Large Array-Data Stewardship System.' URL http://www.nsof.class.noaa.gov/saa/, **2012**. Accessed Aug 2012.

Nogueira, P. J., Falcão, J. M., Contreiras, M. T., Paixão, E., Brandão, J., and Batista, I. 'Mortality in Portugal associated with the heat wave of August 2003: early estimation of effect, using a rapid method.' *Euro surveillance : bulletin européen sur les maladies transmissibles = European communicable disease bulletin*, 10(7):150–153, **2005**.

Noyes, E., Sòria, G., Sobrino, J., and Remedios, J. 'AATSR land surface temperature product algorithm verification over a WATERMED site.' *Advances in Space Research*, 39:171–178, **2007**.

Obukhov, A. M. 'Turbulence in an atmosphere with a non-uniform temperature.' *Boundary-Layer Meteorology*, 2:7–29, **1971**. ISSN 0006-8314. 10.1007/BF00718085.

Office for National Statistics. 'Key Population and Vital Statistics 2007.' URL http://www.statistics.gov.uk/StatBase/Product.asp?vlnk=539., **2009**. Accessed Jan 2010.

Office for National Statistics. 'Super Output Areas Explained.' URL http://www.neighbourhood.statistics.gov.uk/dissemination/Info.do?page=nessgeography/superoutputareasexplained/output-areas-explained.htm, **2011**. Accessed Mar 2011.

Oke, T. 'Inadvertent modification of the city atmosphere and the prospects for planned urban climates.' *Proceedings, Symposium on Meteorology Related to Urban and Regional Land-Use Planning*, pages 151–175, **1976**.

Oke, T. *Boundary Layer Climates*. Routledge: London and New York, 2 edition, **1987**.

Oke, T. 'Towards better scientific communication in urban climate.' *Theoretical And Applied Climatology*, 84(1-3):179–190, **2006**. doi:10.1007/s00704-005-0153-0.

O'Neill, M. and Ebi, K. 'Temperature extremes and health: impacts of climate variability and change in the United States.' *Journal of Occupational and Environmental Medicine*, 51(1):13–24, **2009**. doi:10.1097/JOM.0b013e318173e122.

Openshaw, S. *The modifiable areal unit problem (concepts and techniques in modern geography)*. Geo Books, **1984**.

Osei, F. and Duker, A. 'Spatial and demographic patterns of Cholera in Ashanti region- Ghana.' *International Journal of Health Geographics*, 7(1):44, **2008**.

Ottle, C. and Vidal-Madjar, D. 'Estimation of land surface temperature with NOAA9 data.' *Remote Sensing of Environment*, 40(1):27–41, **1992**. doi:10.1016/0034-4257(92)90124-3.

Oven, K. J., Curtis, S. E., Reaney, S., Riva, M., Stewart, M. G., Ohlemüller, R., Dunn, C. E., Nodwell, S., Dominelli, L., and Holden, R. 'Climate change and health and social care: Defining future hazard, vulnerability and risk for infrastructure systems supporting older people's health care in England.' *Applied Geography*, 33(C):16–24, **2012**. doi:10.1016/j.apgeog.2011.05.012.

Owen, S., MacKenzie, A., Bunce, R., Stewart, H., Donovan, R., Stark, G., and Hewitt, C. 'Urban land classification and its uncertainties using principal component and cluster analyses: A case study for the UK West Midlands.' *Landscape And Urban Planning*, 78(4):311–321, **2006**. doi:10.1016/j.landurbplan.2005.11.002.

Palutikof, J. 'The view from the front line: Adapting Australia to climate change.' *Global Environmental Change*, 20:218–219, **2010**.

Parenteau, M. and Sawada, M. 'The modifiable areal unit problem (MAUP) in the relationship between exposure to NO 2 and respiratory health.' *International Journal of Health Geographics*, 10(1):1–15, **2011**. doi:10.1186/1476-072X-10-58.

Pasquill, F. and Smith, F. *Atmospheric Diffusion*. Ellis Horwood Limited: Chichester., 3rd edition, **1983**.

Patt, A. G., Vuuren, D. P. v., Berkhout, F., Aaheim, A., Hof, A. F., Isaac, M., and Mechler, R. 'Adaptation in integrated assessment modeling: where do we stand?' *Climatic Change*, 99(3-4):383–402, **2010**. doi:10.1007/s10584-009-9687-y.

Peterson, T., Basist, A., and Williams, C. 'A Blended Satellite–In Situ Near–Global Surface Temperature Dataset.' *Bulletin of the American Meteorological Society*, 81(9):2157–2164, **2000**.

Petropoulos, G., Carlson, T., Wooster, M., and Islam, S. 'A review of Ts/VI remote sensing based methods for the retrieval of land surface energy fluxes and soil surface moisture.' *Progress in Physical Geography*, 33(2):224–250, **2009**. doi:10.1177/0309133309338997.

Pidgeon, N. and Butler, C. 'Risk analysis and climate change.' *Environmental Politics*, 18(5):670–688, **2009**. doi:10.1080/09644010903156976.

Pinker, R. T., Sun, D., Hung, M.-P., Li, C., and Basara, J. B. 'Evaluation of Satellite Estimates of Land Surface Temperature from GOES over the United States.' *Journal of Applied Meteorology and Climatology*, 48(1):167–180, **2009**. doi:10.1175/2008JAMC1781.1.

Pirard, P., Vandentorren, S., Pascal, M., Laaidi, K., Le Tertre, A., Cassadou, S., and Ledrans, M. 'Summary of the mortality impact assessment of the 2003 heat wave in France.' *Euro surveillance : bulletin européen sur les maladies transmissibles = European communicable disease bulletin*, 10(7):153–156, **2005**.

Platt, C. M. R. and Prata, A. J. 'Nocturnal effects in the retrieval of land surface temperatures from satellite measurements.' *Remote Sensing of Environment*, 45(2):127–136, **1993**. doi:DOI: 10.1016/0034-4257(93)90037-X.

Pongrácz, R., Bartholy, J., and Dezső, Z. 'Remotely sensed thermal information applied to urban climate analysis.' *Advances in Space Research*, 37(12):2191–2196, **2006**. doi:10.1016/j.asr.2005.06.069.

Pongrácz, R., Bartholy, J., and Dezső, Z. 'Application of remotely sensed thermal information to urban climatology of Central European cities.' *Physics and Chemistry of the Earth*, 35(1-2):95–99, **2010**. doi:10.1016/j.pce.2010.03.004.

Pouteau, R., Rambal, S., Ratte, J., Gogé, F., Joffre, R., and Winkel, T. 'Downscaling MODIS-derived maps using GIS and boosted regression trees: The case of frost occurrence over the arid Andean highlands of Bolivia.' *Remote Sensing of Environment*, 115:117–129, **2010**. doi:10.1016/j.rse.2010.08.011.

Prata, A. 'Land Surface Temperature determination from satellites.' *Advances in Space Research*, 14(3):15–26, **1994**. doi:10.1016/0273-1177(94)90186-4.

Prata, A. 'Land surface temperature measurement from space: AATSR algorithm theoretical basis document.' *Contract Report to ESA, CSIRO Atmospheric Research, Aspendale, Victoria, Australia, 2002*, pages 1–34, **2002**.

Price, J. 'Assessment of the urban heat island effect through the use of satellite data.' *Monthly Weather Review*, 107(11):1554–1557, **1979**. doi:10.1175/1520-0493(1979)107<1554:AOTUHI>2.0.CO;2.

Prichard, B. 'Weather news.' *Weather*, 66(4):86–86, **2011**. doi:10.1002/wea.694.

Prieto-Lopez, T., Chapman, L., and Hamilton, C. 'A low cost air temperature sensor network for urban climate studies.' Technical report, University of Birmingham, **2011**.

Pu, R., Gong, P., Michishita, R., and Sasagawa, T. 'Assessment of multi-resolution and multi-sensor data for urban surface temperature retrieval.' *Remote Sensing of Environment*, 104(2):211–225, **2006**. doi:10.1016/j.rse.2005.09.022.

Rajasekar, U. and Weng, Q. 'Urban heat island monitoring and analysis using a non-parametric model: A case study of Indianapolis.' *ISPRS Journal of Photogrammetry and Remote Sensing*, 64(1):86–96, **2008**. doi:doi:10.1016/j.isprsjprs.2008.05.002.

Reid, C., O Neill, M., Gronlund, C., Brines, S., Brown, D., Diez-Roux, A., and Schwartz, J. 'Mapping community determinants of heat vulnerability.' *Environmental Health Perspectives*, 117(11):1730–1730, **2009**. doi:10.1289/ehp.0900683.

Retalis, A., Paronis, D., Lagouvardos, K., and Kotroni, V. 'The heat wave of June 2007 in Athens, Greece - Part 1: Study of satellite derived land surface temperature.' *Atmospheric Research*, 98(2-4):458–467, **2010**. doi:10.1016/j.atmosres.2010.08.005.

Rigo, G., Parlow, E., and Oesch, D. 'Validation of satellite observed thermal emission with in-situ measurements over an urban surface.' *Remote Sensing of Environment*, 104(2):201–210, **2006**. doi:10.1016/j.rse.2006.04.018.

Rizwan, A., Dennis, L., and Liu, C. 'A review on the generation, determination and mitigation of Urban Heat Island.' *Journal of Environmental Sciences*, 20(1):120–128, **2008**. doi:10.1016/S1001-0742(08)60019-4.

Roberts, J. J., Best, B. D., Dunn, D. C., Treml, E. A., and Halpin, P. N. 'Marine Geospatial Ecology Tools: An integrated framework for ecological geoprocessing with ArcGIS, Python, R, MATLAB, and C++.' *Environmental Modelling and Software*, 25(10):1197–1207, **2010**. doi:10.1016/j.envsoft.2010.03.029.

Rooney, C., Mcmichael, A. J., Kovats, R. S., and Coleman, M. P. 'Excess mortality in England and Wales, and in Greater London, during the 1995 heatwave.' *Journal Of Epidemiology And Community Health*, 52(8):482–486, **1998**. doi:10.1136/jech.52.8.482.

Sandau, R., Brieß, K., and D errico, M. 'Small satellites for global coverage: Potential and limits.' *ISPRS Journal of Photogrammetry and Remote Sensing*, 65(6):492–504, **2010**. doi:10.1016/j.isprsjprs.2010.09.003.

Sarrat, C., Lemonsu, A., Masson, V., and Guedalia, D. 'Impact of urban heat island on regional atmospheric pollution.' *Atmospheric Environment*, 40:1743–1758, **2006**. doi:10.1016/j.atmosenv.2005.11.037.

Schmetz, J., Pili, P., Tjemkes, S., Just, D., Kerkmann, J., Rota, S., and Ratier, A. 'Supplement to An Introduction to Meteosat Second Generation (MSG).' *Bulletin of the American Meteorological Society*, 83(7):992–992, **2002**. doi:10.1175/BAMS-83-7-Schmetz-2.

Semenza, J., Rubin, C., Falter, K., Selanikio, J., Flanders, W., Howe, H., and Wilhelm, J. 'Heat-Related Deaths during the July 1995 Heat Wave in Chicago.' *The New England Journal of Medicine*, 335(2):84, **1996**. doi:10.1056/NEJM199607113350203.

Senay, G. B., Budde, M., Verdin, J. P., and Melesse, A. M. 'A coupled remote sensing and simplified surface energy balance approach to estimate actual evapotranspiration from irrigated fields.' *Sensors*, 7(6):979–1000, **2007**.

Sherwood, S. and Huber, M. 'An adaptability limit to climate change due to heat stress.' *Proceedings of the National Academy of Sciences (early view)*, **2010**.

Simón, F., Lopez-Abente, G., Ballester, E., and Martínez, F. 'Mortality in Spain during the heat waves of summer 2003.' *Euro surveillance : bulletin européen sur les maladies transmissibles = European communicable disease bulletin*, 10(7):156–161, **2005**.

Smith, C. L., Lindley, S. J., and Levermore, G. 'Estimating spatial and temporal patterns of urban anthropogenic heat fluxes for UK cities: the case of Manchester.' *Theoretical And Applied Climatology*, 98:19–35, **2009**. doi:10.1007/s00704-008-0086-5.

Smith, C. L., Webb, A., Levermore, G. J., Lindley, S. J., and Beswick, K. 'Fine-scale spatial temperature patterns across a UK conurbation.' *Climatic Change*, **2011**a. doi:10.1007/s10584-011-0021-0.

Smith, S., Hanby, V., and Harpham, C. 'A probabilistic analysis of the future potential of evaporative cooling systems in a temperate climate.' *Energy And Buildings*, 43:507–516, **2011**b. doi:10.1016/j.enbuild.2010.10.016.

Snyder, W., Wan, Z., Zhang, Y., and Feng, Y. 'Requirements for satellite land surface temperature validation using a silt playa.' *Remote Sensing of Environment*, 61(2):279–289, **1997**. doi:10.1016/S0034-4257(97)00044-8.

Snyder, W., Wan, Z., Zhang, Y., and Feng, Y. 'Classification-based emissivity for land surface temperature measurement from space.' *International Journal Of Remote Sensing*, 19(14):2753–2774, **1998**. doi:10.1080/014311698214497.

Soanes, C. and Stevenson, A., editors. *Oxford Dictionary of English, Second Edition, Revised*. Oxford University Press, **2005**.

Sobrino, J. 'Land surface temperature retrieval from MSG1-SEVIRI data.' *Remote Sensing of Environment*, 92(2):247–254, **2004**. doi:10.1016/j.rse.2004.06.009.

Sobrino, J., Jimenez-Munoz, J., Zarco-Tejada, P., Sepulcre-Canto, G., and Miguel, E. 'Land surface temperature derived from airborne hyperspectral scanner thermal infrared data.' *Remote Sensing of Environment*, 102(1-2):99–115, **2006**. doi:10.1016/j.rse.2006.02.001.

Sòria, G. and Sobrino, J. 'ENVISAT/AATSR derived land surface temperature over a heterogeneous region.' *Remote Sensing of Environment*, 111(4):409–422, **2007**. doi:10.1016/j.rse.2007.03.017.

Souch, C. and Grimmond, S. 'Applied climatology: urban climate.' *Progress in Physical Geography*, 30(2):270–279, **2006**. doi:10.1191/0309133306pp484pr.

Stabler, L., Martin, C., and Brazel, A. 'Microclimates in a desert city were related to land use and vegetation index.' *Urban Forestry & Urban Greening*, 3:137–147, **2005**. doi:10.1016/j.ufug.2004.11.001.

Stafoggia, M., Forastiere, F., Agostini, D., Biggeri, A., Bisanti, L., Cadum, E., Caranci, N., de Donato, F., de Lisio, S., de Maria, M., Michelozzi, P., Miglio, R., Pandolfi, P., Picciotto, S., Rognoni, M., Russo, A., Scarnato, C., and Perucci, C. A. 'Vulnerability to heat-related mortality: a multicity, population-based, case-crossover analysis.' *Epidemiology*, 17(3):315–323, **2006**. doi:10.1097/01.ede.0000208477.36665.34.

Stathopoulou, M. and Cartalis, C. 'Daytime urban heat islands from Landsat ETM+ and Corine land cover data: An application to major cities in Greece.' *Solar Energy*, 81(3):358–368, **2007**.

Stathopoulou, M. and Cartalis, C. 'Downscaling AVHRR land surface temperatures for improved surface urban heat island intensity estimation.' *Remote Sensing of Environment*, 113:2592–2605, **2009**.

Stathopoulou, M., Cartalis, C., and Chrysoulakis, N. 'Using midday surface temperature to estimate cooling degree-days from NOAA-AVHRR thermal infrared data: An application for Athens, Greece.' *Solar Energy*, 80(4):414–422, **2006**.

Stewart, I. 'A systematic review and scientific critique of methodology in modern urban heat island literature.' *International Journal of Climatology*, 31(2):200–217, **2010**. doi:10.1002/joc.2141.

Stimpson, J. 'Analysis - Are risks from heatwaves being taken seriously.' *New Civil Engineer*, pages 14–15, **2011**.

Stott, P., Stone, D., and Allen, M. 'Human contribution to the European heatwave of 2003.' *Nature*, 432(7017):610–614, **2004**. doi:10.1038/nature03089.

Streutker, D. 'Satellite-measured growth of the urban heat island of Houston, Texas.' *Remote Sensing of Environment*, 85(3):282–289, **2003**. doi:10.1016/S0034-4257(03)00007-5.

Su, J., Morello-Frosch, R., Jesdale, B., Kyle, A., Shamasunder, B., and Jerrett, M. 'An Index for Assessing Demographic Inequalities in Cumulative Environmental Hazards with Application to Los Angeles, California.' *Environmental science & technology*, 43(20):7626–7634, **2009**. doi:10.1021/es901041p.

Suddle, S. and Ale, B. 'The third spatial dimension risk approach for individual risk and group risk in multiple use of space.' *Journal of hazardous materials*, pages 35–53, **2005**. doi:10.1016/j.jhazmat.2005.04.024.

Sun, D. 'Estimation of land surface temperature from a Geostationary Operational Environmental Satellite (GOES-8).' *Journal of Geophysical Research*, 108(D11):1–15, **2003**. doi:10.1029/2002JD002422.

Sun, D., Pinker, R., and Basara, J. 'Land Surface Temperature Estimation from the Next Generation of Geostationary Operational Environmental Satellites: GOES M–Q.' *Journal of applied meteorology*, 43:363–372, **2004**. doi:10.1175/1520-0450(2004)043<0363:LSTEFT>2.0.CO;2.

Sun, D., Pinker, R. T., and Kafatos, M. 'Diurnal temperature range over the United States: A satellite view.' *Geophysical Research Letters*, 33(5):1–4, **2006**. doi:10.1029/2005GL024780.

Sun, Y., Wang, J., Zhang, R., Gillies, R., Xue, Y., and Bo, Y. 'Air temperature retrieval from remote sensing data based on thermodynamics.' *Theoretical And Applied Climatology*, 80(1):37–48, **2005**. doi:10.1007/s00704-004-0079-y.

Sustainability West Midlands. 'A Summary of Climate Change Risks for the West Midlands.' **2012**.

Sutherland, R., Hansen, F., and Bach, W. 'A quantitative method for estimating Pasquill stability class from windspeed and sensible heat flux density.' *Boundary-Layer Meteorology*, 37(4):357–369, **1986**. doi:10.1007/BF00117483.

Svensson, M. 'Sky view factor analysis–implications for urban air temperature differences.' *Meteorological Applications*, 11(03):201–211, **2004**. doi:10.1017/S1350482704001288.

Synnefa, A., Santamouris, M., and Akbari, H. 'Estimating the effect of using cool coatings on energy loads and thermal comfort in residential buildings in various climatic conditions.' *Energy And Buildings*, 39(11):1167–1174, **2007**. doi:10.1016/j.enbuild.2006.01.004.

Takahashi, K., Honda, Y., and Emori, S. 'Assessing Mortality Risk from Heat Stress due to Global Warming.' *Journal of Risk Research*, 10(3):339–354, **2012**. doi:doi: 10.1080/13669870701217375.

Tan, J. 'Commentary: People's vulnerability to heat wave.' *International Journal of Epidemiology*, 37(2):318, **2008**. doi:10.1093/ije/dyn023.

Tan, J., Zheng, Y., Song, G., Kalkstein, L., Kalkstein, A., and Tang, X. 'Heat wave impacts on mortality in Shanghai, 1998 and 2003.' *International journal of biometeorology*, 51(3):193–200, **2007**. doi:10.1007/s00484-006-0058-3.

Taramelli, A., Melelli, L., Pasqui, M., and Sorichetta, A. 'Estimating hurricane hazards using a GIS system.' *Natural Hazards And Earth System Sciences*, 8(4):839–854, **2008**.

Taylor, D. 'HRPT Reader.' URL `http://www.satsignal.eu/software/hrpt.htm`, **2012**. Accessed Aug 2012.

Tertre, A. L., Lefranc, A., Eilstein, D., Declercq, C., Medina, S., Blanchard, M., Chardon, B., Fabre, P., Filleul, L., Jusot, J.-F., Pascal, L., Prouvost, H., Cassadou, S., and Ledrans, M. 'Impact of the 2003 heatwave on all-cause mortality in 9 French cities.' *Epidemiology*, 17(1):75–79, **2006**.

The Economist. 'Russia's heatwave.' URL `http://www.economist.com/node/16703362`, **2010**. Accessed Nov 2011.

The Government Office for Science. *Foresight International Dimensions of Climate Change, Final Project Report*. London., **2011**.

The Mersey Forest and The University of Manchester. 'Surface temperature and runoff tools for assessing the potential of green infrastructure in adapting urban areas to climate change.' URL `http://82.69.33.138/grabs/`, **2011**. Accessed Aug 2012.

The Royal Commission on Environmental Pollution. 'Adapting Institutions to Climate Change.' Technical report, The Royal Commission on Environmental Pollution, **2010**.

The Sydney Morning Herald. 'Sydney swelters in record heatwave.' URL `http://www.smh.com.au/environment/weather/sydney-swelters-in-record-heatwave-20110201-1abm9.html`, **2011**. Accessed Nov 2011.

The University of Manchester Centre for Urban Regional Ecology. 'Adaptation Strategies for Climate Change in the Urban Environment (ASCCUE).' URL `http://www.sed.manchester.ac.uk/research/cure/research/asccue/`, **2012**. Accessed Aug 2012.

Tomlinson, C. J., Chapman, L., Thornes, J. E., and Baker, C. J. 'Including the urban heat island in spatial heat health risk assessment strategies: a case study for Birmingham, UK.' *International Journal of Health Geographics*, 10(1):42, **2011**. doi:10.1186/1476-072X-10-42.

Tomlinson, C. J., Chapman, L., Thornes, J. E., and Baker, C. J. 'Derivation of Birmingham's summer surface urban heat island from MODIS satellite images.' *International Journal of Climatology*, 32:214–224, **2012**a. doi:10.1002/joc.2261.

Tomlinson, C. J., Chapman, L., Thornes, J. E., Baker, C. J., and Prieto-Lopez, T. 'Comparing night-time satellite land surface temperature from MODIS and ground measured air temperature across a conurbation.' *Remote Sensing Letters*, 3(8):657–666, **2012**b. doi:10.1080/01431161.2012.659354.

Torok, S., Morris, C., Skinner, C., and Plummer, N. 'Urban heat island features of southeast Australian towns.' *Australian Meteorological Magazine*, 50(1):1–13, **2001**.

Trigo, I. F., Monteiro, I. T., Olesen, F., and Kabsch, E. 'An assessment of remotely sensed land surface temperature.' *Journal of Geophysical Research*, 113(D17):1–12, **2008**. doi:10.1029/2008JD010035.

UK Climate Projections. '99th percentile of daily minimum temperature (warmest night of the season).' URL `http://ukclimateprojections.defra.gov.uk/content/view/2135/690/`, **2011**a. Accessed Feb 2012.

UK Climate Projections. 'Case Studies.' URL `http://ukclimateprojections.defra.gov.uk/content/view/865/521/`, **2011**b. Accessed Feb 2012.

UK Climate Projections. 'Do the UKCP09 projections include the Urban Heat Island (UHI) effect?' URL `http://ukclimateprojections.defra.gov.uk/content/view/831/500/`, **2011**c. Accessed Feb 2012.

UK Climate Projections. 'Key findings for the West Midlands.' URL `http://ukclimateprojections.defra.gov.uk/content/view/2158/499/`, **2011**d. Accessed Feb 2012.

UK Meteorological Office. 'MIDAS Land Surface Stations data (1853-current).' URL `http://badc.nerc.ac.uk/data/ukmo-midas`, **2006**. Accessed Jan 2010.

UKCIP. 'A local climate impacts profile: how to do an LCLIP.' Technical report, UKCIP, **2009**a.

UKCIP. 'Risk Framework.' URL `http://www.ukcip.org.uk/index.php?option=com_content&task=view&id=62&Itemid=9`, **2009**b. Accessed Jan 2009.

Ulivieri, C. and Cannizzaro, G. 'Land surface temperature retrievals from satellite measurements.' *Acta Astronautica*, 12(12):977–985, **1985**. doi:10.1016/0094-5765(85)90026-8.

Umamaheshwaran, R., Bijker, W., and Stein, A. 'Image mining for modeling of forest fires from meteosat images.' *IEEE Transactions on Geoscience and Remote Sensing*, 45(1):246–253, **2007**. doi:10.1109/TGRS.2006.883460.

Unger, J. 'Intra-urban relationship between surface geometry and urban heat island: review and new approach.' *Climate Research*, 27(3):253–264, **2004**. doi:10.3354/cr027253.

Unger, J. 'Modelling of the annual mean maximum urban heat island using 2D and 3D surface parameters.' *Climate Research*, 30:215–226, **2006**. doi:10.3354/cr030215.

United Nations. 'World Urbanization Prospects: The 2007 Revision.' **2008**.

Unwin, D. 'The Synoptic Climatology of Birmingham's Urban Heat Island, 1965-74.' *Weather*, 35:43–50, **1980**.

USEPA. 'Reducing Urban Heat Islands: Compendium of Strategies. Urban Heat Island Basics.' Technical report, U.S. Environmental Protection Agency, **2008**.

USGS. 'Landsat Data Continuity Mission.' URL `http://pubs.usgs.gov/fs/2007/3093/`, **2007**. Accessed Aug 2012.

USGS. 'EarthExplorer.' URL `http://earthexplorer.usgs.gov/`, **2012**a. Accessed Aug 2012.

USGS. 'Global Visualization Viewer.' URL `http://glovis.usgs.gov`, **2012**b. Accessed Aug 2012.

Vancutsem, C., Ceccato, P., and Dinku, T. 'Evaluation of MODIS land surface temperature data to estimate air temperature in different ecosystems over Africa.' *Remote Sensing of Environment*, 114:449–465, **2010**. doi:10.1016/j.rse.2009.10.002.

Vandentorren, S., Bretin, P., Zeghnoun, A., Mandereau-Bruno, L., Croisier, A., Cochet, C., Riberon, J., Siberan, I., Declercq, B., and Ledrans, M. 'August 2003 heat wave in France: risk factors for death of elderly people living at home.' *The European Journal of Public Health*, 16(6):583–591, **2006**. doi:10.1093/eurpub/ckl063.

Vaneckova, P., Beggs, P. J., and Jacobson, C. R. 'Spatial analysis of heat-related mortality among the elderly between 1993 and 2004 in Sydney, Australia.' *Social Science & Medicine*, 70(2):293–304, **2010**. doi:10.1016/j.socscimed.2009.09.058.

Vaneckova, P., Hart, M. A., Beggs, P. J., and Dear, R. J. 'Synoptic analysis of heat-related mortality in Sydney, Australia, 1993–2001.' *International journal of biometeorology*, 52(6):439–451, **2008**. doi:10.1007/s00484-007-0138-z.

Vázquez, D. P., Reyes, F. J. O., and Arboledas, L. A. 'A comparative study of algorithms for estimating land surface temperature from AVHRR Data.' *Remote Sensing of Environment*, 62(3):215–222, **1997**. doi:10.1016/S0034-4257(97)00091-6.

Vescovi, L., Rebetez, M., and Rong, F. 'Assessing public health risk due to extremely high temperature events: climate and social parameters.' *Climate Research*, 30(1):71–78, **2005**.

Voogt, J. and Oke, T. 'Thermal remote sensing of urban climates.' *Remote Sensing of Environment*, 86(3):370–384, **2003**. doi:10.1016/S0034-4257(03)00079-8.

Walker, S., Liberti, L., and McAuslane, N. 'Refining the Benefit-Risk Framework for the Assessment of Medicines: Valuing and Weighting Benefit and Risk Parameters.' *Clin Pharmacol Ther*, 89(2):179–182, **2011**.

Wan, Z. 'MODIS Land-Surface Temperature Algorithm Theoretical Basis Document (LST ATBD).' Technical report, University of California, **1999**.

Wan, Z. 'Validation of the land-surface temperature products retrieved from Terra Moderate Resolution Imaging Spectroradiometer data.' *Remote Sensing of Environment*, 83(1-2):163–180, **2002**. doi:10.1016/S0034-4257(02)00093-7.

Wan, Z. 'New refinements and validation of the MODIS Land-Surface Temperature/Emissivity products.' *Remote Sensing of Environment*, 112(1):59–74, **2008**. doi:10.1016/j.rse.2006.06.026.

Wan, Z. 'MODIS Land Surface Temperature Products collection 5.' Technical report, University of California, **2009**.

Wan, Z. and Dozier, J. 'A generalized split-window algorithm for retrieving land-surface temperature from space.' *IEEE Transactions on Geoscience and Remote Sensing*, 34(4):892–905, **1996**. doi:10.1109/36.508406.

Wan, Z., Zhang, Y., Zhang, Q., and Li, Z. 'Quality assessment and validation of the MODIS global land surface temperature.' *International Journal Of Remote Sensing*, 25(1):261–274, **2004**. doi:10.1080/0143116031000116417.

Wang, K. and Liang, S. 'Evaluation of ASTER and MODIS land surface temperature and emissivity products using long-term surface longwave radiation observations at SURFRAD sites.' *Remote Sensing of Environment*, 113:1556–1565, **2009**.

Wang, W. 'Validating MODIS land surface temperature products using long-term nighttime ground measurements.' *Remote Sensing of Environment*, 112(3):623–635, **2008**. doi:10.1016/j.rse.2007.05.024.

Warwickshire LAA. 'Warwickshire LAA – Climate Change and Environment RISK MATRIX – Risk Evaluation and Scoring.' **2008**. Email correspondence October 2008.

Watkins, R., Palmer, J., and Kolokotroni, M. 'The London Heat Island: results from summertime monitoring.' *Building Services Engineering Research and Technology*, 23(2):97–106, **2002**. doi:10.1191/0143624402bt031oa.

Weller, J. and Thornes, J. E. 'An investigation of winter nocturnal air and road surface temperature variation in the West Midlands, UK under different synoptic conditions.' *Meteorological Applications*, 8(4):461–474, **2001**. doi:10.1017/S1350482701004078.

Weng, Q. 'Fractal analysis of satellite-detected urban heat island effect.' *Photogrammetric Engineering and Remote Sensing*, 69(5):555–566, **2003**.

Weng, Q. 'Thermal infrared remote sensing for urban climate and environmental studies: Methods, applications, and trends.' *ISPRS Journal of Photogrammetry and Remote Sensing*, 64(4):335–344, **2009**. doi:10.1016/j.isprsjprs.2009.03.007.

Weng, Q., Lu, D., and Schubring, J. 'Estimation of land surface temperature-vegetation abundance relationship for urban heat island studies.' *Remote Sensing of Environment*, 89(4):467–483, **2004**. doi:10.1016/j.rse.2003.11.005.

Wilby, R. 'Past and projected trends in London's urban heat island.' *Weather*, 58(7):251–260, **2003**. doi:10.1256/wea.183.02.

Wilby, R. 'Constructing climate change scenarios of urban heat island intensity and air quality.' *Environment and Planning B: Planning and Design*, 35(5):902–919, **2008**. doi:10.1068/b33066t.

Wilby, R. and Dessai, S. 'Robust adaptation to climate change.' *Weather*, **2010**.

Wilby, R., Jones, P., and Lister, D. 'Decadal variations in the nocturnal heat island of London.' *Weather*, **2011**.

Williams, C. N., Basist, A., Peterson, T. C., and Grody, N. 'Calibration and Verification of Land Surface Temperature Anomalies Derived from the SSM/I.' *Bulletin of the American Meteorological Society*, 81(9):2141–2156, **2000**. doi:10.1175/1520-0477(2000)081<2141:CAVOLS>2.3.CO;2.

Williams, N. S., Rayner, J. P., and Raynor, K. J. 'Green roofs for a wide brown land: Opportunities and barriers for rooftop greening in Australia.' *Urban Forestry & Urban Greening*, **2010**. doi:10.1016/j.ufug.2010.01.005.

Wilson, Nicol, E., Nanayakkara, F., Ueberjahn-Tritta, L., and Anja. 'Public Urban Open Space and Human Thermal Comfort: The Implications of Alternative Climate Change and Socio-economic Scenarios.' *Journal of Environmental Policy & Planning*, 10(1):31–45, **2008**. doi:10.1080/15239080701652615.

Xian, G. and Crane, M. 'An analysis of urban thermal characteristics and associated land cover in Tampa Bay and Las Vegas using Landsat satellite data.' *Remote Sensing of Environment*, 104(2):147–156, **2006**. doi:10.1016/j.rse.2005.09.023.

Yamaguchi, Y., Kahle, AB, Tsu, H., Kawakami, T., and Pniel, M. 'Overview of Advanced Spaceborne Thermal Emission and Reflection Radiometer (ASTER).' *IEEE Transactions on Geoscience and Remote Sensing*, 36(4):1062–1071, **1998**.

Yan, H., Zhang, J., Hou, Y., and He, Y. 'Estimation of air temperature from MODIS data in east China.' *International Journal Of Remote Sensing*, 30(23):6261–6275, **2009**. doi:10.1080/01431160902842375.

Yaron, M. and Niermeyer, S. 'Clinical description of heat illness in children, Melbourne, Australia–a commentary.' *Wilderness & environmental medicine*, 15:291–292, **2004**.

Yu, Y., Privette, J. L., and Pinheiro, A. C. 'Evaluation of Split-Window Land Surface Temperature Algorithms for Generating Climate Data Records.' *IEEE Transactions on Geoscience and Remote Sensing*, 46(1):179–192, **2008**. doi:10.1109/TGRS.2007.909097.

Yunyue, Y., Tarpley, D., Privette, J. L., Goldberg, M. D., Rama Varma Raja, M. K., Vinnikov, K. Y., and Hui, X. 'Developing Algorithm for Operational GOES-R Land Surface Temperature Product.' *IEEE Transactions on Geoscience and Remote Sensing*, 47(3):936–951, **2009**. doi:10.1109/TGRS.2008.2006180.

Zhu, K., Blum, P., Ferguson, G., Balke, K.-D., and Bayer, P. 'The geothermal potential of urban heat islands.' *Environmental Research Letters*, 5(4):044,002, **2010**. doi:10.1088/1748-9326/5/4/044002.

Appendices

Appendix A

Published Papers

INTERNATIONAL JOURNAL OF CLIMATOLOGY
Int. J. Climatol. **32**: 214–224 (2012)
Published online 3 December 2010 in Wiley Online Library
(wileyonlinelibrary.com) DOI: 10.1002/joc.2261

Derivation of Birmingham's summer surface urban heat island from MODIS satellite images

C. J. Tomlinson,[a]* L. Chapman,[b] J. E. Thornes[b] and C. J. Baker[a]
[a] *School of Civil Engineering, University of Birmingham, Edgbaston, Birmingham, B15 2TT, UK*
[b] *School of Geography, Earth and Environmental Sciences, University of Birmingham, Edgbaston, Birmingham, B15 2TT, UK*

ABSTRACT: This study investigates the summer (June, July, August) night urban heat island (UHI) of Birmingham, the UK's second most populous city. Land surface temperature remote sensing data is used from the MODIS sensor on NASA's Aqua satellite, combined with UK Met Office station data to map the average variation in heat island intensity over the Birmingham conurbation. Results are presented of average UHI events over four Pasquill-Gifford stability classes D, E, F, and G between 2003 and 2009, as well as a specific heatwave event in July 2006. The results quantify the magnitude of the Birmingham surface UHI as well as the impact of atmospheric stability on UHI development. During periods of high atmospheric stability, a UHI of the order of 5 °C is evident with a clear peak in the central business district. Also identified, are significant cold spots in the conurbation. In one city park, recorded surface temperatures are up to 7 °C lower than the city centre.

KEY WORDS urban heat island; MODIS; remote sensing; GIS; Birmingham; surface temperatures

Received 1 April 2010; Revised 13 September 2010; Accepted 19 October 2010

Tomlinson et al. International Journal of Health Geographics 2011, 10:42
http://www.ij-healthgeographics.com/content/10/1/42

INTERNATIONAL JOURNAL OF HEALTH GEOGRAPHICS

METHODOLOGY Open Access

Including the urban heat island in spatial heat health risk assessment strategies: a case study for Birmingham, UK

Charlie J Tomlinson[1*], Lee Chapman[2], John E Thornes[2] and Christopher J Baker[1]

Abstract

Background: Heatwaves present a significant health risk and the hazard is likely to escalate with the increased future temperatures presently predicted by climate change models. The impact of heatwaves is often felt strongest in towns and cities where populations are concentrated and where the climate is often unintentionally modified to produce an urban heat island effect; where urban areas can be significantly warmer than surrounding rural areas. The purpose of this interdisciplinary study is to integrate remotely sensed urban heat island data alongside commercial social segmentation data via a spatial risk assessment methodology in order to highlight potential heat health risk areas and build the foundations for a climate change risk assessment. This paper uses the city of Birmingham, UK as a case study area.

Results: When looking at vulnerable sections of the population, the analysis identifies a concentration of "very high" risk areas within the city centre, and a number of pockets of "high risk" areas scattered throughout the conurbation. Further analysis looks at household level data which yields a complicated picture with a considerable range of vulnerabilities at a neighbourhood scale.

Conclusions: The results illustrate that a concentration of "very high" risk people live within the urban heat island, and this should be taken into account by urban planners and city centre environmental managers when considering climate change adaptation strategies or heatwave alert schemes. The methodology has been designed to be transparent and to make use of powerful and readily available datasets so that it can be easily replicated in other urban areas.

Keywords: Urban Heat Island, UHI, Birmingham, Experian, Heat Risk, Spatial Risk Assessment, GIS, Remote Sensing, MODIS

Background

The aim of this paper is to integrate remotely sensed urban heat island data alongside commercial social segmentation data through a spatial risk assessment methodology in order to highlight potential heat health risk areas. This will build the foundations for a climate change risk assessment using the city of Birmingham, UK as a case study area.

Heat Risk and Urban Areas

There is a growing recognition in the fields of bio-meteorology, epidemiology, climatology and environmental health that heat risk in urban areas is a problem, with literature considering cities in Europe [1], the USA [2,3], Australia [4] and Asia [5,6]. Elevated temperatures cause increased human mortality [7] which is exacerbated in heatwaves resulting in excess deaths. A number of examples are available in the literature such as in the 1995 UK heatwave [8], the 1995 Chicago heatwave [9] or the 2003 European heatwave [10] which affected France [11-14], England [15,16], the Netherlands [17], Portugal [18] and Spain [19]. There is growing evidence that the intensity, frequency and duration of heatwaves is likely to increase in the future [20]. This is prompting increased research into heat health risk projections [21,22], often as part of the broader remit concerning climate change and health [23-26].

* Correspondence: cjt512@bham.ac.uk
[1]School of Civil Engineering, University of Birmingham, Edgbaston, Birmingham, B15 2TT, UK
Full list of author information is available at the end of the article

The urban heat island (UHI) is a well documented phenomenon [27,28] that results in a conurbation being warmer than the surrounding rural areas. It is an example of an unintentional modification of the local climate and is principally caused by alterations to the energy balance influenced by variations of landuse, surface properties (e.g. surface roughness, albedo, emissivity) and geometry of the of the urban area [29,30]. Increased population in the city also promotes warming from anthropogenic heat release [31]. Hence, those that live in inner city areas are subsequently exposed to the UHI effect and can therefore be under increased heat health risk [2,8,32]. However, previous spatial risk assessment studies generally don't include the UHI [33]. With rates of urbanisation continuing to increase (the United Nations [34] predicting that population growth to 2050 will be absorbed exclusively in urban areas), the need for detailed heat risk assessments is paramount. Although this is an emerging research area [35,36], existing climate change work does not include a UHI component [37,38], despite it having a considerable influence on the mesoscale climate. Some work has been done to integrate the UHI within the United Kingdom Climate Projections 2009 (UKCP09) [39], but this is at a much larger scale than this paper considers. The result is a present need to integrate climate change projections with UHI data via a piecemeal methodology. Recent work utilising remote sensing techniques [40,41] has allowed the spatial extent of the UHI to be measured at a higher resolution than previously, and this paper focuses on using this data for heat health risk studies.

Vulnerable Sections of the Population

There is evidence to suggest there are upper limits to human adaptation to temperature [42], which makes the consequences of increased temperatures important to understand. Although defining human thresholds for heat risk has many problems [43], it is possible to identify vulnerable groups (Table 1). High population density has been shown to correlate with areas of higher temperatures [44], and is to be expected given that high population density is often within inner city areas that are also impacted by the UHI. With specific reference to heat health risk, multiple studies have shown that increased population density results in increased risk [45-47]. Therefore it is reasonable to include people living in areas of high population density as vulnerable to heat risk.

Table 1 Groups vulnerable to heat risk

Vulnerable Group	References
Elderly People	[32,48-57]
Ill Health	[9,11,55,58,59]
High Population Density	[45-47]
High Rise Living	[9,32,59]

The elderly population has a relatively high percentage of illness and disability which increases their vulnerability [48]. Older, frail individuals are thought to have a lower tolerance to extremes of heat [49], and compounding factors, such as lack of mobility, further increase vulnerability [50]. This has been illustrated in the literature by studies in Switzerland [51], Italy [52], the Netherlands [53], Spain [54], Italy [55] and Latin America [56]. Within the UK, academic research [57] and the national Department of Health [32] recognise that the elderly are vulnerable to heat.

Another vulnerable group can be defined as those in "ill health". This includes those with pre-existing illness or impaired health, which could be physical or mental [58,59]. Known medical problems and those unable to care for themselves or with limited mobility are at increased risk [3,9,55], and diseases mentioned specifically include respiratory, cardiovascular and the nervous system [11].

People living on the top floor of flats or high rise buildings have also been found to have increased heat risk, with studies in Chicago in both 1995 [9] and 1999 [59] having similar results, finding that those living on higher floors were subject to increased risk. Within the UK, those in south facing top floor flats are classed as "high risk" by the Department of Health [32]. The reasons for this increased risk include the build up of temperatures in larger and taller buildings, and the increased exposure to incoming solar radiation resulting in higher temperatures.

Finally, young children are another group that could be at risk, with studies in Australia [60], America [61] and the UK [62] outlining the vulnerability of the very young. However, in this paper children have not been included because of the difficulties in locating detailed data (a consequence of the requirement to target parents or guardians in order to communicate). An effective way to reduce this research gap could be to target schools and embed heat risk education where appropriate.

Spatial Risk Assessment Methodologies

The use of Geographical Information Systems (GIS) for spatial risk assessment work is a growing field, and covers a diverse range of hazards. These include various environmental hazards [63,64], flooding and geological hazards [65], technological hazard [66], hurricanes [67], fuel poverty [68] and many more. Work exploring spatial heat risk has so far been limited, but includes work in Australia [69], Canada [70] and the United States [71]. However the work that is most closely related to

this paper is that of the field of climate change adaptation in the UK [33,72,73].

A critique of risk assessment methods in relation to climate change [74] details how problematic the process can be. However, given the increasing demand for "evidence based decisions" within governance, a form of risk assessment framework is required. The Adaptation Strategies for Climate Change in the Urban Environment (ASCCUE) project (more details available at http://www.sed.manchester.ac.uk/research/cure/research/asccue/) developed a risk assessment methodology based on "Crichton's Risk Triangle" [75]. This has been utilised in the UK as part of a broader methodology to assess flood hazard at both a neighbourhood and conurbation scale [65,73] and to assess heat risk in relation to climate change [33,72]. This paper builds on the methodologies developed in these papers and adds some important developments. In particular, this paper focuses on the impact of the UHI as well as developing objective methods that can easily be replicated nationally.

Methods

Study Area

The study area of Birmingham is the second most populous city in the United Kingdom, covering over 270 km^2 and with a population over one million [76]. Birmingham can be seen as representative of many inland mid-latitude cities worldwide, and using it as a case study offers a change from papers focussing on mega-cities such as London or New York which are too unique to have results which can easily be translated elsewhere.

This study utilises the "Lower layer Super Output Area" (LSOA) [77] as a spatial scale. LSOA is a geographical hierarchy designed for small area statistics, and although they do not have consistent physical size, they are not subject to boundary changes in the future, unlike other areas such as wards or postcodes. This makes them ideal for ongoing studies. A LSOA has a minimum population of 1,000 and an average population of 1,500, allowing data to be distributed easily without identifying individuals. As the LSOA is part of a hierarchy it is easy to change the scale, for example combining a number of LSOA into a single Medium layer Super Output Area (MSOA) which adds flexibility to the methodology as it allows comparison with datasets that may only be available at MSOA. There are 641 LSOA within the Birmingham area, numbered from 8881 to 9521 inclusive, with size (km^2) ranging between 0.062 - 8.739, mean 0.418, standard deviation 0.541.

Health research with specific reference to the Birmingham area has taken place both within academia; exploring the relationship between mortality and temperature [78], looking at the 1976 heatwave [79] and through the public sector; looking at climate change and health [80]. This previous work has not included a spatial aspect, which is an important research gap given the size and diversity within Birmingham, and particularly when including a UHI component. Detailed work on Birmingham's UHI has recently been undertaken [41] and data is readily available, allowing this important effect to be considered in detail.

Spatial Risk Assessment

The methodology utilised in this paper has deliberately been kept simple and transparent in order to remove excessive complicated jargon and help explanation to stakeholders including local authorities. However, at this stage it is important to clarify the terminology used in this paper, as throughout the risk assessment literature there are various terms that have multiple definitions.

The main risk assessment theory focuses on "Crichton's Risk Triangle" (Figure 1) that states that risk is a function of hazard, exposure and vulnerability, and all must be spatially coincident for a risk to exist. The advantages of splitting the definition are that it makes the process clear and transparent and simplifies analysis within a layering system in a GIS. A hazard is something that may cause a risk, and in this method the spatial and temporal aspects of the hazard are required, alongside the magnitude. This could be historical, measured or predicted, and in this case the increase in temperature from the UHI is being considered, measured from remotely sensed satellite data. The exposure represents what is exposed to the hazard and at a basic level is simply a spatial coincidence between the hazard and the exposure of interest. Various items could be exposed and relevant data about each is required spatially for this method to

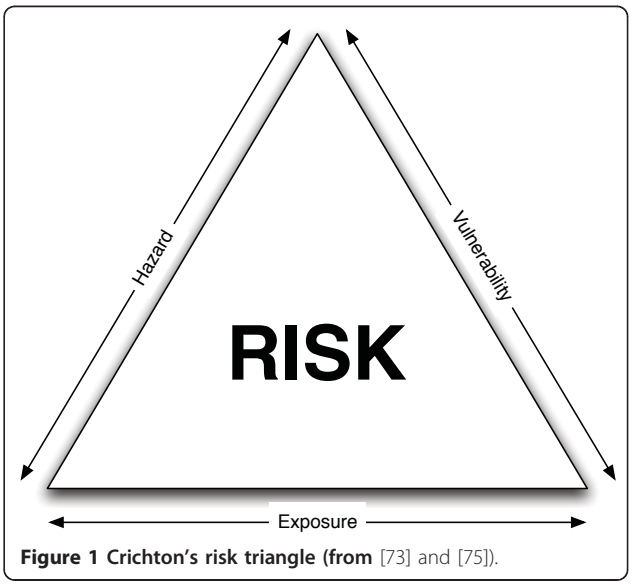

Figure 1 Crichton's risk triangle (from [73] and [75]).

be useful. Examples could be buildings (with corresponding metadata such as types or value) or people (with metadata such as age or health problems) and this paper uses high resolution commercial social segmentation data. Vulnerability refers to which aspects of the exposed elements are vulnerable to a given hazard, and this is generally defined by referencing a vulnerability table. Certain groups are more vulnerable to heat risk, for example the elderly. The final risk layer is generated from the spatial coincidence of the hazard layer and the *exposed and vulnerable* layer. This is a simplification of the ASCCUE work and a flowchart visually illustrates the workflow (Figure 2). These methodological changes, which remove the "hazard-exposure" layer and place more emphasis on the "*exposed and vulnerable*", were chosen due to simplification of data manipulation and ease of explaining to stakeholders. A more detailed explanation of Crichton's risk triangle and real world examples of use are available [33,65,72,73,75]. In order to spatially represent each of the hazard, exposure, vulnerability and risk layers a coherent spatial scale is required across all layers. All items of interest are merged at the LSOA scale.

A standardisation technique has been employed, in order to illustrate each variable on the same scale and ensure ease of combining layers of a different nature. This technique helps quantify the process and enables statistical analysis and comparisons to be carried out more effectively. This is based on the Hazard Density Index (HDI) [66] that a number of studies have used successfully [63,81]. Individual variables are standardised by dividing each variable value from the maximum value of that variable across the complete study area. The formula used is: "*LSOA score/max LSOA score across Birmingham = standardised score for each LSOA*". This standardises the variable to between zero (low) and one (high).

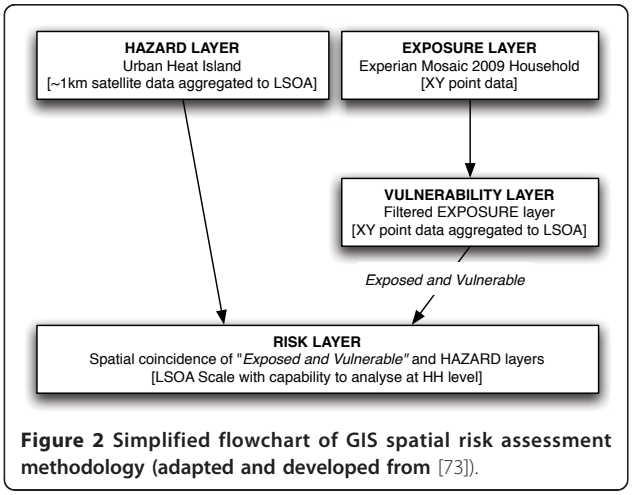

Figure 2 Simplified flowchart of GIS spatial risk assessment methodology (adapted and developed from [73]).

When combining layers it is possible to vary the weighting of values based on relative importance. However, in this paper all weightings have been kept equal in the interests of transparency. Other studies have used equal weighting methods with success [63,64]. If weighting of values is varied the process becomes subjective and the resultant maps open to manipulation. Appropriate use of weightings requires considerable knowledge concerning all the variables and techniques. It is anticipated that the results of this work will be incorporated into a spatial decision support tool where the weightings can be altered according to specific user requirements.

Hazard Layer: Urban Heat Island

High resolution UHI mapping can be obtained through remote sensing methods, including airborne (such as NASA's ATLAS sensor [82]) or satellite platforms. The highest resolution (~60 m) satellite sensors used for UHI work include Landsat ETM+ [83] and ASTER [84]. This paper uses the Moderate Resolution Imaging Spectroradiometer (MODIS) on NASA satellites (due to the increased temporal coverage and thermal accuracy) to measure Land Surface Temperature (LST) at a ~1 km resolution on cloud free days and this has been analysed and manipulated (full details available [41]) in order to measure the magnitude of the surface UHI. The relationship between LST (and therefore surface UHI) and measured air temperature is complicated, with techniques such as statistical regression [85], solar zenith angle models [86] or thermodynamics [87] often used to explore the relationship. LST and air temperature are not directly comparable, however in the case of the UHI, it is reasonable to believe that spatial trends will be similar when comparing LST and air temperature, and therefore remotely sensed data is a useful dataset as absolute values are not vital in this methodology.

Detailed UHI work has been carried out for Birmingham [41] and it is this dataset that has been used in this paper. The MODIS remotely sensed image of the night of the 18th July 2006, used as a "heatwave" example was resampled and then zonal statistics were carried out in order to facilitate generalisation at the LSOA scale. The mean UHI magnitude (°C) for each LSOA was taken to standardise the LSOA output on a scale between zero and one, as for other layers. The resultant layer illustrates the spatial pattern of the UHI across the conurbation on a specific heatwave day, representative of a day with ideal conditions for UHI generation (low windspeed and low cloud cover). However the spatial pattern of the UHI has been shown to be similar across a number of different meteorological conditions [41].

The main alternatives to satellite data for calculating the UHI include ground sensor measurements or model output. There is a paucity of ground sensors in

Birmingham, and other approaches (for example transect based [88]) require extensive fieldwork. UHI model's [36,89] have been developed, but require considerable work to collate accurate input variables and validate the results. Satellite data is readily available globally, increasing the utility of the methodology.

Overall, the inclusion of the UHI as the hazard layer explicitly fills a specific research gap from other heat risk studies. The work could be expanded on, for example to include the possible effects of both climate change and the UHI, however this is outside the scope of this paper.

Exposure Layer: Experian Mosaic 2009 Data

The exposure layer in this paper is made up of detailed commercial data from Experian on every household in Birmingham. Experian are a global company focussed on providing information to help business and in the UK they are commonly known for being one of the three credit reference agencies the financial industry uses. Within this paper, the Experian Mosaic UK 2009 product is used which is a consumer classification for the United Kingdom, providing "an accurate understanding of the demographics, lifestyles and behaviour of all individuals and households in the UK" [90], classifying each household into one of 15 groups, and below that one of 67 types. This exact method is suitable for the UK, but Experian have a number of consumer segmentation products for 29 countries that classify over a billion consumers, so it could be easily adapted to other parts of the developed world. The Mosaic classification is built using 440 data elements, and is updated and verified bi-annually [90].

The Mosaic 2009 dataset was supplied for all of Birmingham at household (HH) level, with each HH including attributes of X and Y location, Mosaic Type and Mosaic Group. For the purposes of this paper, HH data is generally aggregated up to LSOA levels as this can be distributed without personal identities being disclosed, whilst still giving a relatively high resolution. However, having access to the HH data gives additional flexibility both for the methodology and analysis. Supplied alongside the raw data was the key to Mosaic types, a document that gave in depth qualitative information for each Mosaic type, including a general overview followed by specific demographic information related to where the type lives, how they live, world views, financial situation and online behaviour. Using a single dataset to underpin the methodology and analysis was a deliberate choice, designed to remove problems of availability and contextual differences that have been illustrated in previous studies [63]. The data used in this project is at HH level, and details the 427,914 HH contained within Birmingham city extents. Experian offer a risk dataset (Perils), encompassing flood, subsidence, windstorm and freeze risk [91] however heat risk is notably absent, and therefore this work also acts as a proof of concept for expanding Experian's risk dataset product portfolio. The exposure layer is point shapefile with one point for each household containing attribute data including Mosaic type; data is summarised into LSOA at a later stage using GIS techniques. Titles of the Mosaic types used in this paper are detailed in Table 2, and more details are available in the Mosaic 2009 brochure (available online [90]).

An alternative data source is the British Census (a decadal survey of every person and household in the UK), and this has been used in other studies [33,57]. However, it will take time for data from the recent 2011 Census to become available after being verified and quality assured, and available data from the 2001 Census is now outdated. This paper does not use Census data, given the time delay and the future uncertainty over the survey given the current governmental spending cuts. Mosaic uses current year estimates of Census data for 38% of the information used to create the classification, alongside additional datasets and verification. This makes the data more useful as it is upto date. For more information on the classification system, see the brochure online [90].

Vulnerability Layer(s): Specific Vulnerable Types

The vulnerability layer in this paper is made up of vulnerable types extracted from the exposure layer, made

Table 2 Titles of relevant Mosaic type identified for specific vulnerabilities

Mosaic Number	Mosaic Titles	Vulnerability
20	Golden Retirement	Elderly
21	Bungalow Quietude	Elderly
22	Beachcombers	Elderly
23	Balcony Downsizers	Elderly
38	Settled Ex-Tenants	III
39	Choice Right to Buy	III
42	Worn-Out Workers	III
43	Streetwise Kids	III
44	New Parents in Need	III
45	Small Block Singles	III
47	Deprived View	III
50	Pensioners in Blocks	Elderly
51	Sheltered Seniors	Elderly
52	Meals on Wheels	Elderly
53	Low Spending Elders	Elderly
65	Anti-Materialists	III

*All 67 Mosaic types were used to calculate density and high rise vulnerabilities

up of Experian Mosaic HH types. Vulnerable types have been defined through a literature review and justifications for each layer are given in Table 1. The following details how each specific vulnerable type was identified and extracted from the data available in the Mosaic dataset.

Elderly people were identified as Mosaic group E, "Active Retirement" (type 20,21,22,23) and L, "Elderly Needs" (type 50,51,52,53). Within these groups, there is a wide range of socioeconomic factors, however all are elderly. The literature identified elderly as a vulnerable type, and whilst affluence can reduce vulnerability, for example by financing air conditioning units, it cannot totally mitigate the vulnerability. The number of HH classed as "elderly" per LSOA was counted and then standardised as discussed.

Other heat risk studies [33] discuss how analysing flats or high rise buildings could be a possible addition to their study. This paper uses a combination of datasets to calculate people living in high rise buildings. The Mosaic data gave household locations (including multiple households at the same XY coordinates). Ordnance Survey Mastermap, the highest resolution vector mapping solution available in the UK, details individual buildings at polygon level. Individual building polygons across Birmingham were extracted from Mastermap, and then the number of HH points falling within each polygon was counted. This was then filtered to show only polygons with greater than ten HH within. The rationale behind this number is that buildings with less than ten households are not likely to be sufficiently high rise. This number would be easily altered for use in different cities. Light Detection and Ranging (LIDAR) height data could be combined in order to obtain true height of buildings but this approach was not used because this methodology focuses on using Experian data for ease of repeatability.

Density of households per LSOA was calculated simply by using following formula, for each LSOA "*HH density per LSOA = number of HH in LSOA/area of LSOA (km^2)*". The result is household density per km^2 that was standardised as per the technique already detailed.

The vulnerable group "ill health" was created by a literature and keyword search of the Mosaic 2009 key document for keywords "health" or "illness" followed by qualitative interpretation of the results by a single interpreter to avoid bias. This identified Mosaic types 38, 39, 42, 43, 44, 45, 47, and 65 as including people with ill health. Not all HH will be of ill health, but examples of the way these groups are described includes "they have health problems " or "higher levels of illness" or "many have health issues, including mental health issues". The number of HH classed as "ill health" per LSOA was counted, and then standardised as described.

Risk Layer

To create the final risk layer, the four vulnerability layers were combined into a single "*exposed and vulnerable*" layer (each weighted at 25%) which was then spatially combined with the hazard layer (each weighted at 50%), a technique that has been used successfully for previous spatial risk assessment [63]. This process is illustrated in Figure 3.

Results and Discussion

When interpreting the results it is important to note that when generalising at the LSOA scale, some data will be masked in a small number of cases. For example, the Sutton Park area in the north of the city that contains the actual park has to be extended to include an area with approximately 1,500 people in order to match the LSOA geography. As this LSOA is physically one of the biggest by area within Birmingham, maps can look skewed.

Spatial Trend between the UHI and Exposed and Vulnerable

The UHI under heatwave conditions at LSOA level (Figure 4) reflects the results (from [41]) and gives confidence that the generalisation to LSOA has not compromised the dataset. A full discussion of the spatial trends is available [41] but in summary, the highest temperatures are found in the city centre where as the Sutton Park area in the north of the city is the coolest area. As expected, there is a general trend towards lower temperatures in the suburban areas.

The four main "*exposed and vulnerable*" layers were displayed in a GIS with natural breaks (Jenks) symbology (Figure 5) in order to view groupings inherent in the data. Concentrations of old people are scattered throughout the city, with distinct clusters in the north. This is not surprising as the northern Sutton Coldfield area is generally regarded as having a slower pace of life,

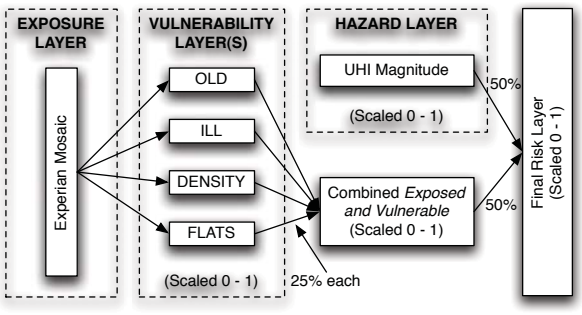

Figure 3 Detailed flowchart of spatial risk assessment methodology. All are at LSOA level except the Exposure Layer which is HH points.

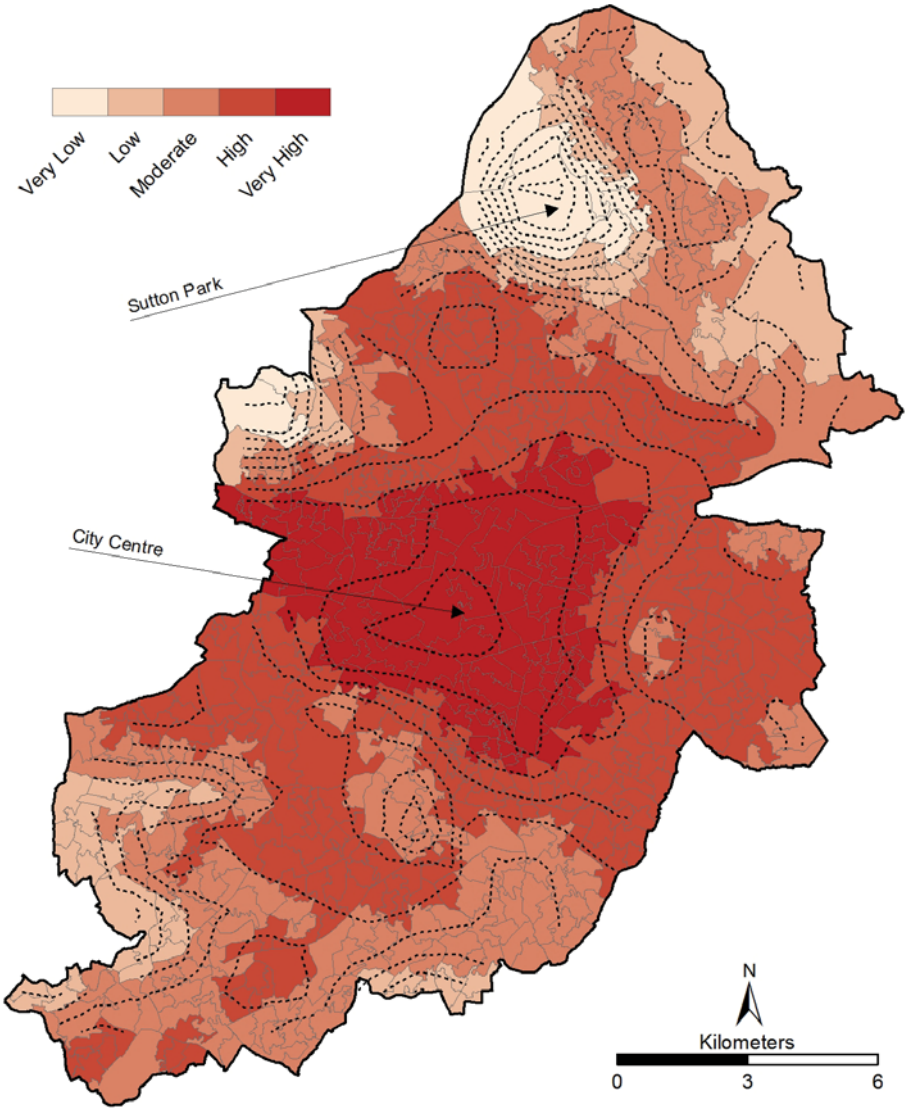

Figure 4 Birmingham UHI under heatwave conditions at LSOA level. 18th July 2006 from MODIS remotely sensed data. Shown with contour lines for validation.

with close proximity to countryside being appealing to the older generation. This also helps explain the lack of elderly people in the city centre, where they are conspicuously absent. There are additional concentrations of older people in the east and towards the south.

Conversely when looking at flats, there is a significant concentration in the city centre, a result of high land costs forcing the development of high rise flats. This property type is unappealing for the majority of elderly people, given the difficulties of access (e.g. stairs/lifts) and greater noise levels. Away from the centre, there are other LSOA's with high levels of flats, including small numbers in the north, and even less in the south. For example, clusters can be found in student areas, such as the high rise student housing located on Birmingham City University campus (Area Z, Figure 5).

There is less of a visible range when looking at density (detailed in HH per km^2). Again, the highest density LSOA's are located in the city centre, extending north westwards into areas renowned for having a high immigrant population. Conversely, density reduces heading south from the city. For example, Edgbaston (Area Y, Figure 5) is an affluent area that also includes the University of Birmingham, Edgbaston golf course and other land uses not associated with households. The north east quarter of the city centre (Area N, Figure 5) is also low density, and is an area traditionally associated with industry. However, the overall density levels across the city are generally

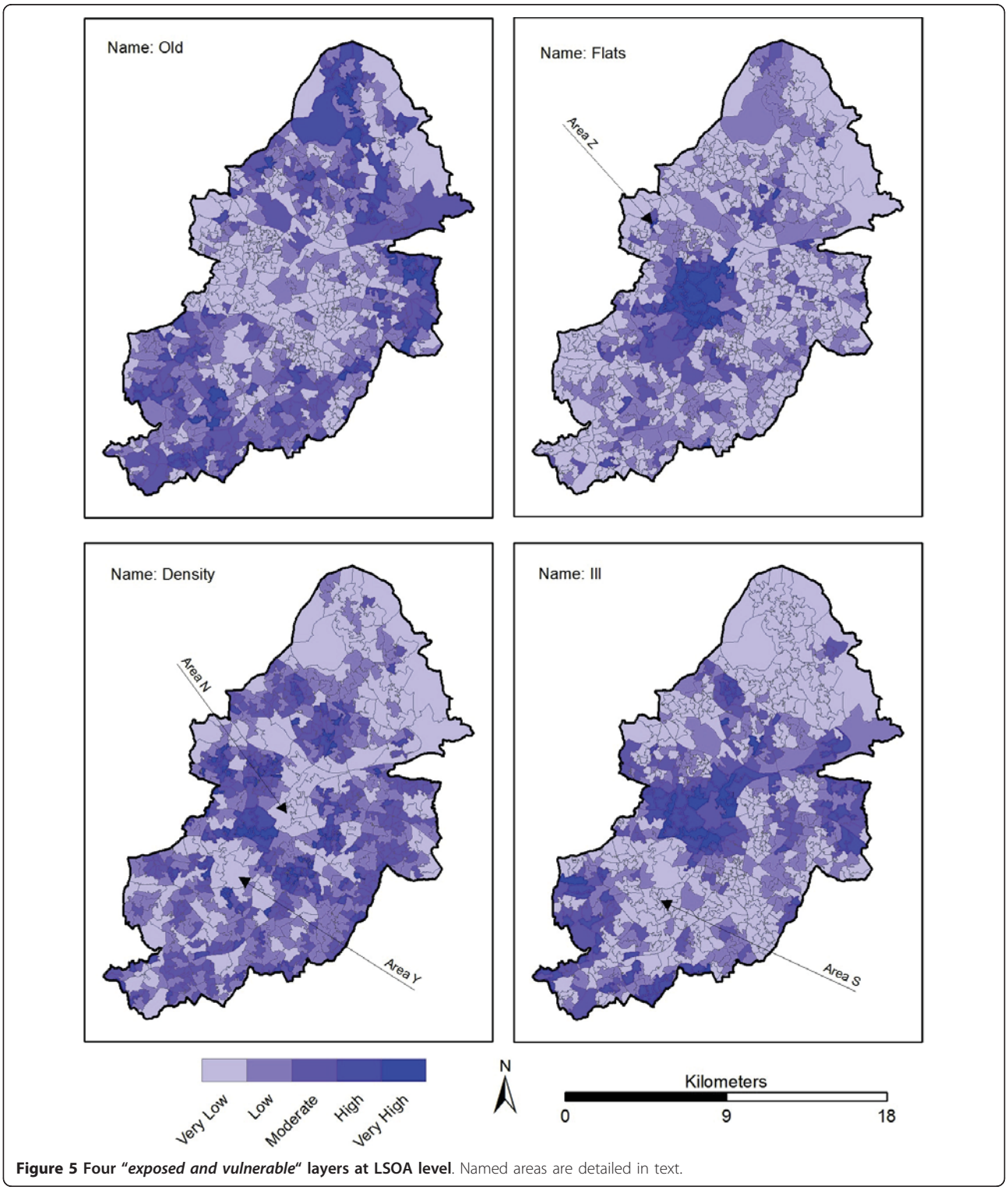

Figure 5 Four "*exposed and vulnerable*" layers at LSOA level. Named areas are detailed in text.

similar, with local variations between LSOA's dependent on the presence of greenspace (which increase the size of the LSOA area but not numbers of HH).

Finally, significant concentrations in the spatial pattern of people with ill health exist. This is particularly evident across the city centre and in a belt north east of the city centre and towards the cities eastern edge. Pockets are also visible in the south, after noticeable lows in the affluent area of Edgbaston and the transient student population of Selly Oak (Area S, Figure 5), who

are unlikely to stay in the same place long enough for reliable health statistics to be compiled.

A Spearman's rank order correlation was carried out to determine the statistical relationships between each "*exposed and vulnerable*" group and the UHI at the LSOA level ($n = 641$). Table 3 shows that the results generally agree with the visual interpretation and all relationships are statistically significant ($p < 0.01$) except density *vs* flats. There is a weak positive correlation between density, flats and illness with the UHI, showing that as the UHI increases, the number of "*exposed and vulnerable*" groups also increases. There is a stronger negative correlation between old people and the UHI that agrees with the visual interpretation already discussed.

When the above four vulnerable groups are combined and equally weighted (Figure 6) it is clear to see that the very high risk areas are concentrated around the city centre. This is to be expected due to the individual distributions already discussed, and agrees with previous work in the USA which has found that vulnerability increased in warmer neighbourhoods [45] and that these neighbourhoods had a tendency to be located within the inner city [71]. Although equal weightings for all layers have been used in this study, it is recognised that features of urban form (e.g. density) can also act as predictors for the UHI. As a result, this can impact the output risk, and is an area that could be explored more in the future when considering different weightings for layers.

The Final Risk Layer

Figure 7 shows that the majority of the "very high" risk LSOA's are grouped together in the city centre. It is here where the highest temperatures are experienced as well as the highest number of ill people, number of flats and density. However, additional pockets of "very high" risk also exist and these require additional explanation. As already discussed, a high concentration of flats increases the density of a LSOA. Outside of the city centre, these flats are frequently high rise social housing that is often associated with increased illness in the poorer sections of communities. A typical "high risk" pocket has significant high rise social housing which increases the density, scores highly for flat and often for illness as well.

Table 3 Spearman's rank correlation coefficient matrix

	Density	Flats	Ill	Old
Density	-	-	-	-
Flats	0.058*	-	-	-
Ill	0.161**	0.254**	-	-
Old	-0.256**	0.241**	0.158**	-
UHI (mean)	**0.329****	**0.125****	**0.224****	**-0.396****

* Correlation is not significant at the 0.01 level.

** Correlation is significant at the 0.01 level.

The lowest risk areas are found in the north west (Sutton Park area) and north east of the city. This is explained by the low and very low UHI risk coupled with very low "*exposed and vulnerable*" populations. An anomaly of this area is that it actually has the highest concentration of elderly people, but they are less vulnerable to heat due to their distance from the city centre. Other very low risk areas are evident west of the city centre and scattered south of the city centre. In general these are heavily linked to greenspace; which has the dual effect of ameliorating the UHI and reducing the number of people living in an area. Indeed, a more explicit look at the distribution of greenspace within the conurbation could be useful (e.g. using surface cover analysis [92] or energy exchange models [93]), given the benefits of reducing the UHI [94] and improving health inequalities [95].

Household Level

A strength of the methodology detailed in this paper is that once the risk areas have been identified, a subsequent detailed analysis down to HH level can be conducted. Such high resolution work within urban areas is a logical development of previous broader scale work, such as the province wide analysis carried out in Quebec, Canada [70]. A GIS was used to identify 37,477 HH's (or ~8.76% of 427,914) that fall within the "very high" risk LSOA's (33 out of 641). These HH's can then be profiled using Mosaic type (Figure 8), which illustrates the vast majority are either 47 (Deprived view) or 64 (Bright young things), accounting for ~7,000 HH each. This illustrates a clear divide within the "very high" risk area which is only able to be explored by having access to high resolution underlying datasets such as Mosaic. Type 47 are "poor people who live in high rise blocks of socially owned housing...many have disabilities...characterised by extreme poverty". Type 64 are "well educated young high flyers...live in smart inner city areas...mostly modern, purpose built or converted apartments". Despite living in broadly the same area, the populations are generally separated (Figure 9) and are at polarised levels of heat risk. Type 64 typically live in new apartments located within the inner city. These dwellings may have good insulation, air conditioning or even passive cooling. This is a contrast to type 47, who live in older, social apartments located in less desirable areas surrounding the urban core. Unlike type 64, this group is unlikely to have the finances available to make themselves comfortable or safe.

Conclusions

This study has illustrated a simple methodology for quantifying risk, through a process where each stage can

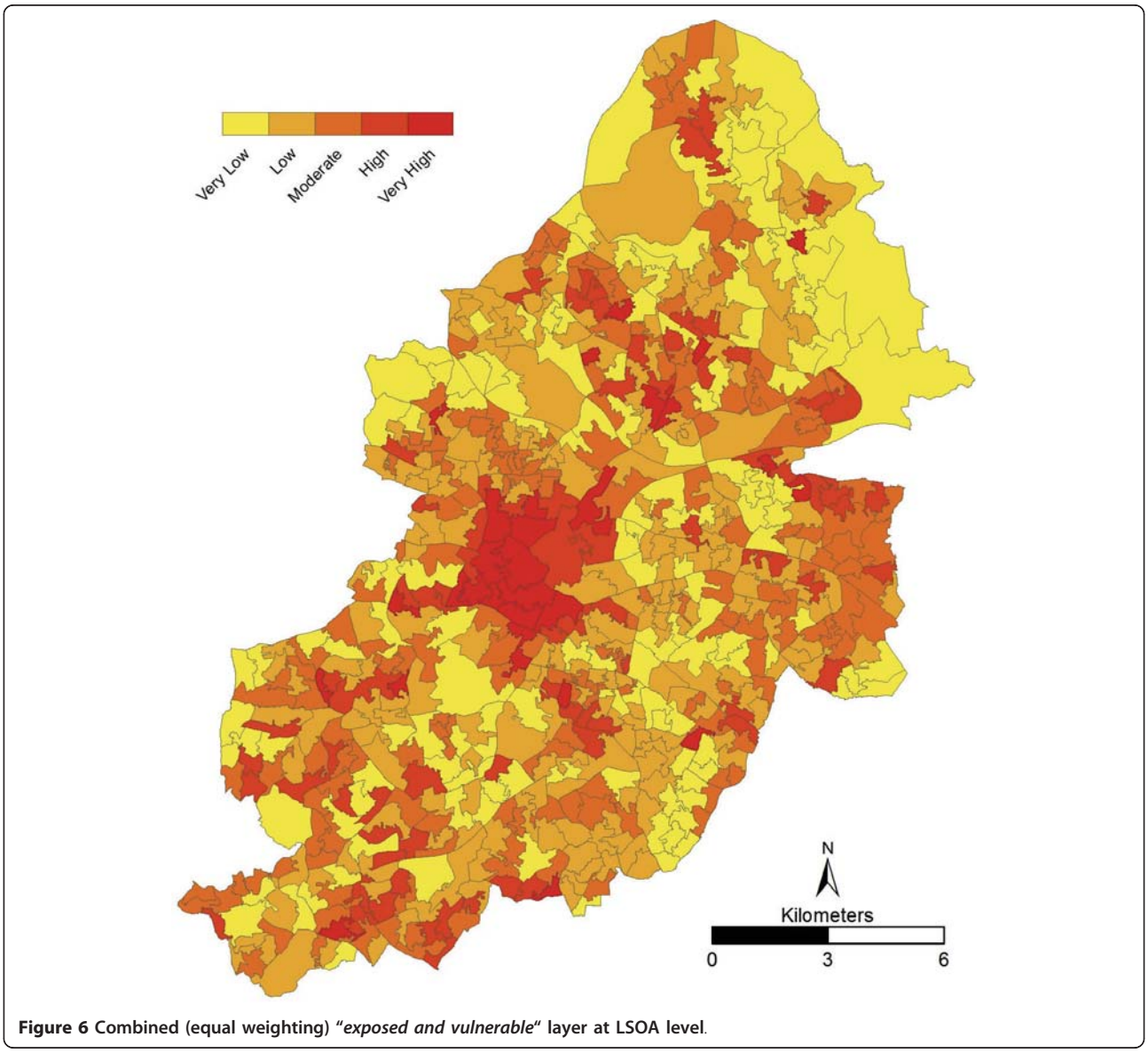

Figure 6 Combined (equal weighting) "*exposed and vulnerable*" layer at LSOA level.

clearly be explained and understood. It offers suggestions for the output to be customised, for example with different weightings or replacement with different hazards or risk groups as appropriate. This work offers the foundations for a spatial decision support tool that could be linked to climate change and projection models in order to consider climate change adaptation with a focus on heat health risks. Indeed, such data is potentially of great use to local authorities and health agencies when deciding on targeted campaigns.

The highest vulnerability is shown to exist in the inner city areas. This result agrees with similar work done in the USA [45,71] and is a direct consequence of the increased temperatures associated with the UHI in this area. Furthermore, many of the root causes of the UHI (for example lack of greenspace, high anthropogenic heat output, significant built form) can be linked to vulnerable groups and therefore a feedback loop is created.

The simplicity of the methodology could be significantly refined through further research. For example, throughout this paper no explicit temperature values have been mentioned. This is deliberate as the focus has been the spatial identification of risk groups. This paper assumes that a single day "snapshot" of UHI data is representative of varying conditions, but an alternative heat hazard layer could be developed using outputs from UHI models, which would allow for flexibility when considering varying conditions.

A significant research gap in this paper is the verification of the results, for example against health and

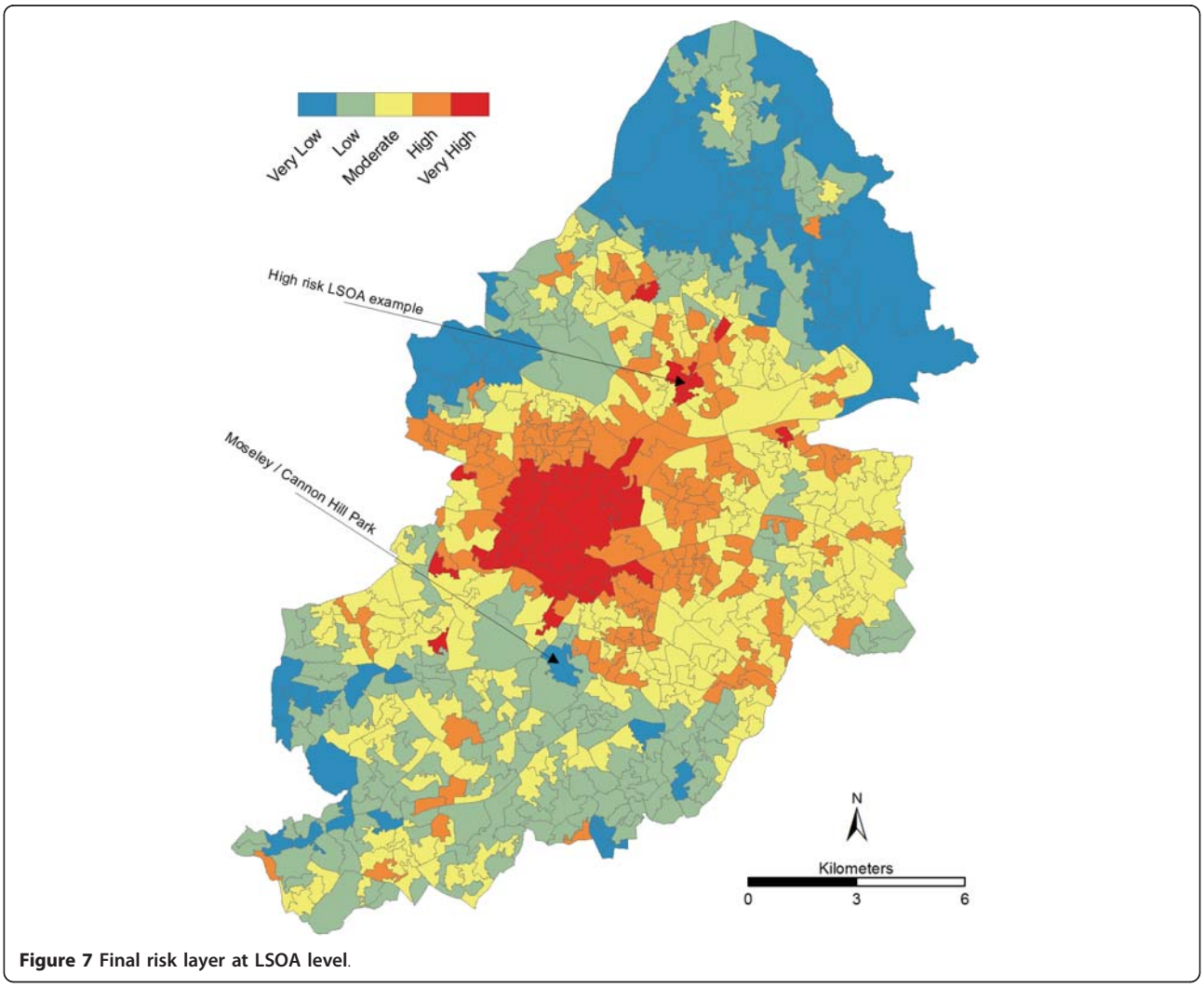

Figure 7 Final risk layer at LSOA level.

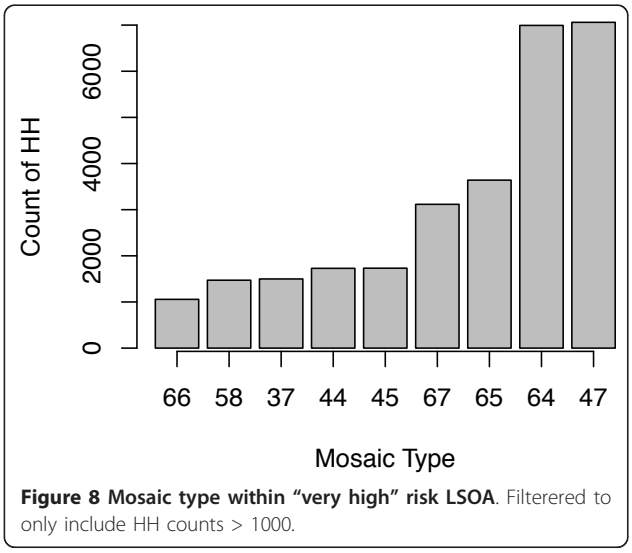

Figure 8 Mosaic type within "very high" risk LSOA. Filterered to only include HH counts > 1000.

mortality records in association with previous heat events (e.g. heatwave events in 2003 or 2006). This is the focus of ongoing work, but the data is presently not available at both a high temporal and spatial scale, which would be required in order to test for links at LSOA level. The data that is available is of limited utility as it is hard to quantify heat related health issues or mortality with any degree of certainty, and records have unreliable spatial attributes; in that they may relate to a patients home or to the hospital, and significant distances may be present between these. Hospital discharge data could potentially help quantify heat-related health admissions, although again the utility may be restricted due to small datasets and restricted availability.

In summary, the methods shown offer a repeatable methodology that can be utilised in many countries. This is made possible by the flexibility of a GIS based approach, the worldwide availability of the MODIS

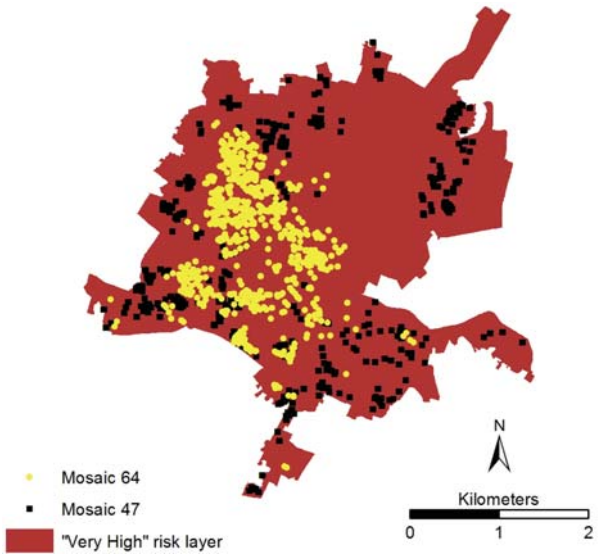

Figure 9 Mosaic type 64 and 47 spatial distribution within "very high" risk city centre area.

satellite data and the significant coverage of Experian's segmentation data throughout the developed world.

List of Abbreviations

ASCCUE: Adaptation Strategies for Climate Change in the Urban Environment; GIS: Geographical Information System; HDI: Hazard Density Index; HH: Household; LSOA: Lower layer Super Output Area; MODIS: MODerate resolution Imaging Spectroradiometer; MSOA: Middle layer Super Output Area; UHI: Urban Heat Island; UKCP09: United Kingdom Climate Projections 2009; UMT: Urban Morphology Type.

Acknowledgements

This research has been funded by a Doctoral Training Award issued by the Engineering and Physical Sciences Research Council and supported by Birmingham City Council. It would not have been possible without demographic data from Experian and satellite data from NASA. Experian data is available direct from Experian (http://www.experian.co.uk/). The satellite data is distributed by the Land Processes Distributed Active Archive Center (LP DAAC), located at the U.S. Geological Survey (USGS) Earth Resources Observation and Science (EROS) Center (lpdaac.usgs.gov).

Author details

[1]School of Civil Engineering, University of Birmingham, Edgbaston, Birmingham, B15 2TT, UK. [2]School of Geography, Earth and Environmental Sciences, University of Birmingham, Edgbaston, Birmingham, B15 2TT, UK.

Authors' contributions

CJT carried out the risk analysis and drafted the manuscript. LC, JET and CJB offered advice throughout the research and feedback on the draft manuscript. All authors read and approved the final manuscript.

Competing interests

The authors declare that they have no competing interests.

Received: 17 March 2011 Accepted: 17 June 2011
Published: 17 June 2011

References

1. Kovats RS, Hajat S: **Heat Stress and Public Health: A Critical Review.** *Annu Rev Publ Health* 2008, **29**:41-55.
2. Basu R, Samet JM: **Relation between elevated ambient temperature and mortality: a review of the epidemiologic evidence.** *Epidemiol Rev* 2002, **24**:190-202.
3. O'Neill M, Ebi K: **Temperature extremes and health: impacts of climate variability and change in the United States.** *J Occup Environ Med* 2009, **51**:13-24.
4. Vaneckova P, Hart MA, Beggs PJ, Dear RJ: **Synoptic analysis of heat-related mortality in Sydney, Australia, 1993-2001.** *Int J Biometeorol* 2008, **52**:439-451.
5. Honda Y: **Impact of climate change on human health in Asia and Japan.** *Global Environ Res* 2007, **11**:33-28.
6. Tan J, Zheng Y, Song G, Kalkstein L, Kalkstein A, Tang X: **Heat wave impacts on mortality in Shanghai, 1998 and 2003.** *Int J Biometeorol* 2007, **51**:193-200.
7. Gosling SN, Lowe JA, McGregor GR, Pelling M, Malamud BD: **Associations between elevated atmospheric temperature and human mortality: a critical review of the literature.** *Climatic Change* 2009, **92**:299-341.
8. Rooney C, Mcmichael AJ, Kovats RS, Coleman MP: **Excess mortality in England and Wales, and in Greater London, during the 1995 heatwave.** *J Epidemiol Commun H* 1998, **52**:482-486.
9. Semenza J, Rubin C, Falter K, Selanikio J, Flanders W, Howe H, Wilhelm J: **Heat-Related Deaths during the July 1995 Heat Wave in Chicago.** *New Engl J Med* 1996, **335**:84-90.
10. Kovats R, Kristie L: **Heatwaves and public health in Europe.** *Eur J Public Health* 2006, **16**:592-599.
11. Fouillet A, Rey G, Laurent F, Pavillon G, Bellec S, Guihenneuc-Jouyaux C, Clavel J, Jougla E, Hémon D: **Excess mortality related to the August 2003 heat wave in France.** *Int Arch Occup Env Hea* 2006, **80**:16-24.
12. Le Tertre A, Lefranc A, Eilstein D, Declercq C, Medina S, Blanchard M, Chardon B, Fabre P, Filleul L, Jusot JF, Pascal L, Prouvost H, Cassadou S, Ledrans M: **Impact of the 2003 heatwave on all-cause mortality in 9 French cities.** *Epidemiology* 2006, **17**:75-79.
13. Pirard P, Vandentorren S, Pascal M, Laaidi K, Le Tertre A, Cassadou S, Ledrans M: **Summary of the mortality impact assessment of the 2003 heat wave in France.** *Euro Surveill* 2005, **10**:153-156.
14. Filleul L, Filleul L, Cassadou S, Cassadou S, Médina S, Médina S, Fabres P, Fabres P, Lefranc A, Lefranc A, Eilstein D, Eilstein D, Tertre AL, Tertre AL, Pascal L, Pascal L, Chardon B, Chardon B, Blanchard M, Blanchard M, Declercq C, Declercq C, Jusot JF, Jusot JF, Prouvost H, Prouvost H, Ledrans M, Ledrans M: **The Relation Between Temperature, Ozone, and Mortality in Nine French Cities During the Heat Wave of 2003.** *Environ Health Persp* 2006, **114**:1344-1347.
15. Johnson H, Kovats RS, McGregor G, Stedman J, Gibbs M, Walton H: **The impact of the 2003 heat wave on daily mortality in England and Wales and the use of rapid weekly mortality estimates.** *Euro Surveill* 2005, **10**:168-171.
16. Kovats RS, Johnson H, Griffith C: **Mortality in southern England during the 2003 heat wave by place of death.** *Health Stat Q* 2006, **29**:6-8.
17. Garssen J, Harmsen C, de Beer J: **The effect of the summer 2003 heat wave on mortality in the Netherlands.** *Euro Surveill* 2005, **10**:165-168.
18. Nogueira PJ, Falcão JM, Contreiras MT, Paixão E, Brandão J, Batista I: **Mortality in Portugal associated with the heat wave of August 2003: early estimation of effect, using a rapid method.** *Euro Surveill* 2005, **10**:150-153.
19. Simón F, Lopez-Abente G, Ballester E, Martínez F: **Mortality in Spain during the heat waves of summer 2003.** *Euro Surveill* 2005, **10**:156-161.
20. Meehl G, Tebaldi C: **More intense, more frequent, and longer lasting heat waves in the 21st century.** *Science* 2004, **305**:994-997.
21. Knowlton K, Lynn B, Goldberg RA, Rosenzweig C, Hogrefe C, Rosenthal JK, Kinney PL: **Projecting heat-related mortality impacts under a changing climate in the New York City region.** *Am J Public Health* 2007, **97**:2028-2034.
22. Luber G, McGeehin M: **Climate Change and Extreme Heat Events.** *Am J Prev Med* 2008, **35**:429-435.
23. Haines A, Kovats RS, Campbell-Lendrum D, Corvalan C: **Climate change and human health: Impacts, vulnerability and public health.** *Publ Health* 2006, **120**:585-596.
24. Costello A, Abbas M, Allen A, Ball S, Bell S, Bellamy R, Friel S, Groce N, Johnson A, Kett M, Lee M, Levy C, Maslin M, Mccoy D, Mcguire B, Montgomery H, Napier D, Pagel C, Patel J, Oliveira JAPd, Redclift N, Rees H,

Rogger D, Scott J, Stephenson J, Twigg J, Wolff J, Patterson C: **Managing the health effects of climate change.** *Lancet* 2009, **373**:1693-1733.
25. Guest C, Willson K, Woodward A, Hennessy K, Kalkstein L, Skinner C, Mcmichael A: **Climate and mortality in Australia: retrospective study, 1979-1990, and predicted impacts in five major cities in 2030.** *Climate Res* 1999, **13**:1-15.
26. Kovats R, Haines A, Stanwell-Smith R, Martens P, Menne B, Bertollini R: **Climate change and human health in Europe.** *Brit Med J* 1999, **318**:1682-1685.
27. Arnfield AJ: **Two decades of urban climate research: a review of turbulence, exchanges of energy and water, and the urban heat island.** *Int J Climatol* 2003, **23**:1-26.
28. Stewart I: **A systematic review and scientific critique of methodology in modern urban heat island literature.** *Int J Climatol* 2010, **31**:200-217.
29. Oke TR: *Boundary Layer Climates Second Edition.* Second edition. London and New York: Routledge; 1987.
30. Stabler L, Martin C, Brazel A: **Microclimates in a desert city were related to land use and vegetation index.** *Urban For Urban Green* 2005, **3**:137-147.
31. Smith C, Lindley S, Levermore G: **Estimating spatial and temporal patterns of urban anthropogenic heat fluxes for UK cities: the case of Manchester.** *Theor Appl Climatol* 2009, **98**:19-35.
32. Department of Health: **NHS Heatwave Plan for England - Protecting Health and Reducing Harm from Extreme Heat and Heatwaves, 2009 Edition.** 2009, 1-39.
33. Lindley SJ, Handley JF, Theuray N, Peet E, McEvoy D: **Adaptation Strategies for Climate Change in the Urban Environment: Assessing Climate Change Related Risk in UK Urban Areas.** *J Risk Res* 2006, **9**:543-568.
34. United Nations: **World Urbanization Prospects: The 2007 Revision.** 2008.
35. McCarthy MP, Best MJ, Betts RA: **Climate change in cities due to global warming and urban effects.** *Geophys Res Lett* 2010, **37**:1-5.
36. Grimmond C, Blackett M, Best M, Barlow J, Baik JJ, Belcher S, Bohnenstengel S, Calmet I, Chen F, Dandou A, Fortuniak K, Gouvea M, Hamdi R, Hendry M, Kawai T, Kawamoto Y, Kondo H, Krayenhoff E, Lee SH, Loridan T, Martilli A, Masson V, Miao S, Oleson K, Pigeon G, Porson A, Ryu YH, Salamanca F, Shashua-Bar L, Steeneveld GJ, *et al*: **The International Urban Energy Balance Models Comparison Project: First results from Phase 1.** *J Appl Met Clim* 2010, **49**:1268-1292.
37. Gawith M, Street R, Westaway R, Steynor A: **Application of the UKCIP02 climate change scenarios: Reflections and lessons learnt.** *Global Environ Chang* 2009, **19**:113-121.
38. Jenkins GJ, Murphy JM, Sexton DS, Lowe JA, Jones P, Kilsby CG: **UK Climate Projections: Briefing report.** 2009, 1-60.
39. Kershaw T, Sanderson M, Coley D, Eames M: **Estimation of the urban heat island for UK climate change projections.** *Build Serv Eng Res Technol* 2010, **31**:1-13.
40. Cheval S, Dumitrescu A: **The July urban heat island of Bucharest as derived from modis images.** *Theor Appl Climatol* 2009, **96**:145-153.
41. Tomlinson CJ, Chapman L, Thornes JE, Baker CJ: **Derivation of Birmingham's summer surface urban heat island from MODIS satellite images.** *Int J Climatol* .
42. Sherwood S, Huber M: **An adaptability limit to climate change due to heat stress.** *P Natl Acad Sci Usa* 2010, **107**:9552-9555.
43. Meze-Hausken E: **On the (im-)possibilities of defining human climate thresholds.** *Climatic Change* 2008, **89**:299-324.
44. Coutts AM, Beringer J, Tapper NJ: **Impact of increasing urban density on local climate: Spatial and temporal variations in the surface energy balance in Melbourne, Australia.** *J Appl Meteorol* 2007, **46**:477-493.
45. Harlan S, Brazel A, Prashad L, Stefanov W, Larsen L: **Neighborhood microclimates and vulnerability to heat stress.** *Soc Sci Med* 2006, **63**:2847-2863.
46. Dolney T, Sheridan S: **The relationship between extreme heat and ambulance response calls for the city of Toronto, Ontario, Canada.** *Environ Res* 2006, **101**:94-103.
47. Hajat S, Kosatky T: **Heat-related mortality: a review and exploration of heterogeneity.** *J Epidemiol Commun H* 2010, **64**:753-760.
48. Tan J: **Commentary: People's vulnerability to heat wave.** *Int J Epidemiol* 2008, **37**:318-320.
49. Flynn A, Mcgreevy C, Mulkerrin E: **Why do older patients die in a heatwave?** *Q J Med* 2005, **98**:227-229.
50. Vandentorren S, Bretin P, Zeghnoun A, Mandereau-Bruno L, Croisier A, Cochet C, Riberon J, Siberan I, Declercq B, Ledrans M: **August 2003 heat wave in France: risk factors for death of elderly people living at home.** *Eur J Public Health* 2006, **16**:583-591.
51. Grize L, Huss A, Thommen O, Schindler C, Braun-Fahrländer C: **Heat wave 2003 and mortality in Switzerland.** *Swiss Med Wkly* 2005, **135**:200-205.
52. Conti S, Meli P, Minelli G, Solimini R, Toccaceli V, Vichi M, Beltrano C, Perini L: **Epidemiologic study of mortality during the Summer 2003 heat wave in Italy.** *Environ Res* 2005, **98**:390-399.
53. Huynen MM, Martens P, Schram D, Weijenberg MP, Kunst AE: **The impact of heat waves and cold spells on mortality rates in the Dutch population.** *Environ Health Persp* 2001, **109**:463-470.
54. Díaz J, Jordán A, García R, López C, Alberdi J, Hernández E, Otero A: **Heat waves in Madrid 1986-1997: effects on the health of the elderly.** *Int Arch Occup Env Hea* 2002, **75**:163-170.
55. Stafoggia M, Forastiere F, Agostini D, Biggeri A, Bisanti L, Cadum E, Caranci N, de' Donato F, De Lisio S, De Maria M, Michelozzi P, Miglio R, Pandolfi P, Picciotto S, Rognoni M, Russo A, Scarnato C, Perucci CA: **Vulnerability to heat-related mortality: a multicity, population-based, case-crossover analysis.** *Epidemiology* 2006, **17**:315-323.
56. Bell ML, O'Neill MS, Ranjit N, Borja-Aburto VH, Cifuentes LA, Gouveia NC: **Vulnerability to heat-related mortality in Latin America: A case-crossover study in Sao Paulo, Brazil, Santiago, Chile and Mexico City, Mexico.** *Int J Epidemiol* 2008, **37**:796-804.
57. Hajat S, Kovats RS, Lachowycz K: **Heat-related and cold-related deaths in England and Wales: who is at risk?** *Occup Environ Med* 2007, **64**:93-100.
58. Kaiser R, Rubin C, Henderson A: **Heat-related death and mental illness during the 1999 Cincinnati heat wave.** *AM J Foren Med Path* 2001, **22**:303-307.
59. Naughton M, Henderson A, Mirabelli M: **Heat-related mortality during a 1999 heat wave in Chicago.** *Am J Prev Med* 2002, **22**:221-227.
60. Yaron M, Niermeyer S: **Clinical description of heat illness in children, Melbourne, Australia–a commentary.** *Wild Environ Med* 2004, **15**:291-292.
61. McGeehin M, Mirabelli M: **The Potential Impacts of Climate Variability and Change on Temperature-Related Morbidity and Mortality in the United States.** *Environ Health Persp* 2001, **109**:185-189.
62. Kovats RS, Hajat S, Wilkinson P: **Contrasting patterns of mortality and hospital admissions during hot weather and heat waves in Greater London, UK.** *Occup Environ Med* 2004, **61**:893-898.
63. Collins T, Grineski S, de Lourdes Romo Aguilar M: **Vulnerability to environmental hazards in the Ciudad Juárez (Mexico)-El Paso (USA) metropolis: A model for spatial risk assessment in transnational context.** *Appl Geogr* 2009, **29**:448-461.
64. Su J, Morello-Frosch R, Jesdale B, Kyle A, Shamasunder B, Jerrett M: **An Index for Assessing Demographic Inequalities in Cumulative Environmental Hazards with Application to Los Angeles, California.** *Environ Sci Technol* 2009, **43**:7626-7634.
65. Fedeski M, Gwilliam J: **Urban sustainability in the presence of flood and geological hazards: The development of a GIS-based vulnerability and risk assessment methodology.** *Landsc Urban Plann* 2007, **83**:50-61.
66. Bolin B, Nelson A, Hackett EJ, Pijawka KD, Sicotte D, Sadalla EK, Matranga E, O'Donnell M: **The ecology of technological risk in a Sunbelt city.** *Environ Plann A* 2002, **34**:317-339.
67. Taramelli A, Melelli L, Pasqui M, Sorichetta A: **Estimating hurricane hazards using a GIS system.** *Nat Hazard Earth Sys Sci* 2008, **8**:839-854.
68. Morrison C, Shortt N: **Fuel poverty in Scotland: Refining spatial resolution in the Scottish Fuel Poverty Indicator using a GIS-based multiple risk index.** *Health Place* 2008, **14**:702-717.
69. Vaneckova P, Beggs PJ, Jacobson CR: **Spatial analysis of heat-related mortality among the elderly between 1993 and 2004 in Sydney, Australia.** *Soc Sci Med* 2010, **70**:293-304.
70. Vescovi L, Rebetez M, Rong F: **Assessing public health risk due to extremely high temperature events: climate and social parameters.** *Climate Res* 2005, **30**:71-78.
71. Reid C, O'Neill M, Gronlund C, Brines S, Brown D, Diez-Roux A, Schwartz J: **Mapping community determinants of heat vulnerability.** *Environ Health Persp* 2009, **117**:1730-1736.
72. Lindley SJ, Handley JF, McEvoy D, Peet E: **The Role of Spatial Risk Assessment in the Context of Planning for Adaptation in UK Urban Areas.** *Built Environ* 2007, **33**:46-69.
73. Gwilliam J, Fedeski M, Lindley SJ, Theuray N, Handley JF: **Methods for assessing risk from climate hazards in urban areas.** *Municip Eng* 2006, **159**:245-255.

74. Pidgeon N, Butler C: **Risk analysis and climate change.** *Environ Politics* 2009, **18**:670-688.
75. Crichton D: **The Risk Triangle.** *Natural disaster management: a presentation to commemorate the International Decade for Natural Disaster Reduction (IDNDR), 1990-2000* Ingleton J: Tudor Rose; 1999.
76. **Key Population and Vital Statistics.** 2007 [http://www.statistics.gov.uk/StatBase/Product.asp?vlnk=539].
77. **Super Output Areas Explained.** [http://www.neighbourhood.statistics.gov.uk/dissemination/Info.do?page=nessgeography/superoutputareasexplained/output-areas-explained.htm].
78. Fisher PA: **An Examination of the Association between Temperature and Mortality in the West Midland from 1981 to 2007 (Masters Thesis).** University of Birmingham, Department of Public Health and Epidemiology; 2009.
79. Ellis FP, Princé HP, Lovatt G, Whittington RM: **Mortality and morbidity in Birmingham during the 1976 heatwave.** *Q J Med* 1980, **49**:1-8.
80. May E, Baiardi L, Kara E, Raichand S, Eshareturi C: **Health Effects of Climate Change in the West Midlands: Technical Report.** 2010.
81. Grineski SE, Collins TW: **Exploring patterns of environmental injustice in the Global South: Maquiladoras in Ciudad Juárez, Mexico.** *Popul Environ* 2008, **29**:247-270.
82. Gluch R, Quattrochi D, Luvall J: **A multi-scale approach to urban thermal analysis.** *Remote Sens Environ* 2006, **104**:123-132.
83. Stathopoulou M, Cartalis C: **Daytime urban heat islands from Landsat ETM + and Corine land cover data: An application to major cities in Greece.** *Sol Energy* 2007, **81**:358-368.
84. Nichol JE, Fung WY, Lam Ks, Wong MS: **Urban heat island diagnosis using ASTER satellite images and 'in situ' air temperature.** *Atmos Res* 2009, **94**:276-284.
85. Yan H, Zhang J, Hou Y, He Y: **Estimation of air temperature from MODIS data in east China.** *Int J Remote Sens* 2009, **30**:6261-6275.
86. Cresswell MP, Morse AP, Thomson MC, Connor SJ: **Estimating surface air temperatures, from Meteosat land surface temperatures, using an empirical solar zenith angle model.** *Int J Remote Sens* 1999, **20**:1125-1132.
87. Sun Y, Wang J, Zhang R, Gillies R, Xue Y, Bo Y: **Air temperature retrieval from remote sensing data based on thermodynamics.** *Theor Appl Climatol* 2005, **80**:37-48.
88. Smith CL, Webb A, Levermore GJ, Lindley SJ, Beswick K: **Fine-scale spatial temperature patterns across a UK conurbation.** *Climatic Change* .
89. Martilli A: **Current research and future challenges in urban mesoscale modelling.** *Int J Climatol* 2007, **27**:1909-1918.
90. **Mosaic UK - the consumer classification of the United Kingdom.** [http://www.experian.co.uk/assets/business-strategies/brochures/mosaic-uk-2009-brochure-jun10.pdf].
91. **Natural & Man-Made Risk Identification for Insurance Risk | Insurance Perils | Experian.** [http://www.experian.co.uk/consumer-information/perils.html].
92. Gill SE, Handley JF, Ennos AR, Pauleit S, Theuray N, Lindley SJ: **Characterising the urban environment of UK cities and towns: A template for landscape planning.** *Landsc Urban Plann* 2008, **87**:210-222.
93. Gill S, Handley J, Ennos A, Pauleit S: **Adapting Cities for Climate Change: The Role of the Green Infrastructure.** *Built Environ* 2007, **33**:115-133.
94. Bowler DE, Buyung-Ali L, Knight TM, Pullin AS: **Urban greening to cool towns and cities: A systematic review of the empirical evidence.** *Landsc Urban Plann* 2010, **97**:147-155.
95. Mitchell R, Popham F: **Effect of exposure to natural environment on health inequalities: an observational population study.** *Lancet* 2008, **372**:1655-1660.

doi:10.1186/1476-072X-10-42
Cite this article as: Tomlinson *et al.*: Including the urban heat island in spatial heat health risk assessment strategies: a case study for Birmingham, UK. *International Journal of Health Geographics* 2011 **10**:42.

METEOROLOGICAL APPLICATIONS
Meteorol. Appl. **18**: 296–306 (2011)
Published online in Wiley Online Library
(wileyonlinelibrary.com) DOI: 10.1002/met.287

RMetS
Royal Meteorological Society

Review

Remote sensing land surface temperature for meteorology and climatology: a review

Charlie J. Tomlinson,[a]* Lee Chapman,[b] John E. Thornes[b] and Christopher Baker[a]

[a] *Department of Civil Engineering, University of Birmingham, Birmingham B15 2TT, UK*
[b] *Department of Geography, Earth and Environmental Sciences, University of Birmingham, Birmingham B15 2TT, UK*

ABSTRACT: The last decade has seen a considerable increase in the amount and availability of remotely sensed data. This paper reviews the satellites, sensors and studies relevant to land surface temperature measurements in the context of meteorology and climatology. The focus is on using the thermal infrared part of the electromagnetic spectrum for useful measurements of land surface temperature, which can be beneficial for a number of uses, for example urban heat island measurements.

KEY WORDS LST; remote sensing; UHI; satellite; MODIS; Landsat

Received 30 June 2011; Revised 15 July 2011; Accepted 20 July 2011

Remote Sensing Letters
Vol. 3, No. 8, 20 December 2012, 657–666

Taylor & Francis
Taylor & Francis Group

Comparing night-time satellite land surface temperature from MODIS and ground measured air temperature across a conurbation

CHARLIE J. TOMLINSON*†, LEE CHAPMAN‡, JOHN E. THORNES‡, CHRISTOPHER J. BAKER† and TATIANA PRIETO-LOPEZ‡

†School of Civil Engineering, University of Birmingham, Edgbaston, Birmingham B15 2TT, UK

‡School of Geography, Earth and Environmental Sciences, University of Birmingham, Edgbaston, Birmingham B15 2TT, UK

(*Received 14 September 2011; in final form 16 January 2012*)

The relationship between remotely sensed land surface temperature (LST) data and ground-measured air temperature is important for a number of applications. This article details a pilot project over the summer (June, July, August) 2010 using Moderate Resolution Imaging Spectroradiometer (MODIS) LST data and air temperature data from a custom network of data loggers across the conurbation of Birmingham, UK. The results show that at night-time air temperature is consistently higher than the satellite-measured LST, but significant station-specific variability exists.